Evaluation of Stable Chlorine and Bromine Isotopes in Sedimentary Formation Fluids

by

Orfan Shouakar-Stash

A thesis
presented to the University of Waterloo
in fulfillment of the
thesis requirement for the degree of
Doctor of Philosophy
in
Earth Sciences

Waterloo, Ontario, Canada, 2008

I hereby declare that I am the sole author of this thesis. This is a true copy of the thesis, including any required final revisions, as accepted by my examiners.

I understand that my thesis may be made electronically available to the public

ABSTRACT

Two new analytical methodologies were developed for chlorine and bromine stable isotope analyses of inorganic samples by Continuous-Flow Isotope Ratio Mass Spectrometry (CF-IRMS) coupled with gas chromatography (GC). Inorganic chloride and bromide were precipitated as silver halides (AgCl and AgBr) and then converted to methyl halide (CH_3Cl and CH_3Br) gases and analyzed. These new techniques require small samples sizes (1.4 μmol of Cl^- and 1 μmol of Br^-). The internal precision using pure CH_3Cl gas is better than ±0.04 ‰ (±STDV) while the external precision using seawater standard is better than ±0.07 ‰ (±STDV). The internal precision using pure CH_3Br gas is better than ±0.03 ‰ (±STDV) and the external precision using seawater standard is better than ±0.06 ‰ (±STDV). Moreover, the sample analysis time is much shorter than previous techniques. The analyses times for chlorine and bromine stable isotopes are 16 minutes which are 3-5 times shorter than all previous techniques.

Formation waters from three sedimentary settings (the Paleozoic sequences in southern Ontario and Michigan, the Williston Basin and the Siberian Platform) were analyzed for ^{37}Cl and ^{81}Br isotopes. The $\delta^{37}Cl$ and $\delta^{81}Br$ values of the formation waters from these basins are characterized by large variations (between -1.31 ‰ and +1.82 ‰ relative to SMOC and between -1.50 ‰ and +3.35 ‰ relative to SMOB, respectively). A positive trend between $\delta^{81}Br$ and $\delta^{37}Cl$ values was found in all basins, where an enrichment of $\delta^{81}Br$ is coupled by an enrichment of $\delta^{37}Cl$.

In the Paleozoic sequences in southern Ontario and Michigan, the $\delta^{37}Cl$ and $\delta^{81}Br$ signatures of formation water collected from northwest of the Algonquin Arch are distinct from those collected from southeast of the Arch. All of the brines from the northwest of the Algonquin Arch are characterized by depleted isotopic values in comparison with the isotopic values from the brines from southeast of the Arch. The $\delta^{81}Br$ signatures of the two brines show total separation with no overlaps. The $\delta^{37}Cl$ values show some overlap between the two groups. One of the scenarios that can be put forward is that the Arch forms a water divide, where sediments southeast of the Arch are dominated by Appalachian Basin formation waters, and the sediments located northwest of the Arch are dominated by the Michigan Basin formation waters.

The $\delta^{81}Br$ and $\delta^{37}Cl$ signatures of the Williston Basin brines suggest the existence of several different brines that are isotopically distinct and located in different stratigraphic units, even though they are chemically similar. The relatively wide range of $\delta^{37}Cl$ and $\delta^{81}Br$ of the formation waters suggests that the ocean isotopic signatures were variable over geologic time. A seawater temporal curve for $\delta^{81}Br$ and $\delta^{37}Cl$ was proposed with a larger variation of $\delta^{81}Br$ in comparison with $\delta^{37}Cl$. The isotopic variations of these two elements agree very well with $^{87}Sr/^{86}Sr$ seawater variation during the same period.

In general, the use of chlorine and bromine stable isotopes can be very useful in assessing the origin and the evolutionary processes involved in evolving formation waters and also in distinguishing different brines (end members). Furthermore, they can be employed to investigate the hydrogeological dynamics of sedimentary basins.

ACKNOWLEDGEMENTS

First and foremost, I would like to sincerely thank my supervisor, Professor Shaun K. Frape, for his generous guidance, support and constructive critical insights throughout this thesis. I would like also to express my genuine appreciation to Shaun for giving me the opportunity to attend several important conferences and for introducing me to highly respected scientists. I certainly gained valuable experience and contacts during these meeting and these resulted in several co-operative projects. I am proud to call you and your lovely wife Nori friends.

Also, I am grateful to my PhD committee members, Professor Ramon Aravena, Professor Jim Barker and Professor Mario Coniglio from the University of Waterloo and Professor Ben Rostron from the University of Alberta for their valuable time, advice, constructive comments and guidance throughout this study. A special appreciation goes to Ben for sharing his samples and database to conduct a study on the Williston Basin (Chapter 6). Ben, thank you very much for trusting me and for supporting my work, and for the fast responses to my phone calls and emails. I would also like to extend my appreciation to Ramon for his friendship and support over the years.

I also extend my appreciation to my external examiner Professor Don Siegel for his valuable time and his critical and constructive comments that enriched my thesis.

Further, I would like to express my gratefulness to Dr. Sergey Alexeev and Dr. Ludmila Alexeeva for sharing their Siberian Platform samples, providing me with valuable information and supporting my study.

I would also like to gratefully acknowledge the support and assistance of Bob Drimmie who always encouraged me, trusted me and inspired me. I thank him also for giving me the opportunity to work at the Environmental Isotope Laboratory (EIL), which got me involved in different analytical challenges and sparked my interest in the method development aspects of isotopes.

The faculty and staff of the Department of Earth and Environmental Sciences created a supportive and highly stimulating environment in which to work. I especially want to acknowledge the support of my fellow EIL staff members. I consider myself lucky not only to have had the opportunity to work in the EIL, but also to work with wonderful people and make unforgettable colleagues and friends. I would like also to extend my thanks to Sue Fisher and Lorraine Albrecht.

I wish to extend my thanks to Dr. Monique Hobbs and Dr. Min Zhang for their friendship, support and enlightening discussions that I have had over the years.

Special thanks are also due to Bill Mark and Richard Elgood for their friendship and support. I very much enjoyed our irregular lunches. I certainly think that we need to get a life, so let us schedule regular lunches. Rich I think you should be in charge of that.

I cannot thank Oya Albak, Humam Elmugammar, Asma Kaghdou and Tania Stas enough for their friendship, support and encouragement. I wish all the best for them in their career, and personal life.

I also would like to thank Mary Ellen Patton for her support, friendship and proofreading several papers. My gratitude goes also to Randy Stotler my fellow graduate student over the last few years for interesting discussions and friendship.

Above all else, I am indebted to my parents for their support, endless patience and unconditional love. They inspired me to work hard and they taught me the value of education. My gratitude to them exceeds the boundaries of this formal acknowledgement. My heartfelt appreciations are also extended to my in-laws for their continuous support and undying encouragement to pursue my dreams.

Finally, I dedicate this work to my lovely wife Mirna and my little two angels Enaal and Anzor. The development and completion of this work would not have been possible without their support, encouragement, belief in me and understanding. I am very grateful to God who blessed me with my wife and kids. I know that school took a lot of my time and that I could not be there as much as I should have been. However, now that my formal education is complete, I can only hope that there will be many happy years ahead of us. Mirna, no matter what I say, I cannot thank you enough. I ask Almighty God to keep us together forever.

TABLE of CONTENTS

LIST OF TABLES

LIST OF FIGURES

FOREWORD

This thesis was written in paper format with the intention that each chapter (with the exception of chapters 1 and chapter 7) will be published separately. Due to this format, there is some repetition between chapters. Chapter 1 is an introduction chapter that demonstrates the chemical and isotopic characteristic of chlorine and bromine and their distribution in nature. Chapters 2 and 3 are technical papers that describe the development of two new methodologies for analyzing chlorine and bromine stable isotopes by Continuous-Flow Isotope Ratio Mass Spectrometry (CF-IRMS). These two chapters are already published and the full references for these two chapters are as follow:

***Chapter 2*:** Shouakar-Stash, O., Drimmie, R.J., and Frape, S.K. (2005) Determination of inorganic chlorine stable isotopes by Continuous Flow Isotope Ratio Mass spectrometry. Rapid Communication in Mass Spectrometry. Vol. 19, 121-127. (DOI: 10.1002/rcm.1762)

***Chapter 3*:** Shouakar-Stash, O., Frape, S.K., and Drimmie, R.J. (2005) Determination of bromine stable isotopes using Continuous-Flow Isotope Ratio Mass Spectrometry. Analytical Chemistry. vol. 77, No. 13, 4027-4033. (10.1021/ac048318n CCC:)

Chapters 4 through 6 are individual study areas; The southern Ontario sedimentary sequences in Canada, the Siberian Platform in Russia, and the Williston Basin in Canada and the United States of America. Of these three chapters, chapter 5 is already published in Applied Geochemistry and the full reference of this paper is given below:

***Chapter 5*:** Shouakar-Stash, O., Alexeev, S. V., Frape, S.K., Alexeeva, L. P., Drimmie, R. J. (2007) Geochemistry and stable isotopic signatures, including chlorine and bromine isotopes, of the deep groundwaters of the Siberian Platform, Russia. Applied Geochemistry. vol. 22, 589-605. (doi:10.1016/j.apgeochem.2006.12.005).

The discussion in Chapter 5 is slightly different from that published in Applied Geochemistry. This section was modified during the final stage of the thesis to add clarity, but it doest not change the conclusions of the published paper.

Chapter 4 and 6 are to be submitted for publication in Geochimica et Cosmochimica Acta and Applied Geochemistry.

Chapter 7 is the last chapter which is composed of a general summary of all chapters.

CHAPTER 1

INTRODUCTION

1.1 Background

Of all halogens, chlorine was the first to be discovered, being prepared by Scheele in 1774 by heating hydrochloric (muriatic) acid with manganese dioxide (Downs and Adams, 1975), though the fumes of the gas must have been known from the time of the thirteenth century by all those who made and used aqua regia (a mixture of concentrated nitric acid and concentrated hydrochloric acid). Sodium chloride (Halite) also known as 'salt' is referred to by Pliny in the first century A.D. in his *Naturalis Historiae* (Downs and Adams, 1975). Salt was an object of barter trade as early as the Stone Age. The "salt routes" crossed the ancient world from India to the Dead Sea; Marco Polo even noted salt coins bearing the seal of the Great Khan of Cathay. The busy traffic on the European salt routes persisted until modern time (Harben and Kužvart, 1996).

Bromine was discovered by A.J. Balard in 1825 and its atomic weight was determined gravimetrically for the first time in the 1860's by J. S. Stas (Yaron, 1966). Bromine is the only nonmetallic element that is liquid at room temperature, which readily volatilizes to a red vapour that is extremely irritating to the eyes, nose, and throat. It has a pungent odour as described by its Greek derivation *bromo*, meaning stench. The first bromine-bearing mineral, apparently bromyrite (silver bromide), was recognized in 1846 by Berthier (Harben and

Kužvart, 1996). The discovery of bromine and the invention of photography were made at about the same time. In 1840, the use of silver bromide was introduced in photography and through this, bromine became an industrial chemical (Yaron, 1966). The initial commercial production of bromine developed by David Alter at Freeport, Pennsylvania was based on native salt brines. An additional source was discovered in 1858 as a by-product of potash production from the Stassfurt salt deposits in Germany.

1.2 Distribution in Nature

1.2.1 Chlorine

Of the ninety two natural elements, chlorine is the eighteenth in order of abundance (Graedel and Keene, 1996). Chlorine exists predominantly as chloride ion, a trace component of all the Earth's geological compartments other than the oceans, its primary sink (Reimann and de Caritat, 1998). Chlorine resides in several major reservoirs (Figure 1.1); rock (the mantle and crust), soil (the pedosphere), freshwater (groundwater, lakes and rivers), salt-waters (the oceans, saline lakes, inland seas, and subsurface crystalline and sedimentary brines), ice caps (the cryosphere), the lower atmosphere (the troposphere), and the middle atmosphere (the stratosphere). The total chlorine content of these reservoirs differs enormously. The chlorine contents in these different reservoirs were calculated by the author and presented in Table 1.1.

Table 1.1 The natural chlorine contents of Earth's reservoirs[a]

Reservoir	Chlorine content[a]	Percentage of total	Form	Sources[b]
Mantle	4.61×10^{24} g	98.170 %	Mineral	[1], [2]
Crust	60×10^{21} g	1.272 %	Mineral	[3]
Igneous and Metamorphic Rocks	6.67×10^{21} g	0.142%	Mineral	[4]
Sedimentary Rocks	53.33×10^{21} g	1.13 %	Mineral	[3],[4]
Ocean	26×10^{21} g	0.553191 %	Ionic	[5], [6]
Pedosphere	24×10^{15} g	5.11×10^{-7} %	Mineral	[3]
Fresh surface waters	7.35×10^{14} g	1.56×10^{-8} %	Ionic	[5], [7]
Groundwater	380×10^{15} g	8.09×10^{-6} %	Ionic	[5], [8]
Cryosphere	5.15×10^{14} g	1.10×10^{-8} %	Ionic	[3], [5]
Troposphere	4.3×10^{12} g	9.15×10^{-11} %	Gaseous	[3], [5]
Troposphere	$1.0 - 1.5 \times 10^{12}$ g	2.66×10^{-11} %	Areosol	[3], [5]
Stratosphere	0.4×10^{12} g	8.51×10^{-12} %	Gaseous	[3], [5]
Earth (total)	4.7×10^{24} g	100 %		

[a] The Chlorine contents are calculated from information obtained from the references listed below. Calculations are described in more details in Appendix A.

[b] Sources: [1] Anders and Ebihara, 1982; [2] Press and Siever, 1978; [3] Graedel and Keene, 1996; [4] Yoshida et al., 1971; [5] Berner and Berner, 1987; [6] Wilson, 1975; [7] Meybeck, 1994; [8] Freeze and Cherry, 1979.

Figure 1.1 demonstrate a useful summary that was prepared by Graedel and Kneene (1996) for the major reservoirs and the flow between them. As a result of their aqueous solubility, inorganic chloride salts enter the hydrosphere and distribute between the hydrosphere's sub-

compartments coupled to the hydrological cycle. Chlorine is distributed in the hydrosphere in the following order: Oceans (97 %), ice sheets and glaciers (2 %), deep (0.4 %) and shallow (0.3 %) groundwater, lakes (0.01 %), soil moisture (0.005 %), rivers (0.0001 %) and the atmosphere (0.001 %).

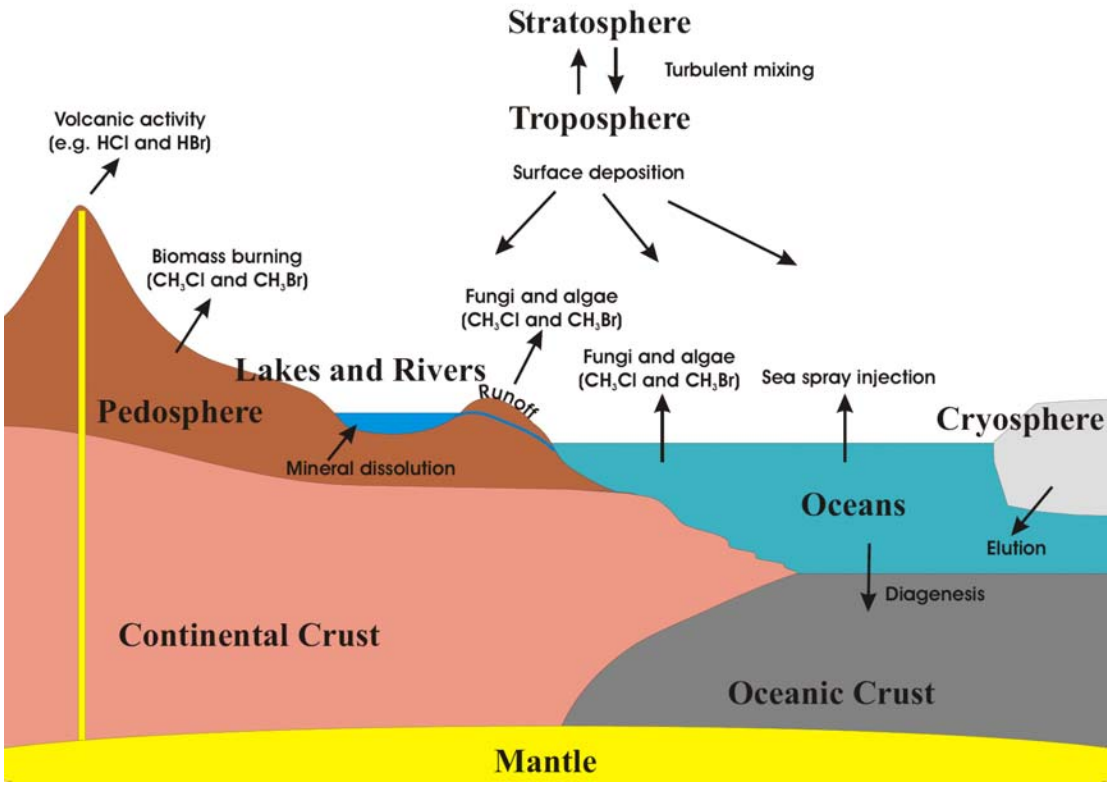

Figure 1.1 The Earth's major reservoirs of chlorine and bromine and some natural processes that transfer these two elements between these reservoirs (modified after Graedel and Keene, 1996).

1.2.2 Bromine

Bromine is widely distributed in nature but in relatively small concentrations compared to chlorine. Elemental bromine follows chlorine through the geological cycle (Harben and Kužvart, 1996) (Figure 1.1). In accordance with the similarity of radius of the chloride and bromide ions, their mineral chemistry is closely related, and bromine is known to replace chlorine in numerous minerals (Yaron, 1966). The bulk of the chlorine and bromine present in sedimentary and volcanic rocks takes the place of OH groups in hydroxide-bearing minerals such as amphibols, phylosilicates (mica), clay materials and aluminum hydroxide (feldspathoids) (e.g. sodolite) (Downs and Adams, 1975). There are relatively few minerals composed chiefly of bromide compounds, those that exist usually contain silver bromide (AgCl), and they have no commercial significance with regard to bromine manufacture. The chief mineral sources used to obtain bromine include sylvinite (KCl.NaCl) and carnallite ($KCl.MgCl_2.6H_2O$) where Br content seldom exceeds 0.35% w/w (Price et al., 1988).

The other main sources of bromine are the seas, salt lakes, brine wells and salt springs. Although the bromine content of seawater is only 0.0065 %, some isolated water bodies are much richer in bromine. Worldwide, the two most important brine sources with regard to bromine manufacture are the Arkansas subsurface sedimentary brine field in the USA which has a typical bromide content of 4 g/litre and the Dead Sea where the bromide level is about 5 g/litre (Price et al., 1988).

The bromine contents of the Earth's various reservoirs are presented in Table 1.2. These contents are calculated based on information obtained from several references that are listed

in Table 1.2. The bromine content of the mantle (10.471×10^{21} g) was calculated by subtracting the sum of all reservoirs from the total content listed for Earth. This is most likely an over estimation since the author did not address the bromine content in the cryosphere and the pedosphere, due to the lack of information in the literature. However, the bromine content in these two reservoirs is relatively small in comparison to the mantle and leaving these two out of the equation will not change the overall distribution picture and the bromine content in the mantle. Detailed information on the calculations is presented in Appendix A. Figures 1.1 illustrates the main reservoirs for chlorine and bromine and the relationship between these various reservoirs.

Table 1.2 The natural bromine content of Earth's eservoirs*

Reservoir	Bromine content	Percentage of total	Form	Sources***
Mantle	10.471×10^{21} g	98.924 %	Mineral	[1], [2]
Crust*	2.21×10^{19} g	0.209 %	Mineral	[3]
Ocean	9.18×10^{19} g	0.867 %	Ionic	[4]
Fresh surface waters	25.34×10^{11} g	2.39×10^{-8} %	Ionic	[4], [5], [6]
Groundwater**	1.267×10^{15} g	1.20×10^{-5} %	Ionic	[4], [7], [8]
Atmosphere	3.98×10^{10} g	3.76×10^{-10} %	Gaseous	[9]
Earth (total)	10.585×10^{21} g	100 %		

*based on the average content of Br in igneous rock that makes up over 95% of the crust. Calculations are described in more details in Appendix A.

**by estimating an average Cl/Br of 300

*** Sources: [1] Anders and Ebihara, 1982; [2] Press and Siever, 1978; [3] Yoshida et al., 1971; [4] Berner and Berner, 1987; [5] Martin and Meybeck, 1979; [6] Chester, 2000; [7] Freeze and Cherry, 1979. [8] Downs and Adams, 1975; [9] Schilling et al., 1978.

1.3 Physical and Chemical Properties

Some of the physical and chemical properties of chlorine and bromine are presented in Table 1.3.

Table 1.3 Physical properties of chlorine and bromine*

Property	Chlorine	Bromine
Atomic number	17	35
Atomic weight	35.453	79.904
Physical state (at 20ºC and 1 atm)	Green-Yellow gas	Dark red liquid
Melting point	172.31 K (-100.84ºC)	266.05 K (-7.1ºC)
Boiling point	239.25 K (-33.9ºC)	332.4 K (59.25ºC)
Electronegativity (Pauling)	3.16	2.96
Density ($g.ml^{-1}$)20ºC	3.214	3.119
Vapour pressure	1300	5800 (at -7.1 ºC)
Atomic radius	0.97 Å	1.12 Å
Covalent radius	0.99 Å	1.14 Å
Ionic radius	1.81 Å	1.96 Å
Ionization potential		
First	12.967	11.814
Second	23.81	21.8
Third	39.611	36
Valence electron potential (¯eV)	-7.96	-7.35
Electrode potential $E^0_{298/volts}$	-1.358	-1.065
Electron affinity eV	3.613	3.363

* Data are from Environmental Chemistry (http://environmentalchemistry.com/yogi/chemistry/), Bassett et al., 1988 and Wieser, 2006 (IUPAC, 2006).

1.4 Isotopes

1.4.1 Chlorine

Isotopes are atoms whose nuclei contain the same number of protons but a different number of neutrons. The term "isotope" is derived from Greek (meaning equal places) and indicates that isotopes occupy the same position in the periodic table (Hoefs, 2004). The newest CRC Handbook of Chemistry and Physics lists 24 chlorine isotopes, ranging in mass from 28 to 51 (CRC, 2005), all of which are radioactive isotopes except for two (^{35}Cl and ^{37}Cl) that are stable. The majority of the radioactive isotopes have a very short half-life in the range of nano-seconds. Chlorine-36 (half-life 3.01 x 10^5 years) is probably the most well known of all radioactive chlorine isotopes. The Atomic Mass (m_a/u) of these two stable isotopes, are 34.96885272 and 36.96590260, respectively (De Laeter et al., 2003 (IUPAC, 2003)). The lighter isotope ^{35}Cl is the dominant isotope in nature with an abundance of 75.76 % and the heavier isotope ^{37}Cl is the second most common isotope with an abundance of 24.24 % (De Laeter et al., 2003 (IUPAC, 2003)).

Aston (1919) was probably the first to show that chlorine has two stable isotopes ^{35}Cl and ^{37}Cl. Several other researchers (Curie, 1921; Gleditsch and Sandahl, 1922; Harkins and Stone, 1926; Nier and Hanson, 1936; Graham et al., 1951; Shields et al., 1962) attempted to measure the chlorine isotopic ratios, however, due to the relatively small isotopic variation and poor precision, no measurable variations were found. After the development of a new mass spectrometer with double ion collectors (Nier, 1947; Nier et al., 1947; McKinney et al., 1950; Nier, 1955) it was possible to measure chlorine isotope ratios with a precision of ± 1

‰. Hoering and Parker (1961) analyzed various rocks and minerals (81 samples) for chlorine isotope ratios and they concluded no significant variations from standard. They also analyzed three perchlorate samples and they did not find any significant isotopic differences between their chloride and perchlorate samples. Recently, Coleman et al. (2003) reported large isotope fractionation (-15.8 ± 4 ‰) between pechlorate and chloride during microbial reduction of perchlorate. Furthermore, Böhlke et al. (2005) reported $\delta^{37}Cl$ values between -3.1 ‰ and +1.6 ‰ for syntactic perchlorate and $\delta^{37}Cl$ values between -14.5 ‰ and -9.2 ‰ for natural perchlorate extracted from Atacama nitrate ore and from Chilean nitrate fertilizer products. In 1954, Langvard developed a technique for measuring chlorine stable isotopes on methyl chlorides. This technique was improved later by Hill and Fry (1962) and later by Taylor and Grimsrud (1969). However, Kaufmann (1984) was the first to show measurable variations of chlorine stable isotopes in natural samples after modifying the above methodology and achieving a precision of ± 0.24 ‰. Kaufmann's work was followed by several other studies that investigated the variations of chlorine stable isotopes (Kaufmann et al., 1984; Gifford et al., 1985; Desaulniers et al., 1986; Kaufmann and Arnórsson 1986; Kaufmann et al., 1987; Kaufmann et al., 1988; Eastoe et al., 1989; Kaufmann, 1989; Eastoe and Guilbert, 1992; Kaufmann et al., 1992; Kaufmann et al., 1993). Currently, chlorine stable isotopes are determined by three different analytical techniques, two of which use thermal ionization mass spectrometry (TIMS). The first technique (N-TIMS) is based on measuring [Cl^-] negative ions (Shields et al., 1962; Vengosh et al., 1989). This has reasonably high sensitivity; however, the technique is difficult and the precision is poor (> ±0.4 ‰). The second

technique (P-TIMS) is based on measuring positive ions [Cs_2Cl^+] (Xiao and Zhang, 1992; Magenheim et al., 1994; Xiao et al., 1995; Numata et al., 2001; Xiao et al., 2002). This technique is best for analyzing very small samples (1–50 μg Cl) and has good precision (±0.2‰) for such small samples. The third technique is based on analyzing methyl chloride gas using dual inlet isotope ratio mass spectrometry (DI-IRMS) (Long et al., 1993). This last technique is reported to have the best precision available in analyzing chlorine stable isotopes; however, the technique is limited by the sample size requirement (300–1000 μg of Cl^-) and also by the lengthy preparation process which limits the number of samples that can be analyzed in a prescribed period of time. Beside methods that focused on measuring Cl isotope compositions in inorganic compounds, several methods were developed for analyzing chlorine stable isotopes in organic compounds (Tanaka and Rye 1991; van Warmerdam et al., 1995; Holt et al., 1997; Jendrezejewski et al., 1997; Holt et al., 2001; Holmstrand et al., 2004; Shouakar-Stash et al., 2006).

1.4.2 Bromine

Bromine has 31 isotopes, ranging in mass between 67 and 97 (CRC, 2005). Out of this large number of isotopes there are only two stable isotopes (^{79}Br and ^{81}Br) that are by far the two dominant isotopes. The rest are radioactive isotopes that have very short half-lives that range between nano-seconds and several hours. When neglecting the very small contribution from unstable isotopes produced in nature by spontaneous fission and nuclear reactions induced by cosmic radiation, bromine consists mainly of the two stable isotopes. The Atomic Mass

(m_a/u) of these two stable isotopes, are 78.9183379 and 80.916291, respectively (De Laeter, 2003 (IUPAC, 2003)). Relative abundances of these isotopes have been measured and they are 50.69 % and 49.31 %, respectively (De Laeter, 2003 (IUPAC, 2003)).

Attempts to measure bromine stable isotopes were made as early as 1920 (Aston, 1920). In 1936, more attempts were made using a Dempster-type mass spectrograph (Blewett, 1936). The measurement was done by analyzing positive and negative ions (Br^+, Br_2^+, Br^{2+} and Br^-), and a precision of ± 25 ‰ was reported. Ten years later, Williams and Yuster (1946) used a mass spectrograph of the Nier type to analyze bromine stable isotopes, and the results were obtained from measuring positive ions (Br^+, Br_2^+, and Br^{2+}) formed from electronic bombardment of bromine vapour. In this study, Williams and Yuster (1946) achieved a precision of ± 4 ‰. In 1955, isotopic compositions of elemental bromine from various suppliers and diverse origins were determined by N-TIMS (Cameron and Lippet, 1955); however, no significant differences between these samples were found, which is probably due to the poor precision (± 4 ‰). Another attempt to use TIMS for bromine stable isotope measurement was followed by Catanzaro et al. (1964) and they reported an improvement in the precision (± 1.8 ‰). A much more precise technique was introduced in 1993 by the means of positive-TIMS (Xiao et al., 1993), based on measuring positive ions of Cs_2Br^+. This technique is useful for analyzing very small samples (4-32 μg of Br) and has good precision (± 0.12 ‰) for such small samples. DI-IRMS was used for the first time to determine bromine stable isotope composition in 1978 (Willey and Taylor, 1978). The technique is based on analyzing methyl bromide gas. More recently, Eggenkamp and Coleman (2000)

published a paper on bromine separation and isotopic determination of bromine by DI-IRMS. In their technique they reported a precision of ± 0.18 ‰.

1.5 Isotopic Distribution of Chlorine and Bromine

1.5.1 Chlorine

A summary of the chlorine stable isotope ranges of various materials is presented in Figure 1.2. All ranges are reported relative to seawater "Standard Mean Ocean Chloride (SMOC)" as first proposed by Kaufmann (1984) and it has the value of 0 ‰. Recently, Godon et al. (2004) conducted a study on seawater chlorine isotopic composition where they analyzed 24 samples from different oceans and seas that confirmed the homogeneity and consistency of the 0 ‰ value assigned to SMOC by reporting that all values are within ±0.08 ‰ (2σ).

In general, chlorine isotopes that exist in the chloride form in various natural materials and phases are found to range between ~ -8 ‰ and ~ +8 ‰. However, the vast majority of samples lie between -2 ‰ and +2 ‰. It seems that minerals and rocks are responsible, more than other sources, for extending the chlorine isotopic range to extreme positive values, while pore waters in ocean and lake sediments are responsible for extending it to the other extreme. It is important to note that the most negative isotopic values of chlorine were found in perchlorate (ClO_4^-) extracted from Atacama nitrate ore and from Chilean nitrate fertilizer products (values range between -14.5 ‰ and -9.2 ‰, Böhlke et al., 2005).

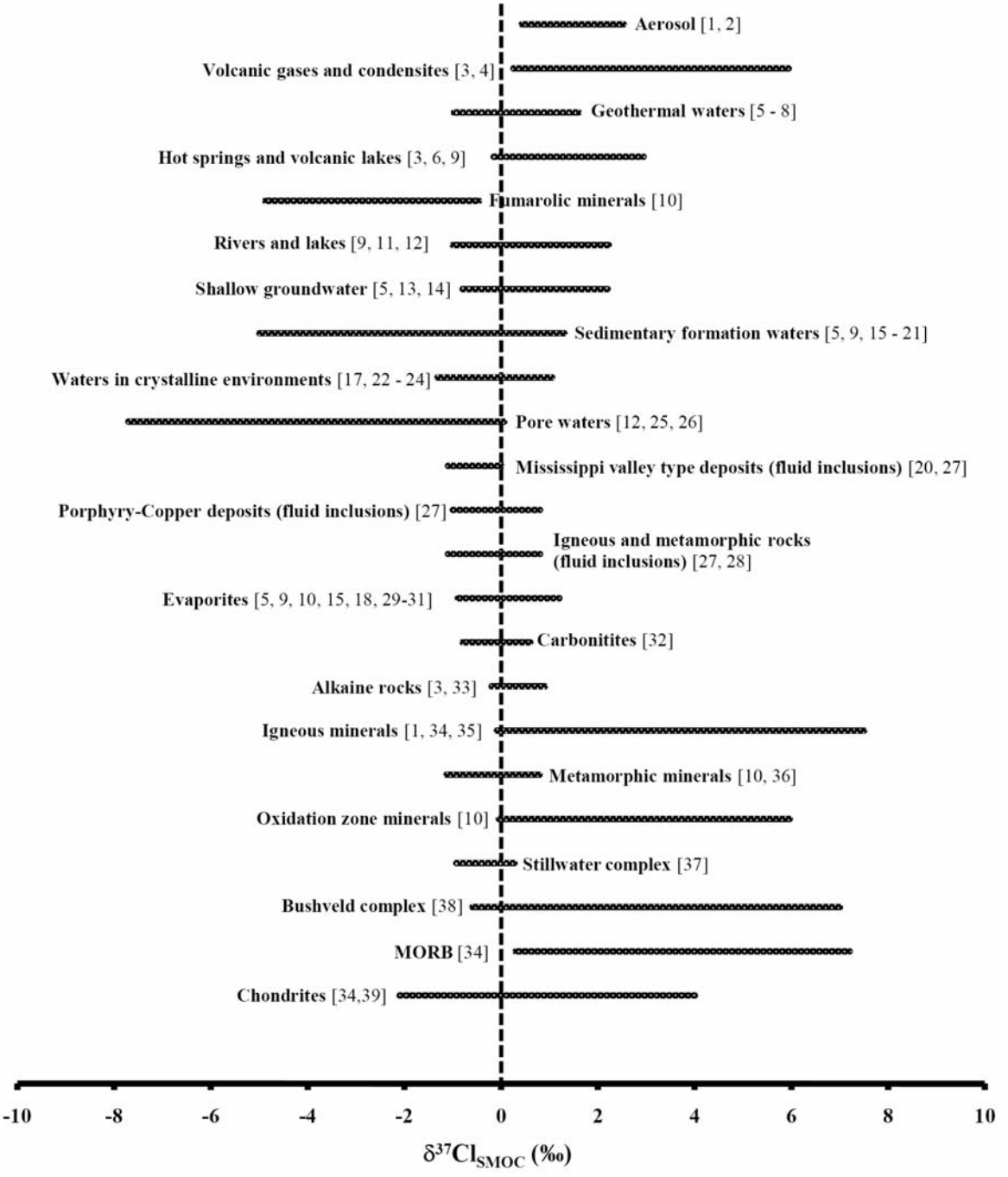

Figure 1.2 A summary of $\delta^{37}Cl$ ranges of various natural materials. Bracketed numbers refers to the source of data. References are presented in Table 1.4. This figure does not include the highly negative values (-14.5 ‰ and -9.2 ‰) obtained for the perchlorate (Böhlke et al., 2005).

Table 1.4 References of the source data presented in Figure 1.2

Number	Reference	Number	Reference
[1]	Magenheim et al., 1994	[21]	This study
[2]	Volpe and Spivack, 1994	[22]	Frape et al., 2004
[3]	Eggenkamp, 1994	[23]	Sie and Frape, 2002
[4]	Godon et al., 2004	[24]	Frape et al., 1996
[5]	Kaufmann et al., 1984	[25]	Hesse et al., 2006
[6]	Kaufmann and Arnorsson, 1986	[26]	Ransom et al., 1995
[7]	Kaufmann, 1989	[27]	Eastoe et al., 1989
[8]	Bonifacie et al., 2005	[28]	Kaufmann et al., 1987
[9]	Liu et al., 1997	[29]	Eggenkamp et al., 1995
[10]	Eggenkamp and Schilling, 1995	[30]	Eastoe et al., 2007
[11]	Lyons et al., 1999	[31]	Eastoe and Peryt 1999
[12]	Drimmie and Frape, 1996	[32]	Eggenkamp and Koster van Groos, 1997
[13]	Desaulniers et al., 1986	[33]	Musashi et al., 1998
[14]	Hendry et al., 2000	[34]	Magenheim et al., 1995
[15]	Eastoe et al., 2001	[35]	Frape (Unpblished)
[16]	Kaufmann et al., 1988	[36]	Markl et al., 1997
[17]	Kaufmann et al., 1992	[37]	Stewart et al., 1996
[18]	Eastoe et al., 1999	[38]	Willimore et al., 2002
[19]	Eggenkamp and Coleman, 1998	[39]	Bonifacie et al., 2006
[20]	Eastoe and Guilbert, 1992		

1.5.2 Bromine

A study that was conducted by Cameron and Lippet (1955) on elemental bromine products from various suppliers concluded that there are no significant isotopic differences between the materials analyzed. They reported their isotopic results as absolute values. The re-calculation of their results using the delta notation after considering one of their samples as a standard showed some variation (~ 2.84 ‰), however this variation was uncertain due to the poor precision (± 4 ‰ on average) of their methodology. Xiao et al. (1993) reported a ~1 ‰ variation between different bromide salts from different manufactures that were analyzed. Eggenkamp and Coleman (2000) were the first to propose the bromine isotopic composition of the ocean as standard and they called it Standard Mean Ocean Bromide (SMOB). They were also the first to report the bromine value in the standard delta notation (δ^{81}Br) as the per mil deviation from the seawater composition that was assigned the value of 0 ‰. In their study they analyzed 11 oil field formation waters and they reported a range of 1.19 ‰ (+ 0.08 ‰ and + 1.27 ‰) for these samples. During this Thesis (Chapters 3 – 6) various water samples from sedimentary and crystalline environments (Southern Ontario, Siberian Platform, Williston Basin, Canadian Shield, and the Fennoscandian Shield) were analyzed for bromine stable isotopes. The results revealed a total range of bromine stable isotopes between -1.43 ‰ and +3.35 ‰. The sedimentary formation waters encompassed a larger range of isotopic variation (-1.43 ‰ to +3.35 ‰) in comparison to the waters from the crystalline environments (+0.01 ‰ to +1.77 ‰). Figure 1.3 illustrates the δ^{81}Br ranges of different waters from sedimentary and crystalline environments.

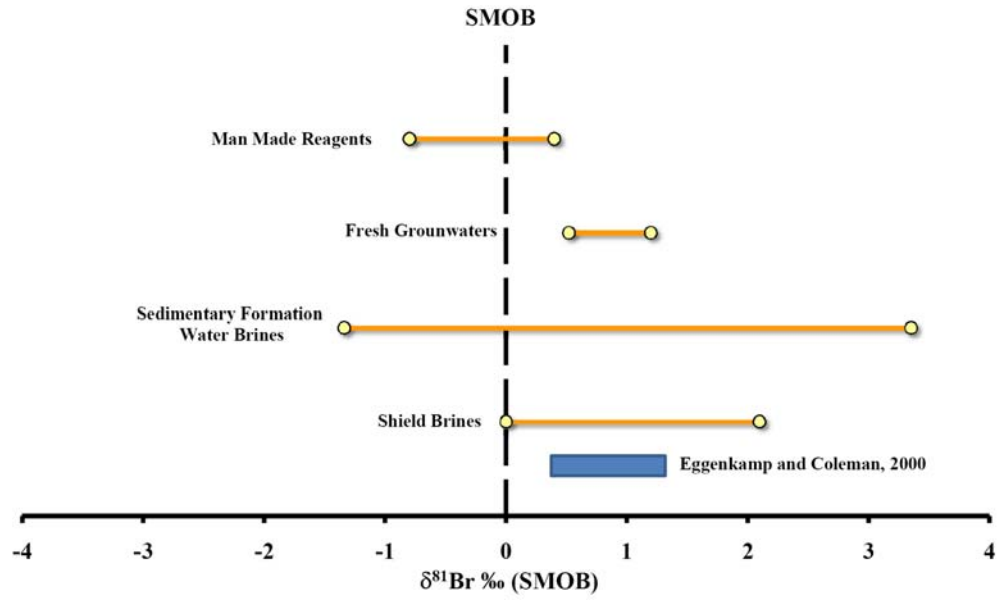

Figure 1.3 A summary of δ^{81}Br ranges of waters from sedimentary and crystalline environments. Sources are: [1] Eggenkamp and Coleman, 2000; [2] Frape et al., 2007; [3] this study; [4] Shouakar-Stash et al., 2005a.

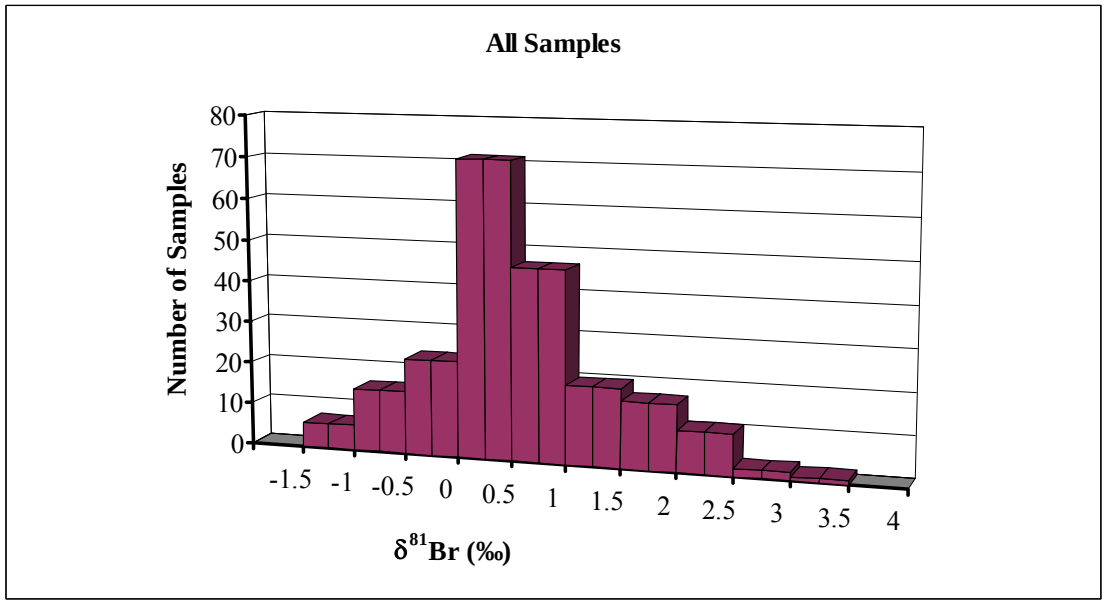

Figure 1.4 Histogram of all δ^{81}Br values of sedimentary and crystalline formation waters from this thesis (198 samples) and Eggenkamp and Coleman (2000) (11 samples). Samples range between -1.43 ‰ and 3.35 ‰.

Figure 1.4 illustrates a histogram of all samples that were analyzed in this thesis (198 samples; 187 of which are sedimentary formation waters and 11 crystalline samples), besides 11 samples that were reported by Eggenkamp and Coleman (2000). The summary of all known $\delta^{81}Br$ samples shows that the vast majority of samples (95.69 %) fall between -1 ‰ and +2 ‰. The data also shows that 78.95 % of all samples are positive ($\delta^{81}Br \geq 0$ ‰) and 21.05 % are negative ($\delta^{81}Br < 0$ ‰).

1.6 Natural Processes and Isotopic Fractionation

The majority of natural processes are associated with isotopic fractionation. In order to use isotopes as tolls when investigating the origin or fate of formation waters, it is crucial to understand the isotopic behaviours associated with various natural processes.

The behaviour of chlorine stable isotopes associated with various processes were examined and determined mathematically and experimentally by various researches in the last two decades (Hanshaw and Coplen, 1973; Fritz and Marine, 1983; Campbell, 1985; Desaulniers et al., 1986; Phillips and Bentley, 1987; Kaufmann et al., 1988; Eggenkamp, 1994; Volpe and Spivack, 1994; Eggenkamp et al., 1995; Coleman et al., 2001; Eastoe et al., 2001; Coleman et al., 2003; Schauble et al., 2003; Zhang and Frape, 2003; Böhlke et al., 2005; Lavastre et al., 2005; Hesse et al., 2006; Eastoe et al., 2007). However, the behaviour of bromine stable isotopes has not been explored at this time. The new methodology developed to analyze bromine stable isotopes and the large bromine isotopic variation reported from different

sedimentary and crystalline environments in this thesis is designed to encourage researchers to pursue further investigations into the behaviour of bromine stable isotopes in natural processes. The behaviour of bromine stable isotopes is expected to follow that of the chlorine stable isotopes due to their chemical similarities. However, the extent of the isotopic fractionations of these two isotopes will not be the same as several differences exist including their mass and isotopic abundances. Figure 1.5 illustrates the known behaviour of chlorine stable isotopes coupled with the possible behaviour of bromine stable isotopes during various geochemical processes such as evaporation, dissolution, precipitation, diffusion, ion filtration, water-rock interaction, freezing, oxidation and reduction.

1.7 Implications

The use of chlorine and bromine stable isotopes can be a valuable tool to investigate the origins of formation waters or to explore the geochemical evolution processes that influence formation water chemistry in sedimentary basins and crystalline shield environments. This knowledge can be very crucial when assessing hydrogeological dynamics of sedimentary basins and accordingly, applications to various fields as diverse as petroleum exploration or nuclear waste storage. They can be also useful in the petroleum industry as exploration tools or trouble shooting tools in cross-formational leak issues. As well, they can be used in investigating mine leakage issues (fingerprinting). Moreover, they might aid in understanding and resolving some of the scientific controversies in the earth's history. Broad applications of

these isotopes will be a major focus of future investigations concerning the systematic of bromine isotopes.

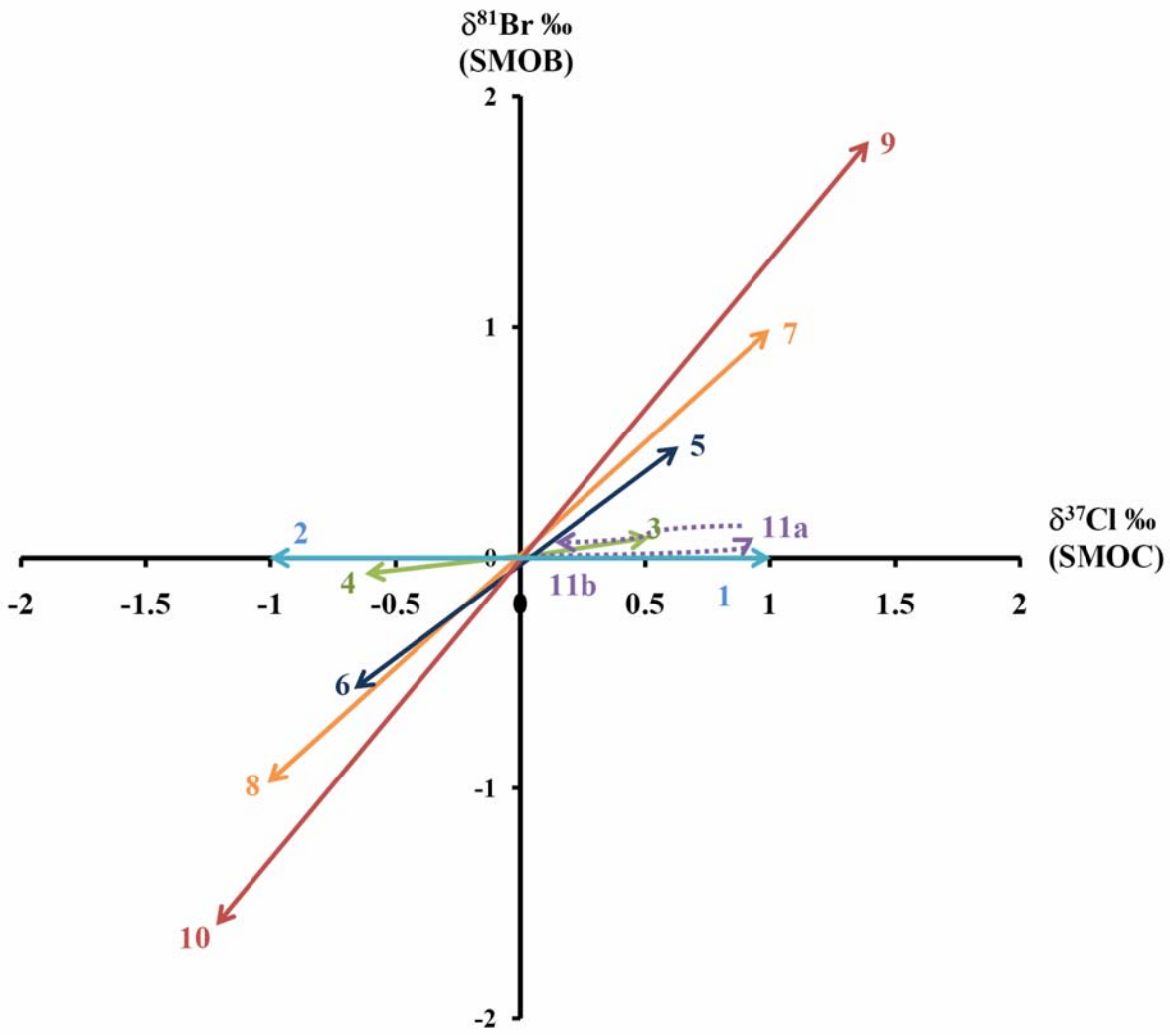

Figure 1.5 The predicted behaviours of $\delta^{81}Br$ values during natural processes coupled with the known behaviour of $\delta^{37}Cl$. 1-2) Halite dissolution (Water signature), 3) Halite precipitation (halite), 4) Halite precipitation (residual water), 5) Diffusion (residual water) / Ion filtration front, 6) Ion filtration (residual water) / Diffusion front, 7) Water Rock-interaction (isotopic signature of the rock), 8) Water Rock-interaction (isotopic signature of the water), 9) Oxidation to compounds with high oxidation state (isotopic signature of the residual), 9) Reduction to compound with low oxidation state (isotopic signature of the residual), 10) Oxidation (isotopic signature of the produced compound), 10) Reduction (isotopic signature of the produced compound), 11) Freezing (a- enrichment followed by b- depletion toward original signature).

CHAPTER 2

DETERMINATION OF INORGANIC CHLORINE STABLE ISOTOPES BY CONTINUOUS-FLOW ISOTOPE RATIO MASS SPECTROMETRY (CF-IRMS)

2.1 Introduction

Natural chlorine has two stable isotopes, ^{35}Cl and ^{37}Cl, with abundances of 75.76% and 24.24%, respectively (De Laeter et al., 2003 (IUPAC, 2003)). Chlorine in the natural environment occurs almost exclusively in the [-1] oxidation state as chloride ion [Cl^-], which means that chlorine participation in oxidation-reduction reactions is very limited. This fact is the major reason behind the small range of variation of stable chlorine isotopes in comparison to other environmental stable isotopes such as hydrogen, oxygen, carbon and sulfur (Eastoe et al., 1989 and Eggenkamp, 1994).

The largest reservoir of chloride at the Earth's surface is in the ocean, and chloride is also the major anion in almost all crustal and magmatic fluids and in mineral fluid inclusions, and the main complexing ligand for many metals (Hoering and Parker, 1961 and Eggenkamp, 1994). The natural variation of $\delta^{37}Cl$ values in different water types, including seawater, rivers, lakes, hot springs, shield brines, oil-field brines, basin formation waters and chlorine-bearing minerals, range from ~ -8 ‰ to ~ +8 ‰ (Hoering and Parker, 1961; Kaufmann et al.,

1984; Desaulniers et al., 1986; Kaufmann et al., 1987; Kaufmann et al., 1988; Kaufmann et al., 1992; Eggenkamp, 1994; Volpe and Spivack 1994; Eggenkamp et al., 1995; Magenheim et al., 1995; Ransom et al., 1995; Drimmie and Frape 1996; Frape et al., 1996; Liu et al., 1997; Eggenkamp and Coleman, 1998; Eastoe et al., 1999; Eastoe and Peryt 1999; Banks et al., 2000; Hesse et al., 2000; Eastoe et al., 2001; Sie and Frape 2002; Hesse et al., 2006). However, the vast majority of inorganic chlorine samples have $\delta^{37}Cl$ values that range between ~ -2 ‰ and ~ +2 ‰ (Eggenkamp, 1994). The use of stable chlorine isotopes in inorganic studies has been well established; some examples include distinguishing transport mechanisms in groundwaters (Desaulniers et al., 1986; Kaufmann et al., 1987; Kaufmann et al., 1988), identifying the origin of solutes in formation waters, in both shield and sedimentary environments (Kaufmann et al., 1988; Eastoe and Peryt 1999; Eastoe et al., 2001), hydrothermal processes (Eastoe et al., 1989), lake sediment studies (Drimmie and Frape 1996), processes in the evolution of salt lake brines (Liu et al., 1997), the formation of evaporate deposits (Eggenkamp et al., 1995; Eastoe et al., 1999), mineral fluid inclusion research (Banks et al., 2000), and in oceanic crustal studies (Magenheim et al., 1995; Ransom et al., 1995). Furthermore, it can be used to evaluate inorganic chloride contamination of water bodies as a result of road salt contamination of groundwater aquifers by determining sources of contamination (Rosen 1999). The use of chlorine stable isotope ratio measurements is not limited to inorganic studies. Rather, it is also used in determining organic contaminant sources and their behaviour in the subsurface. Chlorinated solvents are the most common organic contaminant in groundwater. They are found as multiple sources and their degradation products often lead to complex groundwater plumes and sources are

difficult to trace and assign ownership. In recent years, various research studies have used stable carbon isotopes in assessing groundwater contamination by organic compounds (Beneteau et al., 1999; Hunkeler et al., 1999; Bloom et al., 2000; Hunkeler and Aravena, 2000; Sherwood Lollar et al., 2001). Researchers in the field of organic contamination of groundwater have examined the possibility of using chlorine stable isotopes to better understand the fate of organic contaminants in the subsurface (van Warmerdam et al., 1995; Holt et al., 1997; Jendrzejewski et al., 1997; Sturchio et al., 1998; Heraty et al., 1999; Huang et al., 1999; Poulson and Drever 1999; Drenzek et al., 2002; Shouakar-Stash et al., 2003; Holmstrand et al., 2004). The range of variations of $\delta^{37}Cl$ in organic compounds is between -5.1 ‰ and +6.0 ‰ (van Warmerdam et al., 1995; Holt et al., 1997; Jendrzejewski et al., 1997; Sturchio et al., 1998; Heraty et al., 1999; Huang et al., 1999; Poulson and Drever 1999; Drenzek et al., 2002; Shouakar-Stash et al., 2003; Holmstrand et al., 2004).

Currently, chlorine stable isotopes are determined by three different analytical techniques, two of which use thermal ionization mass spectrometry (TIMS). The first technique (NTIMS) is based on measuring [Cl^-] negative ions (Shields et al., 1962; Vengosh et al., 1989). This has reasonably high sensitivity; however, the technique is difficult and the precision is poor (> ±0.4 ‰). The second technique (P-TIMS) is based on measuring positive ions [Cs_2Cl^+] (Xiao and Zhang, 1992; Magenheim et al., 1994; Xiao et al., 1995; Numata et al., 2001; Xiao et al., 2002). This technique is best for analyzing very small samples (1–50 μg Cl) and has good precision (±0.2 ‰) for such small samples. The third technique is based on analyzing methyl chloride gas using dual inlet isotope ratio mass spectrometry (DI-IRMS) (Long et al.,

1993). This last technique is reported to have the best precision (±0.09 ‰) available in analyzing chlorine stable isotopes; however, the technique is limited by the sample size requirement (300–1000 μg of Cl^-) and also by the lengthy preparation process which limits the number of samples that can be analyzed in a prescribed period of time. Therefore, there is an interest in improving the methodology by lowering the required sample size without compromising the precision as well as shortening the analysis time in order to improve sample throughput.

In the last decade, continuous flow isotope ratio mass spectrometry (CF-IRMS) has allowed more rapid analysis, reduced the required sample sizes and improved the precision on a variety of isotope analysis such as ^{13}C, ^{15}N, ^{18}O, ^{2}H and ^{34}S (Begley et al., 1996; Brand 1996; Morrison et al., 2001). The objective of this paper is to present a new technique based on CF-IRMS to determine $\delta^{37}Cl$ composition in inorganic samples. This technique will enhance the use of chlorine stable isotopes and will allow the use of this analytical technique in studies where chlorine concentration is low and analytical precision is important.

2.2 Experimental

2.2.1 Materials

The following chemicals are used in the preparation process of silver chloride (AgCl): nitric acid (Omni trace, cat # NX0407-2); sodium phosphate dibasic anhydrous (EM Science, cat # SX0720-1); citric acid monohydrate (EMScience, cat # CX1725-1); potassium nitrate 99.0%

(Alfa Aesar, cat # 13443); silver nitrate 99.9+ % min. (Alfa Aesar, cat # 11414). Methyl iodide (CH_3I) 99.5% (Alfa Aesar, cat # 31876) is used in the preparation of methyl chloride (CH_3Cl). The following items are used in the preparation of CH_3Cl: 20 mL amber headspace vials, 23x75 mm (LabSphere, Inc., cat # 20-6000); crimp seals, magnetic, 20 mm (Chromatographic Specialties, cat # SB405038); Tegrabond discs (septa), 125/10 MIL silicone/Teflon, 20 mm (Chromatographic Specialties, cat # C8812120M); helium gas (ultra-high purity 5.0); inflatable glove chamber (I2R1 Glove Bag™, model R-17.17); 20 mm crimper (Kimble, cat# 69901-20).

2.2.2 Instruments

A continuous flow isotope ratio mass spectrometer (Iso-Prime, Micromass, currently GV Instruments) was used in this study. The mass spectrometer is also capable of running in the dual inlet mode. This instrument has nine collectors, consisting of standard triple collectors and six dedicated collectors, two for masses 50/52 (CH_3Cl), two for masses 62/64 (vinyl chloride) and two for masses 94/96 (CH_3Br) (Figure 2.1). Methyl chloride gas is toxic and not safe to run in a continuous-flow mode from a reference tank, therefore, one of the bellows on the dual inlet part of the isotope ratio mass spectrometer is used as a reservoir for the CH_3Cl reference gas.

An Agilent 6890 gas chromatograph equipped with a CTC Analytics CombiPAL autosampler is attached to the isotope ratio mass spectrometer (Figure 2.2). A DB-5 MS GC column, 60 m x 0.320 mm, 1 μm film thickness (J&W Scientific Inc., cat # 1235563), is used

in the gas chromatograph for gas separations. A direct injection sleeve, 1.5 mm i.d. (Supelco, cat# 2-0517,05), is used as an inlet liner. The autosampler can hold 32 vials (20 mL) and samples are injected into the gas chromatograph via a 1.0 mL gastight syringe, 23 gauge, pt#5 (Lab-Sphere, Inc., cat# L120.00041).

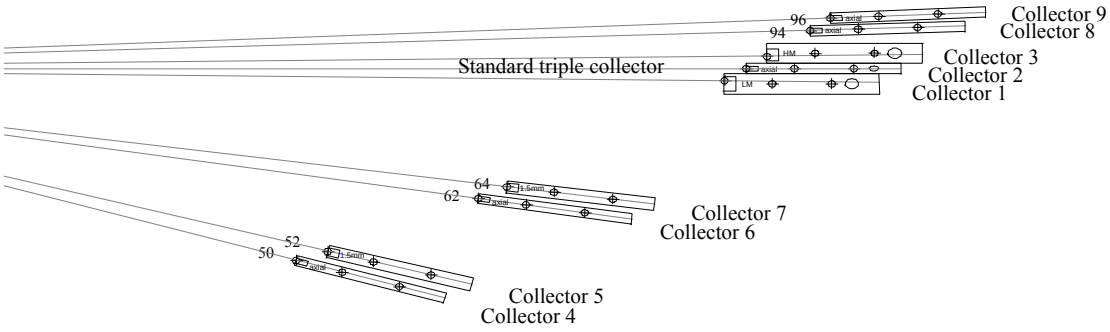

Figure 2.1 Schematic of the multi-collector array on the CF-IRMS (IsoPrime GV Instruments). Collectors 1, 2 and 3 are the standard triple collector and collectors 4-9 are dedicated collectors for specific masses.

A four-way Valco valve with two positions is installed between the gas chromatograph and the isotope ratio mass spectrometer. The end part of the GC column is connected to one of the two in-ports of the valve, while the other in-port is connected with ultra-pure helium gas (Figure 2.3).

Figure 2.2 The CF-IRMS system attached to the gas chromatograph which is equipped with an autosampler.

The two out-ports are connected to the isotope ratio mass spectrometer and to a flame ionization detector (FID) mounted on the gas chromatograph (Figure 2.3). This setup is designed to allow a constant flow of helium into the isotope ratio mass spectrometer. In position A, flow from the gas chromatograph is directed to the FID, while helium gas is flowing into the isotope ratio mass spectrometer, and, in position B, the out flow from the gas chromatograph is directed to the isotope ratio mass spectrometer and the helium flow is directed to the FID. This setup is important to direct only desired compounds to flow into the isotope ratio mass spectrometer (CH_3Cl in this case) and direct all other compounds to the

FID to be burned. A 100 µm deactivated capillary column is used to connect the valve port with the isotope ratio mass spectrometer. An open split is installed on this line to lower the pressure in the capillary before it flows into the isotope ratio mass spectrometer to 2 - 3 x 10^6 mbar. The open split is vented into the fumehood via a Teflon tube, because CH_3Cl gas is a toxic gas and should not be vented to the laboratory atmosphere. All vent ports on the gas chromatograph are vented into a fumehood. The helium flow that feeds the valve is balanced to the flow from the GC column. This is important to achieve the same background level when switching between the two positions A and B.

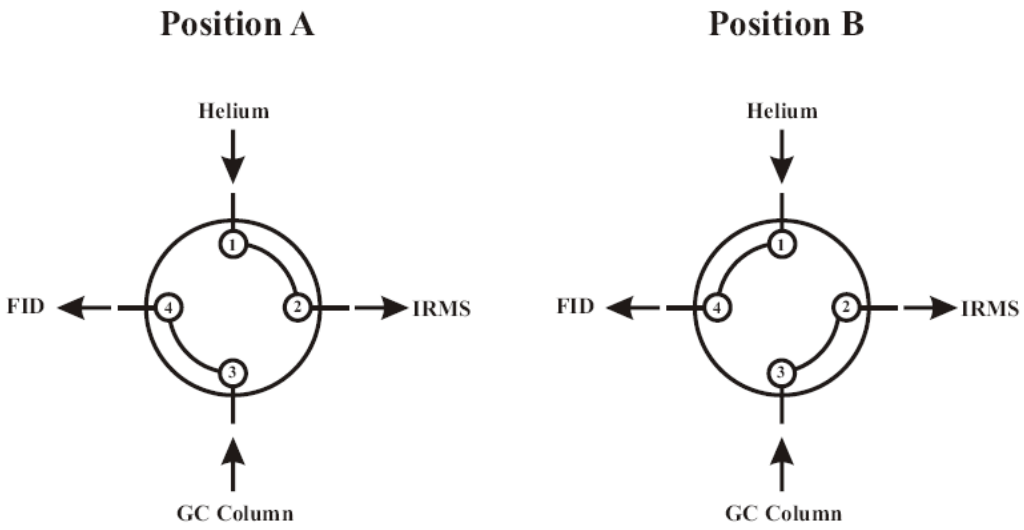

Figure 2.3 Schematic of the four way Valco valve installed between the GC and the IRMS. The figure illustrates the two positions, A and B.

2.2.3 Silver Chloride Preparation

The first step in sample preparation for measurement of chlorine stable isotope ratios is precipitating inorganic chlorides in the form of silver chloride (AgCl). The method used in this technique follows that described in earlier studies (Eggenkamp, 1994; Holt et al., 1997). Briefly, the method aims at precipitating AgCl from solution at fixed [Cl^-] content, fixed ionic strength and fixed pH. The solution containing [Cl^-] is first diluted by ultra-pure water or evaporated gently to bring the solution to the desired concentration. Secondly, it is acidified to pH ~2 with ultra-pure nitric acid (HNO_3) and heated at 80°C for a few minutes to drive off CO_2 (Long et al., 1993). Then, 0.4 M potassium nitrate (KNO_3) solution is added to reach a high ionic strength which helps to form small crystals of AgCl. Anhydrous sodium phosphate dibasic (Na_2HPO_4) and citric acid monohydrate ($HOC(CH_2CO_2H)_2CO_2H.H_2O$) (0.0004 and 0.0098 mol, respectively) are added to buffer pH at ~2. This is important to remove small amounts of sulfide, phosphate and carbonate from the precipitate by keeping them in solution. Then 1 mL silver nitrate ($AgNO_3$) solution (0.2 M) is added to precipitate AgCl. The beakers are stored in a dark place overnight for the precipitation to come to completion. AgCl is stored in a dark place at all times, as it is sensitive to light in which it will photo-decompose. Once precipitation is completed, precipitates are transferred into amber vials, where they are left to settle. Then, they are rinsed a couple of times with 5% HNO_3. Samples are then placed into the oven overnight to dry. Dried samples are stored in a dark place until CH_3Cl preparation.

2.2.4 Methyl Chloride Preparation

The preparation procedure was first developed in 1954 to obtain the maximum yield of CH_3Cl (Langvard 1954). Later, it was improved to achieve an even higher yield (98%) (Hill and Fry, 1962). However, the procedure was producing isotopic fractionation and, therefore, additional improvements were introduced during subsequent studies to solve previous problems (Taylor and Grimsrud 1969; Kaufmann et al., 1984; Eggenkamp 1994). AgCl is converted into CH_3Cl by reacting it with methyl iodide (CH_3I). Samples are weighed (0.2 mg) into 20 mL crimp amber vials where the reaction takes place. Vials are stored in a dark place if not to be prepared immediately. Once samples are ready to be prepared, they are placed in an inflatable glove bag connected to an ultra-pure helium tank (Figure 2.4). The glove bag should be placed in a fumehood during this procedure as CH_3I is toxic and prolonged exposure can damage lungs, kidneys, liver and the central nervous system. The helium tank is opened and helium is allowed to inflate the glove bag a few times by sealing the bag then opening it slightly to force the helium to flush out any air in the bag. Finally, the glove bag is sealed and the helium flow is reduced. Vials are tipped on an angle and flushed gently with a very low stream of helium to avoid losing sample. CH_3I (100 mL) is added to the samples and then vials are sealed. It is recommended to add CH_3I to 3 - 4 vials at a time and then seal these vials, and so on, otherwise the CH_3I can evaporate from the early vials by the time addition of CH_3I is finished. Vials are checked and retightened once more at the end, because vials need to be sealed (crimped) very well to avoid any leakage, as the desired final

product (CH_3Cl) is a gas. For the reaction to proceed to completion vials are placed in an oven for 48 hours at 80°C.

Figure 2.4 Methyl iodide is added to samples in an inflatable glove bag connected with an ultra pure helium tank.

2.3 Sample Analysis

Three protocols are involved in the sample analysis. The first is the CombiPAL (sample injection) protocol as follows: filling volume 800 μL; filling speed 300 μL/s; filling strokes 3; pull-up delay 1000 ms; pre-injection delay 300 ms; injection volume 750 μL; injection speed 800 ms; post-injection delay 5000 ms; post-clean with air 4 times; flush with helium for 6 minutes. The syringe is flushed with helium between samples to eliminate any cross-contamination from one sample to another, through a hole in the syringe-barrel especially designed for the flushing purpose.

The second protocol is the GC setup, where the flow is set at 1.2 mL/min, and kept constant during the run. The injection port temperature is set at 270°C. The oven temperature was programmed as follows: initial 35°C for 7 min; ramp at 35°C/min; final 250°C and hold for 2 minutes. The oven temperature programming is important for the separation of the CH_3Cl, CH_3I gases and cleaning the column between samples. Split ratio is set at 10. The third protocol is the mass spectrometry method. This method is set up in a way that allows the flow from the gas chromatograph to be directed to the FID for the first 6 minutes (position A); during that time a set of references pulses are allowed to occur by opening the dual inlet reservoir for 40 seconds for each pulse. After 6 minutes, the flow is directed into the isotope ratio mass spectrometer (position B) to carry the CH_3Cl into the source for the chlorine isotope composition analysis. At 8 minutes, the flow is directed again to the FID (position A) to prevent CH_3I from flowing into the mass spectrometer, during that time another set of reference pulses may be added.

2.4 Results and Discussion

The chlorine isotopic compositions are reported in permil (‰) deviation from isotopic standard reference material using the conventional δ notation, where:

$$\delta = \left(\frac{R_{sample}}{R_{s\tan dard}} - 1 \right) \times 1000$$

$^{37}Cl/^{35}Cl$ is the measured isotopic ratio. The reference material is Standard Mean Ocean Chloride (SMOC) (Long et al., 1993). Three different types of blanks were analyzed to determine any contribution of CH_3Cl from the background. The first blank is an empty vial that contains only air; the other blanks were placed in the glove bag along with other samples. One of the blanks is sealed with only helium gas in the vial, while the other one is sealed after the addition of CH_3I. There was no CH_3Cl signal in any blank (Figure 2.5).

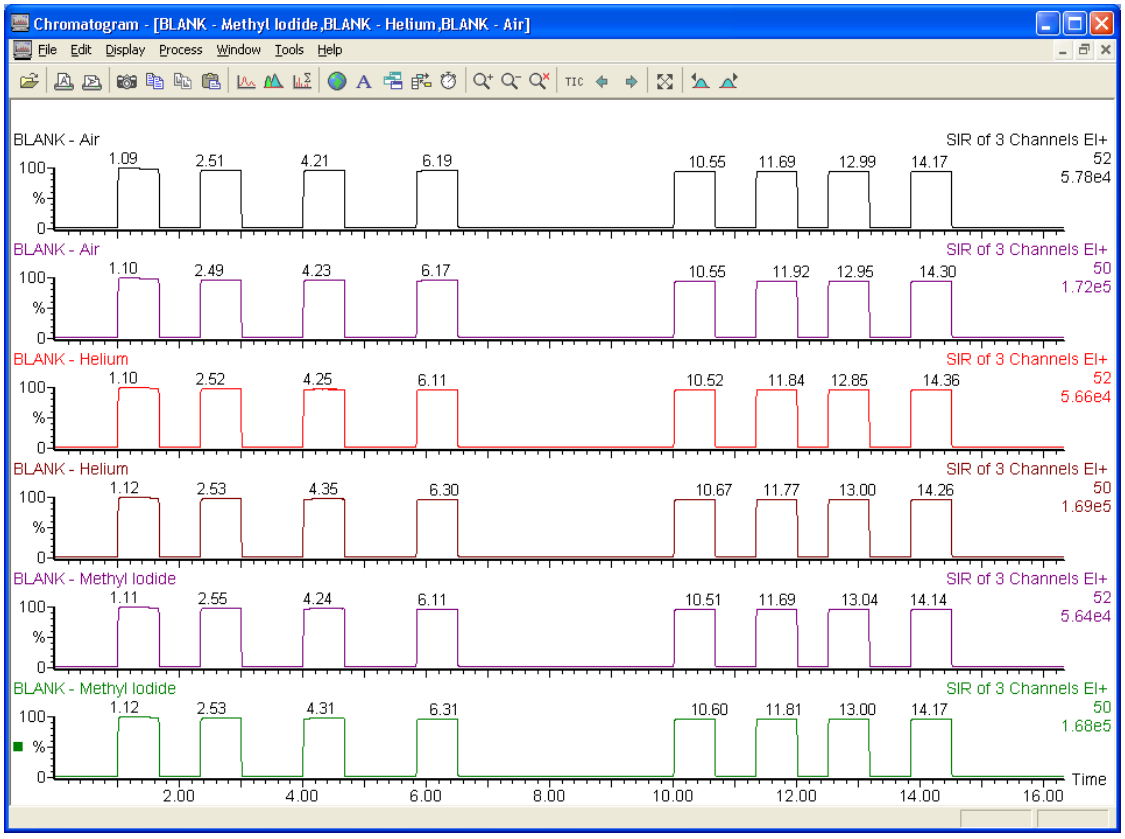

Figure 2.5 Chromatogram of masses 50/52 of different blanks (blank-air, blank-helium, blank-methyl iodide).

Different types of vials and septa were tested. The first vials were 2 mL amber vials (crimp and screw caps); however, there were no suitable septa that could hold gases for 48 hours at 80°C as well as being soft enough for needle penetration without damaging the needle. Septa that sealed the vials appropriately were too thick and often damaged the syringe. Finally, 20 mL amber headspace vials with crimp caps were adopted in this technique along with Tegrabond discs (septa). This combination allowed a very good seal. The septa consist of two layers: silicone and Teflon. Because the Teflon is chemically inert, it was placed facing inwards to be in contact with the chemicals. This minimized/eliminated any possible reactions or contamination between the sample/chemicals and the septa. The thick silicone layer provided a very tight seal to the vials and at the same time it is soft enough for the needle to penetrate without being damaged. The chromatogram in Figure 2.6 illustrates a run of CH_3Cl in the continuous flow mode. The chromatogram shows eight reference pulses and a sample peak. The retention time for the CH_3Cl peak is around 472 seconds. The total length of the run is 15 minutes.

An internal precision was determined by injecting pure CH_3Cl gas. A standard deviation better than ±0.04 ‰ (±STDV) was achieved (n = 10). An external precision was determined by analyzing a seawater standard (separate vials) and the achieved precision was better than ±0.07 ‰ (±STDV) for n = 12. No memory effects were observed during the analysis of three in-house standards that range from -1 ‰ to +1 ‰ (Table 2.1). However, a cleaning protocol of the syringe that consists of four strokes of air and 6 minutes of helium flush through the

syringe was applied to avoid any possible memory effect or cross-contamination between samples.

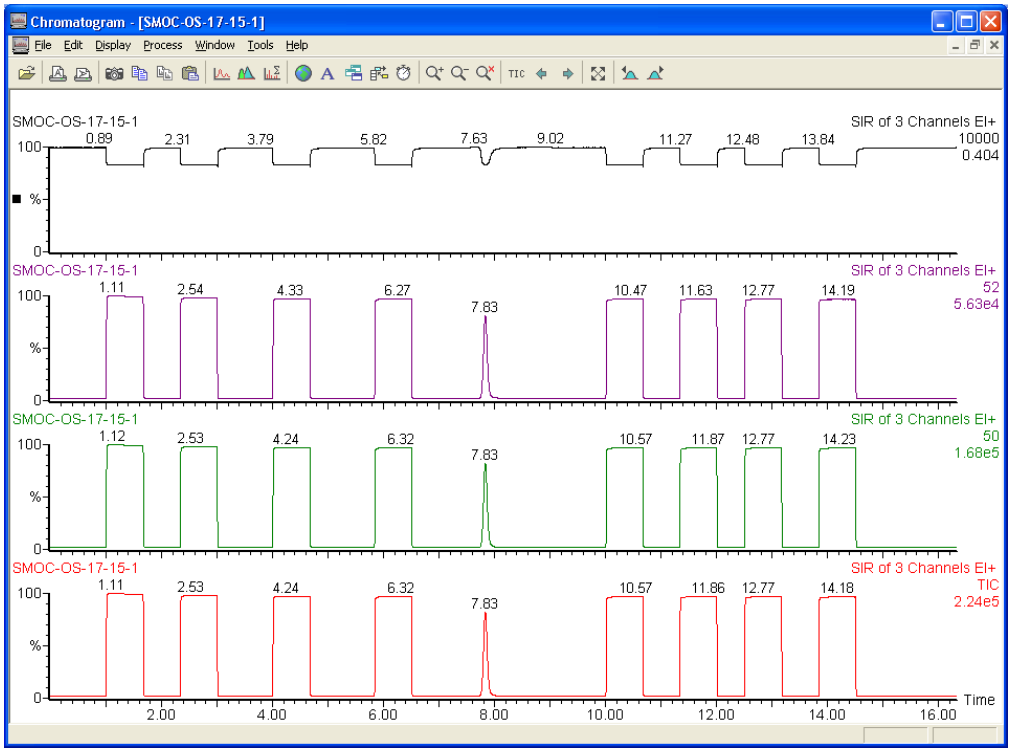

Figure 2.6 Chromatogram of methyl chloride analysis in continuous-flow mode. The chromatogram illustrates 8 reference pulses and a sample peak.

The results from a linearity test (Figure 2.7) showed a linear relationship (R^2 = 0.9831) between peak area and delta values. Therefore, in order to achieve accurate results, peak area correction is necessary when different peak areas are present in a specific run.

An accuracy test was done using a set of samples with a range of chlorine stable isotope composition of 2 ‰ (-1 ‰ to +1 ‰). Figure 2.8 presents a comparison between the results achieved with the new CF-IRMS system and those achieved with the traditional off-line

technique using DI-IRMS. The high correlation coefficient (R^2 = 0.9927) of the linear regression in Figure 2.8 indicates that the technique and machine dependent fractionations are predictable over an approximately 2 ‰ range of $\delta^{37}Cl$ values (as the vast majority of inorganic chlorine samples have $\delta^{37}Cl$ values that range between -1.4 ‰and +1.5 ‰) (Eggenkamp 1994) and can be calibrated by using a simple linear relationship.

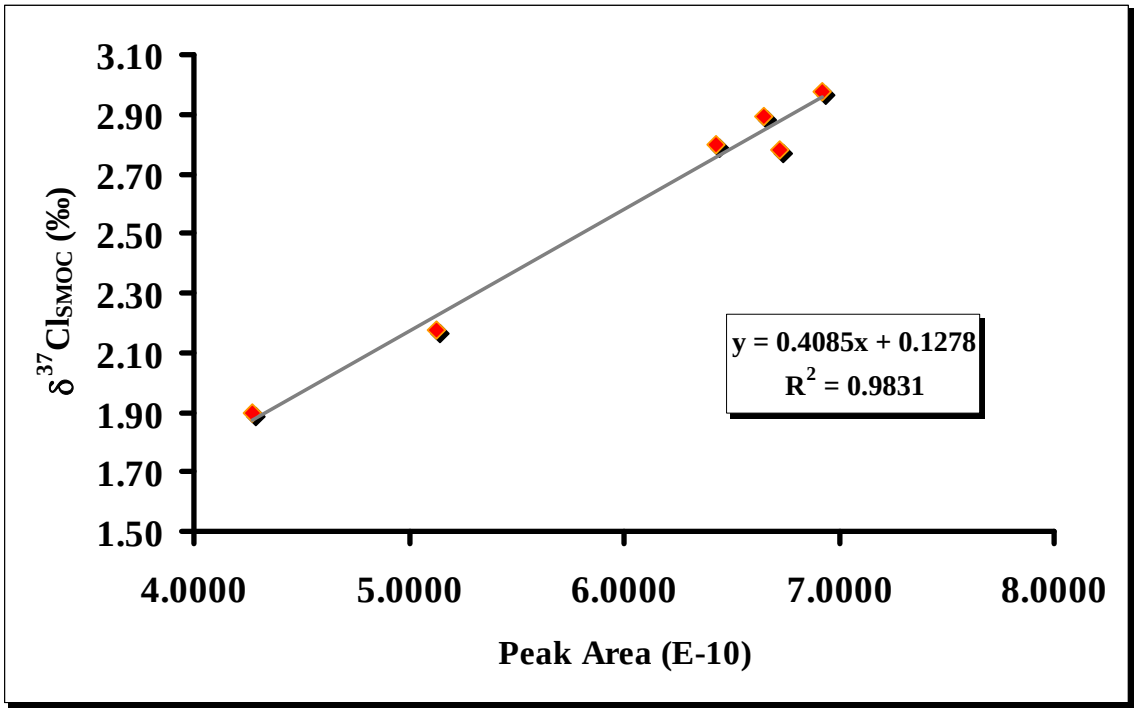

Figure 2.7 Relationship between $\delta^{37}Cl$ values and peak area.

Table 2.1 Test of memory effect of CF-IRMS analysis of chlorine stable isotope.

Order of measurements	U-1 $\delta^{37}Cl$ (‰)	SMOC $\delta^{37}Cl$ (‰)	U-7 $\delta^{37}Cl$ (‰)
1		0.10	
2		-0.02	
3		-0.07	
4			-0.81
5			-0.88
6			-0.92
7		-0.02	
8		-0.01	
9		-0.07	
10	1.14		
11	1.00		
12	0.94		
13		0.12	
14		0.09	
15		0.01	
16			-0.99
17			-0.92
18			-0.80
19		0.08	
20		-0.05	
21		-0.08	
22	0.90		
23	0.96		
24	0.99		
25		-0.07	
26		-0.09	
27		0.04	
Mean Value (‰)	+0.99	0.00	-0.89
STDEV	0.08	0.07	0.07

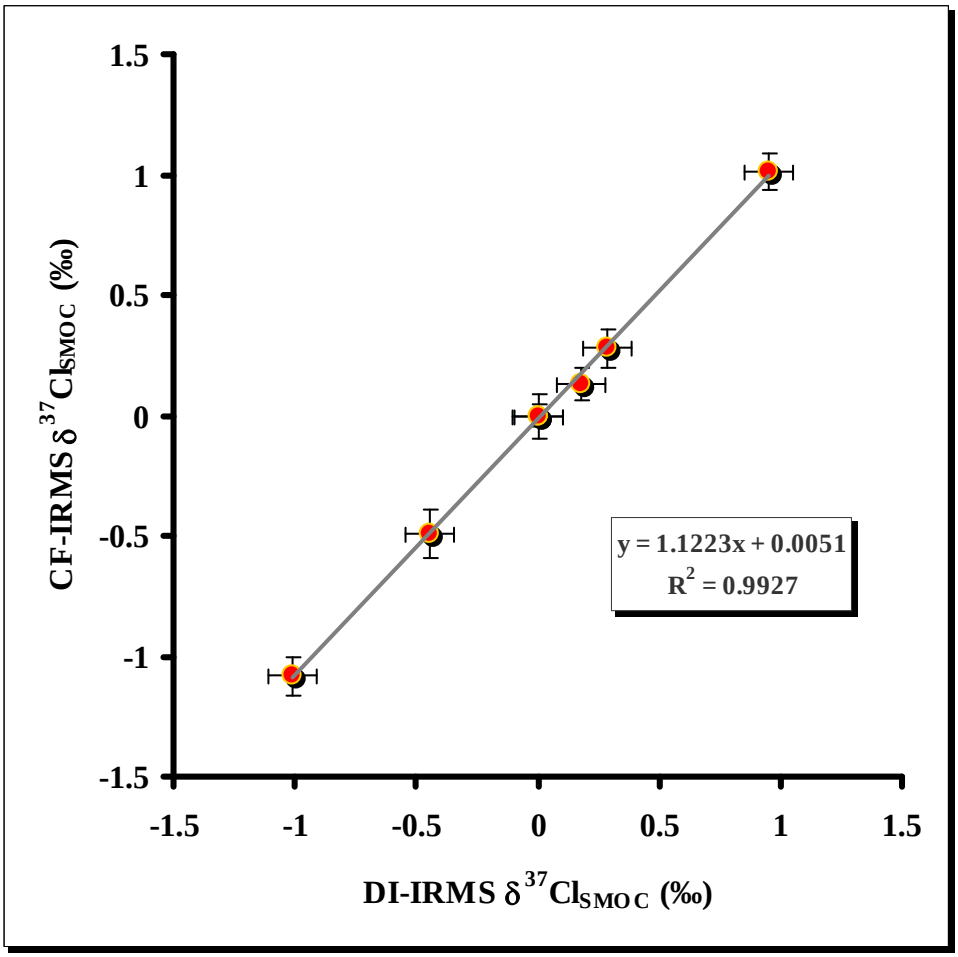

Figure 2.8 Comparison between $\delta^{37}Cl$ values obtained by DI-IRMS and CF-IRMS.

2.5 Conclusions

In this study a new technique was developed to analyze chlorine stable isotope ratios using CF-IRMS. The chlorine stable isotope analysis using continuous-flow technology showed excellent results. This new method combines both online separation and mass spectrometric

analysis in one automated step. This technique is three times faster than the classical off-line method and allows smaller sample sizes (0.2 mg versus 3 mg of AgCl). The technique is also more cost-effective. The precision is better than that achieved by any previous methods. This new technique would allow more samples to be analyzed rapidly and accurately. The CF-IRMS technique will enhance the application of chlorine stable isotope ratio measurements in more research areas and will allow the use of this analysis in studies where chlorine content is small and precision is important.

CHAPTER 3

DETERMINATION OF BROMINE STABLE ISOTOPES USING CONTINUOUS-FLOW ISOTOPE RATIO MASS SPECTROMETRY

3.1 Introduction

Most naturally occurring bromine (neglecting the very small contribution from unstable isotopes produced in nature by spontaneous fission and nuclear reactions induced by cosmic radiation) consists of a mixture of two stable isotopes: ^{79}Br and ^{81}Br. Relative abundances of these isotopes have been measured and they are 50.69 % and 49.31 %, respectively (De Laeter, 2003 (IUPAC, 2003)). Seawater is the largest natural source of bromine. It contains ~0.0065 % bromine, in comparison to 1.9 % of chlorine (representing a chlorine/bromine mass ratio of nearly 300:1) (Downs and Adams, 1975). There are relatively few minerals composed chiefly of bromide compounds; those that do exist usually contain silver bromide.

The natural variation of $\delta^{81}Br$ has been reported in only one study. The results are for oil field formation waters and range from +0.08 ‰ to +1.27 ‰ relative to standard mean ocean bromide (SMOB) (Eggenkamp and Coleman, 2000). This range is smaller than that reported for stable Cl isotopes but is significant enough to indicate that measurable isotopic fractionation processes exist in natural systems. In this paper (chapter), this range has been

increased to between 0.00 ‰ and +1.80 ‰ for natural samples and -0.64 ‰ to +1.80 ‰ in all samples, including man-made reagents. This range, which is obtained from two studies, shows a potential use of bromine stable isotope in determining sources of natural waters and evaluating geological and hydrogeological processes, especially if used in conjunction with other stable isotopes, such as chlorine. Furthermore, the use of bromine stable isotopes as a tool could be extended to inorganic and organic contamination studies. The use of silver bromide was introduced as early as 1840 in photography, and through this, bromine became an industrial chemical. Its use increased with the advent of the photographic film, motion pictures, and X-ray photography (Yaron, 1966). The vast growth of the bromine chemical industry began in 1924 with the commercial application of ethylene dibromide as a lead scavenger additive in gasoline. Since then, other bromine-containing products have followed, including methyl bromide for soil and space fumigation; brominated flame retardants for plastics, textiles, and polymers; high-density clear fluids for oil and gas well completion; and biocides for treating industrial and recreational water, intermediates for agricultural pesticides, and pharmaceuticals (Bassett, et al., 1988).

Attempts to measure bromine stable isotopes were made as early as 1920 (Aston, 1920). In 1936, more attempts were made using a Dempster-type mass spectrograph (Blewett, 1936). The measurement was done by analyzing positive and negative ions (Br^+, Br_2^+, Br^{2+} and Br^-), and a precision of ±25 ‰ was reported. Ten years later, another study used a mass spectrograph of the Nier type to analyze bromine stable isotopes (Williams and Yuster, 1946). Results were obtained from measuring positive ions (Br^+, Br_2^+, and Br^{2+}) formed from

electronic bombardment of bromine vapour. A precision of ±4 ‰ was achieved. In 1955, isotopic compositions of elemental bromine from various suppliers and diverse origins were determined by negative thermal ionization mass spectrometers (N-TIMS) (Cameron and Lippet, 1955); however, no significant differences between these samples were found, and the reported precision was approximately ±4 ‰. In 1964, another study reported the use of TIMS in bromine stable isotope measurement with an improved precision of ±1.8 ‰ (Catanzaro et al., 1964). A much more precise technique was introduced in 1993 by means of positive-TIMS (Xiao et al., 1993), based on measuring positive ions of Cs_2Br^+. This technique is useful for analyzing very small samples (4-32 μg of Br) and has good precision (±0.12 ‰) for such small samples. Dual inlet isotope ratio mass spectrometry (DI-IRMS) was used for the first time to determine bromine stable isotope composition in 1978 (Willey and Taylor, 1978). The technique is based on analyzing methyl bromide gas. More recently, in 2000, a descriptive work was published on bromine separation and isotopic determination of bromine by DI-IRMS (Eggenkamp and Coleman, 2000). The study reported the use of 2-8 mg of Br and a precision of ±0.18 ‰. Although the precision reported in the last technique is highly improved in comparison to previous techniques, there is an interest in improving the precision to better benefit from the small range of variation of the bromine stable isotope composition.

The previous technique is also limited by the sample size requirement and by the lengthy off-line preparation process. Therefore, there is great interest in lowering the required sample size and shortening and simplifying the analytical preparation time. In the past decade,

continuous flow isotope ratio mass spectrometry (CF-IRMS) allowed more rapid analysis, reduced the required sample sizes, and improved the precision on different stable isotope analyses, such as ^{13}C, ^{15}N, ^{18}O, ^{2}H, ^{34}S, and ^{37}Cl (Begley and Scrimgeour, 1996; Brand, 1996; Morrison et al., 2001; Shouakar-Stash et al., 2005b).

The objective of this paper is to present a new technique based on CF-IRMS to determine the bromine stable isotope composition in inorganic samples. This method will allow more work to be done to explore the usefulness of bromine stable isotopes in geochemical, hydrogeological, and ecological studies.

3.2 Experimental

3.2.1 Materials

The following chemicals are used in the bromine separation process: sulfuric acid (trace EMD, Catalogue no. SX1247-2); potassium hydroxide pellets (J. T. Baker, Catalogue no. 3140-01); potassium dichromate (EM Science, Catalogue no. PX1445-1); and zinc powder, median 6-9 μm (Alfa Aesar, Catalogue no. 10835). For the preparation process of silver bromide (AgBr), the following are used: nitric acid (Omni trace EMD, Catalogue no. NX0407-2), potassium nitrate 99.0 % (Alfa Aesar, Catalogue no. 13443), and silver nitrate 99.9+ % minimum (Alfa Aesar, Catalogue no. 11414). Methyl iodide 99.5 % (Alfa Aesar, Catalogue no. 31876) is used in the methyl bromide preparation.

The following items are used in the methyl bromide preparation: 20-mL amber headspace vials, 23 x 75 mm (LabSphere, Inc., Catalogue no. 20-6000); crimp seals, magnetic, 20 mm (Chromatographic Specialties, Catalogue no. SB405038); Tegrabond Disk (septa), 125/10 MIL silicone/Teflon, 20 mm (Chromatographic Specialties, Catalogue no. C8812120M); helium gas (ultrahigh purity 5.0); inflatable glove chamber (I2R Glove Bag, model R-17.17); and 20-mm crimper (Kimble, Catalogue no. 69901-20).

3.2.2 Instruments

A CF-IRMS (IsoPrime, Micromass, currently GV Instruments) was used in this study. The mass spectrometer is designed to work in two modes: continuous flow (CF) and dual inlet (DI). This IRMS has nine collectors, consisting of standard triple collectors and six dedicated collectors: two for *m*/*z* 50 and 52 (CH_3Cl), two for *m*/*z* 62 and 64 (vinyl chloride), and two for *m*/*z* 94 and 96 (CH_3Br) (Figure 3.1). Methyl bromide gas is toxic and not safe to run in a continuous-flow mode from a reference tank. Therefore, one of the bellows on the dual inlet part of the IRMS is used as a reservoir for the methyl bromide reference gas.

An Agilent 6890 gas chromatograph (GC) equipped with a CTC Analytics CombiPAL autosampler was attached to the IRMS. A DB-5 MS gas chromatographic column 60 m x 0.320 mm, 1-μm film thickness (J & W Scientific Inc., Catalogue no. 1235563) was used in the GC for gas separations. A direct injection sleeve, 1.5-mm i.d. (Supelco, Catalogue no. 2-0517,05) was used as an inlet liner. The autosampler can hold 32 vials (20 mL), and samples

were injected into the GC via a 1.0-mL gastight syringe, 23 gauge, part no. 5 (LabSphere, Inc., Catalogue no. L120.00041).

A four-way Valco valve with two positions was installed between the GC and the IRMS. The end part of the GC column was connected to one of the two in ports of the valve, while the other in port was connected to the ultra-pure helium gas. The two out ports were connected to the IRMS and to a FID detector mounted on the GC. This setup is designed to allow a constant flow of helium into the IRMS. In position A, flow from the GC is directed to the FID, while helium gas is flowing into the IRMS, and in position B, the out flow from the GC is directed to the IRMS, and the helium flow is directed to the FID. This setup is important to direct only desired compounds to flow into the IRMS (CH_3Br in this case) and to direct all other compounds to the FID to be burned. A 100-μm deactivated capillary column was used to connect the valve port with the IRMS. An open split was installed on this line to lower the pressure to 2-3 x 10^{-6} mbar in the capillary before helium flowed into the IRMS. The open split was vented into the fume hood via a Teflon tube, because CH_3Br gas is toxic and should not be vented to the laboratory atmosphere.

All vent ports on the GC were vented into a fumehood. The helium flow that feeds the valve was balanced to the flow from the GC column. This is important to ensure the same background level when switching between the two positions, A and B. A separation apparatus (Figure 3.2), specially designed at the University of Waterloo glass shop, consists of the following: three-neck, round-bottom 500-mL flask; two-neck, round-bottom 500-mL flask; simple condenser; 125-mL Erlenmeyer flask; fritted gas dispersion tube; power-

controlled mantle; hemispherical heating round-bottom (Glas-Col apparatus company, Catalogue no. 0406), which is controlled by a variable transformer; cooling bath; and glass connection tube. All glassware joints were designed with either a male ball (29/15) or female socket (29/15) to facilitate grease-free connections between all glassware to eliminate any possible contamination. Viton O-rings (Canadian Bearing, Catalogue no. V-210) were used to seal the glassware joints.

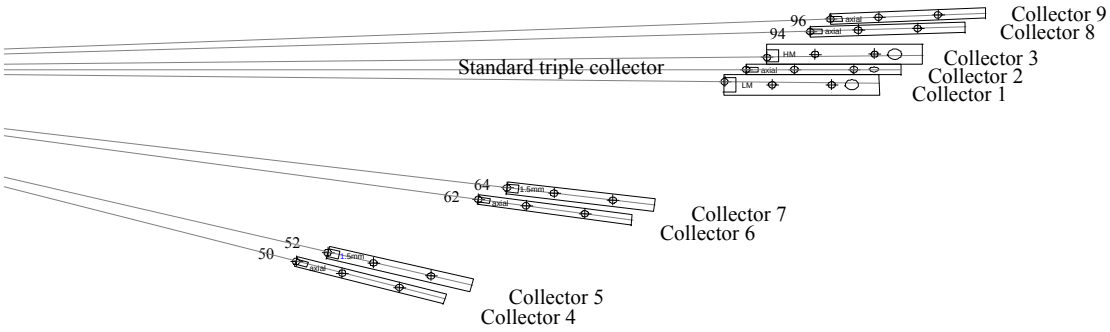

Figure 3.1 Schematic of the multi-collector array on the CF-IRMS (IsoPrime GV Instruments). Collectors 1, 2 and 3 are the standard triple collector and collectors 4-9 are dedicated collectors for specific masses (collectors 8 and 9 are for MeBr).

3.2.3 Bromine Separation

Bromine concentration in natural samples is very low, especially in comparison to chlorine concentration. For example, the Br/Cl ratio in seawater is 0.00342 and it ranges from 0.0002

to 0.04 in different natural water types. Therefore, bromine separation is an essential step. The methodology used for bromine separation follows closely the classical technique presented by earlier studies (Dechan, 1886; Friedheim and Meyer, 1892, Eggenkamp and Coleman, 2000). Briefly, the technique depends on the differences of oxidation-reduction behaviour of different halogens. Halide ions with higher atomic masses are easier to oxidize than ones with lower atomic masses. Therefore, Br is oxidized more easily than Cl. The separation is conducted in the special distillation apparatus shown in Figure 3.2. The three-neck, round-bottom 500-mL flask is filled with sample containing 1-10 mg of Br^-. Ultra-pure water is added to bring the total volume in the flask to 100 mL. Samples with low Br^- concentration are evaporated on a hot plate below boiling (~80°C) to concentrate the Br^- in solution. Then 10 g of $K_2Cr_2O_7$ is added, and 6-mm glass beads are added to facilitate gentle boiling. The graduated addition funnel is connected to the flask and filled with 20 mL of 1:1 H_2SO_4/H_2O (ultra-pure). A fritted gas dispersion tube is connected to the middle port of the flask to feed a steady flow of ultrapure helium to the flask to facilitate the movement of formed gases forward and to avoid back flushes. The two-neck, round-bottom 500-mL flask is filled with 200 mL of solution containing 2 g of KOH. A cooling bath filled with crushed ice is placed under the two-neck flask. The two flasks are connected with a condenser, and the cooling ports are connected to the cooling water system.

A 125-mL Erlenmeyer flask is filled with 100 mL of solution containing 1 g of KOH and connected to the two-neck flask. The power controlled mantle, hemispherical heating round-bottom is placed below the three-neck flask. Once all connections are secured and everything

is ready, the helium tank is opened, and a flow of 200 mL/min is maintained during the entire separation period. Then the stopcock on the addition funnel is opened to allow the H_2SO_4/H_2O mixture to flow into the flask. After the addition of the mixture, 100 mL of ultra-pure water is added via the addition funnel. The flask is then heated slowly to bring the solution to a boiling. It is at this stage that bromine gas (Br_2) (yellow-brown vapour) starts to form and flow, advancing to the second flask via the condenser. In the second flask, Br_2 gas reacts with the KOH solution to form KBr and KBrO. Any escaped Br_2 gas will be reduced in the Erlenmeyer flask with KOH solution. The distillation lasts for 20 minutes after boiling starts to ensure that all Br^- in solution has been oxidized and transferred. This has been tested by calculating the final yield of the Br^- from samples with known bromine concentration. Then the solutions from both the second flask and the Erlenmeyer are transferred to a beaker, 3 g of zinc powder is added, and the mixture is boiled for 10 minutes to reduce all BrO^- ions in the solution to Br^-. The solution is then filtered through a 0.22-μm Millipore Express Plus (PES). It is important to stress that bromine gas is corrosive to all body tissues and may cause serious burns; chronic exposure may cause pulmonary edema, pneumonia, diarrhea, and rashes. Because of these factors and the danger of dealing with strong acids and bases in this separation method, it is highly recommended that all work be done in a fume-hood.

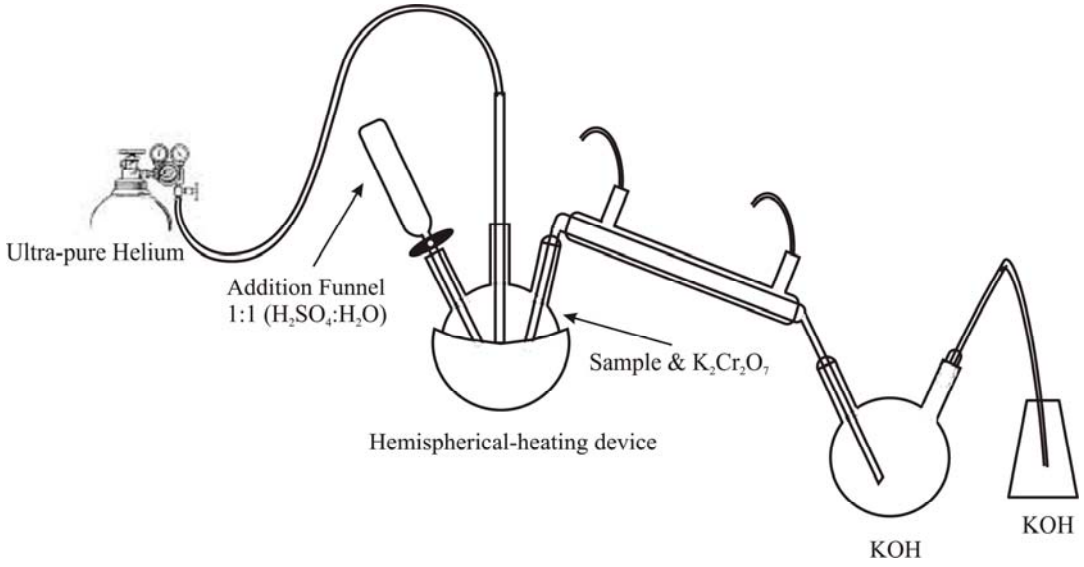

Figure 3.2 Bromine distillation apparatus.

3.2.4 Silver Bromide Preparation

After bromine is separated, it is precipitated as silver bromide (AgBr). The technique used is similar to that used in silver chloride precipitation and follows earlier studies (Taylor and Grimsrud, 1969; Eggenkamp, 1994). Briefly, the method aims at precipitating AgBr from solution at fixed Br- content, fixed ionic strength, and fixed pH. The solution containing Br- is first acidified to pH ~ 2 by adding ultra-pure concentrated nitric acid (HNO_3). Then 18 g of potassium nitrate (KNO_3) is added to the solution to increase the ionic strength, which helps to form small crystals of AgBr. Then 2 mL of silver nitrate ($AgNO_3$) solution (0.2 M) is added to precipitate AgBr. The beakers are stored in a dark place overnight for the precipitation to come to completion. Solutions are tested with a drop of $AgNO_3$ to ensure that

all AgBr is precipitated; if not, more $AgNO_3$ is added and allowed to settle. AgBr is stored in a dark place at all times, because it is sensitive to light and will photodecompose. Once precipitation is complete, it is transferred into an amber vial, and AgBr is allowed to settle. Then it is rinsed twice with 5 % HNO_3 rather than ultra-pure water because the rinsing solution should contain electrolyte to avoid the precipitate's becoming colloidal (nitric acid was chosen because it has no reaction with the precipitate and leaves no residue upon drying). Samples are then placed into an oven at 80°C overnight to dry. Dried samples are stored in a dark place until CH_3Br preparation.

3.2.5 Methyl Bromide Preparation

Silver bromide is reacted with methyl iodide (CH_3I) to form CH_3Br gas. Samples are weighed (0.5 mg) into 20-mL amber crimp vials where the reaction takes place. Vials are stored under vacuum in a desiccator and in a dark place if the samples are not going to be prepared immediately. Once samples are ready to be prepared, they are placed in an inflatable glove-bag connected to an ultrapure helium tank. The glove-bag should be placed in a fume-hood during this procedure because CH_3I is toxic. The helium tank is opened, and helium is allowed to inflate the glove bag a few times by sealing the bag then opening it slightly to force the helium to flush out any air in the bag. Finally, the glove-bag is sealed, and the helium flow is turned down. Vials are tipped on an angle and flushed gently with a very low stream of helium to avoid losing sample.

CH_3I (100 μL) is added to the samples, and then the vials are sealed. It is recommended that CH_3I be added to 4-6 vials at a time and then these vials be sealed, and so on. Otherwise, the CH_3I might evaporate from the early vials by the time addition of CH_3I is finished. Vials are checked and retightened once more at the end of the loading procedure. Vials need to be sealed (crimped) very well to avoid any leakage, because the desired final product (CH_3Br) is a gas. For the reaction to proceed to completion, vials are placed in an oven for 56 ± 5 hours at 80°C.

3.2.6 Sample Analysis

Sample analysis involves three steps. The first step is sample injection, which is done automatically via an autosampler (CombiPAL) following this protocol: filling volume, 750 μL; filling speed, 300 μL/s; filling strokes, 3; pull up delay, 1000 ms; preinjection delay, 300 ms; injection volume, 750 μL; injection speed, 800 ms; postinjection delay, 5000 ms; postclean with air 4 times; and flush with helium for 6 minutes. The syringe is flushed with helium (through a hole in the syringe barrel especially designed for the flushing purpose) between samples to eliminate any cross contamination from one sample to another.

The second step is gas separation via the GC. The GC setup is as follows: flow is set at 1.2 mL/min and kept constant during the run. The injection port temperature is set at 270 °C. The oven temperature is programmed as follows: initial 35°C for 7 min.; ramp at 35 °C/min; final 250 °C and hold for 2 min. The oven temperature programming is important for the

separation of the CH_3Br and CH_3I gases and cleaning the column between samples. Split ratio is set at 5.

The third step is the analysis of the CH_3Br by the mass spectrometer. A method is created for the analysis in a way that allows the flow from the GC to be directed to the FID for the first 360 seconds (position A). During that time, a set of reference pulses are allowed to occur by opening the dual inlet reservoir for 40 seconds for each pulse. After 6 minutes, the flow into the IRMS (position B) is allowed to carry the CH_3Br into the source for the bromine isotope composition analysis. At 600 seconds, the flow is directed again to the FID (position A) to prevent CH_3I from flowing into the IRMS. During that time, another set of reference pulses may be added. When the analyses are completed, the vials should be opened only in a fume-hood to avoid releasing the residual CH_3Br to the laboratory atmosphere. CH_3Br is an extremely toxic gas and easily absorbed through the lungs.

3.3 Results and Discussion

The bromine isotopic compositions are reported in permil (‰) deviation from isotopic standard reference material using the conventional δ notation, where:

$$\delta = \left(\frac{R_{sample}}{R_{standard}} - 1 \right) \times 1000$$

$^{81}Br/^{79}Br$ is the measured isotopic ratio. The reference material is standard mean ocean bromide (SMOB) (Eggenkamp and Coleman, 2000).

3.3.1 Reaction Vials

Amber headspace vials (20 mL) with crimp caps were used in this technique along with Tegrabond Disk (septa). This combination was chosen because it allowed a very good seal for 2-3 days at 80 °C. This was recommended in an earlier study on the determination of chlorine stable isotopes (Shouakar-Stash et al., 2005b). The septa consist of two layers, silicone and Teflon. Because the Teflon is chemically inert, it was placed facing inside to be in contact with the chemicals. This minimized/eliminated any possible reactions or contamination between the sample/chemicals and the septa. The thick silicone layer provided a very tight seal to the vials, and at the same time, it is soft enough for the sampling needle to penetrate without being damaged.

3.3.2 Blanks

Three different types of blanks were analyzed to determine the potential background contribution of CH_3Br other than from samples. The first blank was an empty vial containing only air; two other blanks were placed in the glove-bag along with samples. The second blank was sealed with only helium gas in the vial, and the third one was sealed after the addition of CH_3I. None of the blanks showed a CH_3Br peak; however, blanks were added to every batch in the daily routine of sample analyses.

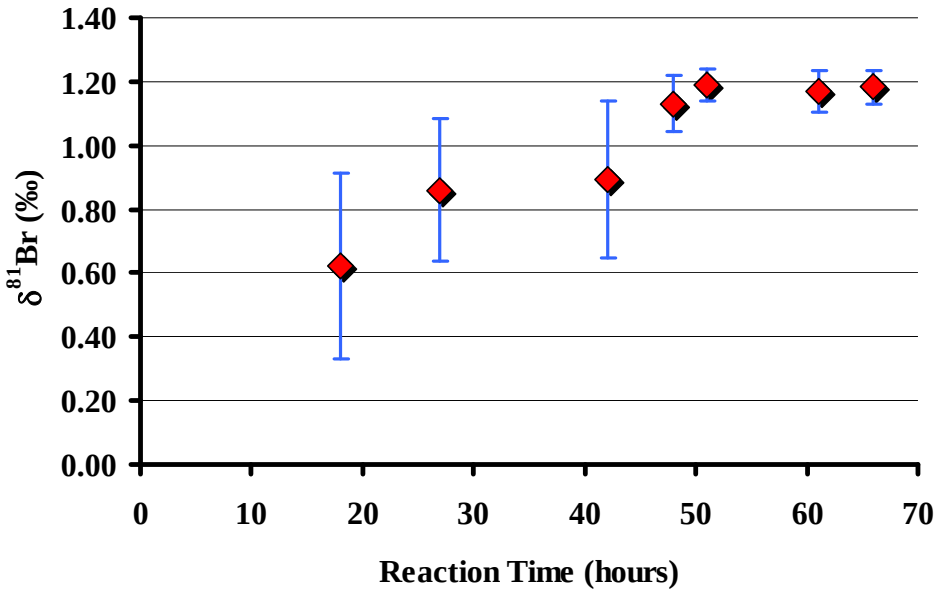

Figure 3.3 δ^{81}Br (‰) values versus Reaction Time (hours). The error bars show that precision is improved significantly at longer reaction time (±0.29 ‰ at 17 hours and ±0.05 ‰ at 66 hours).

3.3.3 Reaction Time

The plot of reaction time (hours) versus δ^{81}Br (‰) in Figure 3.3 shows that the reaction time needed is 56 ± 5 hours at 80°C. This was determined by analyzing one of the in-house standards for different reaction times. Five separate vials were analyzed at each time segment. We found that at short reaction times (18-27 hours), the resultant peak area is smaller than expected and the δ values are more depleted than they should be. At midrange time (42 hours), the peak area appeared as expected; however, the δ value is still depleted, which is the result of a preferential reaction with light isotope atoms. Expected peak area and δ values were achieved at reaction times between 51 and 66 hours. The error bars in Figure

3.3 show that precision is improved significantly at longer reaction times (±0.29 ‰ at 17 hours and ±0.05 ‰ at 66 hours).

3.3.4 Accuracy and Precision

Figure 3.4 illustrates a run of methyl bromide in the continuous flow mode. The chromatogram shows eight reference pulses and a sample peak. The retention time for the CH_3Br peak is around 540 seconds. The total length of the run is 16 minutes. Even though one reference pulse was enough during the analysis, the length of the analysis and the retention time of the CH_3Br peak permitted the introduction of eight reference pulses, and the average result of their isotopic signature values is used in the calculation of the isotopic value of the sample. An accuracy test was performed using a set of samples with a range of bromine stable isotope composition of 1.8 ‰ (0.00 ‰ to +1.80 ‰). Figure 3.5 illustrates a comparison between the results achieved with the new CF-IRMS and those achieved with the traditional off-line technique using the DI-IRMS (Eggenkamp and Coleman, 2000). The high correlation coefficient (R^2 = 0.9899) of the linear regression in Figure 3.5 indicates that the technique and machine-dependent fractionations are predictable over an ~1.8 ‰ range of $\delta^{81}Br$ values and can be calibrated by using a simple linear relationship. An internal precision was determined by injecting pure CH_3Br gas. A standard deviation better than ±0.03 ‰ (±STDV) was achieved (n = 10). An external precision was determined by analyzing two standards, NBS-977 ($\delta^{81}Br_{SMOB}$ = -0.64 ± 0.06 ‰ [±STDV]) for n = 12 and an in-house standard EIL-Br-1 ($\delta^{81}Br_{SMOB}$ = +0.24 ± 0.06 ‰ [±STDV]) for n = 12.

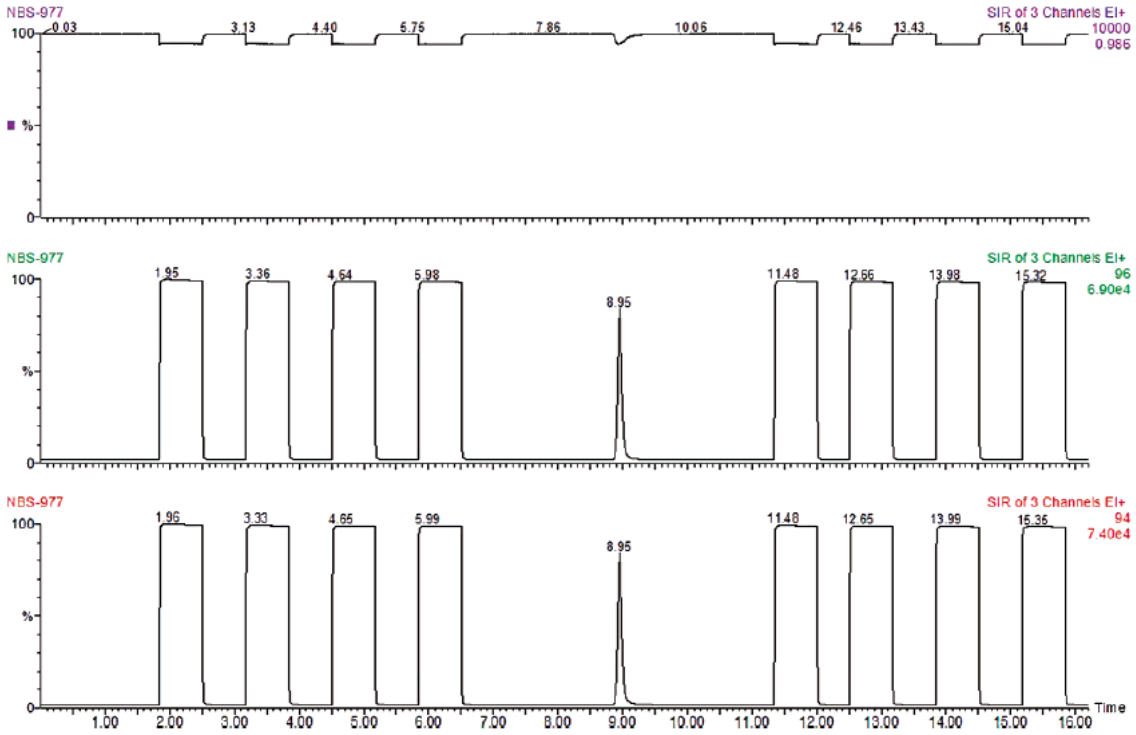

Figure 3.4 Chromatogram of methyl bromide analysis (NBS-977 Standard) in continuous-flow mode. The chromatogram illustrates 8 reference pulses and a methyl bromide peak at 8.95 minutes. Injection time is at time zero. The upper trace is the 94/96 ratio, middle trace is the m/z 96 ion current and the last trace is the m/z 94 ion current.

3.3.5 Linearity

A linearity test was conducted by analyzing an in-house standard several times using different sample sizes (200-1200 μg) covering 10-90 % of the possible peak height and area. The obtained mean value of the raw data is 0.00 ± 0.09 ‰ (n = 13). The results from the linearity test in Figure 3.6 showed a relationship (R^2 = 0.4797) between peak area and δ

values. Both δ values (raw and corrected) are plotted versus peak area and shown in Figure 6. When applying peak area correction, the precision improved somewhat, but the corrected δ^{81}Br values were not accurate (-0.11 ± 0.08 ‰). The plot shows that peak area correction is only needed at peak areas <2 x 10^{-10} As. Applying peak area correction on results with peak area >2 x 10^{-10} As does not improve the precision and negatively affects the accuracy of the results. Therefore, it is best to run the samples at peak area >2 x 10^{-10} As without applying any peak area correction.

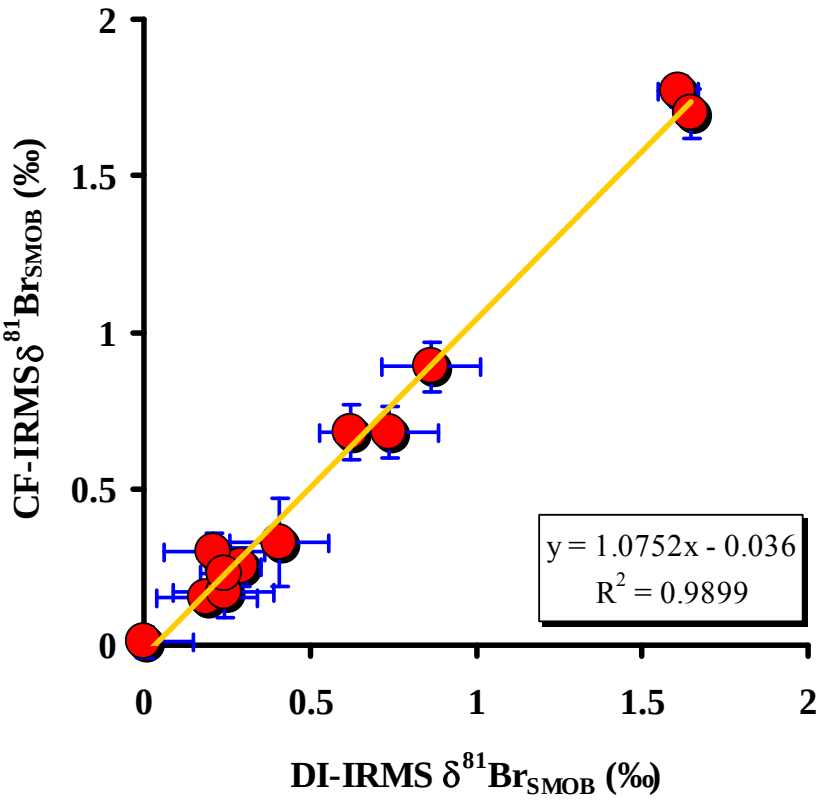

Figure 3.5 Comparison between δ^{81}Br (‰) values obtained by DI-IRMS and CF-IRMS. The comparison indicates a high correlation coefficient (R^2 = 0.9899) of the linear regression.

3.3.6 Memory Effects

A memory effect test was conducted by analyzing three different in-house standards: EIL-Br-9 (-0.64 ‰), EIL-Br-1 (+0.24 ‰), and SS-MI-Br (+1.62 ‰). The δ bromine range is over 2.3 ‰ and covers the entire range of reported bromine δ values in the literature. The results showed no memory effects during the analysis of these three different standards (Figure 3.7). However, a cleaning protocol of the syringe consisting of four strokes of air and 6 minutes of helium flushed through the syringe was applied to avoid any possible memory effect or cross-contamination between consecutive samples.

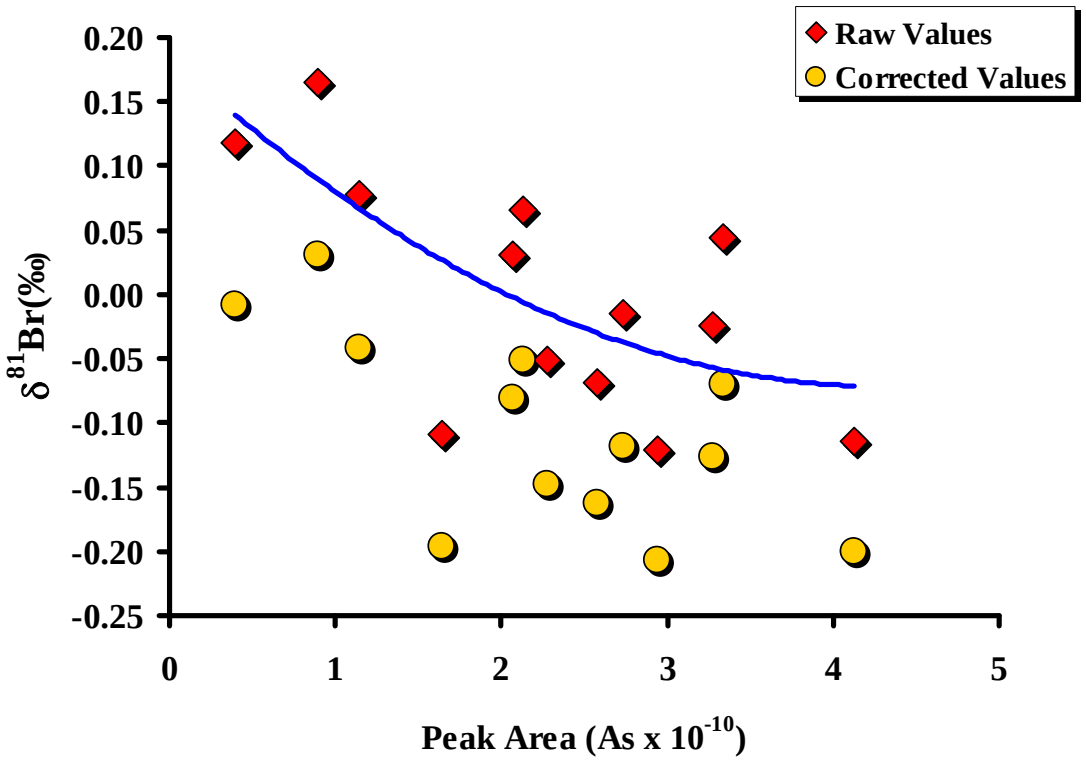

Figure 3.6 δ^{81}Br (‰) values as a function of peak area (Ampere seconds x 10^{-10}). Diamonds represent the raw values obtained from the CF-IRMS and Circles represent the peak area corrected values.

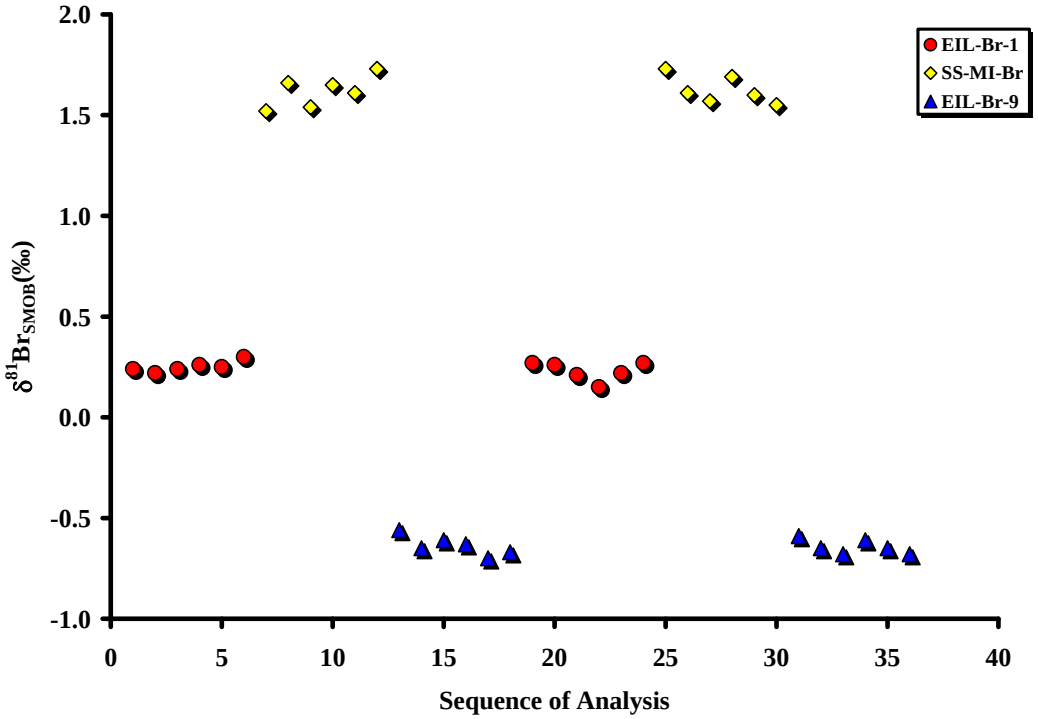

Figure 3.7 Test of memory effect of CF-IRMS analysis of bromine stable isotopes of three standards with a bromine isotopic composition that ranges over 2.3 ‰.

3.4 Potential Application and Data on Natural Samples

A series of natural saline formation waters and brines from sedimentary and crystalline rock environments was measured by the method to test the potential natural range of δ^{81}Br. In addition, this range of samples would test the ability of the methodology to handle very complex chemical matrixes found in these fluids. The isotopic composition of bromine from different samples ranged from 0.00 ‰ to +1.80 ‰. Figure 3.8a shows that the most enriched

$\delta^{81}Br$ occurs in more dilute saline fluids, often NaCl in composition, from the Fennoscandian Shield. Similar results appear to be found in more dilute sedimentary samples as well. Very concentrated Ca-Cl Canadian Shield brines show very little isotopic enrichment, with a slightly increasing isotopic signature with increasing concentration based on a very limited data set. On the basis of the preliminary data presented here, the two crystalline shield areas appear isotopically distinct from one another. Ages of fluids, rock types, and evolutionary history will have to be examined to further refine the reasons behind the differences.

In Figure 3.8b, when $\delta^{81}Br$ is plotted against $\delta^{37}Cl$, the different fluid/rock environments become very distinctive and seem to indicate that these two halogen isotopes used in conjunction should be potentially very useful in distinguishing fluid movement, mixing, processes of fractionation, and possible origin of the chemical components of these very concentrated fluids. A calculated mixing curve between two potential end members is demonstrated in Figure 8b. The calculated mixing curve fits the data obtained from the saline formation waters from the Fennoscandian Shield. Although this is not enough evidence to prove a mixing scenario and further investigation is necessary, it shows promising results and trends worth pursuing. Further work is necessary to improve our understanding of the different processes responsible for bromine stable isotope fractionation and variations in natural systems.

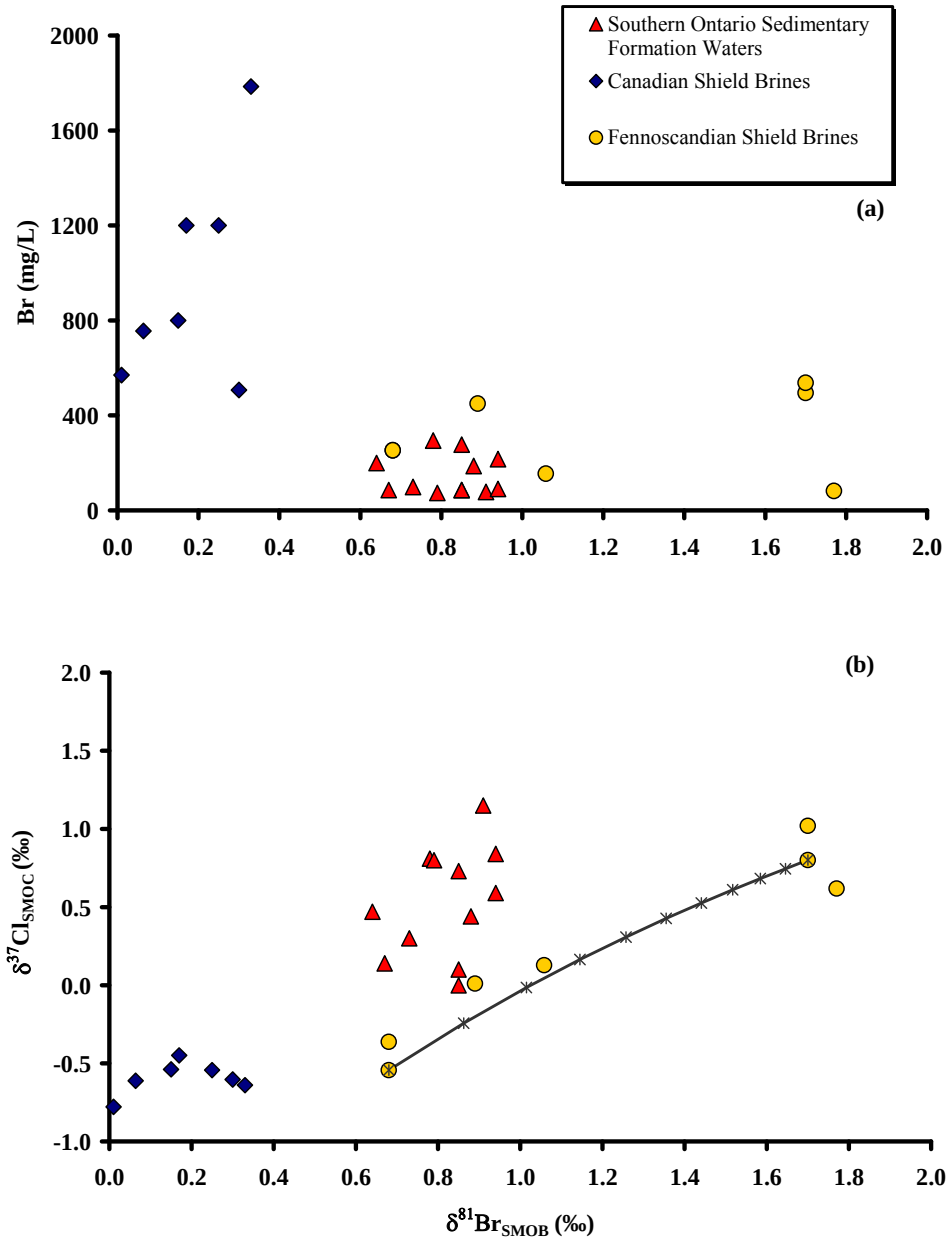

Figure 3.8 **(a) Br (mg/L) versus δ^{81}Br (‰) and (b) δ^{37}Cl (‰) versus δ^{81}Br (‰) values of natural saline formation waters and brines from sedimentary and crystalline rock environments. Triangles represent southern Ontario sedimentary samples, diamonds represent Canadian Shield brines, and circles represent Fennoscandian Shield brines. The Line through the Fennoscandian Samples is a calculated mixing line between two possible end members.**

3.5 Conclusions

In this study, a new methodology was developed for bromine stable isotope determination by CF-IRMS. The bromine stable isotope analysis using continuous flow technology showed excellent results, particularly with the high precision achieved (±0.06 ‰ [±STDV]), for which precision is very important when dealing with small variations in isotopic range. The small sample size (0.2 mg of AgBr) requirement is also an asset, especially for samples with very low concentrations of bromide. Furthermore, this technique is almost five times faster than previous off-line techniques, which will improve sample throughput. The technique is also very cost-effective.

The bromine stable isotope values obtained in this paper extended the range of isotopic variation of stable bromine to values between -0.64 ‰ and +1.80 ‰. Although the range seems to be small, it is large enough to be useful to distinguish differences in standards and samples, especially when combined with the high precision achieved by this new methodology. Isotopic characterization of bromine isotopes could be a powerful tool for determining sources of sedimentary formation waters, geological and hydrogeological processes when used in conjunction with other stable isotopes, such as chlorine. Hopefully, this new technique will encourage researchers to explore the use of stable bromine isotopes in both natural and contaminated systems.

CHAPTER 4

ORIGIN AND EVOLUTION OF WATERS FROM PALEOZOIC FORMATIONS, SOUTHERN ONTARIO, CANADA: ADDITIONAL EVIDENCE FROM δ^{37}CL AND δ^{81}BR ISOTOPIC SIGNATURES

4.1 Introduction

The stratigraphic units underlying southern Ontario are part of two sedimentary basins (the Michigan Basin and the Appalachian Basin). These Paleozoic sedimentary rocks range in age from Cambrian to Mississippian and contain highly saline formation waters (e.g. Dollar et al., 1991). These bedrock units are overlain by Quaternary sediments that mostly contain fresh waters. Several previous studies investigated the origin and movement of highly saline waters in the Paleozoic sedimentary rocks of southern Ontario and Michigan (e.g. McNutt et al., 1987; Long et al., 1988; Dollar et al. 1991; Kaufmann et al. 1993; Wilson and Long, 1993a; 1993b; McIntosh et al., 2002; Husain et al., 2004; McIntosh et al., 2004; McIntosh and Walter, 2005; 2006; Hobbs et al. 2008). McNutt et al., (1987) suggested a paleoseawater origin of these sedimentary formation brines that was modified by water-rock interaction, based on strontium, oxygen and hydrogen isotopic compositions. Long et al. (1988) suggested, but did not confirm that the source of the salinity of the formation waters were due to upward diffusion or advective flow of formation waters that were originally meteoric

waters. Wilson and Long (1993a and 1993b) analyzed brines from the Devonian and Silurian formations in the central part of the Michigan Basin, and concluded that the chemical and isotopic data obtained suggested the brines originated from evapo-concentrated seawater that was further modified by water-rock interaction, halite dissolution and dolomitization. They also concluded that the upper Devonian saline waters had been diluted by meteoric water infiltrating at the basin margins. Dollar et al. (1991) came to a similar conclusion after examining formation waters found in Cambrian to Mississippian units within the central Michigan Basin and Southwestern Ontario. Kaufmann et al. (1993) suggested that mixing could have occurred between Canadian Shield brines and the Michigan sedimentary formation waters based on chemical data in conjunction with chlorine and strontium isotope data.

The interaction of the bedrock formation waters in the marginal area of the basin (outcrop areas) with the overlying shallow groundwater in glacial deposits has been investigated by several researchers. Based on waters from Devonian-aged formations, Weaver et al. (1995) suggested that at least some areas in the Michigan Basin appear to have been hydrogeologically active in the past. Westjohn and Weaver (1997) used geophysical and geological logs to investigate shallow regional aquifers in the Michigan Basin (Mississippian and younger geologic units) and characterize their hydrogeological framework. They concluded that the largest freshwater reservoir is in the Pleistocene glaciofluvial deposits. The uppermost bedrock unit (Jurassic red bed) is a confining unit (aquitard), which probably impedes recharge of freshwater from glacial deposits to the underlying bedrock. The only

fresh water found in the underlying Mississippian and Pennsylvanian aquifers are in the outcrop areas near the edges of the basin, where there is indirect hydraulic connection with glacial deposits. Total dissolved solids (TDS) concentrations were found to increase away from the outcrop areas. Recent studies by McIntosh and Walter (2005, 2006) concluded, based on geochemical data, that hydraulic loading of ice sheets during the Late Pleistocene reversed regional flow patterns, and focused recharge into Paleozoic aquifers in the northern and southern margins of the Michigan Basin, significantly depressing the freshwater–saline water interface.

An understanding of the origin and the evolution of formation waters is important for several reasons, including exploration for hydrocarbon and mineral resources, and for long term waste management strategies and long term regional groundwater resource planning. The focus of this study is to assess the usefulness of $\delta^{37}Cl$ and $\delta^{81}Br$ isotopic measurements of formation waters from the Paleozoic sedimentary sequence in Ontario and Michigan, in conjunction with chemical and water stable isotopic compositions, to better understand the origin of the formation waters and the processes involved in their evolution and interaction.

4.2 Study Area and Geology

Southern Ontario is located between the foreland Appalachian Basin and the intracratonic Michigan Basin in the interior platform of the North American continent (Figure 4.1). The Algonquin and Findlay Arches are broad Precambrian highs (Figure 4.1), separated by the

Chatham Sag, that trend northeast-southwest. These positive structural features, were probably introduced during Late Precambrian time, and then intermittently re-activated during the Paleozoic, forming a broad platform between a more rapidly subsiding Michigan Basin to the west and the Appalachian Basin to the southeast (Sanford et al., 1985).

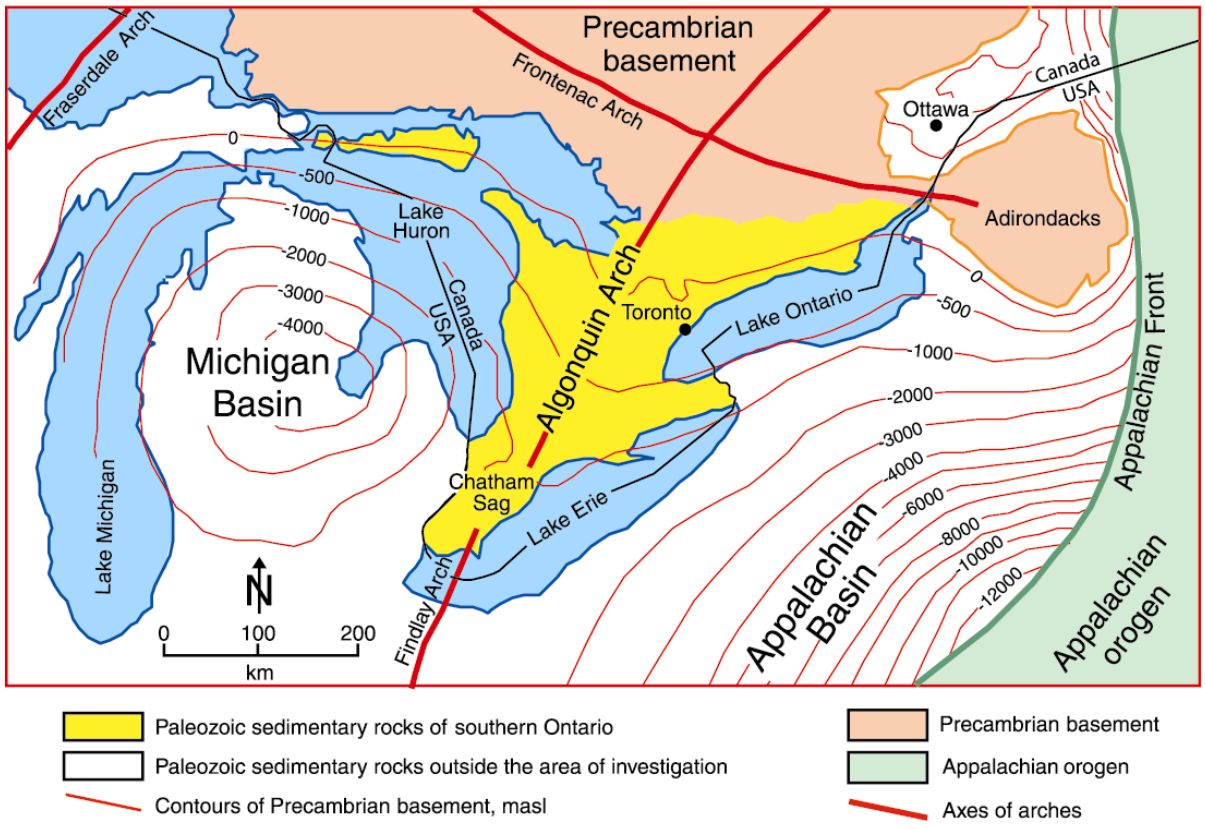

Figure 4.1 Large-scale tectonic elements in southern Ontario and definition of study area, adapted from Johnson et al. 1992 (from Mazurek 2004).

Southern Ontario is underlain by an essentially undisturbed sedimentary succession that rests unconformably on Precambrian basement rocks. Outcrops are largely obscured by Pleistocene glacial drift that reaches thickness of up to 250 m. Sedimentary rocks (Late Cambrian to Early Mississippian) dip to the northwest into the Michigan Basin and to the southeast into the Allegheny Trough of the Appalachian Basin (Figure 4.2). The current regional dip of the rocks to the northwest of the arches is 6 to 9 m/km into the Michigan Basin; to the southeast of the arches, the dip is 6 m/km into the Appalachian Basin (Winder and Sanford, 1972). Paleozoic strata in the Chatham Sag are for the most part horizontal. The sedimentary formations pinch-out against the Canadian Shield in the northeast, where the oldest bedrock outcrop is Cambrian in northeastern Ontario and Ordovician in the study area. Bedrock outcrops are successively younger toward the southwest along the Algonquin Arch.

4.3 Stratigraphy

The maximum thickness of the Paleozoic and Mesozoic sedimentary deposits within the province is 1525 m (Winder and Sanford, 1972). The hydrocarbon reservoir rocks, ranging in age from Late Cambrian to Early Mississippian, are represented in the stratigraphic sections of southwestern Ontario and Michigan (Figure 4.3). A brief description of the stratigraphic units associated with samples examined in this study, are presented in Table 4.1.

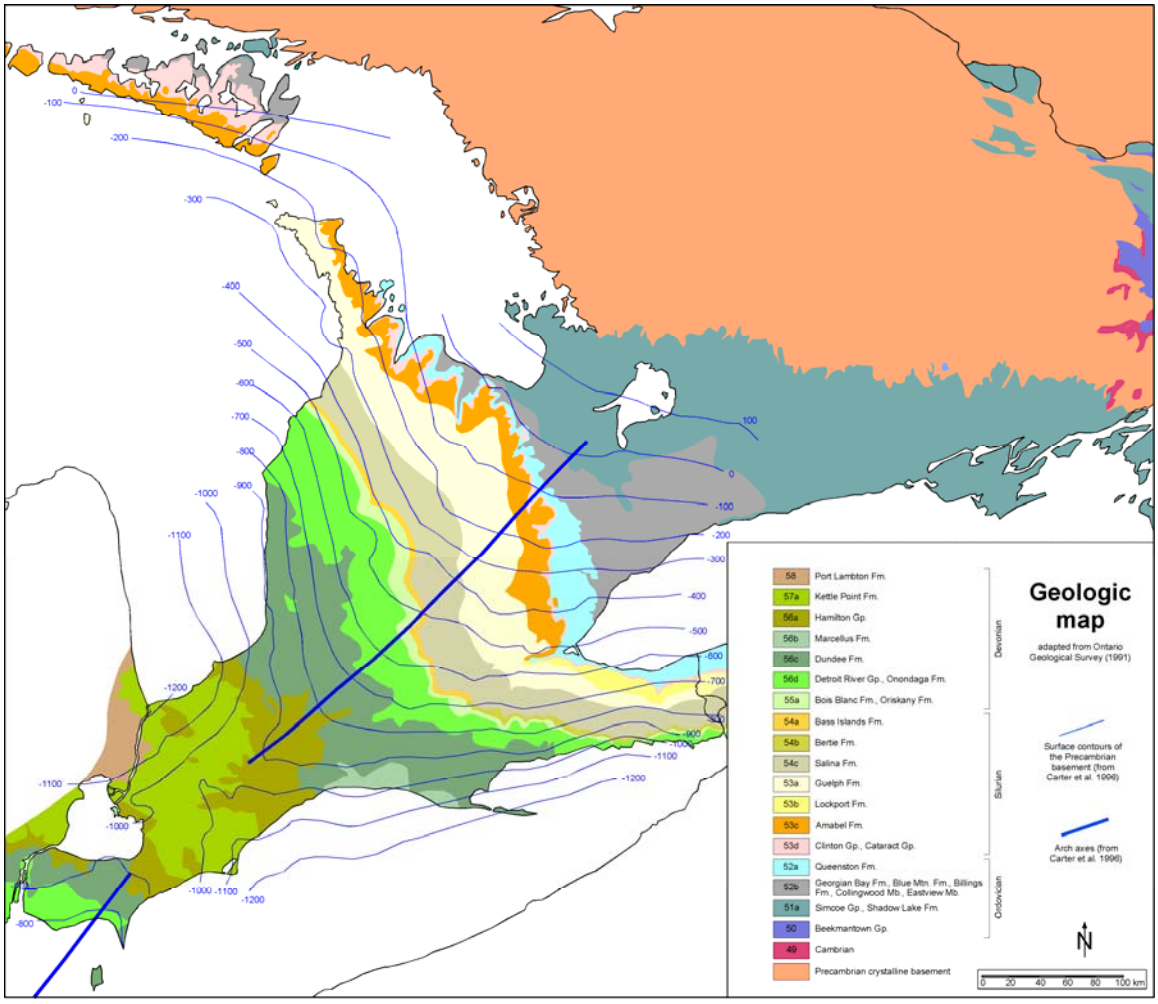

Figure 4.2 Geologic map of southern Ontario (redrawn from Ontario Geological Survey 1991, and surface contours of the Precambrian basement from Carter et al. 1996). Map from Mazurek, 2004.

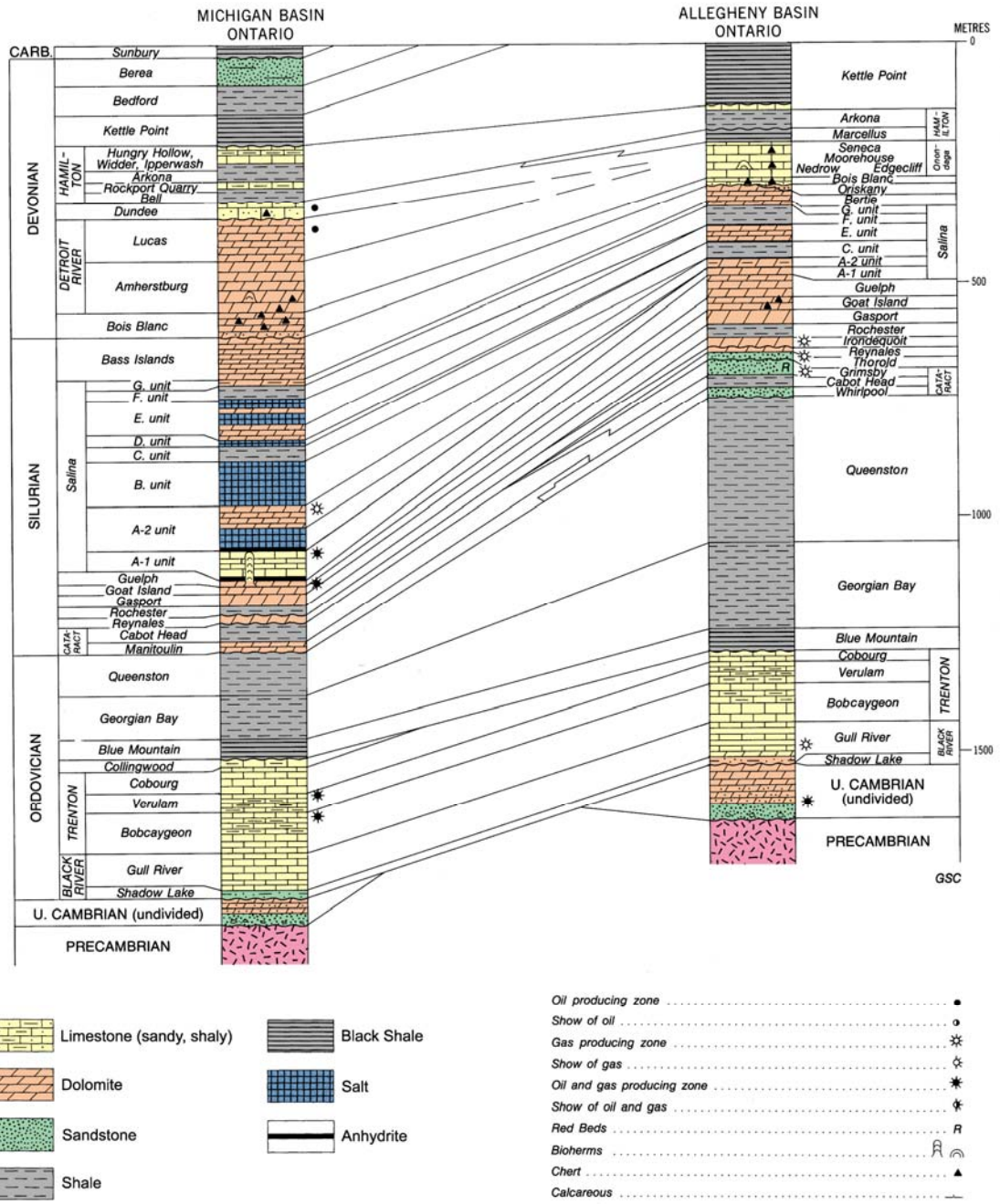

Figure 4.3 Stratigraphic section showing formations and ages, oil and gas producing units. The equivalent units for both the Michigan and the Appalachian (Allegheny) basins are shown. (From Mazurek, 2004; as adapted from Sanford 1993). Although, the Bedford and the Berea formations are listed as Late Devonian in this stratigraphic sketch, it is considered as Mississippian in this study to be consistent with earlier works by Martini et al., 1998 and McIntosh et al., 2002, where some of the samples came from.

Table: 4.1 A brief description of the geology of the stratigraphic units that were sampled

Period	Group	Formation		Description
Mississippian	Port Lambton*	Berea		Sandstones, siltstones and shales (Sanford, 1968 and Johnson et al., 1992)
Devonian		Kettle Point (equivalent to Antrim Shale in the Michigan Basin)		Organic-rich shales (Johnson et al., 1992)
	Hamilton			Mudstone and shale with thin, impure carbonate units (Uyeno et al., 1982)
		Dundee		Limestones (Uyeno et al., 1982)
	Detroit River	Lucas	Richfield Member	The Richfield Member consists mainly of interbedded anhydrites and dolomicrites (Gardner, 1974; Matthews, 1977)
Silurian	Salina	F		Five salt layers, separated by dolomite and shale beds, with numerous anhydrite lenses and stringers (Sanford, 1965, 1969)
		A2		Pinnacle reefs, salt, anhydrite, and overlain by dolostones and minor limestones (Sanford, 1965, 1969)
		A1		Anhydrite overlain by limestones and dolostones (Sanford, 1969).
	Niagaran	Guelph		Dolomitic limestone, reef and interreef deposits (Liberty and Bolton, 1971)
		Lockport		Carbonates (dolomitic limestone) (Bolton, 1957; Hewitt, 1971)
	Clinton	Thorold		Sandstone (Fisher, 1954; Sanford, 1969)
	Cataract	Grimsby		Sandstones (Johnson et al., 1992)
		Whirlpool		Sandstones (Rutka et al., 1991)

		Blue Mountain	Shales (Russell and Telford, 1983)
	Trenton	Cobourg Formation (equivalent to Lindsay Formation in eastern Ontario)	Limestone in the bottom and organic-rich, calcareous shale on the top (Collingwood Member) (Johnson et al., 1992).
		Sherman Fall Formation (equivalent to Verulam Formation in eastern Ontario)	Limestone interbedded with shales (Johnson et al., 1992)
		Kirkfield (equivalent to the upper part of the Bobcaygon in eastern Ontario)	Limestone with interbeds of shale (Liberty, 1969; Williams, 1991)
	Black River	Gull River	Limestone (Liberty 1969; Williams 1991)
		Shadow Lake	craton-derived clastic rocks and impure carbonate rocks (Liberty, 1969)
		Prairie du Chien	Clean quartz sandstone with silica cement (Fisher and Barratt, 1985)
Cambrian		Eau Claire	Sandstones and sandy dolostones (Trevail, 1990)
		Mount Simon	

*According to Johnson et al (1992), these formations could be Late Devonian or Early Mississippian. For simplicity and to be consistent with the earlier works (e.g. Martini et al., 1998; Vugrinovich, 1989; McIntosh et al., 2002), these formations will be referred to in this study as Mississippian.

4.4 Hydrogeology

The aquifer systems in southern Ontario can be divided into two systems. The shallow aquifer system is represented by unconfined, semi-confined and confined aquifers, present in the Quaternary Glacial drift sediments. The deep aquifer system is represented by bedrock aquifers that are part of regional confining units thought to be continuous between the Illinois, Michigan and Appalachian basins (Eberts and George, 2000, McIntosh and Walter, 2005, 2006).

Glacial aquifers typically consist of sand and gravel deposits that result from outwash deposits or discontinuous lenses of ice-contact stratified drift within ground and end-moraine deposits (Westjohn and Weaver, 1997; Eberts and George, 2000). These aquifers are most likely unconfined where the outwash deposits are present along principle streams and locally semi-confined or confined by clayey till elsewhere in the region (Eberts and George, 2000). Usually, these aquifers are associated with seasonally transient flow systems (Eberts and George, 2000). Vugrinovich (1987) suggested that fluid flow in the Devonian and younger rocks, is gravity-driven and topographically controlled. The low topographic gradients and high salinity of underlying basinal formation waters prevent deep circulation of meteoric waters. Westjohn and Weaver (1997) suggested that the fresh water recharge to the underlying bedrock or saline water discharge from the bedrock are prevented by very low permeability Jurassic "red beds", and that recharge of fresh water to the bedrock only occurs where the bedrock outcrops along the margins of the basin, where the glacial deposits are in direct hydraulic connection with the bedrock. Hoaglund et al. (2004) used a model to investigate the extent of modern interaction between groundwater and Saginaw Bay (Michigan). The authors concluded that modern groundwater discharge from the glaciofluvial aquifer to the lake shoreline is relatively low due to low gradients across the Saginaw lowlands and low hydraulic conductivities of the clay-rich lodgement tills. Eberts and George (2000) reported that the vast majority of groundwaters discharge into the Great Lakes catchments, with less than 2% of meteoric water discharging into the deeper basinal-scale flow system. Therefore, modern groundwater flow in the Great Lakes region is primarily restricted to these shallow unconfined glacial drift aquifers (McIntosh and Walter, 2006).

The bedrock aquifers are generally divided into Silurian-Devonian and Cambrian-Ordovician regional systems (McIntosh and Walter, 2005, 2006). The Late Devonian black shales, and Mississippian grey shales and siltstones are the confining units that separate the Silurian-Devonian aquifer system from the overlying shallow glacial drift aquifers. The bedded evaporite (halite and anhydrite) deposits in the Late Silurian section are likely a regional confining unit, separating underlying Silurian carbonates from the overlying Devonian aquifers (Vugrinovich, 1986). The Ordovician Queenston shale or the Utica (equivalent to the Blue Mountain in Ontario) black shale separates the Silurian–Devonian carbonates from the underlying basal Cambrian–Ordovician aquifer system. The Silurian-Devonian and Cambrian-Ordovician aquifer systems outcrop along the margins of the Michigan and Appalachian basins. These outcrops are preserved by deposition of relatively impermeable lake-bed clays and tills during the Pleistocene epoch.

Several researchers (Siegel and Mandle, 1984; Eberts and George, 2000; McIntosh et al., 2002; McIntosh and Walter, 2005, 2006) reported recharge of meteoric waters into the structural Illinois and Michigan basins along the outcrops of the Silurian-Devonian and Cambrian-Ordovician aquifers in the basin marginal areas under cooler climatic conditions, most likely, during the Pleistocene glacial epoch by ice-induced hydraulic loading and basal melting of ice sheets. Weaver et al. (1995) showed that the Early Devonian Dundee Formation in southwestern Ontario was diluted by meteoric water, likely during the Pleistocene. More recently, Hoaglund et al. (2004) suggested that fractures in the Michigan

confining units associated with anticlinal structure presently regulate the degree of communication between Saginaw Bay sediments and the deep brines in the bedrock below.

The presence of paleo-formation waters in shallow bedrock aquifers in the Devonian and Middle Silurian aquifers in southwestern Ontario has been previously documented (Dollar et al. 1991; Weaver et al. 1995; Sklash et al. 1986; Husain et al. 2004; Hobbs et al. 2008). The presence of isotopically depleted waters in Paleozoic aquifers at relatively shallow depths illustrates poor hydraulic connection between these paleowaters and shallow groundwater flow, as these glacial melt-waters have not been flushed by active modern flow systems since the Pleistocene period. Mazurek (2004) suggested that the flow system in the bedrock aquifer system is stagnant or moving very slowly over geological periods of time resulting in long underground residence time for these brines. Furthermore, Raven et al. (1992) reported supernormal fluid pressures within sedimentary sequences in southern Ontario and concluded that the occurrence of such supernormal pressures indicates that the bulk of the enclosing formations are of very low hydraulic conductivity, for otherwise the pressure could not exist.

4.5 Sampling and analyses

Samples were collected by various S.K. Frape students and colleagues (Dollar, 1988; Walter, Pers. Comm.; Cloutier, 1994; Husain, 1996; Weaver, 1994; Sherwood-Lollar and Frape, 1989) over the past 20 years. Samples were collected from various formations (Precambrian

through Mississippian) and various depths ranging from near surface to almost four kilometres. Most waters were sampled following a method modified from Lico et al. (1982) and Kharaka et al. (1987). A detailed demonstration of sample collection and handling is presented by Weaver et al. (1995) and Hobbs et al. (2008).

All of the samples from the Mississippian formations examined in this study are from the Berea Formation and they are from or in close proximity to the central part of the Michigan Basin.

All of the Devonian water samples were collected from southwestern Ontario, except for seven samples that were collected from the central and northern parts of the Michigan basin. Six of the seven samples were collected from the central part of the basin, with one sample from the northern margin of the basin. The samples are from the Middle Devonian Richfield Member and Dundee Formation (carbonate), and the Late Devonian Antrim (shale) Formation (equivalent to the Kettle Point Formation in Ontario). Water samples collected from Ontario are from the Middle Devonian carbonate Detroit River Group and Dundee Formation, and the Late Devonian Hamilton Group and Kettle Point Formation.

Samples were collected from the Middle Silurian carbonates (Guelph, Niagaran and Salina A1) and from salt (Salina F and A2) formations from southern and eastern Michigan and western Ontario. In southeastern Ontario (mainly under Lake Erie), water samples were collected from the Early Silurian (Whirlpool, Grimsby) formations, and Middle Silurian (Thorold Formation), which are predominantly sandstone.

Ordovician water samples were collected from the Prairie du Chien sandstone (Early Ordovician) in the central portion of the Michigan Basin and from the Middle Ordovician carbonates of the Trenton Group in southern Michigan. In southern Ontario, water samples were collected from Middle Ordovician carbonates of the Trenton and Black River Groups, and Late Ordovician shales of the Blue Mountain Formation.

All of the Cambrian samples examined in this study come from southwestern Ontario (south-east of the Algonquin Arch). Because the formations from which the samples were collected were not differentiated, samples are termed Cambrian sandstones samples.

Samples were analyzed for chemical composition and stable isotopes (^{18}O, ^{2}H) by the various studies that were carried out previously and ^{37}Cl and ^{81}Br isotopes were analyzed during this study.

Alkalinity was measured in the laboratory using endpoint titration. The cations compositions were determined by Atomic Adsorption Spectrometry (AAS) and Inductively Coupled Plasma-Atomic Emission Spectrometry (ICP-AES) and the Anions compositions were determined by Ion Chromatography (IC). Reproducibility for the major ions is ± 5% (e.g. Sherwood Lollar and Frape 1989). Analyses of major ions were performed at the University of Waterloo. More detailed information on the methodologies is available in Hobbs et al. (2008).

The ^{18}O, ^{2}H, ^{37}Cl and ^{81}Br stable isotopes were analyzed by Isotope Ratio Mass Spectrometry (IRMS). Oxygen stable isotope measurements were performed on CO_2 by the CO_2–H_2O equilibration method following the procedure of Epstein and Mayeda (1953) and

modified by Moser (1977). Hydrogen stable isotope measurements were performed on H_2 gas using the Zn and Mn reduction methods described by Coleman et al. (1982) and Tanweer and Han (1996). Chlorine stable isotope analyses were performed on methyl chloride (CH_3Cl) gas following the procedure described in Eggenkamp (1994) and Shouakar-Stash et al. (2005b). Bromine stable isotope analyses were carried out on methyl bromide (CH_3Br) gas using a CF-IRMS following (Shouakar-Stash et al., 2005a). The analytical precisions for the ^{18}O, ^{2}H, ^{37}Cl and ^{81}Br isotopes are 0.2 ‰, 1.0 ‰, 0.1 ‰ and 0.1 ‰, respectively.

4.6 Results and Discussion

4.6.1 Chemical Composition

Brine and saline waters are found predominantly in the deep bedrock aquifer systems in southern Ontario, while brackish to fresh waters are found in shallow aquifer systems. Many authors have observed a trend to more concentrated fluids with greater depth in sedimentary basins (e.g. Collins, 1975; Hanor, 1987; Land, 1987; Kharaka and Hanor, 2004).

The chemical compositions of 192 groundwater samples from southern Ontario and Michigan are presented in Table B.1 (Appendix B) (after Hobbs et al., 2008). A large variation in TDS is observed for these waters, with TDS values ranging from less than 1000 mg/L to almost 400,000 mg/L. Applying the classification scheme developed by Carpenter

(1978), 67% of the formation waters are brines, 20% are saline and 10% are brackish. Only 3% of the groundwaters in the database are classified as fresh waters (Hobbs et al., 2008).

Generally, the most concentrated samples are from the central parts of the Michigan Basin and/or from deeper (older) stratigraphic units. Samples from the marginal parts of the basin and especially from younger strata (e.g. Devonian) are relatively less concentrated (i.e. concentration increases with depth and with direction toward the center of the Michigan Basin). In the current database, the most saline formation waters (TDS ≈ 400,000 mg/L) are Ca-Cl type waters, sampled from the Silurian carbonates of the Niagaran formation in central Michigan at depths between 1200 and 1400 metres. The majority of the high TDS samples from the central part of the Michigan Basin are Ca-type waters (e.g. Ca-Cl, Ca-Mg-Cl, Ca-Na-Cl, and Ca-Na-Mg-Cl). Moving away from the center and toward the margins of the Michigan and Appalachian basins, Na-type (Na-Ca-Cl and some Na-Cl) start to predominate. Marginal and shallow samples (mainly Devonian) are characterized by lower TDS value (TDS < 100,000 mg/L) and various Na-type and Na-Ca-type waters (e.g. Na-Ca-Mg-Cl, Na-Mg-Ca-Cl, Na-Cl, Na-Ca-HCO_3 and Na-SO_4-Cl).

Numerous evolutionary processes have been proposed to explain the high TDS of such formation waters, including 1) the evaporation of seawater (e.g. Carpenter, 1978; Kharaka et al., 1987); 2) the dissolution of halite or other evaporites such as potash or gypsum (e.g. Rittenhouse 1967; Land and Prezbindowski 1981; Hitchon, 1996); 3) membrane filtration (Bredehoeft et al., 1963; Berry, 1969; Kharaka and Berry, 1973; Graf, 1982); 4) concentration and metamorphism of waters at great depths assisted by high temperatures and

pressures (Chebotarev, 1955; Krotova, 1958; Pinneker and Lomonosov, 1964); and/or 5) freezing of water or hydration of silicates (clays) with the resulting concentration of solutes (Hanor, 1987). The sediments comprising the Paleozoic rocks underlying southern Ontario were deposited predominantly in shallow inland seas during the Cambrian through the Devonian. Therefore, the formation waters in these sedimentary rocks are assumed to be of marine origin (paleoseawater).

The behaviour of seawater major ions is well understood and documented (e.g. Carpenter, 1978; Kharaka et al., 1987). Figure 4.4 is an illustration of the evolution of modern seawater during evaporation. In fact, in order to evaluate the origin and/or the evolution of brines, major ion (e.g. Ca, Mg, K, Cl and SO_4) concentrations are most often compared to Br concentrations (Valyaskho, 1956; Braitsch and Hermann, 1963; Rittenhouse, 1967; Collins, 1975; Carpenter, 1978; Carpenter and Trout, 1978; Hanor, 1987; Kharaka et al., 1987; Land, 1987; Kharaka and Hanor, 2004). Naturally occurring mineral phases containing bromine are very rare and even at very high ionic strengths, Br partitions predominantly into solution.

Figure 4.5 illustrates the logarithmic relationship between Cl (mg/L) and Br (mg/L) contents of seawater during evaporation. The figure illustrates also the initial precipitation point of evaporite mineral phases as reported by Matray (1988). It also shows some mixing scenarios between several end members (e.g. evaporated seawater, seawater, fresh water). Further it shows the affect of dissolving halite by different fluids such as seawater and brines. These different scenarios were examined and reported previously by several researchers (e.g. Rittenhouse, 1967; Carpenter, 1978; Kharaka and Hanor, 2004). Zherebtsova and Volkova

(1966) showed that during evaporation of seawater essentially all of the potassium, rubidium, lithium and bromide remain in solution until potash salts (e.g. sylvite and carnalite) begin to precipitate, and that most of the Li and Br remain in solution during potash salt deposition. Bromide concentrations were used in this study to determine the degree of evaporation.

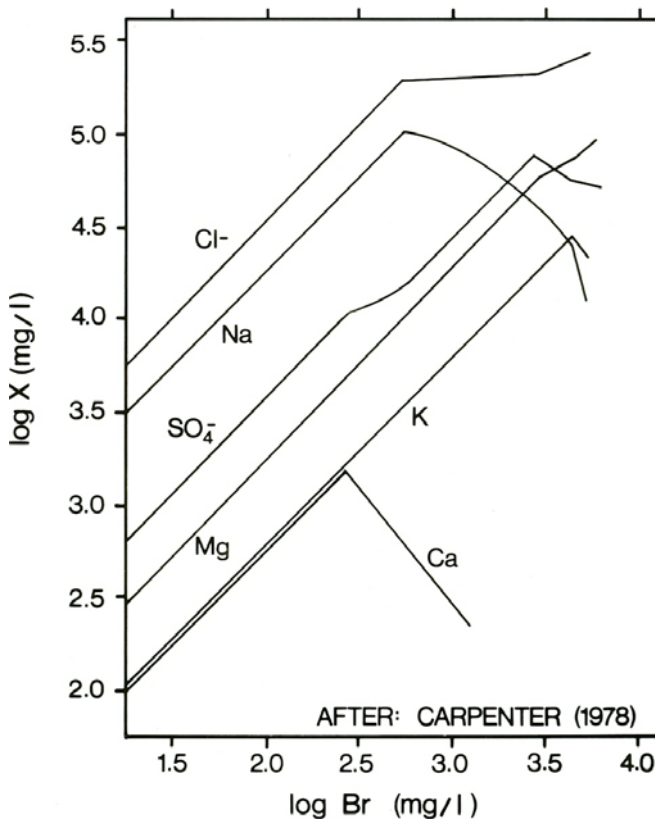

Figure 4.4 Concentration trends of a number of cations and anions in evaporating seawater (From Kharaka et al., 1987, after Carpenter, 1978).

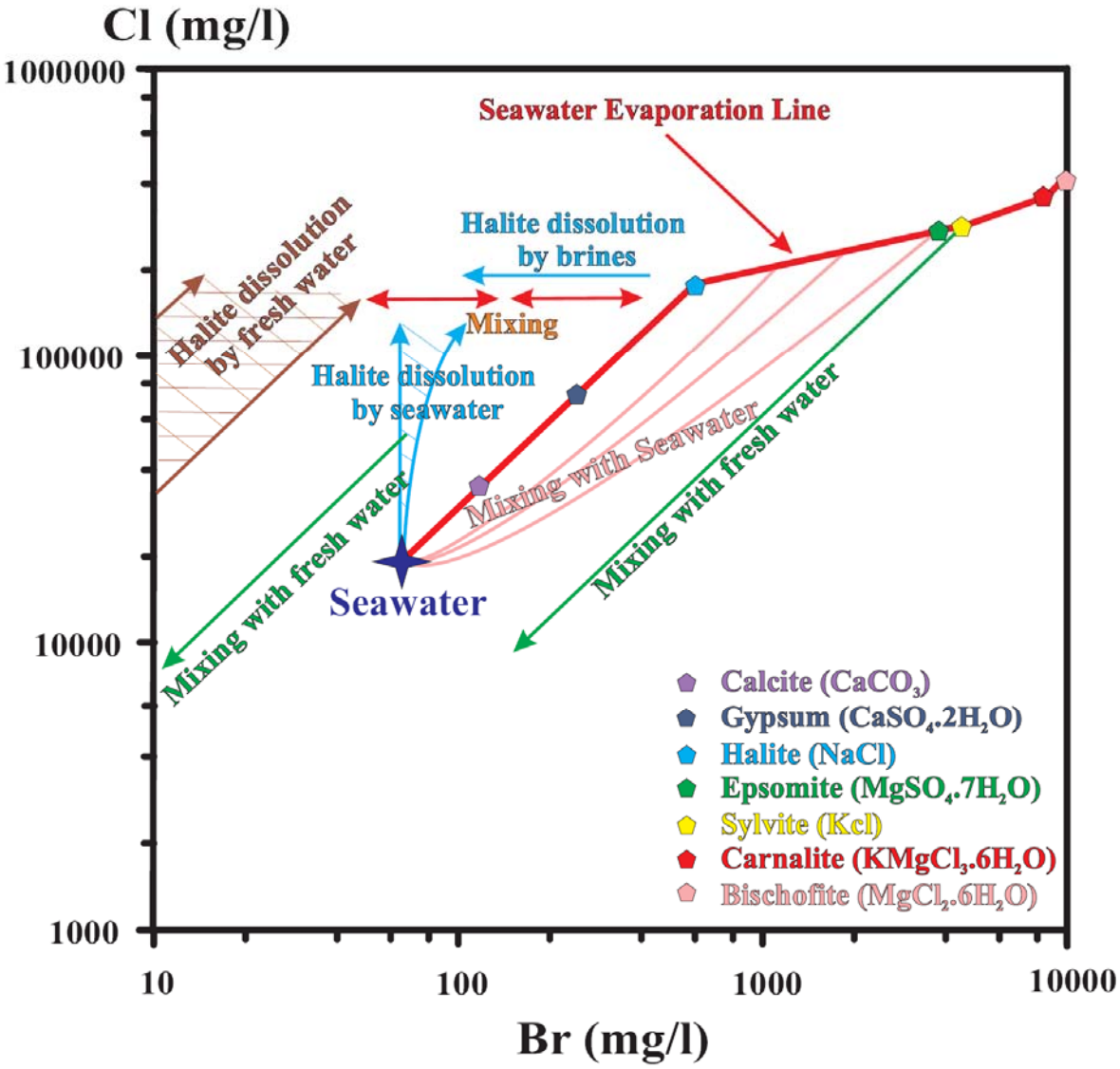

Figure 4.5 A logarithmic plot of the concentration trends of chloride versus bromide during the evaporation of seawater showing the initial precipitation point of evaporite mineral phases (after Matray, 1988). Also shown are some of the possible mixing scenarios after Rittenhouse (1967) with different halite dissolution products and different end member waters (Carpenter, 1978).

Figure 4.6 illustrates the relationship between Cl and Br concentrations of the southern Ontario and Michigan samples based on the stratigraphic units from which they were

sampled. All of the Mississippian samples fall on or just below the seawater evaporation line (halite precipitation stage). All of the samples are Na-Ca-Cl type waters which, suggests the mixing of two end members as the origins of these waters; 1) evaporated paleoseawater and 2) seawaters. The high concentration of almost all of these samples (TDS > 300,000 mg/L) suggests that they consist primarily of the first end member (evaporated paleoseawater).

The Devonian samples illustrated in Figure 4.6 show the largest variations in concentration, which consequently suggests the involvement of diluting end member(s). The samples collected from the central part of the Michigan Basin are characterized by high TDS values (between 123, 000 mg/L and 295,000 mg/L) and they seem to have originated from mixing of end members, such as evaporated paleoseawater, seawater, and halite dissolution by seawater. The rest of the samples that are from the marginal parts of the basin are characterized by several water types, low TDS compositions and they have a Na/Cl ratio close to unity, which is an indication of fresh water and NaCl dissolution components. The low Br contents of these samples are evidence of the greater contribution of these two components. The fresh water (meteoric waters) contribution agrees with conclusion of several researchers (e.g. Weaver et al., 1995; McIntosh et al., 2005; 2006) who reported extensive recharge of Devonian formations near the marginal areas of the Michigan Basin by meteoric waters, presumably during the Pleistocene. In summary the Devonian Formation waters from the marginal parts of the Basin are affected by freshwater recharge and halite dissolution. The presence of seawater and evaporated paleoseawater as mixing end members are also evident, although their contribution is rather small.

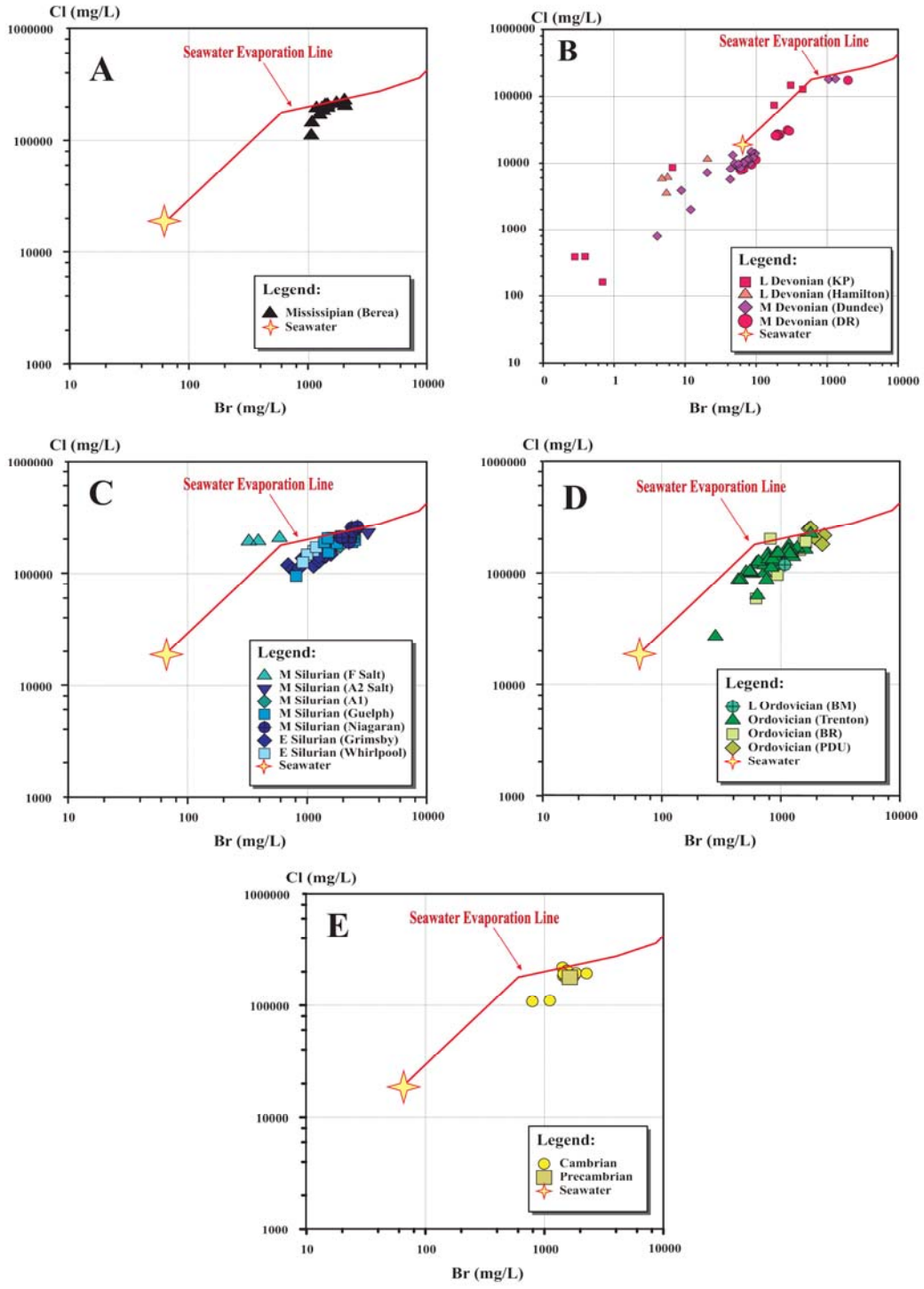

Figure 4.6 Logarithmic plots of Cl (mg/L) versus Br (mg/L) of southern Ontario and Michigan samples based on the stratigraphic units they were sampled from.

Waters sampled from the Silurian formations were collected from several Early and Middle Silurian formations covering a large geographic area ranging from the central parts of the Michigan Basin in Michigan, the marginal parts of the Michigan Basin in southwestern Ontario, and the marginal parts of the Appalachian Basin (southern Ontario and below Lake Erie). The majority of the Silurian samples are Ca-type waters. The Middle Silurian carbonate Niagaran waters are the most concentrated brines found in this study area, especially those collected from the central parts of the Michigan Basin. These samples are Ca type waters that are characterized by high Br contents. This suggests that they are most likely evolved by paleoseawater evaporation. The Middle Silurian carbonate Guelph Formation brines are characterized by Ca-Na-Cl and Na-Ca-Cl type waters and they seem to be more affected by seawater dilution than the carbonate A-1 Formation waters. The process of dilution by seawater mentioned above are in agreement with the evaporative drawdown model suggested by Coniglio et al. (2003) based on a concept from Cercone (1988) to explain the mechanism of dolomitization in these carbonates (Guelph and A-1 formations). Dolomitizing fluids were seawater-derived, and traveled towards the basin by a gravity-driven reflux during the early part of the Late Silurian.

The Early Silurian sandstone formations from the Appalachian Basin (Grimsby and Whirlpool formations) are characterized by Ca-Na-Cl and Na-Ca-Cl type waters and they are also characterized by low TDS (TDS < Middle Silurian brines). These samples seem to suffer greater dilution with seawater than the Middle Silurian formations in the Michigan Basin. Although the brines from the Silurian formations, presented in this chapter, do not show any

contribution of meteoric waters, a study conducted by Hanratty (1996) reported some much more depleted waters in Middle Silurian formations in southern Ontario, indicating an extensive contribution of freshwaters in shallow Silurian formations in their outcrop areas.

The Ordovician water samples belong to a very large geographic area in Michigan and southern Ontario and they are from different Ordovician (Early, Middle and Late) formations. The most concentrated samples are from the Early Ordovician Prairie du Chien sandstone Formation from the central part of the Michigan Basin. These samples are Ca dominated type waters that are highly concentrated (~300,000 mg/L to ~400,000 mg/L). These waters are probably the result of evaporated paleoseawater with some later seawater dilution. The Middle Ordovician Trenton and Black River carbonate formation waters probably experienced a degree of dilution by more recent seawater post the Middle Ordovician. The one sample obtained from the Late Ordovician Blue Mountain Formation is probably of the same origin as the brines from the Black River and Trenton groups. Some of the Trenton Group waters, from the marginal area of the Michigan Basin, are characterized by relatively low TDS (as low as 44,000 mg/L). These samples show high tritium content as well, indicating they experienced recent dilution with fresh water. The quality of these samples was compromised by mixing with drilling fluids (Sherwood-Lollar and Frape, 1989). In summary, aside from some of the UN-2 and OHD-1 samples that are believed to be compromised by drilling fluids, the majority of the Ordovician samples originated by mixing between original evaporated paleoseawater that exist largely in the central part of the Michigan Basin and a more modern saline or seawater.

The majority of the Cambrian and Precambrian brines are characterized by high TDS that are around 300,000 mg/L. However, these samples are most likely the result of evaporated paleoseawater that was diluted by more modern seawater.

The logarithmic plot of chloride versus bromide of the Paleozoic sequences in southern Ontario and Michigan formation waters are presented in Figure B-1 (Appendix B). The change in major ions of the different water types from this study in comparison to the change of their Br concentrations are shown in Appendix B (Figures B-2, B-3, B-4, B-5 and B-6). These figures also illustrate the change in major ions during seawater evaporation and subsequent precipitation of some minerals such as $CaSO_4$ and NaCl.

Generally all major ions show deviations from the expected seawater evaporation trends. The majority of sedimentary formation waters described in the literature have chemistries that vary considerably from what would be expected of evaporated seawater. During the diagenetic evolution of the brines, calcium and strontium concentrations increase by up to an order of magnitude compared to evaporated seawater, while magnesium and potassium concentrations may decrease by as much as an order of magnitude (Kharaka and Hanor 2004). There are several water-rock interaction processes that account for these changes in the major ions. For example, the loss of Na and gain of Ca can be attributed to ion exchange between the water and the host rock.

In summary, the formation waters from the older formations such as Precambrian, Cambrian and Ordovician are mainly originated from dilution of evaporated paleoseawater by more recent saline or seawater. It is not easy to determine whether this dilution occurred in

one event through the outcrops of the various stratigraphic units or via multiple events (i.e. sequential recharge) through a brine reflux. However, it is more reasonable to assume sequential recharges through multiple events as the seawater covered the entire area during the Paleozoic and the opportunity of seawater recharge and mixing with the brines in the uppermost sediments was always a possibility. Generally, the degree of dilution increases with distance from the central part of the basin and towards the marginal areas. The contribution of halite dissolution is minor and it is restricted to marginal areas (McIntosh and Walter, 2005, 2006) such as the, halite dissolution of the Salina salt in southern Ontario (Sanford, 1985). The younger formations such as Devonian and Silurian in the marginal parts of the basins (outcrop areas) are affected by more halite dissolution and contain more fresh water component. This is even more pronounced in the Devonian formation than the Silurian formations.

4.6.2 $\delta^{18}O$ and $\delta^{2}H$ Compositions

The $\delta^{2}H$ versus $\delta^{18}O$ values of the formation waters from southern Ontario and Michigan are presented in Table 4.2. Figure 4.7 illustrates the behaviour of seawater isotopic compositions ($\delta^{2}H$ and $\delta^{18}O$) during evaporation as proposed by Holser (1979). During the early phases of evaporation of seawater the lighter isotopes are preferentially removed from solution and the residual seawater becomes enriched in the heavier isotopes (^{18}O and ^{2}H). Isotopic analysis of an evaporating marine salt pan by Holser (1979) indicated that progressive enrichment of the heavier isotopes does not continue indefinitely, but that the trajectory hooks around as shown

in Figure 4.7 at an evaporation degree of 4 fold. During progressive evaporation the relative amount of water tied up in hydration spheres around cations increases. Isotope exchange between this water, the unbound water, water molecules leaving the liquid-air interface, and atmospheric water vapour may be the cause of the hook-shaped trajectory (Holser, 1979). The shape and the extent of the hook varies depending on local humidity, temperature, average wind speeds, and other climatic variables (Knauth and Beeunas, 1986). The evaporation hook-shaped curve of Holser (1979) was extrapolated by Knauth and Beeunas (1986) to x45 degree of evaporation. Halite precipitation begins at about x11 (Knauth and Beeunas, 1986). Additional processes such as hydrothermal activities (e.g. mixing with geothermal waters) and high temperature water-rock interaction could be important in sedimentary basins as they would cause enrichment of the ^{18}O content of the water. For example, Sheppard (1986) reported that the $\delta^{18}O$ signature enrichments and shifts to the right of the GMWL are predominantly caused by isotopic exchange with ^{18}O-rich sedimentary minerals such as carbonates. The $\delta^{18}O$ compositions are enriched in marine carbonates by 29 ‰ relative to the water they precipitated from at ambient temperature, however, the equilibrium between carbonate and water is reduced to only 8 ‰ at 250°C (Clark and Fritz, 1997). Figure 4.7, also illustrates a few mixing scenarios between the following end members; 1) Seawater (SMOW), 2) saline waters of different degrees of seawater evaporation, 3) modern precipitation, and 4) glacial melt-water. The shaded area represents the mixing area between the main end members.

Table 4.2 Isotopic compositions of formation waters from the southern Ontario and Michigan. Samples were collected from the stratigraphic units shown. (Note: The samples presented in this table were collected by various authors and the δ^2H and $\delta^{18}O$ belong to the authors: [1] Dollar, 1988; [2] Walter, Pers. Comm.; [3] Cloutier, 1994; [4] Husain, 1996; [5] Weaver, 1994; [6] Sherwood-Lollar and Frape, 1989)

No.	Author	Sample Name	$\delta^{18}O$ (VSMOW) (‰)	$\delta^{2}H$ (VSMOW) (‰)	$\delta^{37}Cl$ (SMOC) (‰)	$\delta^{81}Br$ (SMOB) (‰)	3H TU
Mississippian (Berea)							
1	[1]	MB-1	-1.5	-32			<6
2	[1]	MB-2	0.3	-24	0.10		<6
3	[1]	MB-3	-2.1	-45	0.00		<6
4	[1]	MB-4	-3.9	-52			<6
5	[1]	MB-5	0.2	-31			<6
6	[1]	MB-6	0.5	-25	0.10		<6
7	[2]	BRENNAN 122			-0.19		
8	[2]	CAMPBELL #7			-0.40		
9	[2]	CAMPBELL #9			-0.38		
10	[2]	CANNELL #1			0.01		
11	[2]	CARTER			-0.30		
12	[2]	JAMES 122			-0.30		
13	[2]	NKERN #1			-0.20		
Late Devonian (Kettle Point / Antrim)							
14	[3]	LD-90-3-5	-11.1	-69	1.82		
15	[3]	DOW-90-3-4	-8.5	-61			
16	[4]	BRP-143	-16.9	-122	0.01		
17	[4]	BRP-151	-16.9	-122	0.24		
18	[2]	SP A2-32	-4.6	-28	-0.39		
19	[2]	WSMC2-10	-6.7	-40	-1.11		
20	[2]	HGR D4-6	-10.2	-64	-0.35		
Late Devonian (Hamilton)							
21	[3]	LD-90-3-4	-7.5	-52	0.89		
22	[3]	LD-90-3-3	-7.2	-51	0.67		
23	[3]	LD-90-3-2	-6.9	-47	0.18		
24	[3]	DOW-90-3-3	-7.1	-57	0.00		
25	[3]	DOW-90-3-2	-6.8	-50	0.03		
Middle Devonian (Dundee)							
26	[3]	DOW-90-3-1	-6.9	-51	-0.72		
27	[3]	LD-90-3-1	-7.2	-54			
28	[1]	DD-1	-11.4	-86	0.05		<6
29	[1]	DD-2	-15.7	-120			<6
30	[1]	DD-3			-0.19	-0.21	<6
31	[1]	DD-4	-0.9	-34	-0.27	-0.17	<6
32	[5]	PD-COCH	-7.5	-48			
33	[5]	PD-NORTH	-6.9	-41	0.92	0.68	
34	[5]	PD-RAL	-6.8	-43			2.4
35	[5]	PD-WEST	-7.1	-46			
36	[5]	RA-N	-7.6	-49			7.1
37	[5]	RA-NE	-6.8	-46	1.14	0.62	
38	[5]	RA-SE	-7.2	-45	0.95	0.52	
39	[5]	RA-SW	-7.3	-49			
40	[5]	LAI-1	-6.6	-36			
41	[5]	LAI-2	-6.5	-43	1.02		
42	[5]	LAI-3	-6.4	-37			0.8
43	[5]	WB-11	-8.5	-55	1.16		
44	[5]	WB-2	-8.2	-49			7.2
45	[5]	WB-7	-7.6	-48	1.25		
46	[5]	WB-8	-6.9	-42			
47	[5]	LBH-1	-8.7	-59			
48	[5]	LBH-2	-8.8	-62	0.35	0.60	
49	[5]	LBH-3	-8.2	-59			0.8
50	[5]	LBH-4	-8.1	-57	0.33	0.92	

Table 4.2 Continued

No.	Author	Sample Name	$\delta^{18}O$ (VSMOW) (‰)	$\delta^{2}H$ (VSMOW) (‰)	$\delta^{37}Cl$ (SMOC) (‰)	$\delta^{81}Br$ (SMOB) (‰)	3H TU
Middle Devonian (Detroit River)							
51	[5]	LBO-2	-7.5	-53	0.69	0.52	
52	[5]	LBO-3	-7.2	-54			
53	[5]	CFN-14	-9.5	-63	0.50		
54	[5]	CFN-A	-9.0	-60	0.26	0.55	
55	[5]	CFN-B	-9.1	-60			37.7
56	[5]	CFN-161	-6.3	-84	0.63	0.49	1.1
57	[5]	CFN-C	-6.3	-38	0.79	0.35	0.8
58	[5]	CFN-E	-5.9	-56	0.94	0.45	
59	[5]	CFS-A	-6.0	-76	0.69	0.57	
60	[5]	CFS-B	-6.3	-49	0.49		0.8
61	[5]	CFS-C	-6.4	-48	0.72		
62	[5]	CFS-D	-6.3	-68	0.28	0.63	
63	[1]	DR-1	0.2	-55	-0.50	-0.23	<6
Midddle Silurian (F Salt)							
64	[1]	SF-1	-5.5	-55	-0.20		
65	[1]	SF-2					
66	[1]	SF-3	-4.7	-52			<6
Middle Silurian (A2 Salt)							
67	[1]	SA2-1	2.9	-52			
68	[1]	SA2-2	3.2	-48			
Middle Silurian (A1 Carbonate)							
69	[1]	SA1-1			-0.35		
70	[1]	SA1-2	-1.1	-47	-0.35		<6
Middle Silurian (Guelph)							
71	[1]	SG-1	-4.7	-42			
72	[1]	SG-2					<6
73	[1]	SG-3	-0.8	-43	-0.40		<6
74	[1]	SG-4			-0.15	-0.95	<6
75	[1]	SG-5					
76	[1]	SG-6					<6
77	[1]	SG-7			-0.38	-0.83	
78	[1]	SG-8	-0.4	-44	-0.51	-0.61	<6
79	[1]	SG-9					
80	[1]	SG-10			-0.28	-0.75	<6
81	[1]	SG-11					<6
82	[1]	SG-12					
83	[1]	SG-13					
Middle Silurian (Niagaran)							
84	[1]	SN-1	0.2	-42	-1.04	-0.76	
85	[1]	SN-2	-1.4	-48			
86	[1]	SN-3	-2.9	-50	-0.30	-0.28	
87	[1]	SN-4	-4.9	-46	-0.61	-0.70	<6
88	[1]	SN-5	1.2	-40	-0.22	-0.69	
89	[1]	SN-6	-1.0	-47	-0.28	-0.61	<6
90	[1]	SN-7	0.2	-43	-0.30		<6
91	[1]	SN-8	-0.5	-41	-0.30		<6
92	[1]	SN-9	-0.4	-43			<6
93	[1]	SN-10	-0.1	-47	-0.43	-0.92	<6
94	[2]	COLD SPRINGS WH1-29			-0.39		

Table 4.2 Continued

No.	Author	Sample Name	$\delta^{18}O$ (VSMOW) (‰)	$\delta^{2}H$ (VSMOW) (‰)	$\delta^{37}Cl$ (SMOC) (‰)	$\delta^{81}Br$ (SMOB) (‰)	3H TU
Early Silurian (Grimsby/Thorhold)							
95	[1]	STGr-1	-3.5	-43			<6
96	[1]	STGr-2	-2.9	-34			<6
97	[1]	STGr-3	-4.2	-44			
98	[1]	STGr-4	-2.9	-43			<6
99	[1]	ST-5	-4.1	-46	0.78		
100	[1]	ST-6	-3.4	-44			
101	[1]	SGr-7	-3.3	-43			<6
102	[1]	SGr-8	-3.0	-42			<6
103	[1]	STGr-9	-2.8	-44			
104	[1]	STGr-10	-1.9	-42	0.14	0.77	<6
105	[1]	SGr-11	-1.7	-41	0.35	1.36	<6
106	[1]	SGr-12	-3.9	-40			
107	[1]	STGr-13	-3.4	-41	0.35		<6
108	[1]	STGr-14	-1.7	-46	0.21	1.35	<6
109	[1]	SGr-15	-3.5	-39			
110	[1]	SGr-16	-3.4	-35			<6
111	[1]	STGr-17	-2.9	-41	0.13		
112	[1]	SGr-18	-4.3	-44			
113	[1]	SGr-19	-4.5	-44	0.37		<6
114	[1]	SGr-20	-3.7	-38	0.50	1.74	
115	[1]	SGr-21	-3.8	-43	0.50	1.63	<6
Early Silurian (Whirlpool)							
116	[1]	SW-1	-3.0	-39	0.86	2.31	<6
117	[1]	SW-2	-3.7	-41	0.60	2.11	<6
118	[1]	SW-3	-2.5	-39	0.64	2.13	<6
119	[1]	SW-4	-3.8	-42			<6
Late Ordovician (Blue Mountain)							
120	[6]	OHD-1 #15	-5.6	-46	0.09	1.75	26
Middle Ordovician (Trenton)							
121	[1]	OT-1	-2.1	-31	-0.36		<6
122	[1]	OT-2	-1.7	-23	0.00		<6
123	[1]	OT-3	-1.9	-31	0.30		
124	[1]	OT-4	-1.7	-30			
125	[1]	OT-5	-1.9	-29	-0.60		<6
126	[1]	OT-6	-2.2	-28	-0.30		<6
127	[1]	OT-7					
128	[1]	OT-8	-2.1	-30			<6
129	[1]	OT-9	-2.1	-27	-0.59	0.98	<6
130	[1]	OT-10	-2.3	-31	-0.63	0.87	<6
131	[1]	OT-11	-1.9	-26	-0.55	0.76	
132	[1]	OT-12	-2.0	-29	-0.49	0.93	
133	[1]	OT-13	-2.1	-27	-0.50		<6
134	[1]	OT-14	-2.0	-33	-0.52	0.58	<6
135	[1]	OT-15	-2.2	-27	-0.40		<6
136	[1]	OT-16	-2.1	-36	-0.55		<6
137	[1]	OT-17					
138	[1]	OT-18			-0.34	0.62	<6
139	[1]	OT-19	-1.8	-24	-0.70		<6
140	[1]	OT-20	-2.0	-23			<6
141	[1]	OT-21	-3.1	-32	-0.43	0.18	<6
142	[1]	OT-22					
143	[1]	OT-23	-1.3	-45	-0.65	-0.49	<6
144	[1]	OT-24	-1.7	-27	-1.13		<6
145	[1]	OT-25	-2.0	-27			<6

Table 4.2 Continued

No.	Author	Sample Name	$\delta^{18}O$ (VSMOW) (‰)	$\delta^{2}H$ (VSMOW) (‰)	$\delta^{37}Cl$ (SMOC) (‰)	$\delta^{81}Br$ (SMOB) (‰)	3H TU
Middle Ordovician (Trenton)							
146	[1]	OT-26	-2.1	-27			<6
147	[1]	OT-27	-1.9	-26			<6
148	[1]	OT-28					
149	[1]	OT-29	-1.6	-24			<6
150	[1]	OT-30	0.4	-35	-0.31		<6
151	[1]	OT-31	-1.7	-20	-1.31		<6
152	[1]	OT-32	-1.5	-25			<6
153	[1]	OT-33					
154	[1]	OT-34	-1.8	-29			<6
155	[1]	OT-35	-1.8	-25			<6
156	[1]	OT-36					
157	[1]	OT-37	-1.5	-33			<6
158	[1]	OT-38	-2.4	-34			<6
159	[1]	OT-39	-2.7	-26			<6
160	[1]	OT-40	-3.0	-28	-1.09		<6
161	[1]	OT-41	-2.8	-28	-0.60		<6
162	[1]	OT-42	-2.6	-28			<6
163	[6]	UN-2 #13	-6.4	-52	-0.32	2.15	69
164	[6]	OHD-1 #13	-6.1	-52	0.09	1.93	22
165	[6]	UN-2 #11	-5.7	-47	-0.30	2.08	50
Middle Ordovician (Black River)							
166	[6]	OHD-1 #7	-4.8	-41	0.08	1.73	<6
167	[6]	UN-2 #5	-6.0	-46	-0.13	1.18	<6
168	[6]	OHD-1 #5A	-4.8	-42			<6
169	[6]	OHD-1 #5B	-4.6	-42	0.32		<6
170	[6]	OHD-1 #3	-4.6	-41	0.11	1.78	<6
171	[6]	UN-2 #2	-6.7	-49	0.01	1.92	32
172	[6]	UN-2 #4	-5.2	-47	-0.14	1.94	25
173	[6]	OHD-1 #2	-4.5	-42	0.10	1.76	<6
Early Ordovician (Prairie du Chien)							
174	[1]	OP-1	-1.6	-50	-0.95	-0.55	<6
175	[2]	LAHAR 1-7			-0.26		
176	[2]	FOSTER 1-21			-0.18		
177	[2]	PRASS 1-12			-0.34		
178	[1]	OP-2			-1.04	-0.73	
Cambrian							
179	[1]	C-1	-4.0	-29	-0.24		
180	[1]	C-2	-4.4	-28	-0.16	1.17	<6
181	[1]	C-3	-4.6	-28	-0.15	0.93	<6
182	[1]	C-4	-4.6	-35	-0.20	0.72	<6
183	[1]	C-5	-4.1	-36	0.19		<6
184	[1]	C-6	-1.4	-28	-0.50		<6
185	[1]	C-7	-3.3	-21			
186	[1]	C-8	-3.3	-28	-0.31	1.07	
187	[1]	C-9	-3.6	-29	-0.12	0.96	<6
188	[1]	C-10	-3.8	-32	-0.06		
189	[1]	C-11	-2.0	-24	-0.40		
190	[1]	C-12					
191	[1]	C-13			0.10	1.51	
Precambrian							
192	[6]	OHD-1 #1	-5.3	-44	0.30		8

The δ^2H and $\delta^{18}O$ compositions are illustrated based the stratigraphic units from which they were sampled (Figure 4.8) and based on their water type in Figure B.7 (Appendix B). The majority of the formation waters from this study plot below the GMWL and fall around the x45 area. This is in agreement with the conclusion drawn from the chemistry of these samples that they were evaporated beyond the start of halite precipitation and close to the start of epsomite precipitation. Waters sampled at shallow depths in Devonian formations are the exception as they have isotopic signatures that are typical of meteoric water, plotting along the GMWL. Several researchers (Dollar et al. 1991, Weaver et al. 1995, Husain et al. 2004) reported waters from shallow Devonian carbonates or glacial drift aquifers with depleted δ^2H and $\delta^{18}O$ signatures, suggesting a glacial melt-water source.

The illustration of δ^2H and $\delta^{18}O$ results of these formation waters (Figure 4.8) shows that brines from the different-aged formations (Mississippian, Devonian, Silurian, etc.) are characterized by distinctive isotopic signatures. This is suggested by the observed "clustering" of the isotopic signatures for a given formation (Figure 4.8) (Dollar et al., 1991). Some overlaps are also observed between the isotopic signatures of formation waters from different formations (Figure 4.8).

The $\delta^{18}O$ and δ^2H of the various formations shows large variations in both isotopes, this is due to the mixing between various end members (evaporated paleoseawater, seawater, fresh water and glacial melt water). In general, formation waters from the marginal areas of the Michigan Basin (shallow depths) are characterized by depleted $\delta^{18}O$ and δ^2H suggesting a large fresh water component (e.g. Devonian formation waters from southern Ontario). The

large variations of both isotopes of the Devonian formation waters in southern Ontario suggest that they are highly mixed with various water sources. Brines from the central parts of the Basin are more enriched in ^{18}O in comparison to the rest of the samples and this is explained by water-rock interaction by elevated geothermal gradient possibly due to burial diagenesis (e.g. Middle Silurian Niagaran and A-2 salt formation waters). This is supported by the fact that these brines are characterized by high Ca content which could indicate ion exchange during water-rock interaction. Formation waters that were collected geographically between the center and the margins of the basin show mixing between several end members, including seawater (e.g. Trenton Group brines). The conclusions derived from the $\delta^{18}O$ and $\delta^{2}H$ are consistent and lend support to those derived from the chemistry. In some cases, the $\delta^{18}O$ and $\delta^{2}H$ data helped in differentiating between two possible dilution end members (seawater and fresh water). When dilution is not involved variations of the $\delta^{18}O$ and $\delta^{2}H$ can be caused by different climatic conditions during the evaporation of the seawater which would eventually produce different shapes of the seawater evaporation hook.

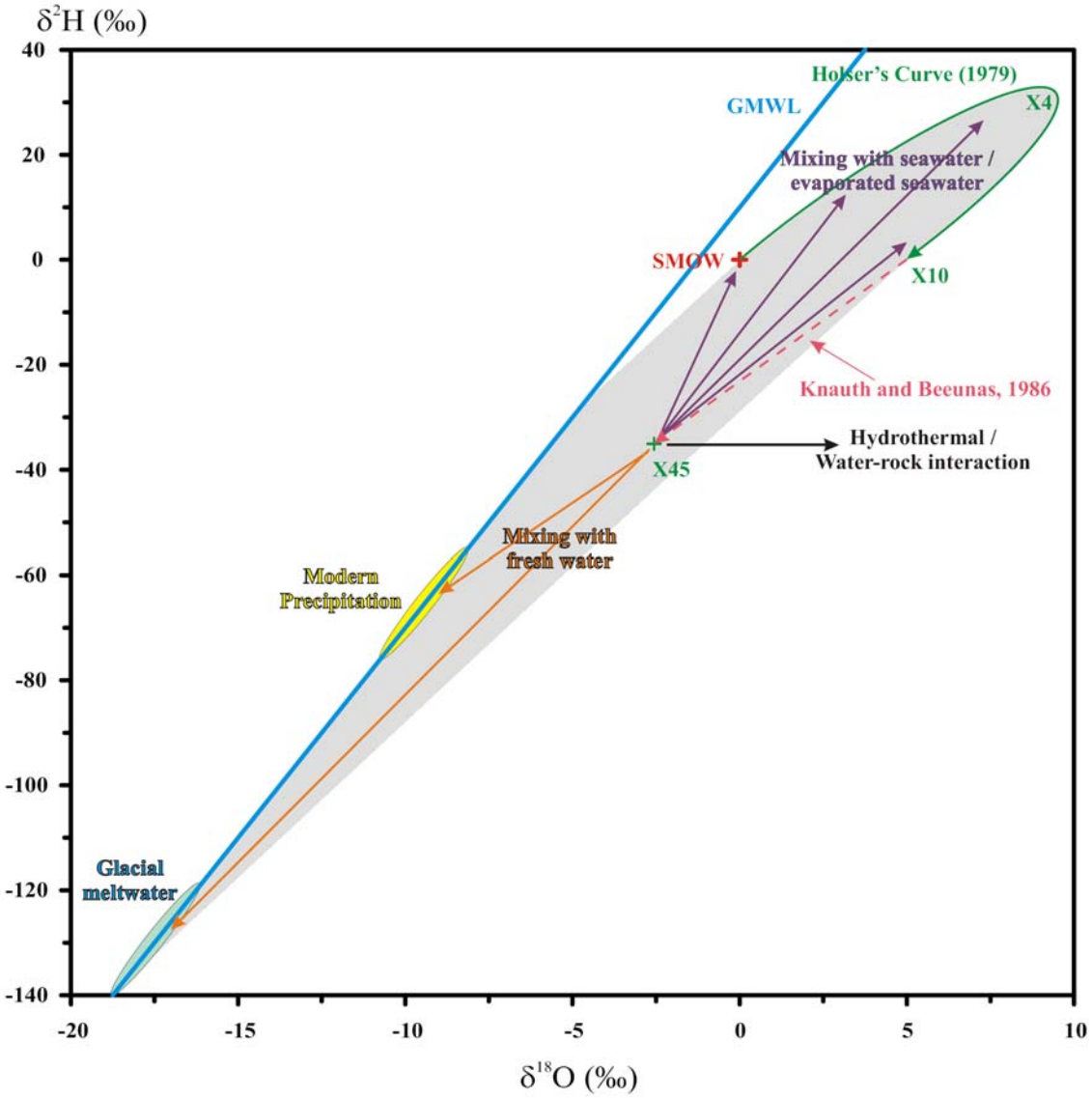

Figure 4.7 The different possible end members and processes that control the oxygen and hydrogen isotopic compositions of the southern Ontario and Michigan formation waters. Seawater (SMOW), different degrees of seawater evaporation, modern precipitation, and glacial melt-water are the main end-members. Mixing between various end members, seawater evaporation, hydrothermal activities, and water-rock interactions are the major processes. The shaded area represents the mixing area between the main end members. The Figure contains the seawater evaporation curve by Holser (1979) and indicates some evaporation degrees (x4 and x10). It contains also the extrapolated evaporation point at 45 fold of evaporation (x45) extrapolated by Knauth and Beeunas (1986).

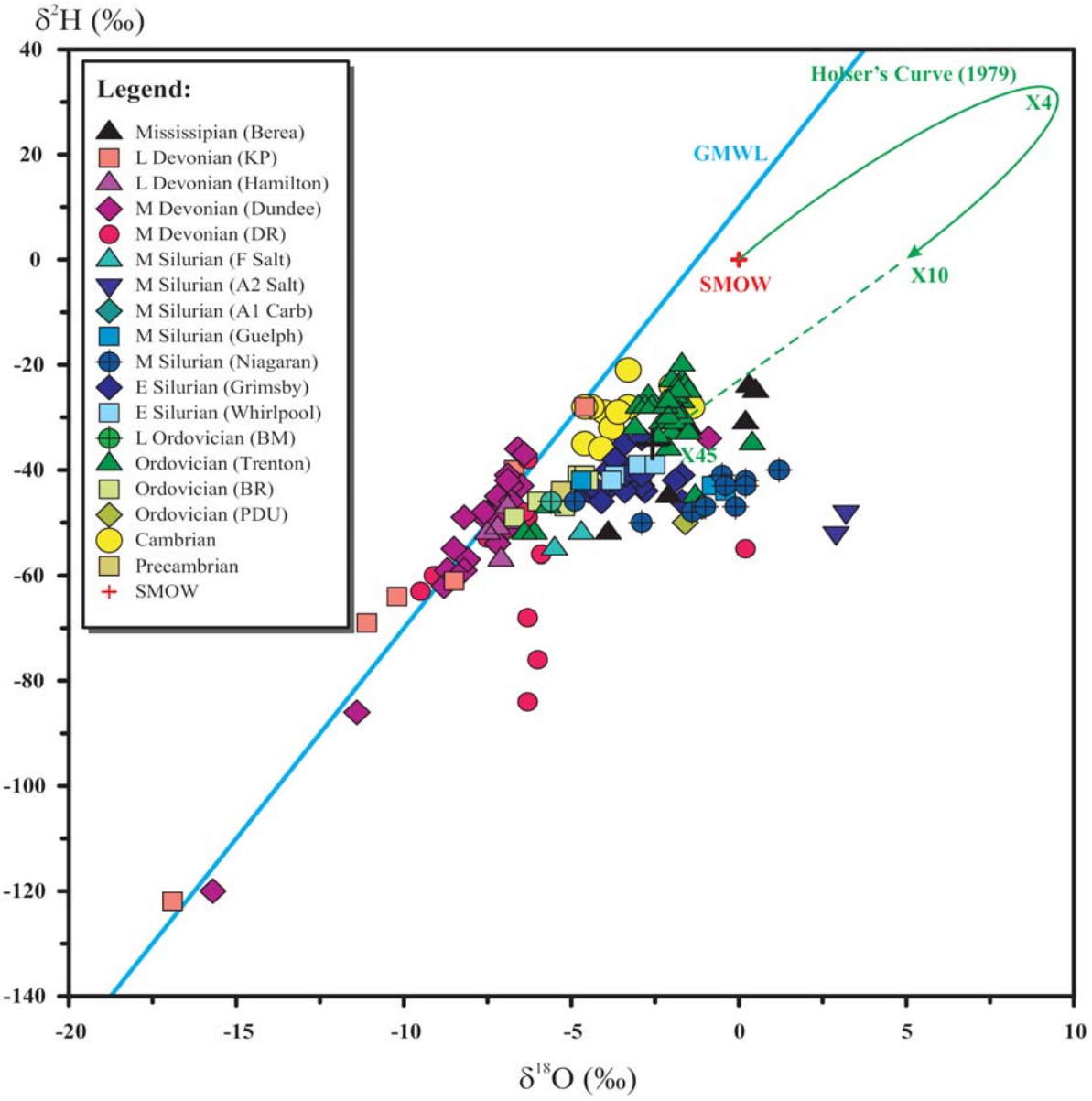

Figure 4.8 δ^2H_{VSMOW} (‰) versus $\delta^{18}O_{VSMOW}$ (‰) of all southern Ontario and Michigan formation waters grouped based on the stratigraphic units from which they were sampled.

4.6.3 $\delta^{37}Cl$ and $\delta^{81}Br$ Compositions

As mentioned earlier, the samples that were investigated in this study were collected by S.K. Frape's students and colleagues over the past twenty years. The fact that some samples no longer existed limited the number of analyses for chlorine and bromine isotopes and imposed a "forced selection" based on the availability of the samples. The $\delta^{37}Cl$ and $\delta^{81}Br$ values of the formation waters show large variations (between -1.31 ‰ and +1.82 ‰ relative to SMOC and between -0.95 ‰ and +2.31 ‰ relative to SMOB, respectively) (Table 4.2). The $\delta^{37}Cl$ range is within the known variation for chlorine stable isotopes of formation waters (Kaufmann et al., 1984; Desauliners et al., 1986; Kaufmann et al., 1988; Eastoe and Guilbert 1992; Kaufmann et al., 1993; Eggenkamp 1994; Liu et al., 1997; Eastoe et al., 1999; Eastoe et al., 2001; Ziegler et al., 2001; Frape et al., 2004; Stewart and Spivack 2004) and $\delta^{81}Br$ values are also within the range reported for formation waters (Eggenkamp and Coleman, 2000; Shouakar-Stash et al., 2005a, 2007).

The $\delta^{81}Br$ and $\delta^{37}Cl$ ranges of the different formation waters are illustrated in Figure 4.9 and presented in Table B.2 (Appendix B). The isotopic results plot in distinctive areas based on the stratigraphic units to which they belong. Figure 4.10 illustrates the $\delta^{81}Br$ and $\delta^{37}Cl$ composition as a function of depth. Generally, the deeper samples are from the central part of the Michigan Basin. In the following sections, these isotopic results will be examined based on the stratigraphic units they belong to and the geographic area from which they were sampled.

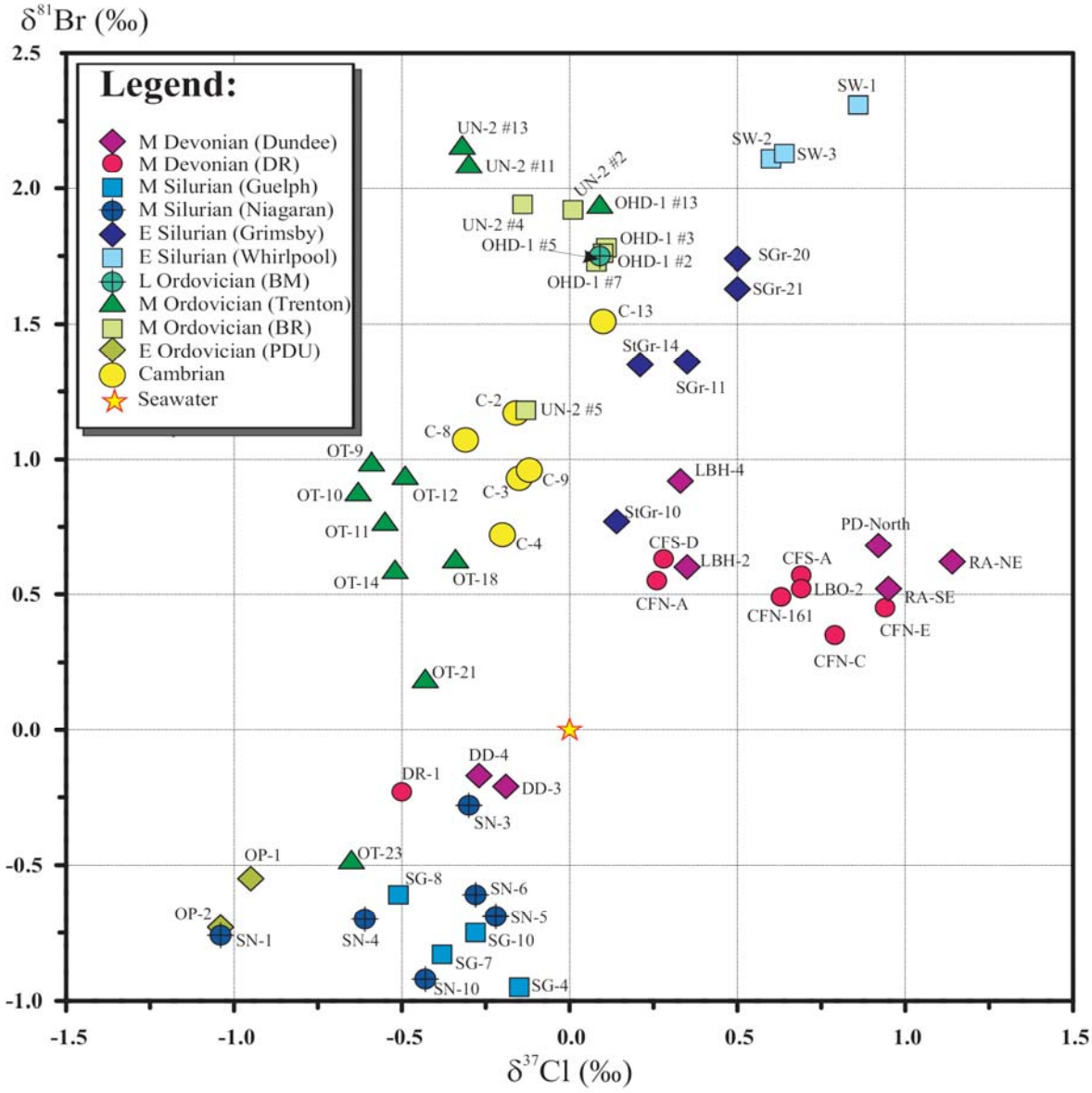

Figure 4.9 δ^{81}Br signatures versus δ^{37}Cl signatures of southern Ontario and Michigan formation waters based on the stratigraphic units they were sampled from.

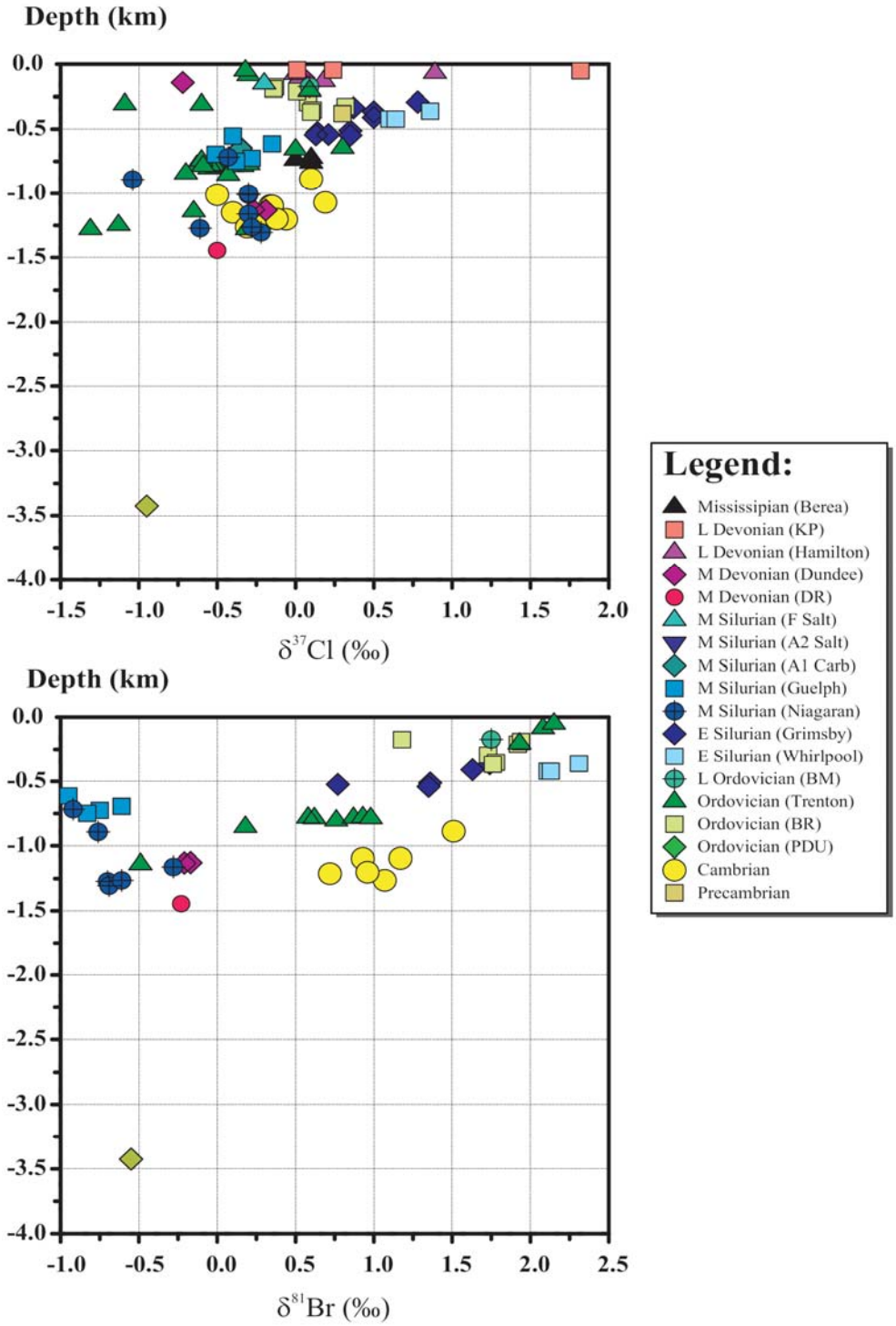

Figure 4.10 $\delta^{37}Cl$ and $\delta^{81}Br$ versus depth of southern Ontario and Michigan formation waters based on stratigraphic units from which they were sampled.

4.6.3.1 Devonian

Three of the Devonian formations waters are from 1200 to 1500 m depth from the central part of the Michigan Basin; DR-1 is from the carbonate Richfield Member of the Detroit River Group and DD-3 and DD-4 are from the carbonate Dundee Formation. The $\delta^{81}Br$ compositions of these three samples are almost identical, however their $\delta^{37}Cl$ are slightly different, where the $\delta^{37}Cl$ composition of DR-1 is more depleted than that of DD-3 and DD-4. The Detroit River Group water (DR-1) is Ca-Na-Cl type water, while the Dundee Formation waters (DD-3 and DD-4) are Na-Ca-Cl type. The water chemistry of the Dundee Formation indicates halite dissolution. As halite has a low Br content, this process is not expected to affect the Br isotopic signature. However, if the chlorine isotopic compositions of the halite involved and the brine are different, the $\delta^{37}Cl$ values are expected to be altered (the reported range of $\delta^{37}Cl$ of evaporites is -0.9 ‰ to +0.9 ‰ (Eastoe et al., 2007)). The similar $\delta^{81}Br$ isotopic compositions of these three samples suggest that the highly concentrated brine in both formations have a common origin. The variations in the $\delta^{37}Cl$ suggest a process (halite dissolution) that affected the brines in one of the formations (Dundee Formation) but not the other (Detroit River Group). This is confirmed by the chemistry (increase of Na and the change of water type). The direction of $\delta^{37}Cl$ shifts toward enriched values indicates the $\delta^{37}Cl$ of the halite involved in this process is relatively enriched in comparison to that of the Ca-rich brine.

Three more samples from Michigan were analyzed for only $\delta^{37}Cl$. The three samples (WSMC2-10, HGRD4-6 from the central part of the basin and sample SPA2-32 from the

northern margins of the basin) are from the Late Devonian Antrim shale Formation (equivalent to Kettle Point Formation in southern Ontario). The $\delta^{37}Cl$ compositions of all three waters are negative (-1.11 ‰, -0.35 ‰ and -0.39 ‰, respectively). These three samples are Na-Cl type waters and they are largely affected by halite dissolution (see Table B.1 and Figure B.8 (Appendix B)). The high salinity of the Antrim Shale formation waters of the Michigan Basin were reported by Martini et al., 1998 and McIntosh et al., 2004 to be the result of mixing between meteoric fresh water recharge which had dissolved halite and Devonian carbonate–hosted brines. Figure B.8 supports the possible impact of halite dissolution. Oxygen and hydrogen isotope signatures indicate that the source of freshwater recharge was likely Pleistocene glacial melt-water or modern precipitation. Although, these samples suffered dilution by fresh water or melt-water, the $\delta^{37}Cl$ values of these samples is mainly controlled by the $\delta^{37}Cl$ signatures of the halite and the original evaporated paleoseawater end members.

The remaining of the Devonian water samples were collected from shallow depths (Figure 4.10) in the marginal parts of the Michigan Basin in southern Ontario. These water samples are also from the Middle Devonian Dundee Formation and the Middle Devonian Detroit River Group. Samples LBH-2, LBH-4, PD-North, RA-NE and RA-SE are from the Dundee Formation, while samples CFS-A, CFS-D, CFN-A, CFN-C, CFN-E, CFN-161 and LBO-2 are from the Detroit River Group. The $\delta^{81}Br$ and $\delta^{37}Cl$ compositions of these samples are totally different from their counterparts in the central parts of the Michigan Basin. The $\delta^{81}Br$ and $\delta^{37}Cl$ compositions of these samples are enriched in both. The larger variation of $\delta^{37}Cl$

when compared to $\delta^{81}Br$ (Figure 4.9) suggest the involvement of end members that are poor in Br but rich in Cl such as halite which is confirmed based on the chemistry. The wide variations of the $\delta^{37}Cl$ of the samples from both formations cannot be explained by the amount of dilution because no systematic relationship is observed between the TDS of these samples and the isotopic values.

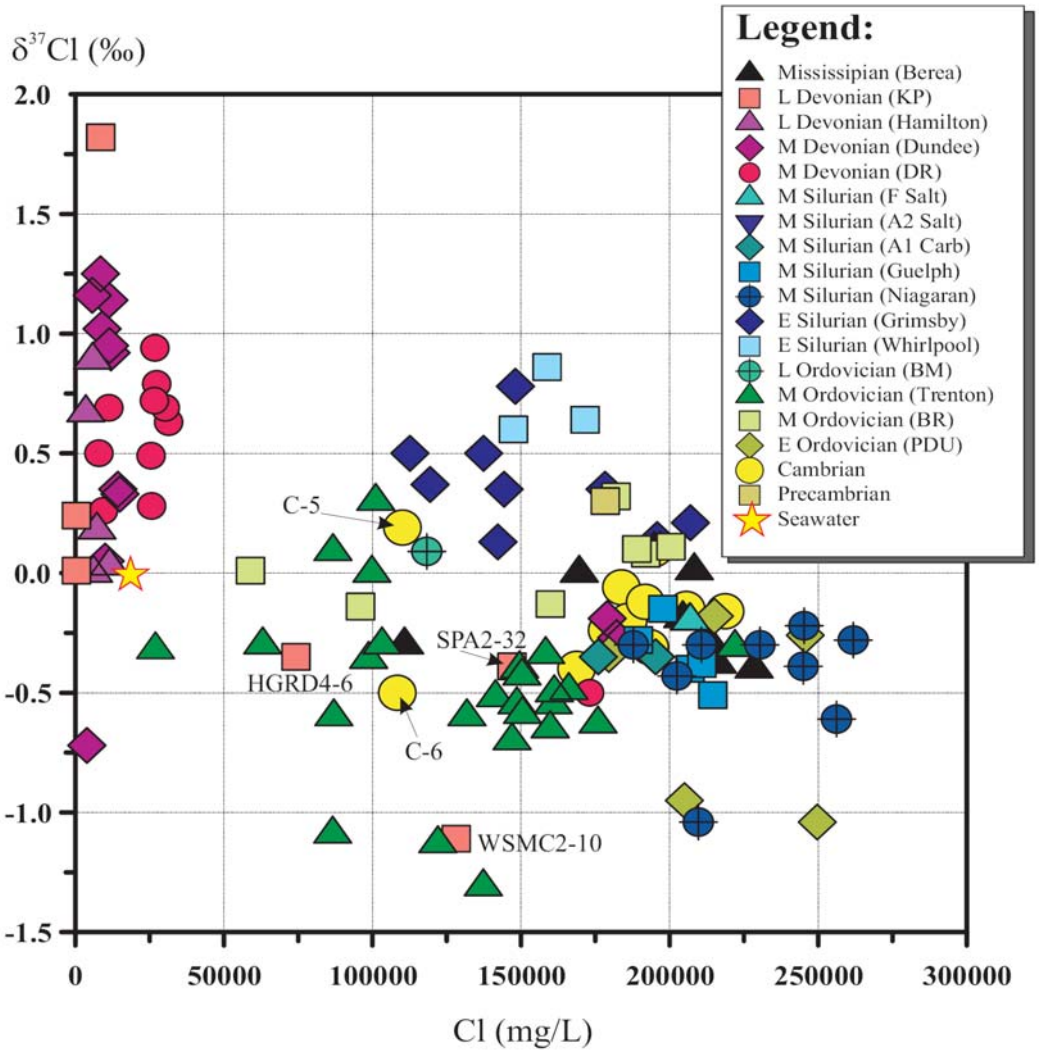

Figure 4.11 $\delta^{37}Cl$ Compositions versus Cl (mg/L) of southern Ontario and Michigan formation waters based on stratigraphic units.

The Late Devonian Kettle Point (shale) Formation and Late Devonian Hamilton (shale) Formation water samples from southern Ontario were only analyzed for $\delta^{37}Cl$. The results showed large $\delta^{37}Cl$ variations of the waters (~1.8 ‰ and ~1.0 ‰, respectively) (Figure 4.11). These values are very similar to those found in the Devonian carbonates underlying the Kettle Point and Hamilton formations which suggest a common origin and evolutionary processes. However, the Br/Cl weight ratio of the carbonate formation waters are larger than that of seawater (Figure 4.12) indicating a residual evaporated paleoseawater end member while shale formation waters are characterized by lower Br/Cl ratios than that of seawater indicating non-marine water component and/or halite dissolution component. The large variation of $\delta^{37}Cl$ values of these samples suggests that the evaporated paleoseawater and halite dissolution are not controlling the $\delta^{37}Cl$ values of these samples. This is a reflection of an active system with various mixing scenarios between diverse end members. This is supported by the fact that most of these samples are from shallow depths which makes them more susceptible to mixing with recharging waters.

4.6.3.2 Silurian

The Silurian water samples belong to two groups: Early Silurian brines from sandstones sourced from the Appalachian basin and Middle Silurian brines from carbonates sourced from Michigan and southern Ontario. The $\delta^{37}Cl$ and $\delta^{81}Br$ values of these two groups are very distinct (Figure 4.9). The brines from the Early Silurian sandstone formations are

enriched in both isotopes relative to the brines from the Middle Silurian carbonate formations.

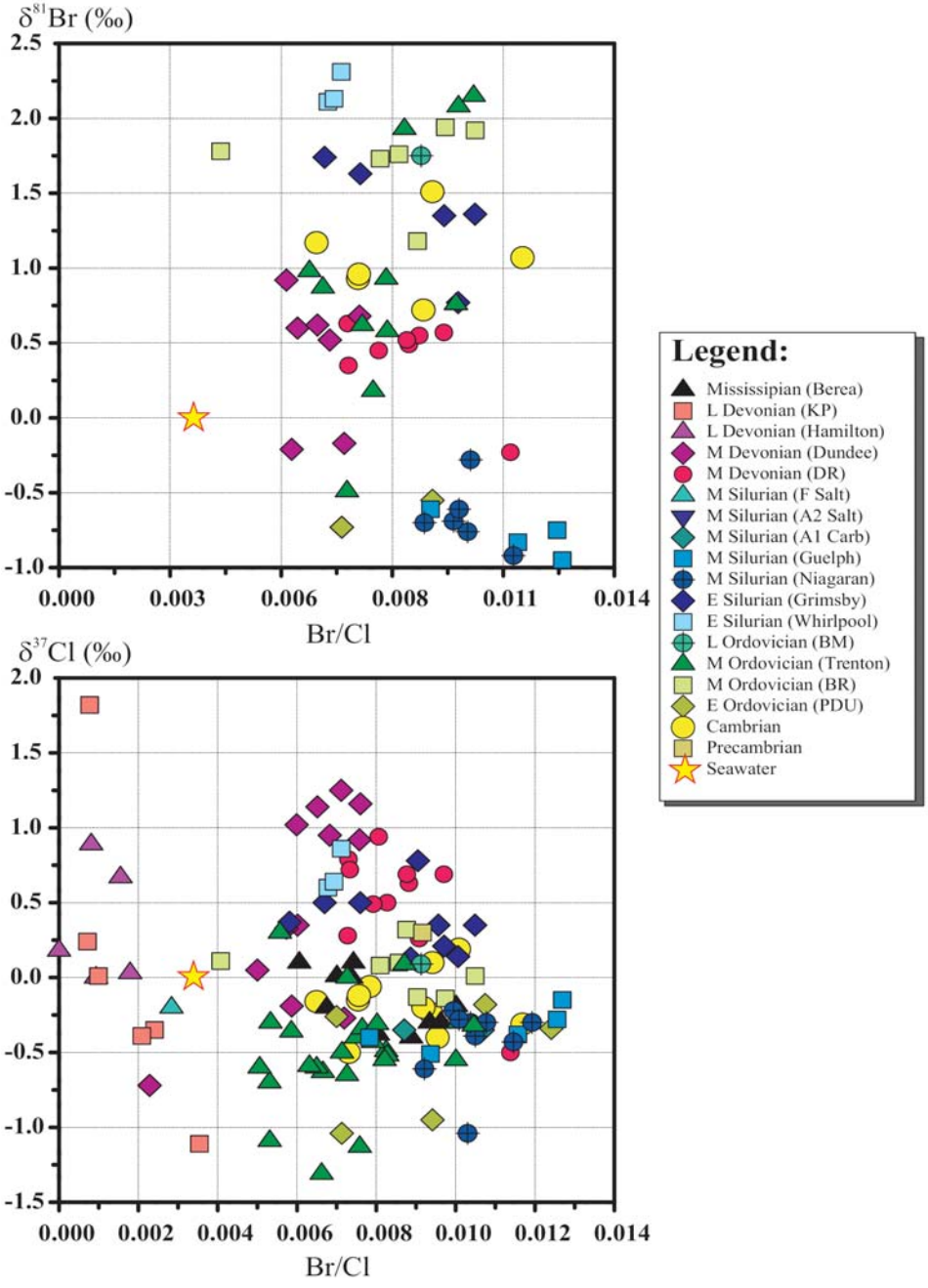

Figure 4.12 $\delta^{37}Cl$ and $\delta^{81}Br$ compositions versus Br/Cl (mg/L) of southern Ontario and Michigan formation waters based on stratigraphic units from which they were obtained.

The first group of Silurian formation waters was collected from two Early Silurian age formations (Whirlpool sandstone Formation and Grimsby sandstone Formation). All of these samples were collected from the Silurian formations below Lake Erie, from the western margin of the Appalachian Basin. The $\delta^{37}Cl$ and $\delta^{81}Br$ of the Whirlpool Formation brines (SW-1, SW-2 and SW-3) fall in narrow ranges (+0.60 ‰ to +0.86 ‰ and +2.11 ‰ and +2.31 ‰, respectively). The $\delta^{37}Cl$ and $\delta^{81}Br$ of the Grimsby Formation brines also fall in narrow ranges (+0.21 ‰ to +0.50 ‰ and +1.35 ‰ and +1.74 ‰, respectively), when excluding one sample (STGr-10; $\delta^{37}Cl$ = +0.14 ‰ and $\delta^{81}Br$ = +0.77 ‰).

The Whirlpool Formation brines seem to have been diluted by seawater or fresh water based on the deviation from the seawater evaporation line in Figure 4.6 and also based on their change in Na and Cl concentrations (Figure B.8). The relatively high TDS (230,000 to 270,000 mg/L) of these samples suggests that their isotopic compositions were not altered dramatically by dilution, unless the diluting end member(s) had extremely enriched isotopic signatures, which is not common. Physical processes that can cause isotopic fractionations such as diffusion and ion filtration cannot explain the $\delta^{81}Br$ values of these brines, which are relatively positive in comparison to $\delta^{37}Cl$ values. This is because these two physical processes should fractionate the chlorine isotopes more than the bromine isotopes due to mass differences between their isotopes. Furthermore, little support exists for extensive water-rock interaction based on the $\delta^{18}O$ values of these waters. Therefore, a possible hypothesis for the origin of these brines is that the original fluid (e.g. seawater) that was concentrated to produce these brines was initially enriched in both isotopes (^{81}Br and ^{37}Cl).

The Grimsby Formation brines are characterized by a larger range of TDS variation (187,000 mg/L to 326,000 mg/L) and by less enriched $\delta^{37}Cl$ and $\delta^{81}Br$ signatures in compared to the Whirlpool Formation brines (Figure 4.9). In general, TDS compositions seem to increase with depth along with depletion in both isotopes. It is possible that the low TDS samples are diluted by less saline waters that are isotopically more enriched than the Grimsby Formation fluids. The isotopic results obtained from the brines of these two formations (Whirlpool and Grimsby) suggest either mixing between the two stratigraphic units (Figure 4.9) or a common evolutionary process that affected both isotopic signatures ($\delta^{37}Cl$ and $\delta^{81}Br$) of these brines and caused larger isotopic fractionations to the bromine isotopes.

Several more samples were analyzed from the Grimsby Formation for $\delta^{37}Cl$ only and the results obtained for $\delta^{37}Cl$ fall in the same range given above. This further confirms that all Early Silurian sandstone formation waters are isotopically enriched (positive).

The second group of Silurian brines is from the Middle Silurian age carbonate Niagaran Group and Guelph Formation (which is also part of the Niagaran Group). All of the Niagaran Group brines were collected from Michigan. Wells SN-1, SN-3, SN-4, SN-5 and SN-6 were sampled in close proximity to the central part of basin and well SN-10 was sampled at the eastern margin of the basin. The Guelph Formation brines (SG-4, SG-7, SG-8 and SG-10) were sampled from the eastern margin of the Michigan Basin in southern Ontario. In general, the Silurian fluids are among the most concentrated brines (TDS between 300,000 mg/L and

400,000 mg/L) in this study. All of these brines are Ca-rich with water types ranging between Ca-Cl, Ca-Mg-Cl and Ca-Na-Cl.

The $\delta^{37}Cl$ and $\delta^{81}Br$ compositions of these formation waters are very distinctive from the Early Silurian sandstone brines discussed above (Figure 4.9). These formation waters are characterized by negative isotopic compositions of $\delta^{37}Cl$ and $\delta^{81}Br$. These differences may be attributed to the fact that these waters are from different ages or to the fact that they are from different basins (the Middle Silurian carbonate formations were sampled from within the Michigan Basin and the Early Silurian sandstone formations were sampled on the margin of the Appalachian Basin). Either way, this can be useful when trying to identify the origin of waters in the marginal areas between the two basins where separation is not easy and mixing is expected to dominate.

The $\delta^{37}Cl$ and $\delta^{81}Br$ signatures of the Niagaran Formation brines range between -1.04 ‰ and -0.22 ‰ and between -0.92 ‰ and -0.28 ‰, respectively. Generally, the brines from Guelph Formation and the Niagaran Group are Ca-Na-Cl type waters and are characterized by the same range of $\delta^{81}Br$. The only sample that is outside this range is SN-3 which is also characterized by a different water type (Ca-Mg-Cl). This might suggest that the change in water type and the more enriched $\delta^{81}Br$ signatures are related and caused by the same process. The presence of dolomitic limestone in the Niagaran Group (Liberty and Bolton, 1971) is probably supporting evidence of a dolomitization process that took place in the Niagaran Group and involved Mg-rich saline water such as seawater as suggested by Coniglio et al. (2003) in their evaporative drawdown model to explain dolomitization.

Additional samples from the Guelph and Niagaran carbonate formations were analyzed for only $\delta^{37}Cl$ only. The $\delta^{37}Cl$ compositions of these samples fall within the same isotopic range as reported in Tables 4.2. In summary, all waters collected from the Silurian carbonate formations are characterized by negative $\delta^{37}Cl$ and $\delta^{81}Br$ compositions. The variations are generally narrow except for few scattered samples that extend the range (Figure 4.9). It is unlikely that the host materials (clastic versus carbonates) contain enough bromine or chlorine to influence or change the fluid isotopic signatures over long periods of time or during a specific event such as orogenic hydrothermal activity. Therefore, it is more likely that the distinctive positive and negative isotopic ($\delta^{37}Cl$ and $\delta^{81}Br$) signatures of the formation waters from the Silurian aged sandstones and carbonates, respectively, are due to geological age differences (seawater isotopic change with time) or the fact that the stratigraphic units are geographically associated with different basins.

4.6.3.3 Ordovician

The Ordovician formation waters analyzed for $\delta^{37}Cl$ and $\delta^{81}Br$ composition were sampled from different stratigraphic units ranging from Early to Late Ordovician at depths ranging from 50 m to 3000 m. Geographically, these Ordovician formation waters cover a large geographic area that extends from the center of the Michigan Peninsula in the west to the north shore of Lake Ontario in the east (Figure 4.1 and Figure 4.18).

Two water samples were collected from the central part of the basin and analyzed for both $\delta^{37}Cl$ and $\delta^{81}Br$ compositions. Sample OP-1 and OP-2, from the Early Ordovician sandstone Prairie du Chien Formation, are characterized by a high TDS (325,400 mg/L and 391,500 mg/L, respectively) and depleted $\delta^{37}Cl$ and $\delta^{81}Br$ compositions (OP-1; $\delta^{37}Cl$ = -0.95 ‰ and $\delta^{81}Br$ = -0.55 ‰, OP-2; $\delta^{37}Cl$ = -1.04 ‰ and $\delta^{81}Br$ = -0.73 ‰). Two additional samples from the same formation and also from the central part of the basin were analyzed for $\delta^{37}Cl$ composition only, and the results showed that both samples are also depleted in $\delta^{37}Cl$ (Lahar-17; $\delta^{37}Cl$ = -0.26 ‰, Prass 1-12; $\delta^{37}Cl$ = -0.34 ‰), confirming the depleted isotopic nature of the brines of the Prairie du Chien Formation.

Sample OT-23 (from the Middle Ordovician carbonate Trenton Group from the southern part of the central area of the Michigan Basin) is also characterized by depleted values for both $\delta^{37}Cl$ and $\delta^{81}Br$ compositions ($\delta^{37}Cl$ = -0.65 ‰ and $\delta^{81}Br$ = -0.49 ‰).

Seven samples (OT-9, OT-10, OT-11, OT-12, OT-14, OT-18 and OT-21) were sampled from the Middle Ordovician carbonate Trenton-Black River Group from the marginal parts of the Michigan Basin in southern Ontario (Chatham Sag). These samples are characterized by positive $\delta^{81}Br$ and negative $\delta^{37}Cl$ composition. The samples show enrichment in $\delta^{81}Br$ and some enrichment in $\delta^{37}Cl$ in comparison to the OT-23 sample from Michigan. The $\delta^{37}Cl$ and $\delta^{81}Br$ signature of these samples range between -0.63 ‰ and -0.34 ‰ and between +0.18 ‰ and +0.98 ‰, respectively. All of these samples are Na-Ca-Cl type waters and are characterized by high TDS (234,000 mg/L – 273,000 mg/L). The chemical compositions of these samples (Table B.1, Figure 4.6 and Figure B.8) suggest that they were diluted by less

saline water such as seawater and they also suggest that they were impacted by halite dissolution. This is supported by the $\delta^{18}O$ and $\delta^{2}H$ composition (Figure 4.8). The relatively large enrichment in $\delta^{81}Br$ is difficult to explain by only dilution and halite dissolution. The $\delta^{81}Br$ results suggests that OT-23 and the other seven OT samples from southwestern Ontario are not of a common origin (i.e. the original brines in these two areas are different) or if they are of a common origin, they underwent different evolutionary processes that affected the $\delta^{81}Br$ signatures in different ways. Budai and Wilson (1991) investigated the diagenetic history of the Trenton Group and they concluded that these formations were diagenetically altered by a complex sequence of events. They concluded that different parts of the basin have distinct types of dolomite suggesting different dolomitization mechanisms. For example regional dolomite, occurs on the west and southwest side of the Michigan Basin where sample OT-23 was collected, while fracture dolomite occurs in south western Ontario where the other OT samples were collected. They concluded that regional dolomite was driven by a mixture of marine and meteoric waters within Trenton and Black River Formations adjacent to the Wisconsin arch, while fracture dolomite in southern Ontario is closely associated with MVT alteration and mineralization of major hydrocarbon reservoirs. They also reported that the latest stage of fracture dolomite cement is coincident with liquid hydrocarbon movement into the reservoirs. The $\delta^{37}Cl$ and $\delta^{81}Br$ signature observed during this study from the Trenton brines, supports the conclusion made by Budai and Wilson (1991) of different fluids affecting different parts of the basin. Furthermore, the $\delta^{37}Cl$ compositions of these waters fall within

the range of $\delta^{37}Cl$ of MVT waters (-1.1 ‰ to 0.0 ‰) found in the literature (Eastoe and et al., 1989; Eastoe and Guilbert, 1992).

Another 12 OT samples were only analyzed for $\delta^{37}Cl$ and the results showed that all $\delta^{37}Cl$ are negative, however, the range was extended slightly to be between -0.7 ‰ and -0.3 ‰. This confirms the negative $\delta^{37}Cl$ isotopic signatures of the OT waters in Michigan.

The rest of the water samples are from north shore of Lake Ontario. The formation waters belong to several stratigraphic units and they were sampled from shallow depths that range between 50 and 368 metre. Samples UN-2 #2, UN-2 #4, UN-2 #5, OHD-1 #2, OHD-1 #3, and OHD-1 #7 are from the Middle Ordovician Black River Group. Samples UN-2 #11, UN-2 #13, and OHD-1 #13 are from the Middle Trenton Group. Sample OHD-1 #15 is from the Late Ordovician Blue Mountain Formation.

These formation waters show more $\delta^{81}Br$ enrichment in comparison to all previous Ordovician samples and they also show small enrichments in $\delta^{37}Cl$. In general, these samples are characterized by. The TDS values of these samples have a large range (44,000 mg/L to 304,000 mg/L) suggesting extensive dilution to some of these samples. This is also supported by the $\delta^{18}O$ and $\delta^{2}H$ results of these samples (Figure 4.8). The presence of tritium in these samples is a reflection of very recent dilution or simply dilution with drilling fluids that compromised the integrity of these samples. It is believed that the Darlington samples were compromised by drilling fluids (Frape, personal communications). However, mixing with drilling waters should not affect the isotopic ($\delta^{37}Cl$ and $\delta^{81}Br$) compositions of the brines, as

the Cl and Br concentration in these waters is dominated by that of the original brines and hence the isotopic compositions are still the reflection of the alteration or mixing that happened prior to this recent incident.

In summary, the $\delta^{37}Cl$ and $\delta^{81}Br$ signature of brines collected from the Ordovician formations illustrate a similarity to those observed from the Silurian formation waters. In both cases (Ordovician and Silurian) formation waters from the central parts of the Michigan Basin are characterized by more depleted isotopic signatures in comparison to the formation waters from the marginal areas. This indicates that the formation waters in these stratigraphic units are either of different origins and/or they experienced different evolutionary processes and/or mixed with different intrusion fluids that altered their isotopic signatures by mixing.

4.6.3.4 Cambrian

Brines from the Cambrian formations are characterized by $\delta^{37}Cl$ and $\delta^{81}Br$ values of -0.50 ‰ to +0.19 ‰ and +0.72 ‰ to +1.51 ‰, respectively (Table 4.2). All of the Cambrian formation waters are from southern Ontario (i.e. the marginal parts of the Michigan and Appalachian basins). These samples are characterized by high TDS compositions (174,000 mg/L to 337,000 mg/L). Although they are isotopically similar or close to the OT samples, their compositions are still distinct (Figure 4.9). All of these samples are Ca-Na-Cl type waters, except for C-6 which is Na-Ca-Cl type water. Based on the TDS values, C-5 and C-6 experienced the most dilution. The $\delta^{18}O$ and $\delta^{2}H$ compositions of these two samples (Table

4.2), however, show that they were not diluted by the same type of waters. This is also supported by the shifts of the $\delta^{37}Cl$ signatures of the two samples (Figure 4.11). The results obtained from the Cambrian formation waters further confirms that the formation waters in southern Ontario are different to those found in the Michigan Basin.

4.6.3.5 Summary

The $\delta^{37}Cl$ values versus Cl concentrations (mg/L) illustrated in Figure 4.11 shows that there is no obvious relationship observed between $\delta^{37}Cl$ and Cl concentrations of these formation waters. In general, samples with similar Cl concentrations are found to have a large range of $\delta^{37}Cl$ and vice versa. Similarly, the $\delta^{81}Br$ versus Br concentrations (mg/L) of all formation waters illustrated in Figure 4.13 does not show any obvious relationship between the concentration of Br and the $\delta^{81}Br$. Therefore, the variations of the isotopes of these two elements cannot be attributed simply to physical processes such as diffusion and ion filtration that are associated by differences in concentrations as well.

Figure 4.14 illustrates the relationship between $\delta^{81}Br$ and K (mg/L) as well as the relationship between $\delta^{37}Cl$ and K (mg/L). These two plots show two trend that are labelled A and B. The first trend (A) shows a small but gradual increase in the concentration of K associated with a depletion of both isotopic signatures ($\delta^{81}Br$ and $\delta^{37}Cl$) and the second trend (B) shows a large increase in the K concentration, however with no obvious change in the isotopic signatures of both elements ($\delta^{81}Br$ and $\delta^{37}Cl$). The first trend (A) suggests mixing

between two end members; 1) K-poor that is isotopically enriched and 2) K-rich which is isotopically depleted. However, the second trend is most likely to represent a process (e.g. water-rock interaction) that enriched these waters with K. Figure 4.15 illustrates the relationship between δ^{81}Br versus K/Br and δ^{81}Br versus Ca/Br. This plot illustrates also the K/Br and Ca/Br of some of the highly concentrated brines of this study relative to seawater.

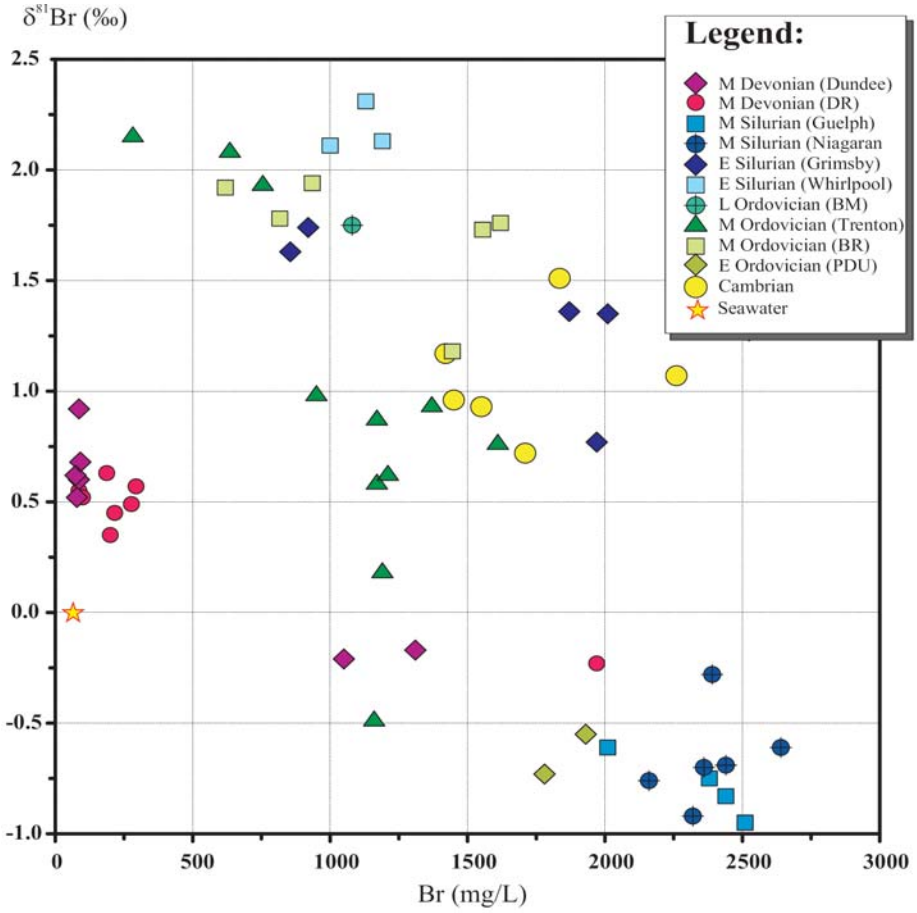

Figure 4.13 δ^{81}Br signatures versus Br (mg/L) of southern Ontario and Michigan formation waters based on stratigraphic units.

All brines show higher Ca/Br ratios than seawater and almost all of the samples show K/Br ratios that are lower than the seawater ratio. The increase of Ca/Br in formation waters is

usually attributed to dolomitization, albitization and dissolution of feldspar (Das et al., 1990; Stueber et al., 1993). Since the increase of Ca and Sr in the brines of this study exceeds the depletion of the Mg, then dolomitization is not the only process and albitization and dissolution of feldspar are also involved in the evolution of these brines. Although the K/Br ratios of these brines are lower than seawater in most of the brines, they are in general higher than what is usually reported for formation waters (Stueber et al., 1993). The depletion of K in formation waters is usually attributed to reactions with low-K clay minerals (Stueber et al., 1993) and the elevation of K in formation waters is usually associated with hotter, K-feldspar/burial diagenetic conditions (Drever, 1988; Lynch et al., 1997). The elevated K of these brines lends support to the dissolution of feldspar suggested above to explain the elevation of Ca and Sr. The enriched $\delta^{18}O$ values of these brines (Figure 4.16) suggest that these brines have undergone elevated temperatures and water-rock interaction in the past which lends support to the suggested process. The process that evolved the K-rich and Ca-rich brines does not seem to cause isotopic changes ($\delta^{81}Br$ and $\delta^{37}Cl$) suggesting that the original brines emplaced or original waters that these brines were formed from were already depleted in both isotopes prior to the digenesis process (i.e. the seawater that these brines originated from was depleted). Although the degree of water-rock interaction can be extensive as we observed from the elevation of Ca and enrichment of the $\delta^{18}O$ values of these brines, the high water/rock ratio and more importantly the high salinity of these brines limits the chlorine and bromine that can be leached or exchanged with rock and consequently alter the isotopic signatures of these two elements. Furthermore, the low K/Br ratio of some of

these brines which is usually associated with reaction with clay minerals does not seem to be associated with any isotopic (δ^{81}Br and δ^{37}Cl) alterations.

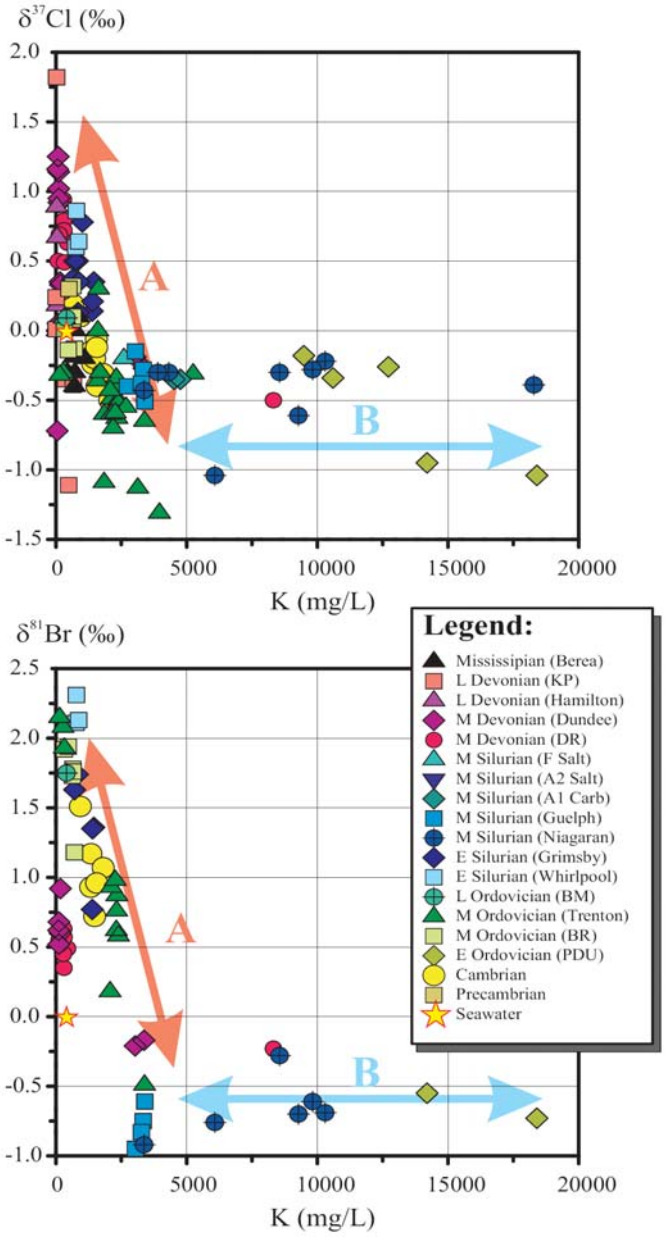

Figure 4.14 δ^{37}Cl versus K (mg/L) and δ^{81}Br versus K (mg/L) of southern Ontario and Michigan formation waters based on stratigraphic units.

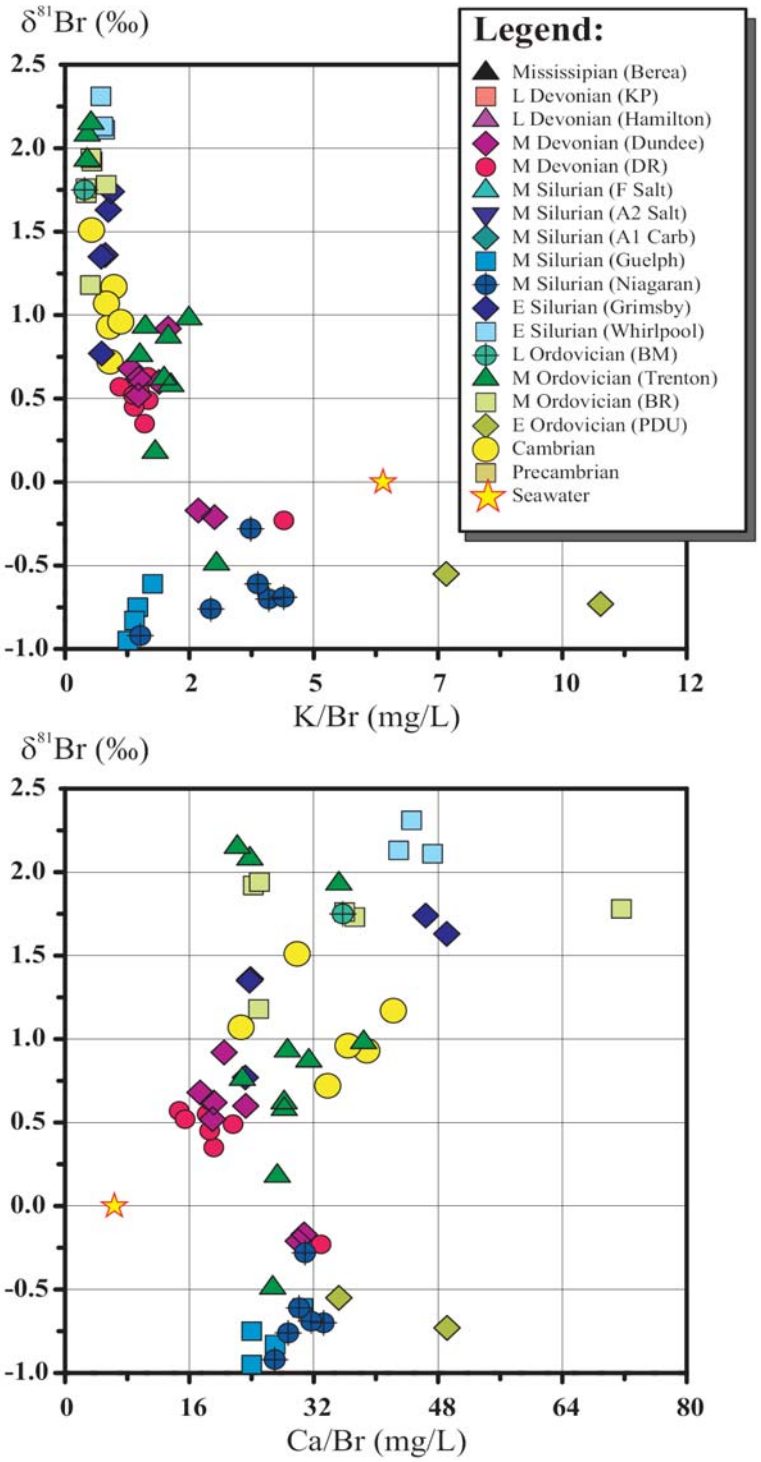

Figure 4.15 δ^{81}Br versus K/Br (mg/L) and Ca/Br (mg/L) of southern Ontario and Michigan formation waters based on stratigraphic units.

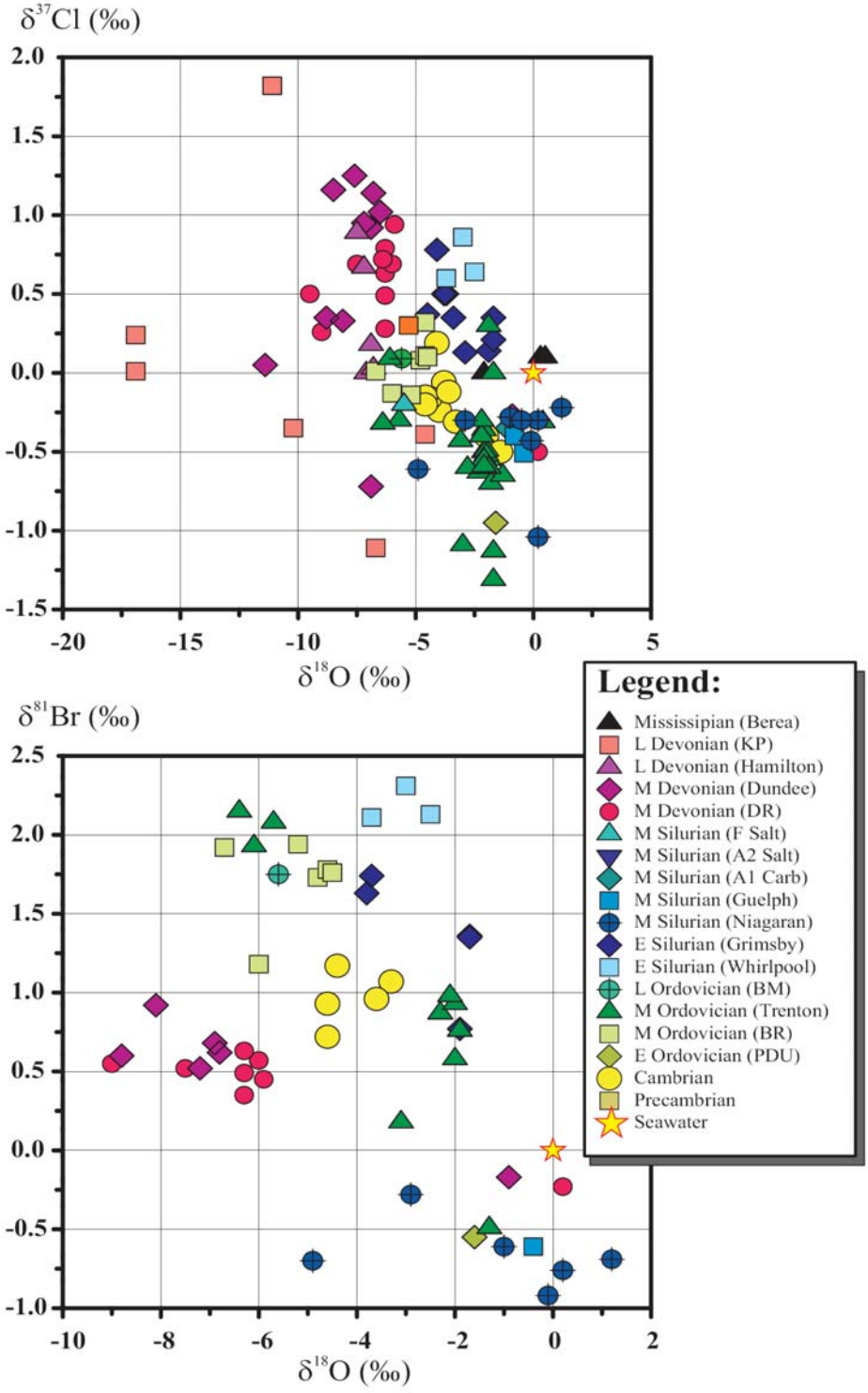

Figure 4.16 $\delta^{37}Cl$ versus $\delta^{18}O$ and $\delta^{81}Br$ versus $\delta^{18}O$ of southern Ontario and Michigan formation waters based on stratigraphic units.

Figure 4.17 illustrates the relationship between (δ^{81}Br versus Br/Cl (mg/L) and δ^{37}Cl versus Br/Cl (mg/L). The Br/Cl ratio of formation waters is typically used to distinguish between different brines originating from various sources (e.g. halite dissolution versus seawater concentration). The formation waters collected from the various stratigraphic units in this study are characterized by large Br/Cl variations, where almost all stratigraphic units are characterized by the same range of Br/Cl variations. Furthermore, although some isotopic (δ^{81}Br and δ^{37}Cl) differences are observed between the different brines from the different formations (Figure 4.9), overlaps do exist and a clear separation is not obvious. Nonetheless, the samples presented in Figure 4.17 can be grouped into groups A and B. Group A are samples collected northwest of the Algonquin Arch and group B are samples collected southeast of the Algonquin Arch (Figure 4.18). The δ^{37}Cl and δ^{81}Br show some distinctive differences between the samples collected from north (west) of the Algonquin Arch, and those collected from southeast of the Algonquin Arch (Figure 4.17 and Figure 4.18). All of the brines from group A are characterized by depleted isotopic values in comparison with the isotopic values from group B. The δ^{81}Br signatures of the two groups show total separation with no overlaps, unlike the δ^{37}Cl values that show some overlap between the two groups. Although, the chemical parameters (e.g. Br/Cl) and also the δ^{18}O and δ^{2}H show some similarities and overlaps between all samples, the δ^{37}Cl and δ^{81}Br show some distinctive differences between these samples. One of the scenarios that can be put forward is that the arch forms a water divide, where sediments southeast of the arch are dominated by Appalachian Basin processes and formation waters, and the sediments located northwest of

the arch are dominated by the Michigan Basin formation waters. The fact that formation waters from either side of the arch are isotopically (^{81}Br) distinct strongly suggests that the evolutionary processes that affected the waters are very different. Barker and Pollock (1984) studied the geochemistry and origin of natural gases in southern Ontario from Silurian through Cambrian stratigraphic units and they concluded that gases from the Appalachian and the Michigan basins can be distinguished on the basis of their ethane/propane ratio to their isobutene/normal butane ratio. Their study showed that the gases have different ratios on either side of the Algonquin Arch, which led them to suggest that natural gas formation and accumulation in the two basins proceeded under slightly different conditions, or from somewhat different sources. Gas migration and accumulation in southern Ontario from deeper distant sources via permeable vertical pathways was also previously hypothesized to explain the supernormal fluid pressures within sedimentary sequences in southern Ontario (Raven et al., 1992).

The differences in the $\delta^{37}Cl$ and $\delta^{81}Br$ values measured in this study for formation waters associated with these two different gases, suggests different origins or different evolutionary processes for brines from either side of the Algonquin Arch. Whether isotopic differences of the brines and the chemical composition differences of the gases are caused by the same evolutionary processes or by different processes is not clear at this point of time. Further in depth investigation and understanding of the behaviour of these isotopes under different conditions are necessary to answer that question and better understand the whole system.

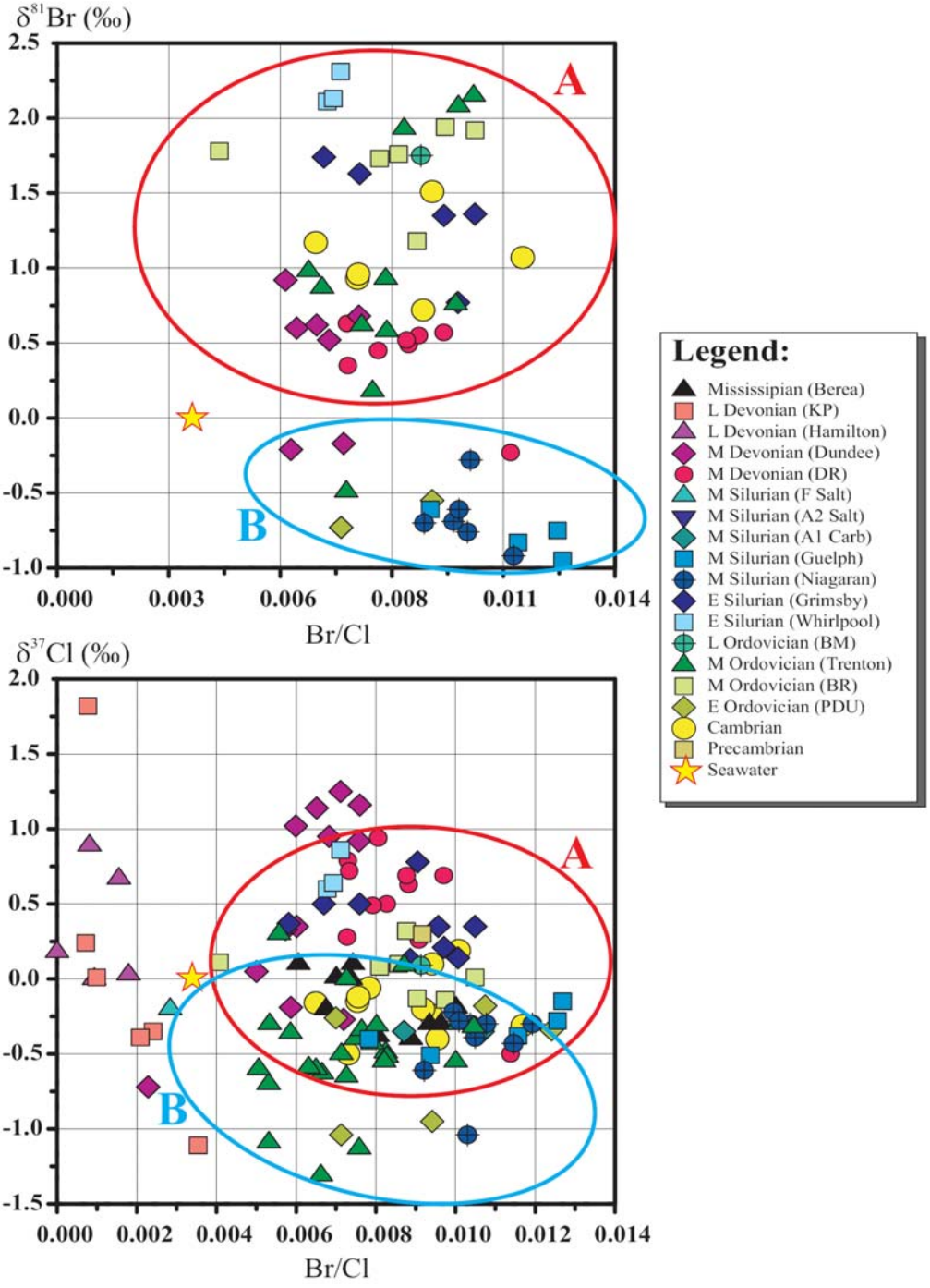

Figure 4.17 $\delta^{37}Cl$ versus Br/Cl (mg/L) and $\delta^{81}Br$ versus Br/Cl (mg/L) of southern Ontario and Michigan formation waters based on stratigraphic units. The plots illustrate two groups (A and B) of brines that were collected northwest and southeast of the Algonquin Arch (Figure 4.18).

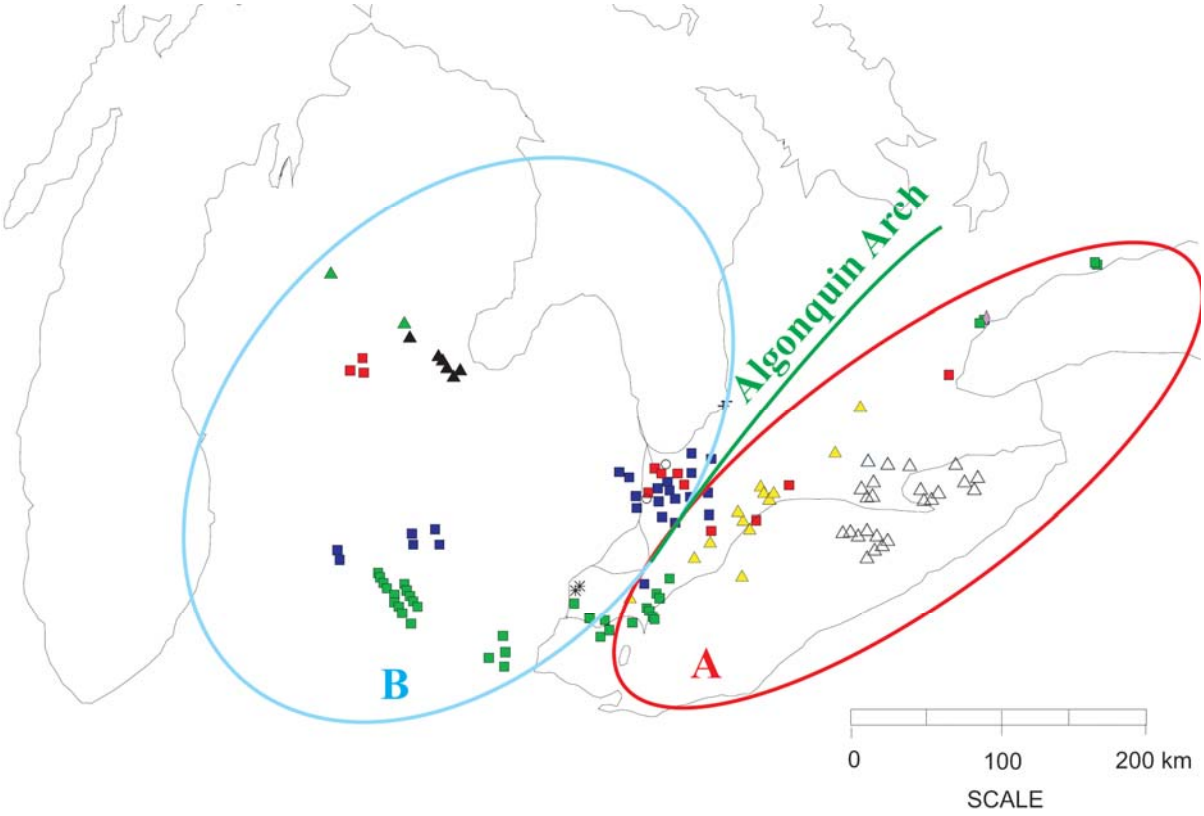

Figure 4.18 Map of the study area that illustrates the sample locations of brines examined in this study. The map shows the location of two groups (A and B) of brines as illustrated in Figure 4.17. These two groups of brines were collected from north west and southeast of the Algonquin Arch.

Similarly, Farquhar et al. (1987) studied the lead isotope ratios in Niagara Escarpment rocks and galenas and they concluded that the isotopic variations they observed are due to separate sources of lead and formation waters originating in the Appalachian Basin and the Michigan Basin. This is consistent also with the hypothesis that was put forward by Haynes and Mostaghel (1979) suggesting that brines migrated northward from the Appalachian Basin

due to the intense compressions in the Paleozoic depocenter caused by the Appalachian orogeny.

The centre of Michigan Basin used to be characterized by a deeper sea than the western margins of the Appalachian Basin (southern Ontario) which is typical for a shallow close to shore environment (Johnson et al., 1992). The deposition during the Ordovician, Late Silurian, Middle to Late Devonian and Mississippian are all characterized by orogen-derived clastic sediments (Uyeno et al., 1982; Johnson et al., 1992), which are more common on the edges of the Appalachian Basin than toward the centre of Michigan Basin where more carbonate sedimentation occurs. It is not possible to relate the isotopic signature and especially bromine isotopic signature to the depositional environment, because formation waters from both clastic and carbonate deposits in the central part of the Michigan Basin are characterized by negative δ^{81}Br signatures (e.g. brines from the Early Ordovician sandstone Prairie du Chien Formation and the Middle Ordovician carbonate Trenton Group). Furthermore, during the Mississippian Period, both the Michigan and the Appalachian basin were dominated by clastic sediments from the Alleghanian Orogeny, with lesser amounts of limestone and coal. Nonetheless, the δ^{37}Cl results of the brines from the Mississippian Berea Formation are all characterized by negative signatures which, based on the results of the current study are typical for the observed values from the Michigan Basin brines. Therefore a relationship between the deposit type and the isotopic signatures cannot be established based on the available data.

4.7 Conclusions

The samples examined in this study are characterized by a large variation in TDS (ranging from less than 1000 mg/L to almost 400,000 mg/L). Generally the most concentrated samples are from the central area of the Michigan Basin and/or from deeper (older) stratigraphic units. Samples from the marginal parts of the basin and especially from younger strata (e.g. Devonian) are relatively less concentrated. The majority of the high TDS samples from the central part of the Michigan Basin are Ca-Na-Cl type waters. Formation waters from the margins of the Michigan Basin and toward the Appalachian Basin are mainly predominated by Na-Ca-Cl type.

The projection of Cl and Br composition on the seawater evaporation line suggests that the origin of these brines is evaporated paleoseawaters, which confirms similar conclusions made by previous researchers (e.g. Dollar et al., 1991). The majority of the formation waters were diluted by less saline waters (e.g. seawater and/or freshwater). Brines from the older formations such as Precambrian, Cambrian and Ordovician most likely originated from evaporated paleoseawater by dilution with more recent seawater. Generally, the degree of dilution increases with distance from the central part of the basin and towards the marginal areas. The contribution of halite dissolution is minor and it is restricted to marginal areas.

The $\delta^{2}H$ and $\delta^{18}O$ values for the various water types show that the Ca-Cl type waters are the least affected by dilution. They also show that most Na-Ca-Cl type waters were affected by dilution with seawaters based on the shifts of the $\delta^{2}H$ toward more enriched values. The

position of the low TDS samples close to the GMWL suggests a large fresh water component in these samples. All of these conclusions are consistent and confirm independently the conclusion found from their chemistry. In general, the $\delta^{2}H$ and $\delta^{18}O$ signatures of these brines confirm the proposed end member and mixing scenarios concluded from the geochemical data.

The $\delta^{37}Cl$ and $\delta^{81}Br$ values of the formation waters are characterized by large variations (between -1.31 ‰ and +1.82 ‰ relative to SMOC and between -0.95 ‰ and +2.31 ‰ relative to SMOB, respectively). Examining the relationship between $\delta^{81}Br$ and $\delta^{37}Cl$ revealed that a generally positive trend between $\delta^{81}Br$ and $\delta^{37}Cl$ signatures of the Ca-Na-Cl type waters. Formation waters from different stratigraphic units were found to have different $\delta^{81}Br$ and $\delta^{37}Cl$ values, however overlaps also do exist. Furthermore, the $\delta^{81}Br$ and $\delta^{37}Cl$ compositions of formation waters from the same stratigraphic units were observed to be different from one part of the basin to another.

The $\delta^{37}Cl$ and $\delta^{81}Br$ values of the brines from the Lower Silurian sandstone formations are enriched compared to the isotopic values of the brines from the Middle Silurian carbonate formations. These differences may be attributed to the fact that these waters are from different ages or to the fact that they are from two different basins. Either way, this can be useful when trying to identify the origin of waters in the marginal areas between the two basins were separation is not easy and mixing is expected to be dominant.

The brines collected from the Ordovician formations illustrated very interesting $\delta^{37}Cl$ and $\delta^{81}Br$ values that are similar to observations from the Silurian formation waters. In both cases (Ordovician and Silurian) formation waters from the central parts of the Michigan Basin are characterized by more depleted isotopic signature in comparison to the formation waters from the marginal areas. This indicates that the formation waters in these stratigraphic units are either of different origins or they experienced different evolutionary processes and/or mixed with different intrusion fluids that altered their isotopic signatures by mixing.

The process that evolved the K-rich and Ca-rich brines does not seem to cause isotopic fractionation ($\delta^{81}Br$ and $\delta^{37}Cl$). This suggests that water-rock interaction does not impact the isotopic signatures of these two elements in such concentrated brines. It also suggests that the original waters that formed these brines were already depleted in both isotopes prior to the diagenesis process (i.e. the seawater that these brines originated from, was depleted).

Although the chemical parameters and also the $\delta^{18}O$ and $\delta^{2}H$ show some similarities and overlaps between all samples, the $\delta^{81}Br$ shows distinctive differences between the samples from northwest of the Algonquin Arch and those from southeast of the Algonquin Arch. All of the brines collected for the northwest of the Algonquin Arch are characterized by depleted isotopic values in comparison with the isotopic values from the brines collected from southeast of the Arch. One of the scenarios that can be put forward is that the arch forms a water divide, where sediments southeast of the arch are dominated by Appalachian Basin formation waters, and the sediments located northwest of the arch are dominated by the Michigan Basin formation waters.

The fact that formation waters from either side of the arch are isotopically (^{81}Br) distinct strongly suggests that the evolutionary processes that affected the waters are very different which in agreement with previous studies that investigated geochemistry and origin of natural gases in southern Ontario (Barker and Pollock, 1984). It is also in agreement with Farquhar et al. (1987) who suggested separate sources of lead and formation waters originating in the Appalachian Basin and the Michigan Basin based on lead isotope ratios in the Niagara Escarpment rocks and galenas.

It was not possible, during this study, to relate the isotopic signature and especially bromine isotopic signature to the depositional environment because formation waters from both clastic and carbonate deposits in the central part of the Michigan Basin are characterized by negative δ^{81}Br signatures.

Whether the isotopic differences of the brines are due to different evolutionary processes in the two basins or simply due to different ages are not clear at this point of time. Further in depth investigation and understanding of the behaviour of these isotopes under different conditions are necessary to answer that question and better understand the whole system.

CHAPTER 5

GEOCHEMISTRY AND STABLE ISOTOPIC SIGNATURES, INCLUDING CHLORINE AND BROMINE ISOTOPES, OF THE DEEP GROUNDWATERS OF THE SIBERIAN PLATFORM, RUSSIA

5.1 Introduction

The origin of concentrated brines in sedimentary basins is of great interest. The geochemistry of formation waters are believed to provide information about a number of important processes that occur within sedimentary basins (Kharaka and Hanor, 2004), such as the generation and accumulation of oil, mineral dissolution and precipitation and their affect on the porosity and permeability of the sedimentary rocks and the hydraulic connections between different geological sections and its applications to various research fields such as waste disposal and oil exploration. In the last few decades, a great number of researchers investigated the origin and the evolution of formation waters in various sedimentary basins around the world (e.g. Bredhoeft et al., 1963; Rittenhouse, 1967; Carpenter, 1978; Land and Prezbindowski, 1981; Graf, 1982; Knauth, 1986; Hanor et al., 1987; Kaufmann et al. 1988; Davisson and Criss, 1996; Hitchon, 1996; Eastoe et al., 1999; Lowenstien et al., 2003; Kharaka and Hanor, 2004). The Siberian Platform was also investigated by several researchers over the years in order to determine the history of the formation waters in the

sedimentary sequences (e.g. Krotova, 1958; Pinneker and Lomonosov, 1964; Borisov, 1976; Lepin and Borisov, 1979; Pinneker et al., 1987; Kraynov and Ryzhenko, 1997; Shvartsev, 1998, 2000; Alexeev and Alexeeva, 2003). These authors concluded that the Siberian Platform brines have different origins that resulted from complex geochemical evolutionary processes. In this study, chemical analyses and several stable isotopes were employed to better understand the origins of the Siberian Platform brines. The data obtained were the most complete data set so far and were evaluated based on the classical approach (e.g. Rittenhouse, 1967; Carpenter, 1978; Knauth, 1988; Kharaka and Hanor, 2004) in investigating formation waters in sedimentary basins using chemical compositions and traditional stable isotopes (^{2}H, ^{18}O). As well, data presented for Cl and Br stable isotopes in order to compare with the conclusions developed from the classical approach.

Eggenkamp and Coleman (2000) were the first to report $\delta^{81}Br$ signatures of 11 oil field brines and established the first natural range of variation for Br stable isotopes. In 2005, a new methodology for analyzing Br stable isotopes by Continuous Flow Isotope Ratio Mass Spectrometry (CF-IRMS) was developed (Shouakar-Stash et al., 2005a). Through examining 26 sedimentary and crystalline shield formation waters, a new range for the natural variation of Br stable isotopes was reported (0.00 ‰ to +1.80 ‰ relative to Standard Mean Ocean Bromide (SMOB)). The range obtained by Eggenkamp and Coleman (2000) and Shouakar-Stash et al. (2005a) showed the potential of using Br stable isotope ratios to determine the solute sources of natural waters and evaluate geochemical and hydrogeological processes.

The objectives of the present study were: (1) the characterization of the geochemistry and isotopic signatures of Siberian Platform waters; (2) the determination of Br and Cl stable isotope ratios in water types found in the Siberian Platform; and (3) the assessment of the usefulness of Cl and Br stable isotopes as tools in evaluating evolutionary processes.

5.2 Study area

The Siberian Platform located in the central part of the Russian Federation extends from approximately 85ºE to 135ºE longitude and 50ºN to 75ºN latitude (Figure 5.1). It is bordered by the Laptev Sea in the North and Lake Baikal in the South. Although samples were not taken from the entire Siberian Platform, those that were collected by various Russian colleagues for this study are from five different sites that cover a large geographic area. Figure 5.1 illustrates the location of these sites: (1) the Daldyn–Alakit area (Site I) which is situated in the central part of the Yakutain diamond-bearing province; (2) the Malo–Botuobinskiy region (Site II) which occupies the southern part of the Yakutain diamond-bearing province; (3) the Nepskiy artesian basin (Site III) which is situated north of the Angara–Lena Terrace; (4) the Tungusskiy artesian basin (Site IV) located in the western part of the Siberian platform; and (5) the Irkutskiy artesian basin (Site V) which is part of the Angara–Lena Province and is located in the southern part of the Siberian Platform.

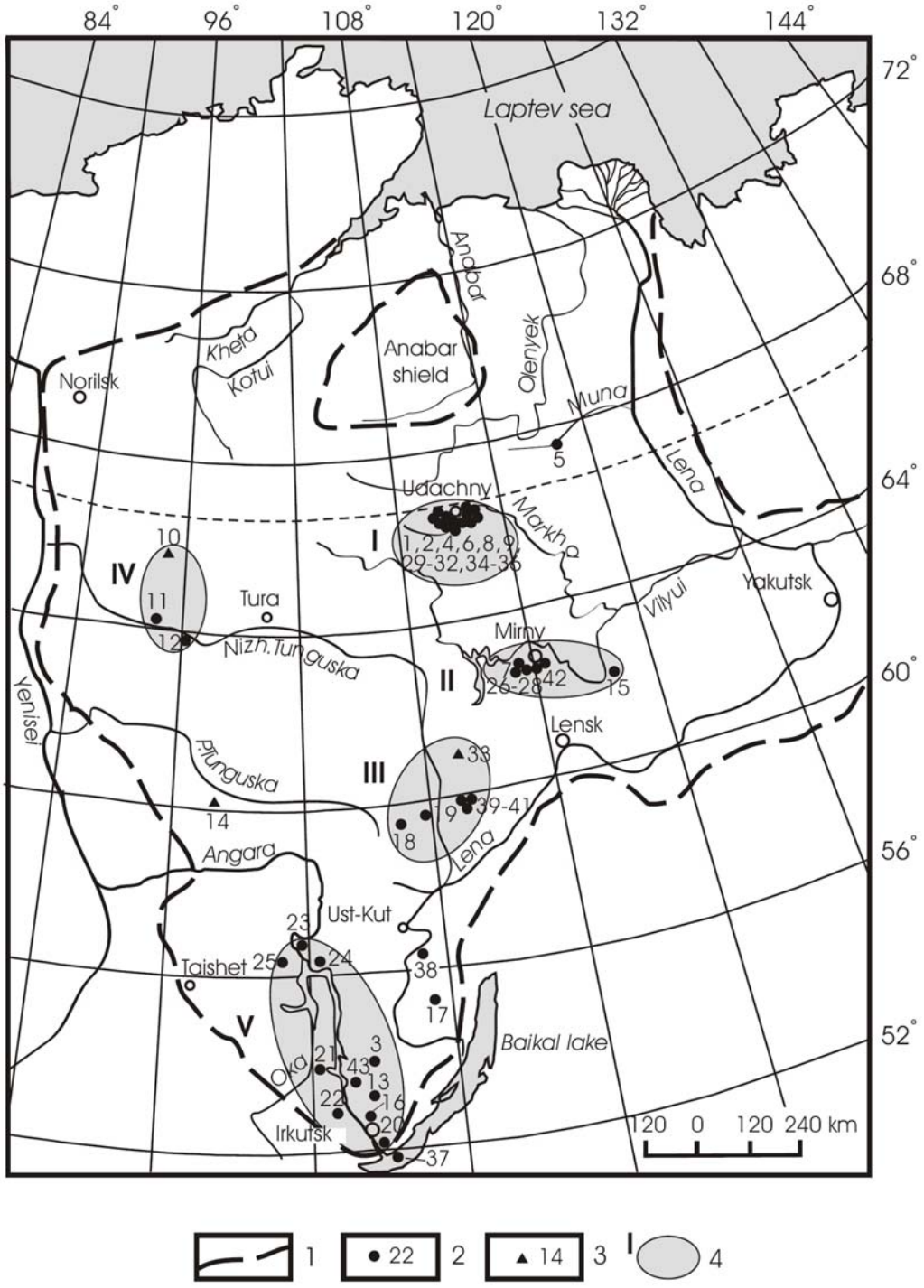

Figure 5.1 Map of the Siberian Platform showing the five sampling sites (after Shouakar-Stash et al., 2007). 1- The boundary of the Siberian Platform, 2- Sampling points, 3- Springs, 4- Study suites.

5.3 Geology

The Siberian Platform consists of thick sedimentary rocks underlain by an Archaean–Proterozoic crystalline basement. The thickness of the sedimentary cover ranges between 2 and 3.5 km and reaches almost 12 km in some areas. The sedimentary cover increases in depth towards the west and the north with the deepest part in the Tungusskiy basin (Site IV) to the west. Although the sedimentary rocks in the Siberian Platform range in age from Jurassic to Cambrian, they are dominated by Cambrian sediments that are mostly terrigenous carbonate and evaporite rocks consisting of gypsum, anhydrite and halite.

The geology of the study area is obtained and summarized from the following references: 1. Pinneker (1966); 2. Geology and gas-petroleum-bearing prospects of the Tungusskaya syneclise and its framing (1968); 3. Petroleum and gas geology of the Siberian platform (1981); 4. Alexeev, (2000); and 5. Tectonics, geodynamics and metallogeny of the Sakha Republic (Yakutia) territory (2001). The geology of the Daldyn–Alakit area (Site I) (Figure 5.2) consists of Archaean basement covered by more than 2.5 km of sedimentary strata ranging from Proterozoic (Vendian) to Paleozoic (Cambrian). The basement consists of gneisses and quartzite–gneisses. The Vendian is mainly dolomites inter-layered with marls and sandstones. The Cambrian sediments consist of dolomite and limestone inter-layered by argillite, clayey limestone and gritstone. There are numerous Late Devonian to Early Carboniferous intruded Kimberlite pipes that are confined to tectonic faults in the area. The stratigraphy of the Malo–Botuobinskiy region (Site II) is illustrated in Figure 5.3. The

basement crystalline rocks are Proterozoic that consist of granite–gneisses, amphibolites and granites. The basement is covered by Vendian–Cambrian sediments that consist primarily of dolomites inter-layered with argillite, anhydrites, limestones, gritstones and rock salts. Immediately above and exposed at the surface are thin layers of sandstones and clays of Jurassic age. Middle Paleozoic kimberlite pipes are also present in this region. The stratigraphy of the Nepskiy artesian basin (Site III) (Figure 5.4) is underlain by Archaean–Proterozoic basement. Overlain the basement is Cambrian sediments that are mainly dolomites inter-layered largely with rock salts at different depths and some beds of limestone and sandstone. The rock salt stratum is the thickest and most persistent strata in the entire area. The stratigraphy of the Tungusskiy artesian basin (Site IV) (Figure 5.5) is the most complex in comparison to the other sites. The crystalline rock Archaean–Proterozoic basement is covered immediately by Proterozoic sediments that consists of carbonaceous–terrigenous rocks. These are overlain by Cambrian to Early Carboniferous sediments consisting of limestone inter-layered with anhydrite and rock salts, and dolomites inter-layered with argillite and gritstones. Above this is a Permo-Triassic cover of sediments made up of limestones, argillites, carbonaceous shales, sandstones, clays and coal strata. Numerous volcanogenic tuffs of Triassic age are also present. In the Irkutskiy artesian basin (Site V) (Figure 5.6), the crystalline basement rocks are of Archaean–Proterozoic age consisting of granites, metamorphic schists and porphyritic volcanics. The basement is covered by Cambrian sediments that consist of dolomites with layers of limestones, rock salts, anhydrites, clays, sandstones, argillites, gritstones, marls and gypsum. The Cambrian sediments are covered by Jurassic sediments made up of sandstones, siltstones and coal beds.

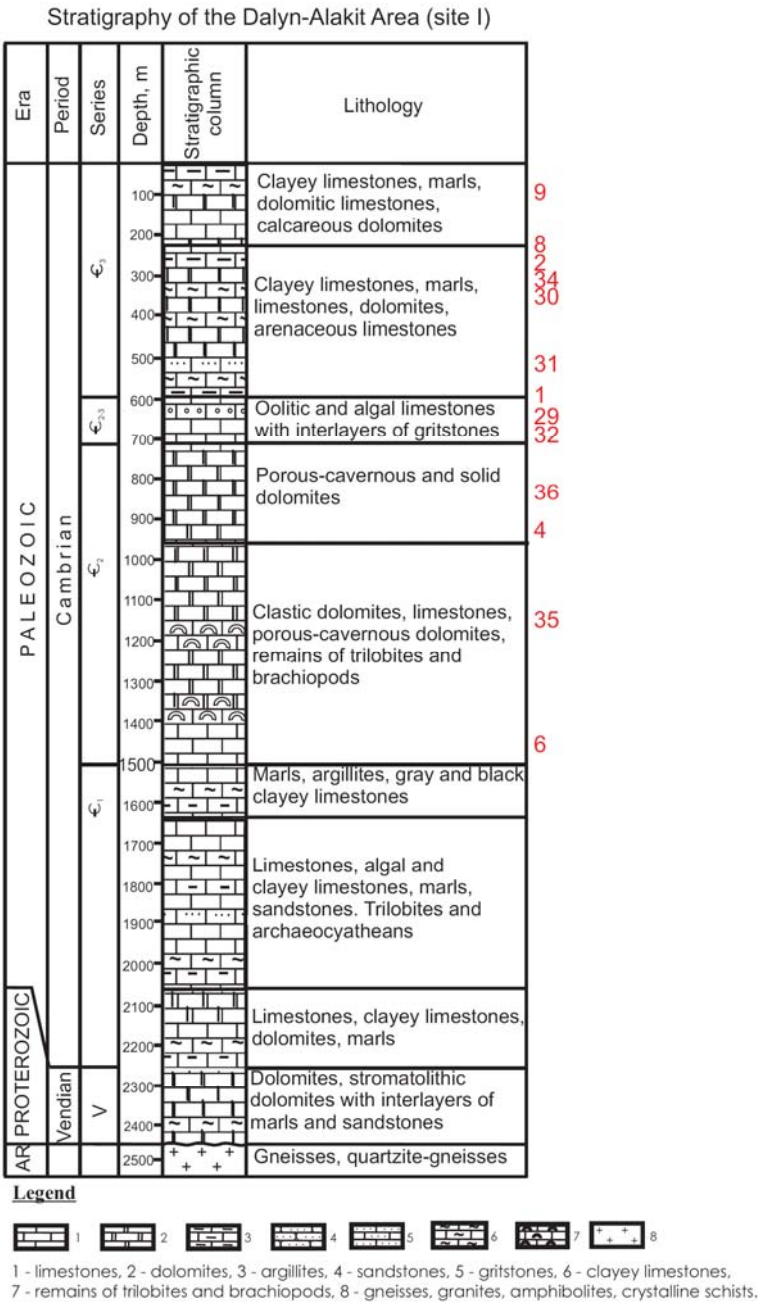

Figure 5.2 Stratigraphic column of the Daldyn-Alakit area (Site I), situated in the central part of the Yakutain diamond-bearing province. Samples collected from this site are illustrated on the stratigraphy (in red) based on the depth they were sampled from. (Pinneker, 1966; Geology and gas-petroleum-bearing prospects of the Tungusskaya syneclise and its framing, 1968; Petroleum and gas geology of the Siberian platform, 1981; Alexeev, 2000; Tectonics, geodynamics and metallogeny of the Sakha Republic (Yakutia) territory, 2001).

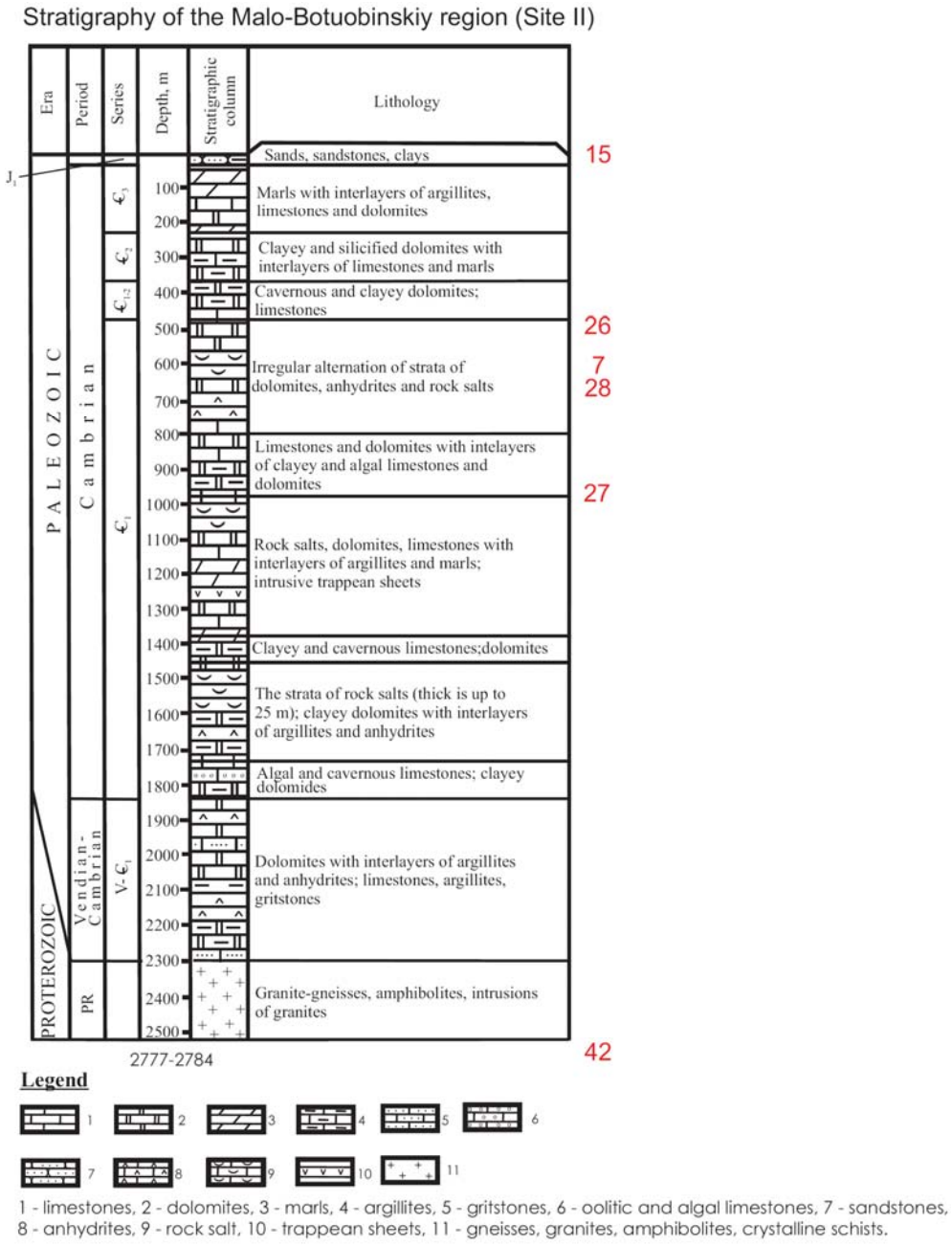

Figure 5.3 Stratigraphic column of the Malo-Botuobinskiy region (Site II) located in the southern part of the Yakutain diamond-bearing province. Samples collected from this site are illustrated on the stratigraphy (in red) based on the depth they were sampled from. (Pinneker, 1966; Geology and gas-petroleum-bearing prospects of the Tungusskaya syneclise and its framing, 1968; Petroleum and gas geology of the Siberian platform, 1981; Alexeev, 2000; Tectonics, geodynamics and metallogeny of the Sakha Republic (Yakutia) territory, 2001).

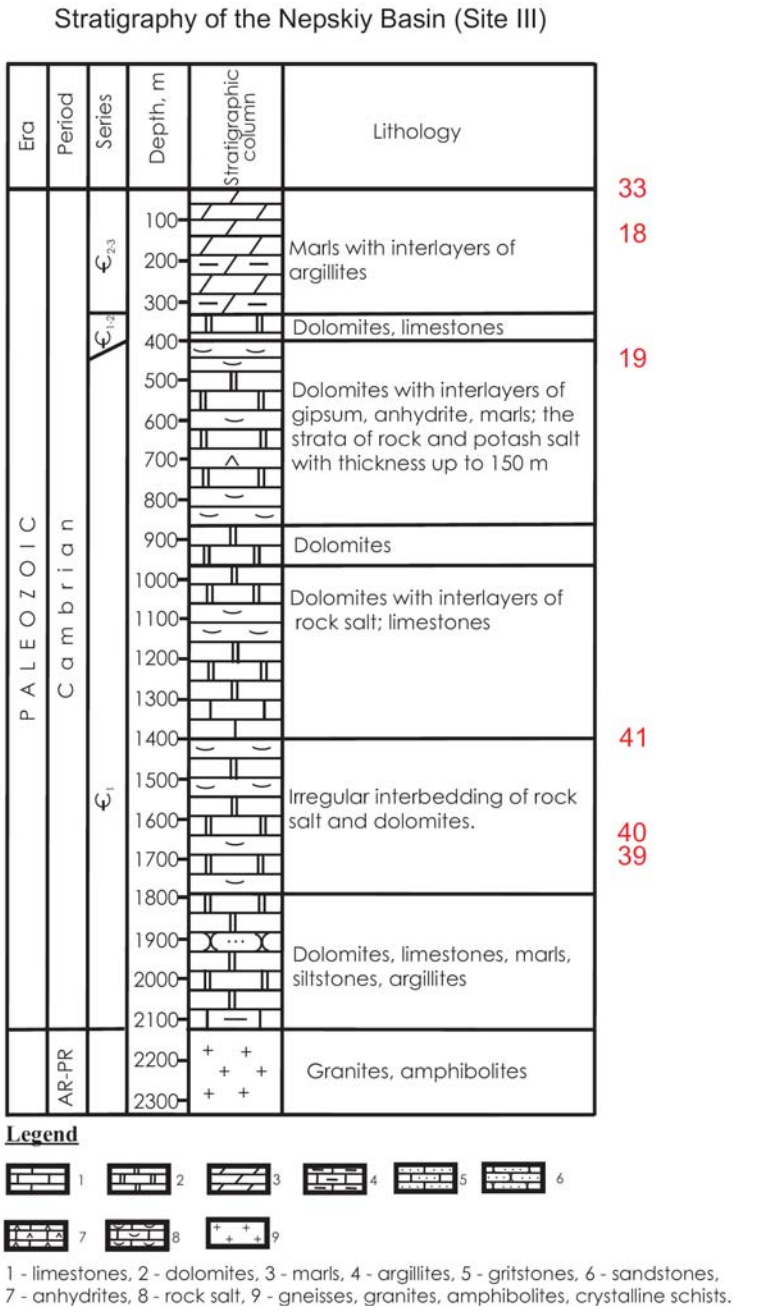

Figure 5.4 Stratigraphic column of the Napskiy artesian basin (Site III) located north of the Angara-Lena Terrace. Samples collected from this site are illustrated on the stratigraphy (in red) based on the depth they were sampled from. (Pinneker, 1966; Geology and gas-petroleum-bearing prospects of the Tungusskaya syneclise and its framing, 1968; Petroleum and gas geology of the Siberian platform, 1981; Alexeev, 2000; Tectonics, geodynamics and metallogeny of the Sakha Republic (Yakutia) territory, 2001).

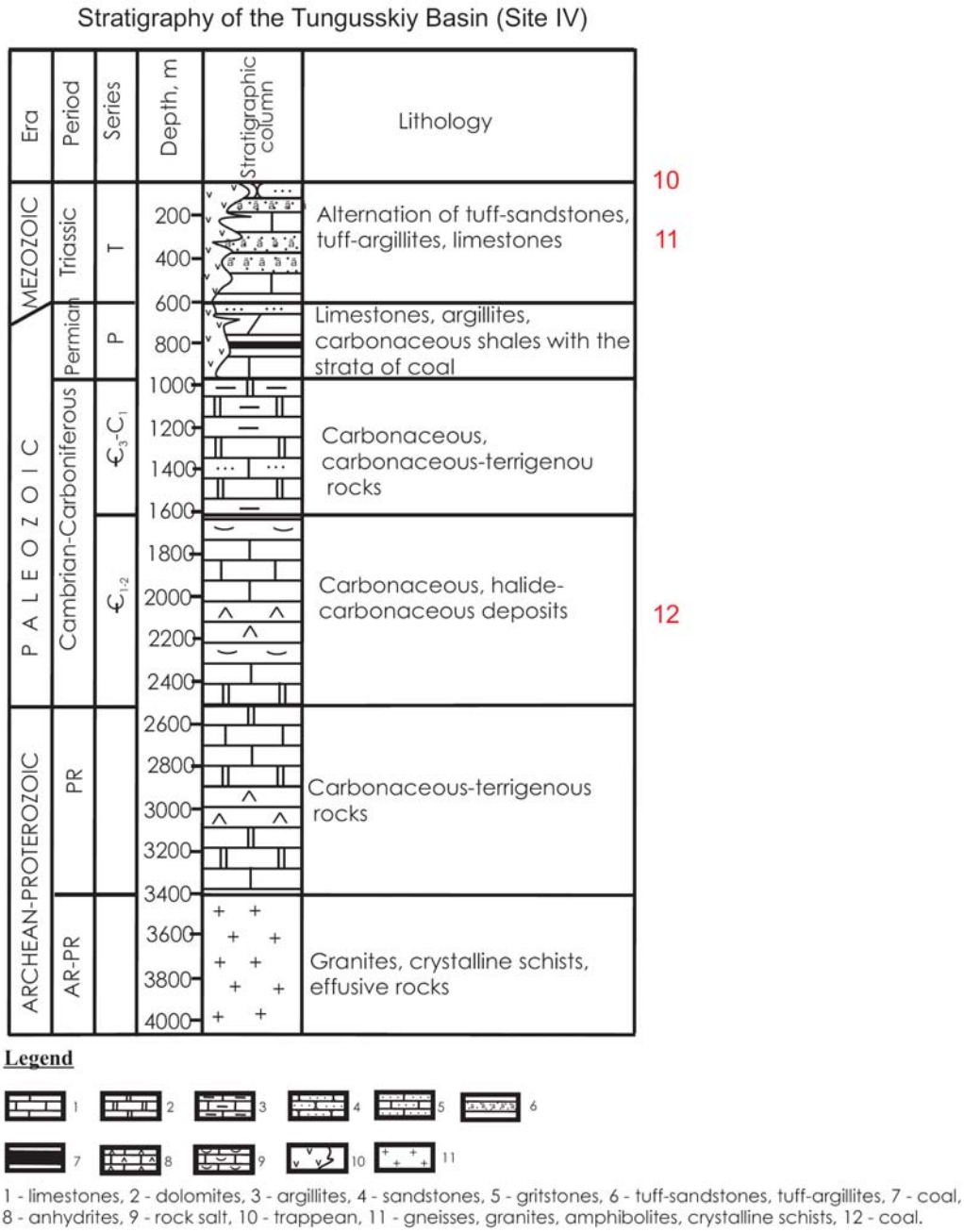

Figure 5.5 Stratigraphic column of the Tungusskiy artesian basin (Site IV) situated in the western part of the Siberian Platform. Samples collected from this site are illustrated on the stratigraphy (in red) based on the depth they were sampled from. (Pinneker, 1966; Geology and gas-petroleum-bearing prospects of the Tungusskaya syneclise and its framing, 1968; Petroleum and gas geology of the Siberian platform, 1981; Alexeev, 2000; Tectonics, geodynamics and metallogeny of the Sakha Republic (Yakutia) territory, 2001).

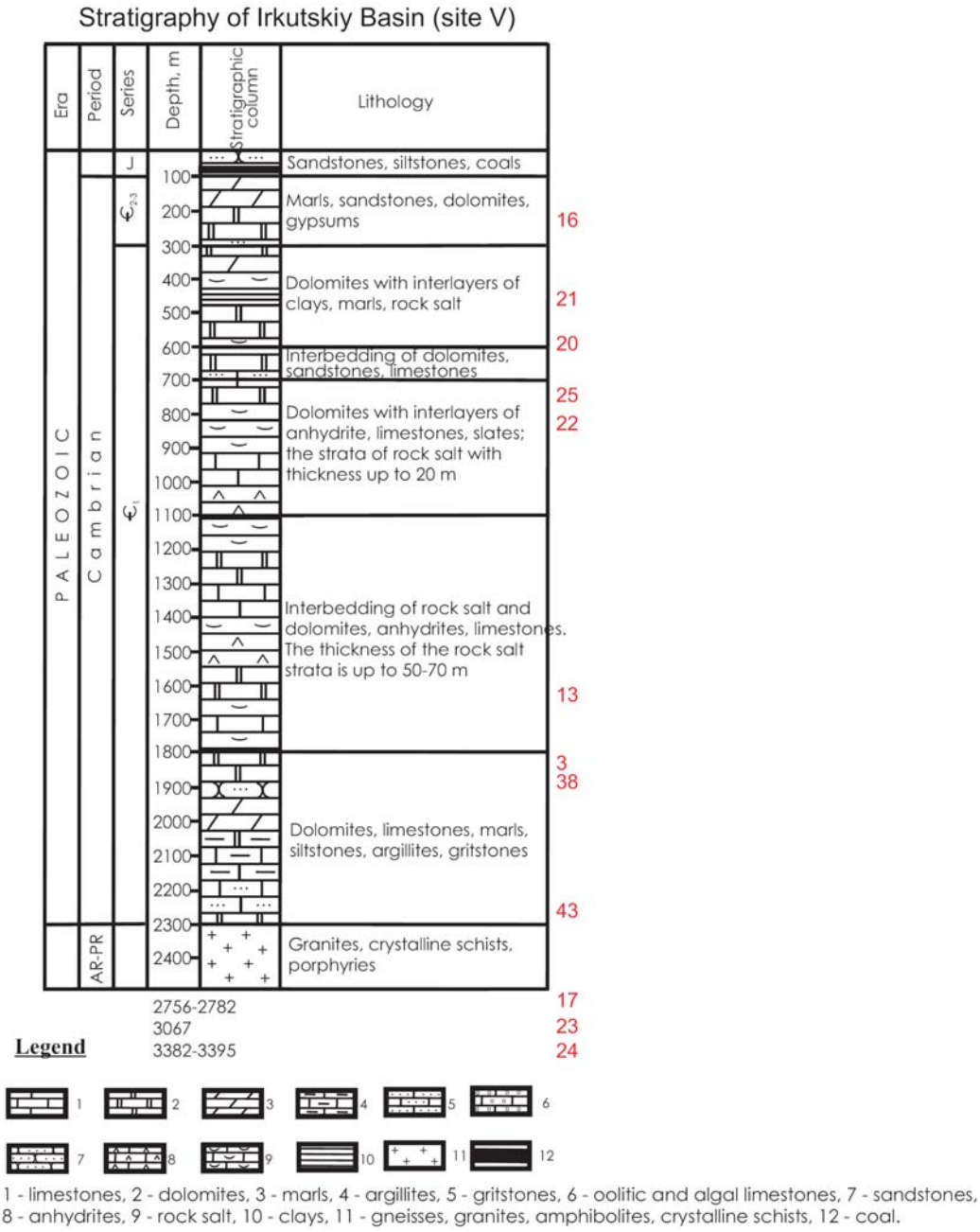

Figure 5.6 Stratigraphic column of the Irkutskiy artesian basin (Site V) which is part of the Angara-Lena Province and located in the southern part of the Siberian Platform. Samples collected from this site are illustrated on the stratigraphy (in red) based on the depth they were sampled from. (Pinneker, 1966; Geology and gas-petroleum-bearing prospects of the Tungusskaya syneclise and its framing, 1968; Petroleum and gas geology of the Siberian platform, 1981; Alexeev, 2000; Tectonics, geodynamics and metallogeny of the Sakha Republic (Yakutia) territory, 2001).

5.4 Hydrogeology

The Siberian Platform is generally characterized by continuous permafrost in the northern and western areas while frozen ground tends to be discontinuous in the southern areas. Data obtained by the researchers of the Permafrost Institute SB RAS (Balobaev et al., 1983; Klimovsky and Gotovcev, 1994) indicated that the temperature of the rocks at base of the permafrost layer fluctuates annually between -2.90°C and -8.75°C in the northern areas of the Siberian Platform and between 0°C and -3°C in southern parts. Recent work by Alexeev and Alexeeva (2002, 2003) has indicated that the total thickness of the cryogenic ground (cryolithozone) that consists of ice-rich permafrost, dry permafrost and frozen sedimentary rocks, including cryopeges (negative temperature waters), ranges from 25 to 1450 metres in depth across the region. In their study, they also identified two hydrodynamic zones in the cryogenic ground of the Siberian Platform: (1) the active water-exchange zone (assumed to have strong elements of advective flow), and (2) the passive water-exchange zone (dominated by diffusive processes). The active and passive water-exchange zones differ from one another by the relative rates of water movement: from a metre per hundreds to thousands of years in the active zone to a metre per over a million years in the passive zone (Alexeev and Alexeeva, 2003).

The minor accumulations of fresh groundwater are confined to the seasonally thawed layer near surface and to active zones of flow under and in unfrozen taliks associated with lakes (Alexeev and Alexeeva, 2003). A dry (unsaturated zone) permafrost layer present below the

active water-exchange zone separates this zone from the passive water-exchange zone located in the frozen sedimentary rocks below. Layers of dry permafrost are also present within the passive water-exchange zone in frozen sedimentary rocks. The thickness of these three zones varies dramatically from one part to another in the Siberian Platform, where all layers are generally thicker in the north and thinner in the south. The water types in the active water-exchange zone are HCO_3–Ca–Mg–Cl and Ca–Mg–Cl. The passive water-exchange zone is characterized by several different types of waters. The northern part of the Siberian Platform (Site I) is characterized by Ca–Mg–Cl and Mg–Ca–Cl type waters; while the southern parts (Site II–V) are characterized by Na–Cl and Ca–Cl type waters (Alexeev and Alexeeva, 2003).

5.5 Sampling and analyses

Sample locations and numbers are shown on Figures 5.1 to 5.6. Samples in this study were collected mainly from deep exploration boreholes and from some springs and lakes. Samples collected from boreholes are usually bailer samples taken periodically during drilling and may in many cases represent fluids from a wide interval in the borehole. Samples were analyzed for chemical composition and stable isotopes (^{18}O, ^{2}H, ^{37}Cl and ^{81}Br). The chemical compositions were determined by ICP-MS/ICPAES and Ion Chromatography (IC) for cations and anions, respectively. Samples were analyzed in the Chemical Laboratory at the Geological Survey of Finland. High concentration samples were diluted 20 times before they were analyzed. The detection limits for Ca, Na, K, Mg, Li and Sr of the ICP-MS/ICP-AES

method are 100, 200, 10, 100, 0.1 and 0.1 µg/L, respectively. The detection limits for Br, Cl and SO_4 of the IC method are 100, 200 and 100 µg/L, respectively. The ^{18}O, ^{2}H, ^{37}Cl and ^{81}Br stable isotopes were analyzed by Isotope Ratio Mass Spectrometry (IRMS) at the Environmental Isotope Laboratory (EIL) at the University of Waterloo.

Oxygen stable isotope measurements were performed on CO_2 by the CO_2–H_2O equilibration method following the procedure of Epstein and Mayeda (1953) and modified by Moser (1977). Hydrogen stable isotope measurements were performed on H_2 gas using the Mn reduction method of Shouakar-Stash et al. (2000). Chlorine stable isotope analyses were performed on methyl chloride (CH_3Cl) gas following the procedure described in Eggenkamp (1994). Bromine stable isotope analyses were carried out on methyl bromide (CH_3Br) gas using a CF-IRMS following the method described by Shouakar-Stash et al. (2005a). The analytical precisions for the ^{18}O, ^{2}H, ^{37}Cl and ^{81}Br isotopes are 0.2 ‰, 1.0 ‰, 0.1 ‰ and 0.1 ‰, respectively.

5.6 Results

The chemical compositions and isotopic signatures of the Siberian Platform samples are presented in Table 5.1. Samples were collected at various depths ranging from near surface to almost 4 km. The results show large variations in TDS ranging from less than 1 g/L to almost 600 g/L. The samples are also characterized by different chemical compositions; the two main chemical compositions of waters found in the Siberian Platform are Ca–Cl and Na–Cl

waters. The Cl content of the samples shows large variations (~1 to >300000 mg/L). Generally, the Br content of the samples varies over a large range (<1 to >8500 mg/L). The Br to Cl weight ratio (Br/Cl) of these samples range between 0.0001 and 0.0389. The low end is typical for fresh waters and the high end exceeds most concentrated brines of marine origin reported in the literature (Frape et al., 2004). The Br/Cl weight ratio for seawater is typically around 0.0034. The $\delta^{2}H$ and $\delta^{18}O$ results range between -195 ‰ and -31 ‰; and -20 ‰ and +2 ‰, respectively. The pattern obtained from the $\delta^{2}H$ and $\delta^{18}O$ values is similar to that previously reported by Pinneker et al. (1987) and typical of results obtained from other sedimentary basins in that they fall to the right of the GMWL. The $\delta^{37}Cl$ values range between -0.67 ‰ and +1.54 ‰. This range is within the known variation for Cl stable isotopes of formation waters (Kaufmann et al., 1984; Desaulniers et al., 1986; Kaufmann et al., 1988; Eastoe and Guilbert, 1992; Kaufmann et al., 1993; Eggenkamp, 1994; Eastoe et al., 1999, 2001; Ziegler et al., 2001; Frape et al., 2004; Stewart and Spivack, 2004). The $\delta^{81}Br$ values have a wide variation and range between -0.80 ‰ and +3.35 ‰. This variation is larger than the previously reported range (0.00 ‰ to +1.80 ‰) for Br stable isotopes for natural samples (Eggenkamp and Coleman, 2000; Shouakar-Stash et al., 2005a).

Table 5.1 Location, depth, major ions, charge balance and stable isotopes of the Siberian platform samples.

Sample ID	Sample Name	Site	Depth m	TDS g/l	Ca mg/l	Mg mg/l	Na mg/l	K mg/l
	Group A							
1	Udachnaya open pit Borehole N 9-G	I	550	323000	48518	13113	16451	9930
3	Znamenka groundwater deposit Borehole N 3A	V	1818-1826	589690	95351	28190	1988	3183
4	Udachnaya area sedimentary rocks Borehole N 308	I	805-1150	353220	37157	7540	10171	8313
6	Udachnaya area deep oil Borehole N 703	I	1390-1567	395800	61202	10983	12098	15656
7	Mir kimberlite pipe Borehole N 82 [S37]	II	600	434850	46417	9853	4025	4432
17	Kazatchinnsk Boehole 89	V	2756-2782	366170	75330	5743	22266	5951
23	Kuturminsk Borehole 156	V	3067	446865	96021	9303	8764	19843
24	Bratsk Borehole 8	V	3382-3395	358900	42733	13311	37177	9871
27	Mir Pipe, Borhole 82	II	884-1024	362910	86041	13870	11294	7574
28	Mir Pie, Borehole 83	II	600	387950	73761	12499	19191	6308
29	Udachnaya Pipe, Borehole 314	I	449-800	316990	74691	12976	15872	13395
31	Udachnaya Borehole 1-OP	I	400-650	315200	63465	12359	21600	10934
32	Udachnaya Borehole 330	I	504-750	316080	70923	11693	19870	12095
35	Udachnaya Borehole 310	I	834-1470	381360	94723	15306	5066	17678
36	Udachnaya Borehole 312	I	583-952	344610	69117	10953	19720	12515
38	Omoloyskaya borehole 13	V	1830-1888	443274	110952	23790	1151	2199
39	Verhnechonskaya Borehole 31	III	1674-1667	384000	100808	10744	8228	7819
40	Verhnechonskaya Borehole 53	III	1623-1633	358000	76395	10134	18559	6383
41	Verhnechonskaya Borehole 77	III	1380-1408	399000	77988	16659	9229	5979
42	Irelyahskaya Borehole 746	II	2777-2784	396000	108747	4005	10406	1195
43	Balagankinskaya Borehole 2	V	2258-2296	511000	119885	9024	2775	15141
	Group B							
14	Spring, near salt factory (OSKOBA)	IV	0	87080	1475	375	27191	118
15	Lake Mohsogoloh, near Kempendrai River	II	0	64189	369	39	22771	11
18	Gazhenka Borehole 6	III	120	77000	792	302	27076	562
19	Nepa Borehole 5-6	III	419-481	44000	1094	484	13427	166
21	Novonukutsk Borehole 3-6M	V	455-500	64000	1275	460	14758	85
22	Usolie Borehole 3	V	700-1000	242020	1114	80	98388	795
26	Mir Pipe, Borehole 28	II	500	87400	1028	739	27996	161
	Group C							
2	Zarnitsa kimberlite pipe Borehole N 14	I	260-270	111330	12737	5285	4843	2060
5	Muna area Hydromineral object Borehole N 20Y	II	600	85650	3707	2232	9569	<0.7
8	Udachnaya area Borehole N 35	I	210	39920	6225	3002	4352	660
9	Udachnaya area polygon Borehole N 6	I	110-120	98340	15479	10247	8545	2418
10	Spring, near Tutonchany River, near Salt factory	IV	0	87550	11270	25	19548	220
12	Nizn. Tunguska Borehole N TP-1	IV	2100	286300	26899	1420	70728	657
13	Osinskaya Borehole N 1	V	1630-1660	46525	986	-	9921	3937
25	Bratsk Borehole 2-S	V	733-760	32000	2656	955	7667	103
30	Daldyn Borehole 24	I	313	91300	14461	4419	19172	2355
	Group D							
11	Nizn. Tunguska Borehole N 44P	IV	300	318	16	3	4	1
16	Mineral water Borehole North Irkutsk	V	3-400	1729	222	82	208	2
20	Zeleniy Mys Borehole 3	V	600	7000	283	127	2218	18
33	Spring, near the Chona River	III	0	11200	270	200	3685	34
37	Lake Baikal	V	0	8659	27	4	20	2

Table 5.1 Continued

Sample ID	Sample Name	Site	Cl mg/l	SO_4 mg/l	Br mg/l	Sr mg/l	Li µg/l	Charge Balance %
	Group A							
1	Udachnaya open pit Borehole N 9-G	I	160931	122	3648	869	126361	0.3
3	Znamenka groundwater deposit Borehole N 3A	V	220840	61	8587	349	366334	2.4
4	Udachnaya area sedimentary rocks Borehole N 308	I	155949	135	3621	548	123946	-15.3
6	Udachnaya area deep oil Borehole N 703	I	179098	44	4910	1198	162493	-0.4
7	Mir kimberlite pipe Borehole N 82 [S37]	II	173338	38	4712	888	25012	-17.7
17	Kazatchinnsk Boehole 89	V	179793	10	4828	3080	43075	2.1
23	Kuturminsk Borehole 156	V	161699	43	4252	4052	166291	5.6
24	Bratsk Borehole 8	V	169649	282	4188	1897	50852	3.2
27	Mir Pipe, Borhole 82	II	158918	100	3816	1791	19459	1.7
28	Mir Pie, Borehole 83	II	163375	86	3421	1584	20693	1.6
29	Udachnaya Pipe, Borehole 314	I	192444	131	4440	1164	125946	3.8
31	Udachnaya Borehole 1-OP	I	151202	88	3229	1040	88628	3.4
32	Udachnaya Borehole 330	I	139435	10	3094	1127	89407	3.5
35	Udachnaya Borehole 310	I	212280	38	5637	1600	177138	4.5
36	Udachnaya Borehole 312	I	199151	87	4354	1138	165178	0.4
38	Omoloyskaya borehole 13	V	231899	23	6317	464	215906	1.3
39	Verhnechonskaya Borehole 31	III	184261	86	5206	2515	25933	1.7
40	Verhnechonskaya Borehole 53	III	171839	314	3928	1764	22585	1.6
41	Verhnechonskaya Borehole 77	III	164859	200	2026	1131	51776	1.8
42	Irelyahskaya Borehole 746	II	187668	183	4725	2279	5245	0.3
43	Balagankinskaya Borehole 2	V	205786	27	5135	3851	119318	3.7
	Group B							
14	Spring, near salt factory (OSKOBA)	IV	44236	3571	49	33	827	-1.2
15	Lake Mohsogoloh, near Kempendrai River	II	34686	945	4	7	24	0.0
18	Gazhenka Borehole 6	III	38423	2656	36	13	207	0.6
19	Nepa Borehole 5-6	III	21857	3946	17	19	436	-1.1
21	Novonukutsk Borehole 3-6M	V	22088	4845	20	29	534	0.2
22	Usolie Borehole 3	V	132866	3111	92	15	328	3.9
26	Mir Pipe, Borehole 28	II	42159	4134	51	32	1401	0.2
	Group C							
2	Zarnitsa kimberlite pipe Borehole N 14	I	59535	688	1167	392	27694	-11.0
5	Muna area Hydromineral object Borehole N 20Y	II	49895	18	749	571	3194	-27.8
8	Udachnaya area Borehole N 35	I	26305	1176	412	186	5922	0.2
9	Udachnaya area polygon Borehole N 6	I	76242	925	1458	308	32492	-2.3
10	Spring, near Tutonchany River, near Salt factory	IV	56021	542	289	198	571	-5.6
12	Nizn. Tunguska Borehole N TP-1	IV	165215	246	1243	449	17887	-1.1
13	Osinskaya Borehole N 1	V	165345	178	258	13	81411	16.7
25	Bratsk Borehole 2-S	V	17538	2162	219	58	3483	0.5
30	Daldyn Borehole 24	I	62810	1349	849	285	11521	1.8
	Group D							
11	Nizn. Tunguska Borehole N 44P	IV	1	63	<0.1	0.1	7	-1.2
16	Mineral water Borehole North Irkutsk	V	303	684	0.3	2	67	0.3
20	Zeleniy Mys Borehole 3	V	3500	894	4	9	903	0.6
33	Spring, near the Chona River	III	639	707	2	8	45	0.3
37	Lake Baikal	V	36	22	0.2	0.2	37	3.6

Table 5.1 Continued

Sample ID	Sample Name	Site	δ^2H_{VSMOW} ‰	$\delta^{18}O_{VSMOW}$ ‰	$\delta^{37}Cl_{SMOC}$ ‰	$\delta^{81}Br_{SMOB}$ ‰
	Group A					
1	Udachnaya open pit Borehole N 9-G	I	-66.4	-3.94	-0.40	0.07
3	Znamenka groundwater deposit Borehole N 3A	V	-47.3	-9.91	-0.53	-0.09
4	Udachnaya area sedimentary rocks Borehole N 308	I	-61.7	-2.43	-0.35	0.07
6	Udachnaya area deep oil Borehole N 703	I	-45.3	1.80	-0.34	0.14
7	Mir kimberlite pipe Borehole N 82 [S37]	II	-39.3	-2.01	-0.32	0.24
17	Kazatchinnsk Boehole 89	V	-35.9	-2.47	-0.16	-0.07
23	Kuturminsk Borehole 156	V	-49.4	-0.20	-0.32	0.00
24	Bratsk Borehole 8	V	-38.4	-0.60	-0.41	-0.05
27	Mir Pipe, Borhole 82	II	-51.8	-5.23	-0.15	0.18
28	Mir Pie, Borehole 83	II	-50.5	-4.94	0.04	0.27
29	Udachnaya Pipe, Borehole 314	I	-67.3	-5.52	-0.22	0.18
31	Udachnaya Borehole 1-OP	I	-69.9	-4.37	-0.23	-0.04
32	Udachnaya Borehole 330	I	-70.5	-4.96	-0.20	0.24
35	Udachnaya Borehole 310	I	-73.3	-8.20	-0.27	-0.07
36	Udachnaya Borehole 312	I	-	-2.00	-0.24	-0.13
38	Omoloyskaya borehole 13	V	-69.6	-10.93	-0.08	0.19
39	Verhnechonskaya Borehole 31	III	-44.9	-1.37	-0.21	0.06
40	Verhnechonskaya Borehole 53	III	-78.3	-7.21	-0.24	0.13
41	Verhnechonskaya Borehole 77	III	-194.6	-12.30	-0.39	-0.01
42	Irelyahskaya Borehole 746	II	-30.6	-6.15	-0.67	-0.31
43	Balagankinskaya Borehole 2	V	-50.7	-4.24	-0.14	-0.11
	Group B					
14	Spring, near salt factory (OSKOBA)	IV	-136.7	-17.51	0.01	0.73
15	Lake Mohsogoloh, near Kempendrai River	II	-93.8	-0.45	0.17	0.65
18	Gazhenka Borehole 6	III	-152.1	-20.01	-0.25	0.71
19	Nepa Borehole 5-6	III	-147.5	-18.47	-0.13	-
21	Novonukutsk Borehole 3-6M	V	-134.0	-16.72	0.08	-
22	Usolie Borehole 3	V	-	-15.20	-0.06	0.20
26	Mir Pipe, Borehole 28	II	-113.2	-9.57	1.54	-
	Group C					
2	Zarnitsa kimberlite pipe Borehole N 14	I	-123.0	-13.10	0.01	0.38
5	Muna area Hydromineral object Borehole N 20Y	II	-108.8	-14.06	1.30	2.31
8	Udachnaya area Borehole N 35	I	-139.6	-16.45	0.52	0.73
9	Udachnaya area polygon Borehole N 6	I	-109.4	-10.22	0.21	0.18
10	Spring, near Tutonchany River, near Salt factory	IV	-124.9	-17.07	-0.17	0.03
12	Nizn. Tunguska Borehole N TP-1	IV	-88.5	-12.31	-0.11	0.70
13	Osinskaya Borehole N 1	V	-90.7	-9.25	-0.29	-0.07
25	Bratsk Borehole 2-S	V	-96.4	-12.20	0.56	3.35
30	Daldyn Borehole 24	I	-95.9	-10.22	-0.40	-0.80
	Group D					
11	Nizn. Tunguska Borehole N 44P	IV	-121.1	-15.22	0.58	-
16	Mineral water Borehole North Irkutsk	V	-131.9	-16.76	-0.13	-
20	Zeleniy Mys Borehole 3	V	-113.2	-15.71	0.10	-
33	Spring, near the Chona River	III	-124.0	-17.65	0.35	-
37	Lake Baikal	V	-103.0	-14.37	-	-

5.7 Discussion

5.7.1 Interpretation based on geochemical parameters

A large number of studies have been carried out to investigate and explain the evolutionary processes that are involved in creating highly saline formation waters. These processes include 1) the evaporation of seawater (e.g. Carpenter, 1978; Kharaka et al., 1987); 2) the dissolution of halite or other evaporites such as potash or gypsum (e.g. Rittenhouse 1967; Land and Prezbindowski 1981; Hitchon, 1996); 3) membrane filtration (Bredehoeft et al., 1963; Berry, 1969; Kharaka and Berry, 1973; Graf, 1982); 4) concentration and metamorphism of waters at great depths assisted by high temperatures and pressures (Chebotarev, 1955; Krotova, 1958; Pinneker and Lomonosov, 1964); and/or 5) freezing of water or hydration of silicates (clays) with the resulting concentration of solutes (Hanor, 1987).

Figure 5.7 illustrates the logarithmic relationship between Cl (mg/L) and Br (mg/L) contents of seawater during evaporation. The figure illustrates also the initial precipitation point of evaporite mineral phases as reported by Matray (1988). It also shows certain mixing scenario between several end members (e.g. evaporated seawater, seawater, fresh water). Further it shows the affect of dissolving halite by different fluids such as seawater and brines. These different scenarios were examined and reported previously by several researchers (e.g. Rittenhouse, 1967; Carpenter, 1978; Kharaka and Hanor, 2004).

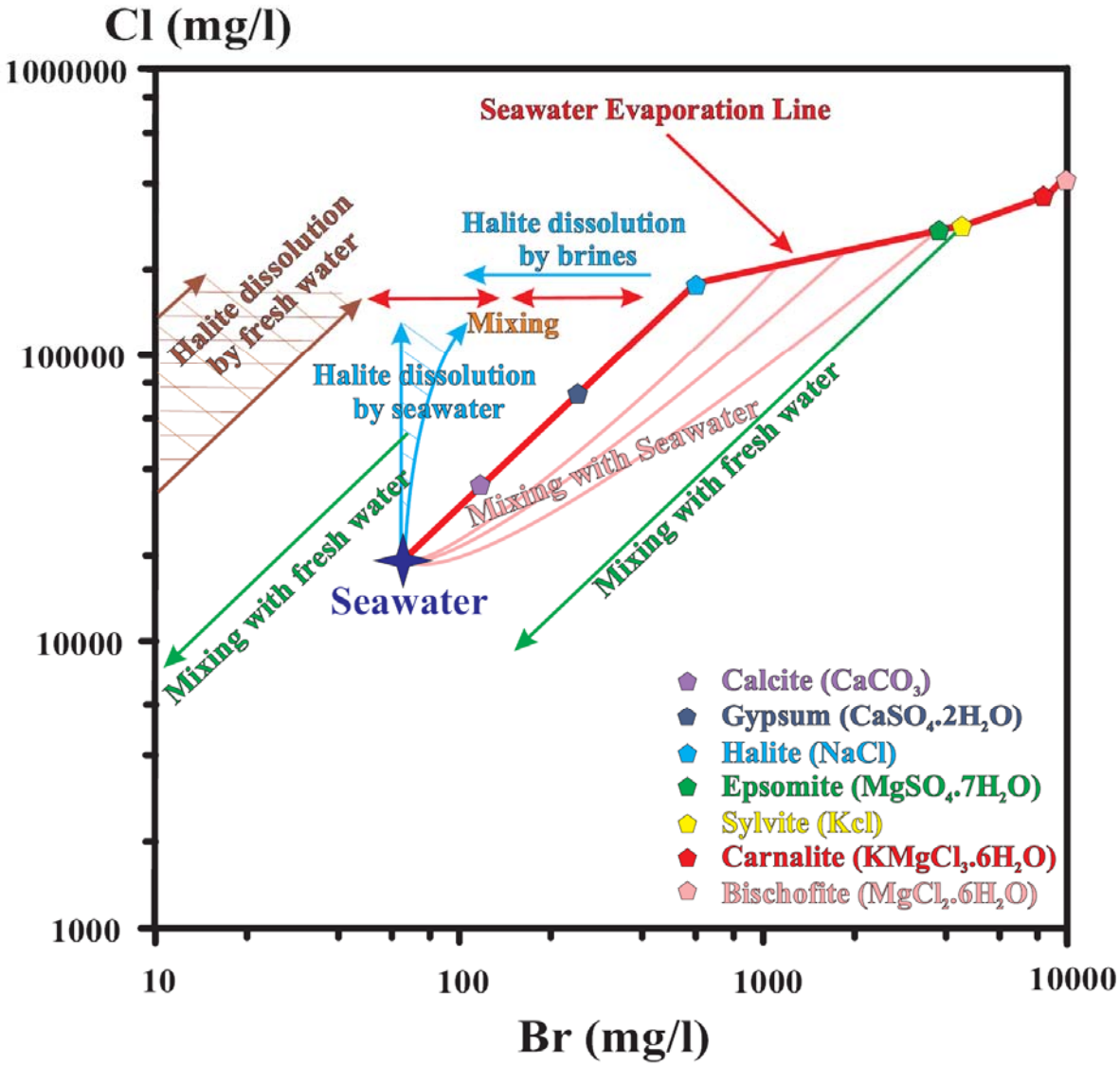

Figure 5.7 A logarithmic plot of the concentration trends of chloride versus bromide during the evaporation of seawater showing the initial precipitation point of evaporite mineral phases (after Matray, 1988). Also shows some of the possible mixing scenarios after Rittenhouse (1967) with different halite dissolution products and different end member waters (Carpenter, 1978).

The samples collected for this study were divided and classified according to their Cl and Br content as well as their location on the log (TDS) versus log (Br) plot relative to the seawater evaporation line (Figure 5.8). Based on this classification, samples were divided into 4 groups; A, B, C and D. Samples in group A are at an advanced stage of seawater evaporation and they plot in the upper right corner of Figure 5.8. All samples of this group are characterized by high TDS values that range between 300,000 mg/L and 600,000 mg/L, and Br contents ranging between 2000 and 8500 mg/L (Figure 5.8). Bromide and chloride or TDS evolutionary schemes would interpret the group A samples to be the result of extreme evaporation followed by a long interval of water rock interaction in the subsurface (Valyaskho, 1956; Rittenhouse, 1967; Carpenter, 1978; Kharaka and Hanor, 2004). These types of fluids have often been associated with evolution beyond or in conjunction with the precipitation of the bitter salts of K, Mg and Ca. The age of the strata, extensive rock salt and anhydrite beds, and the Ca, Mg, K-rich chemistry, would tend to support this evolutionary model.

Group B samples have TDS values higher than seawater. Most of the TDS values of these samples range between 44,000 mg/L and 87,000 mg/L, however, one of the samples (#22) has a higher TDS value that extends the range to 242,000 mg/L (Figure 5.8). The Br content of these samples is less than that expected from simple seawater concentration and they range between 4 and 92 mg/L. The position of these samples on Figure 5.8 would normally be interpreted as a solution interacting with and dissolving halite (Rittenhouse, 1967; Carpenter, 1978; Matray, 1988). During the precipitation of halite bromide preferentially stays in

solution and consequently halite has a low Br/Cl ratio in comparison to the residual solution. The presence of rock salts in the stratigraphic columns (Figures 5.2 – 5.6), the very low Br content, and the dominant Na–Cl chemistry would tend to support the assumption of salt dissolution for the chemical source of group B samples. The bromine contents of these samples (compare with Figure 5.7) suggest that the halite dissolution probably involved both seawater and fresh water.

Eight of nine samples in group C have TDS values that range between 32,000 mg/L and 111,000 mg/L. One sample (#12) of this group has a much higher TDS value (286,000 mg/L) than the rest (Figure 5.8). Samples from this group plot to the right and below the seawater evaporation line. The Br contents of these samples are higher than that expected from simple seawater evaporation. The simplest interpretation of this set of samples would be a mixture of a typical group A brine chemistry with a dilute fresh water or seawater. In some cases it appears that the halite associated group B fluids may be involved in this dilution or mixing scenario.

The fourth type of waters found in the Siberian Platform presented as group D are characterized by low TDS values that range between 318 mg/L and 11,200 mg/L. Their Br content ranges between < 0.1 and 4 mg/L. These samples plot in the lower left corner of Figure 5.8 and below group B samples. The TDS values of these samples are less than that of seawater (35 g/L). Their origins are probably associated with various mixtures of fresh and brackish near-surface waters.

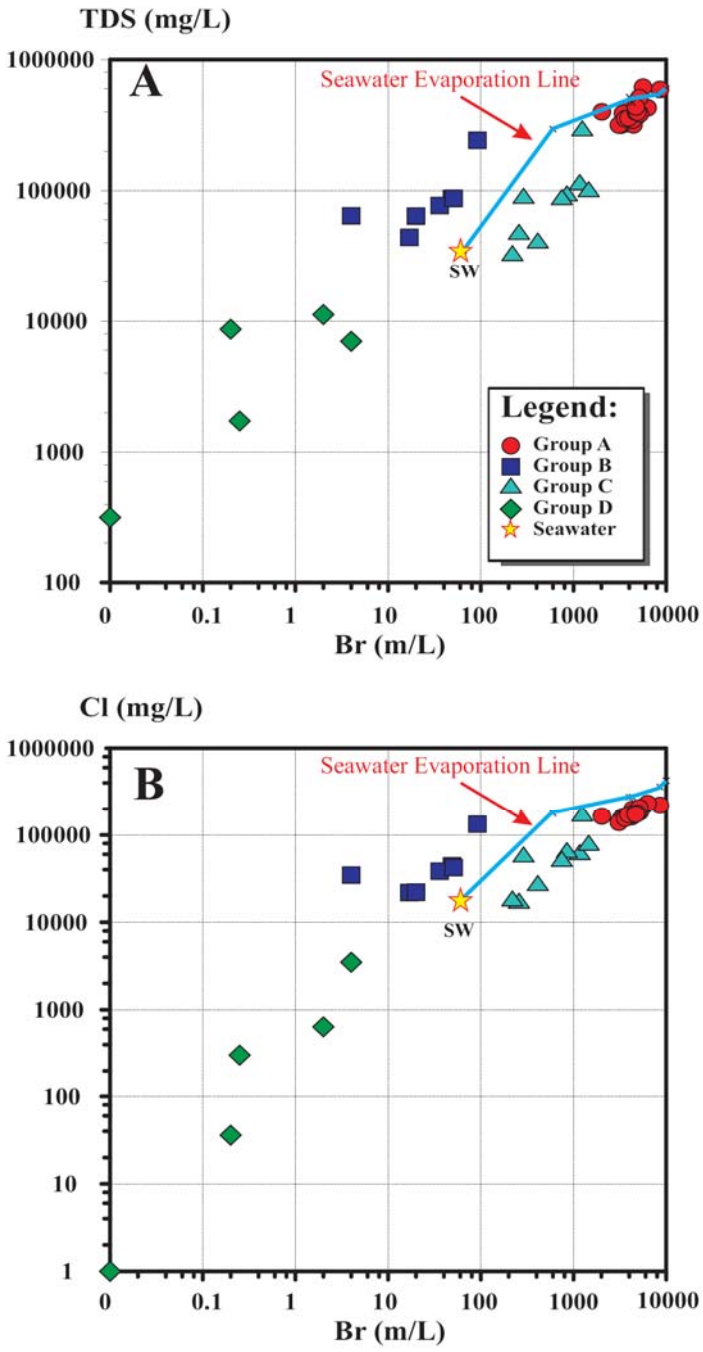

Figure 5.8 (A) Logarithmic plot of TDS (mg/L) versus Br (mg/L) for the Siberian Platform samples. (B) Logarithmic plot for the Cl (mg/L) versus Br (mg/L) of the Siberian Platform samples. The plot includes the seawater evaporation curve and illustrates the position of the four Siberian Platform water groups relative to the seawater evaporation curve. The seawater evaporation line is after Matray, 1988.

The depths at which the four groups of samples were collected are illustrated in Figure 5.9. The majority of group A samples were collected from wells that are below 1000 metres. Group B samples were collected from shallower depths that range between 0 and 1000 metres. Although most of the samples from group C are from depths between 100 and 1000 metres, a couple of samples are from deeper rock units (1650 and 2100 m). Samples in the D group were collected from surface waters and depths down to 600 metres. The great depths at which group A samples were collected supports the previous interpretation drawn from the Br and Cl compositions of these brines (Figure 5.8) where they are considered to result from evaporated paleoseawater. The presence of these brines was probably protected by their density which restrict their movement and also by the presence of thick evaporite units in the upper units that acted as impermeable units. The shallow depths at which the samples of the other groups were collected from also supports the idea of fresh water component in them. In fact the few samples of group B and C that were collected from depths greater than 800 m are characterized by high TDS values and high Cl and Br concentrations, indicating that shallower samples were more susceptible to mixing (dilution) with fresh waters (Figure 5.9).

Further support for the interpretation of origin and evolution of the different groups can be found in Figure 5.10. The piper diagram in Figure 5.10 demonstrates the chemical compositions of the Siberian Platform samples from the various groups. The two main distinctive water groups illustrated in Figure 5.10 are groups A and B. The majority of group A samples are Ca–Cl type brines while group B samples are characterized as Na–Cl type brines. Group C samples, however, show more complex and diverse chemical compositions;

the majority of these samples are either Na–Ca–Cl or Na–Cl water types. Nonetheless, Ca–Mg–Cl and Mg–Ca–Cl type waters also exist. Group C samples appear to have components of A and B but in some cases a third end member or process seems to be influencing the chemical composition. This is very clear when considering the Cl and Br results illustrated in Figure 5.8. The samples of group D have no characteristic water type and are rather different from one another (Figure 5.10).

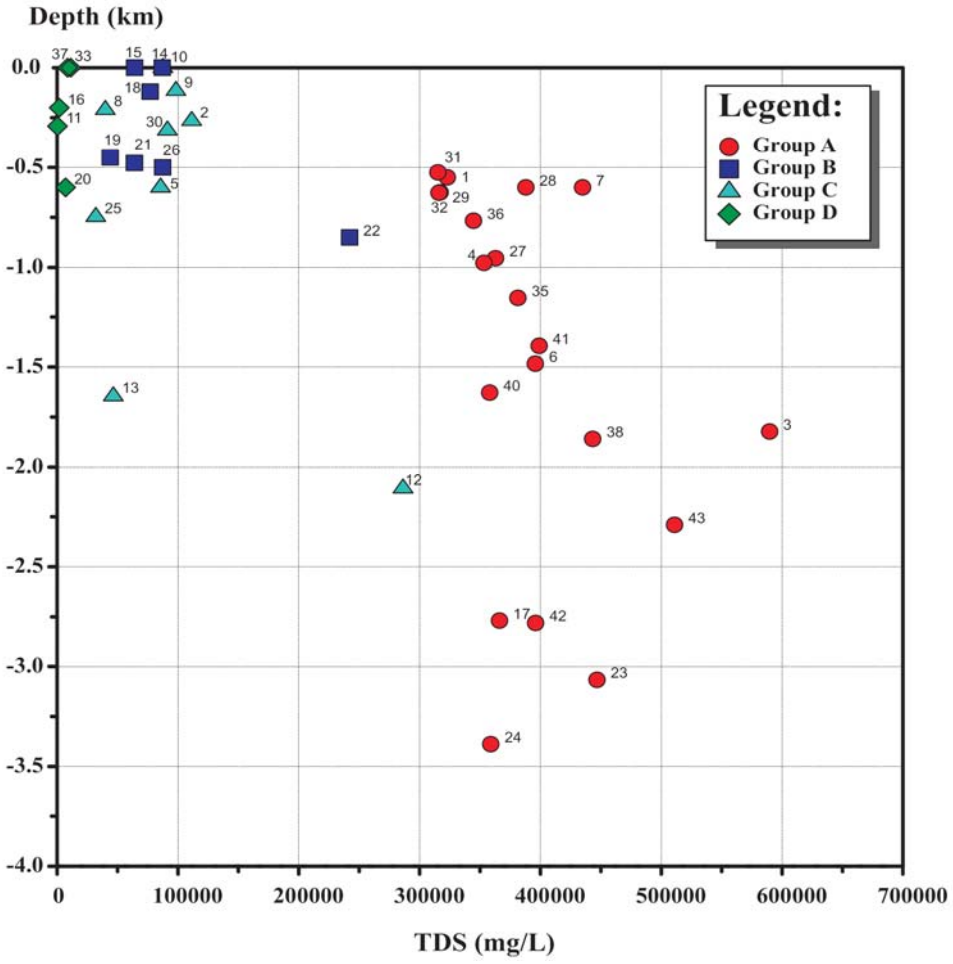

Figure 5.9 Depth (km) versus Total Dissolved Solids (TDS) (mg/L) of the Siberian Platform samples. Group A samples were collected from deeper parts of the basin. They are characterized by higher TDS values relative to the other three groups.

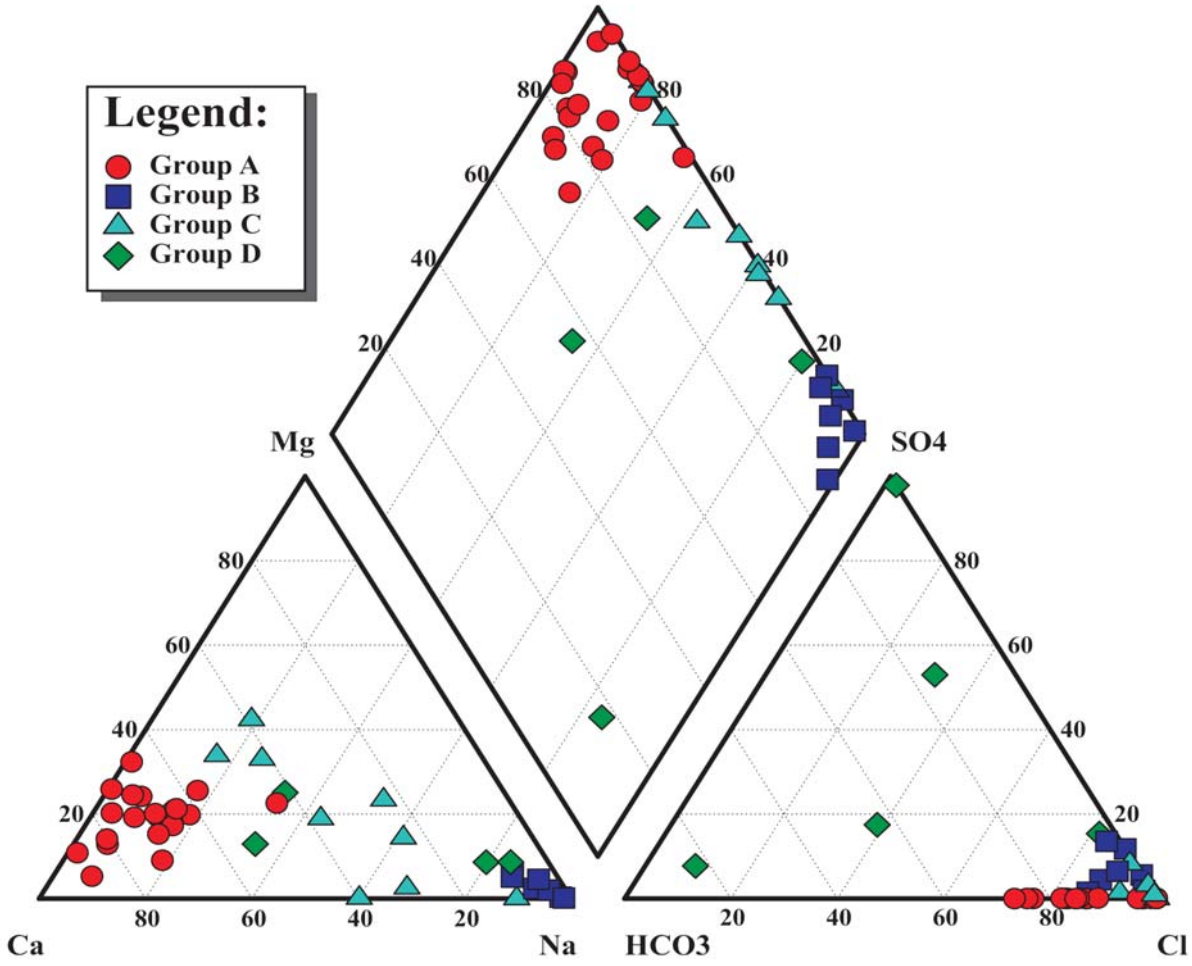

Figure 5.10 Piper diagram of the Siberian Platform samples major ion results. The diagram illustrates the chemical compositions of the four groups. The two major groups are Group A (Ca-Cl) and Group B. (Na-Cl).

Figure 5.11 demonstrates Cl (mg/L) versus Br to Cl (Br/Cl) weight ratios of the Siberian Platform samples and how they compare to the Br/Cl ratio of seawater (0.0034). The Br/Cl ratios of both groups A and C are far greater than the Br/Cl ratio for seawater. The Br/Cl ratios of group A samples are greater than 0.02 and the Br/Cl ratios of group C samples are

between 0.0052 and 0.0196. Group B samples, however, are characterized by Br/Cl ratios less than 0.0012, which are much lower than that of seawater. The Br/Cl ratios of group D samples are between 0.0008 and 0.0100. These values range from less than the seawater Br/Cl ratio to greater than that of the seawater ratio. However, their Cl contents are far less than that of seawater. The most interesting aspect of this diagram is the extreme Br/Cl ratio of many of the group A samples. Very few analyses in the literature for sedimentary or crystalline brines have Br values as concentrated as the Siberian Platform fluids (Frape et al., 2004). This again would support extreme evaporation, long subsurface residence times and/or strong water–rock interaction. Group A and C brines with their high Br/Cl ratios could have interacted with rock salt (halite) and, by selective diffusive processes and/or consecutive dissolution/precipitation reactions, acquired additional Br from the salt (Land and Prezbindowski, 1981). Unlike the dissolution of halite by fresh water that produce brines with low Br content, the interaction between brines and halite causes dissolution and re-crystallization of halite, where a re-distribution of the Br between the brine and the halite body occur and consequently, the halite body loses Br to the brine. This in turn would produce halite bodies that are very poor in Br in comparison to primary halite bodies. In fact, the presence of interbedded salt in the strata and the low Br group B fluids that are believed to be the result of halite dissolution may lend support to this assumption.

The Cl versus Na contents (on milli-equivalent bases) of the Siberian Platform samples is shown in Figure 5.12. This diagram illustrates the position of all samples from all groups relative to the seawater evaporation trend. Groups A and C samples fall above the 1:1 (Na:Cl)

line, while groups B and D samples fall on the 1:1 (Na:Cl) line. In group B brines, Na concentrations range between 2200 mg/L and 98,000 mg/L, while the Cl concentrations range between 3500 mg/L and 133,000 mg/L, and they comprise between 80% and 97% of the major ion composition on a meq basis. This diagram helps to confirm that group B samples are derived or at least heavily affected by halite dissolution. The low concentrations of Ca, Mg, K and Br and low Br/Cl ratios (<0.0012) are consistent with waters derived from halite dissolution.

Figure 5.12 shows that group A samples fall away from the halite dissolution line and from the seawater evaporation line as well. This implies that they have undergone a large degree of diagenetic evolution that changed the water type from Na- to Ca-type waters. The TDS, Cl and Br contents of group A (Figure 5.8) suggest that these brines are the residual of evaporated paleoseawater. If the samples of group A are a residual of evaporated paleoseawater, then according to their Br content, they should have undergone extensive evaporation with an approximate evaporation ratio of 30–128 times. Some of the supporting observations of this scenario are the increasing concentrations of Mg, K, Cl and Br and the decreasing concentration of Ca, Na with progressive evaporation (Carpenter, 1978). All of these trends agree well with what is expected during the evaporation of seawater except for the Ca content of these samples which increases instead of decreases (Table 5.1). This implies that, if evaporated seawater was the precursor, intensive water–rock interactions have replaced Na, Mg and K by Ca (i.e. group A samples followed the seawater evaporation line during their early formation and they deviated from the seawater evaporation line due to the

loss of Na and gain of Ca during water-rock diagenetic processes). This mechanism can be supported by the fact the Na, Mg and K concentrations of these samples are much lower than what is expected as a result of seawater evaporation for samples with such high TDS. Furthermore these waters are characterized by lower concentrations of SO_4, which is again the opposite of what is expected in the case of a seawater evaporation scenario. One mechanism that could remove SO_4 is the formation of gypsum and or anhydrite, which is common in the geological strata of the Siberian Platform. Another theory that may explain the observed high Ca concentrations and low SO_4 concentrations, of these samples would be by starting with a $CaCl_2$ type water that is rich in Ca and poor in SO_4. The presence of $CaCl_2$ oceans in the Paleozoic that are rich in Ca and poor in SO_4 has already been put forward by Lowenstein et al. (2003). They concluded that the paleoseawaters of the Cambrian to Mid-Devonian period were Ca-rich and SO_4-poor. This theory can explain the Ca-rich and SO_4-poor brines found in the Siberian Platform. The elevated concentrations of minor ions such as Li (40 and 240 mg/L) and Sr (1000 and 4000 mg/L) of group A fluids (Table 5.1 and Figure 5.13) are also consistent with evaporated seawater (Davisson and Criss, 1996) and they support the idea of the evolution of these brines via diagenetic processes that changed the brines from Na to Ca type brines as illustrated in Figure 5.12.

Samples 3, 35, 38, and 43 of group A (Figure 5.12) that show the most extensive change from Na to Ca type waters (highly altered by diagenetic processes) are one of the most concentrated brines (>380,000 mg/L) (Table 5.1) and they are from great depths (>1.5 km). On the other hand, samples that suffered less alteration and possibly more dilution such as

samples 31 and 32 are from shallow depths and are characterized by lower TDS values (~300,000 mg/L). The elevated Br concentrations of these samples suggest that they were diluted with less saline fluids such as seawater or fresh water (Figure 5.12). Sample 24 (Figure 5.12) illustrates a shift toward the Na:Cl 1:1 line which implies an interaction of the brine with a halite body. The high Br concentration of this sample suggests a direct interaction between the brine and the halite body rather than mixing between the brine and a halite dissolution fluid.

The elevated Cl concentrations in comparison to Na of group C samples and their location on Figure 5.12 relative to the 1:1 (Na:Cl) line suggest that these samples are not derived from halite dissolution or, at least, halite dissolution is not the major cause in forming these saline waters. The high concentrations of Ca, Mg, K, Br and high Br/Cl ratios further lend support to the conclusion that these samples are not primarily derived from halite dissolution. The chemistry of this group's brines suggests an evaporated seawater origin that suffered dilution with less saline water (e.g. seawater) or fresh water as illustrated in Figure 5.12 (e.g. mixing between group A type waters and seawater or fresh water). The shallow depths of these samples, in general (Figure 5.9), supports the dilution hypothesis.

Samples from group D represent a few examples of fresh to brackish waters. The samples are from three shallow boreholes and two surface waters (a spring near the Chona River (#33) and from Lake Baikal (#37)).

In summary, group A samples are believed to be evolved from evaporated seawaters that were modified by diagenetic processes, while group B samples are product of halite

dissolution. Group C samples on the other hand are believed to be evolved by mixing between two end members; a highly concentrated brine such as group A with a less saline water such as seawater or fresh water, while group D waters are few examples of shallow fresh and brackish waters.

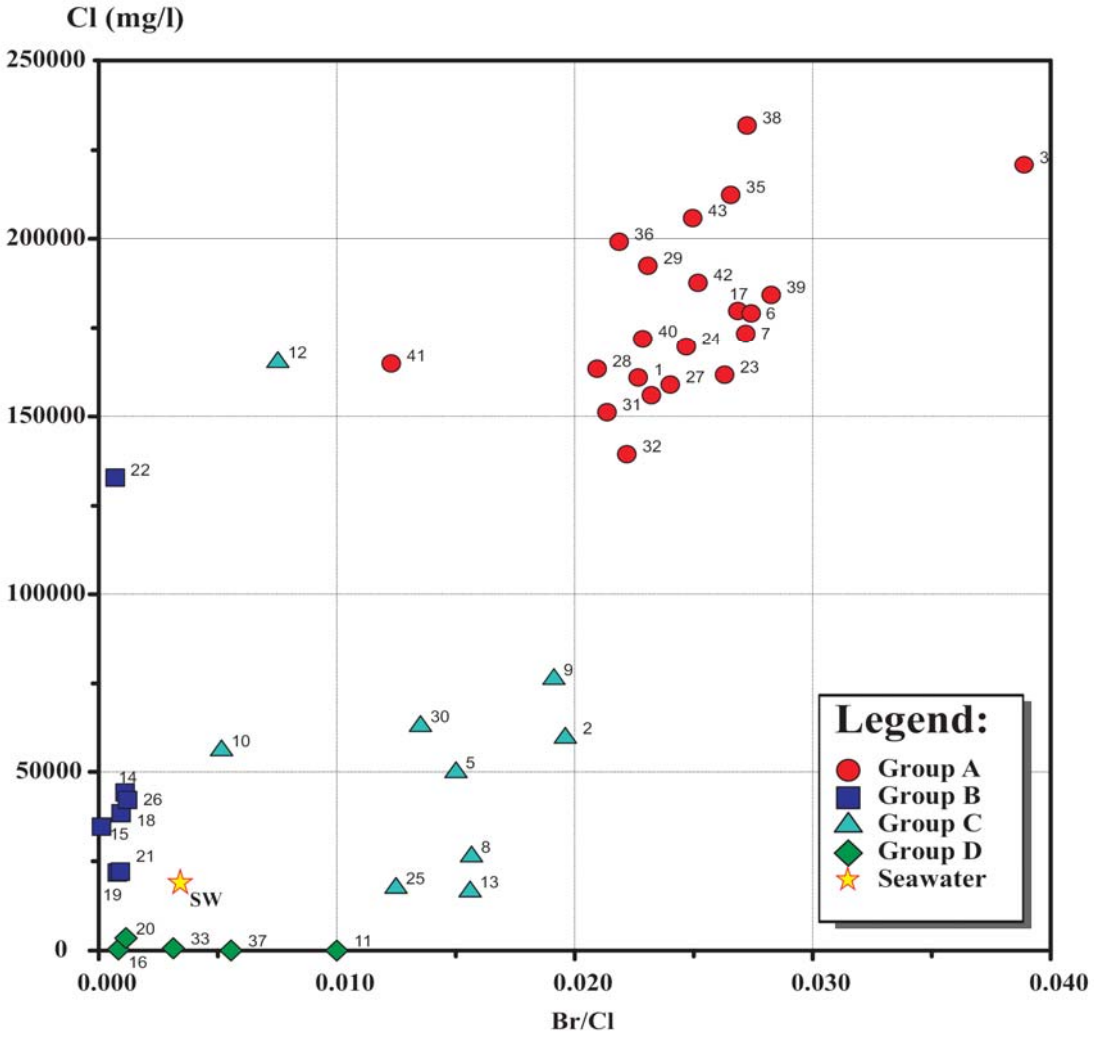

Figure 5.11 Plot of the Cl concentrations (mg/L) versus Br to Cl weight ratio of the Siberian Platform samples. Group A (Ca-Cl) samples are characterized by high Br/Cl ratios while Group B (Na-Cl) samples are characterized by low Br/Cl ratios.

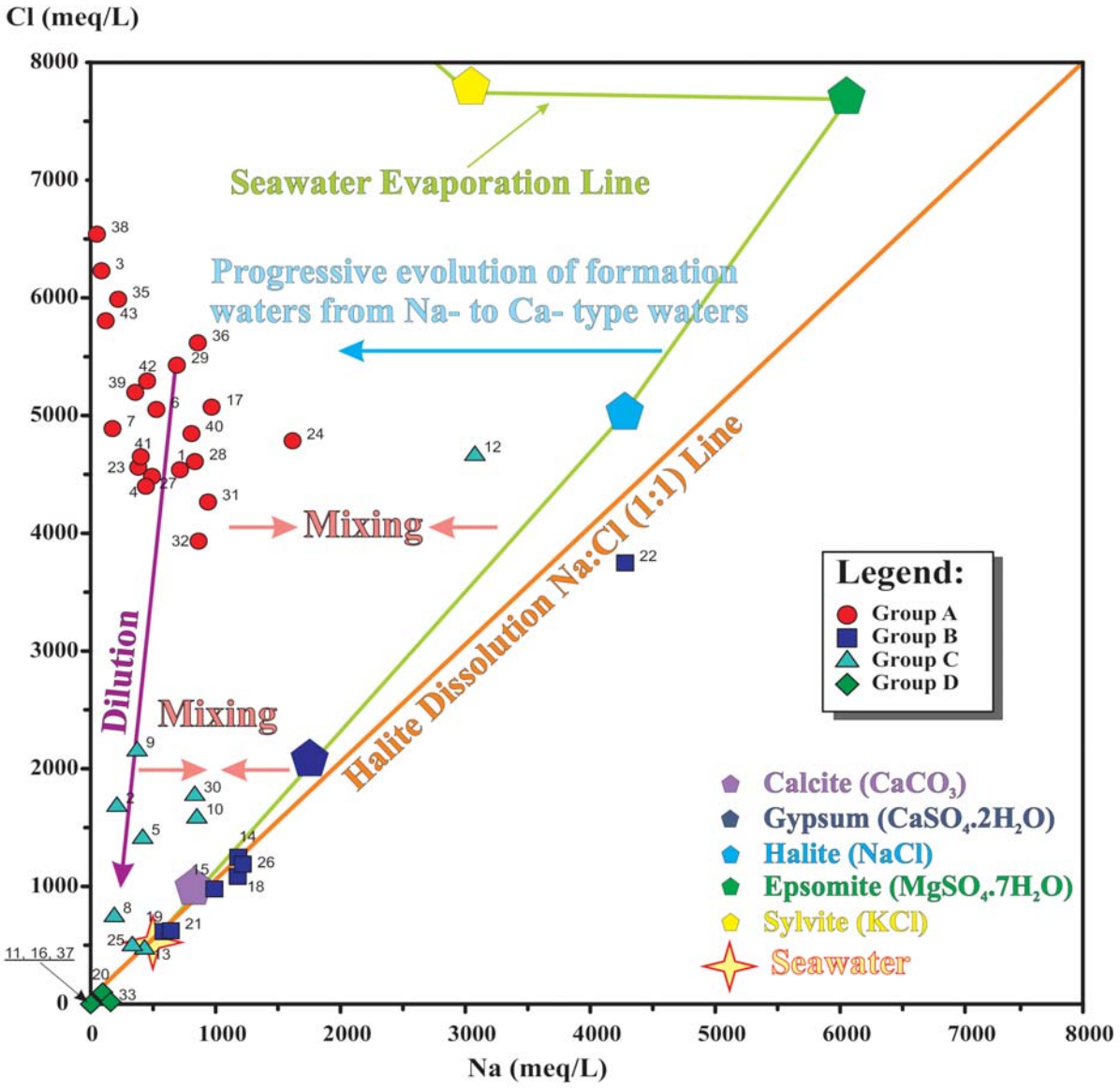

Figure 5.12 Chloride concentrations (meq/L) versus Na concentrations (meq/L) for the Siberian Platform samples. Group B (Na-Cl) samples fall on the 1:1 (Na:Cl) line, while Group A (Ca-Cl) samples are located above the 1:1 (Na:Cl) line. Some of the possible evolutionary processes and mixing scenarios between the end members are also demonstrated.

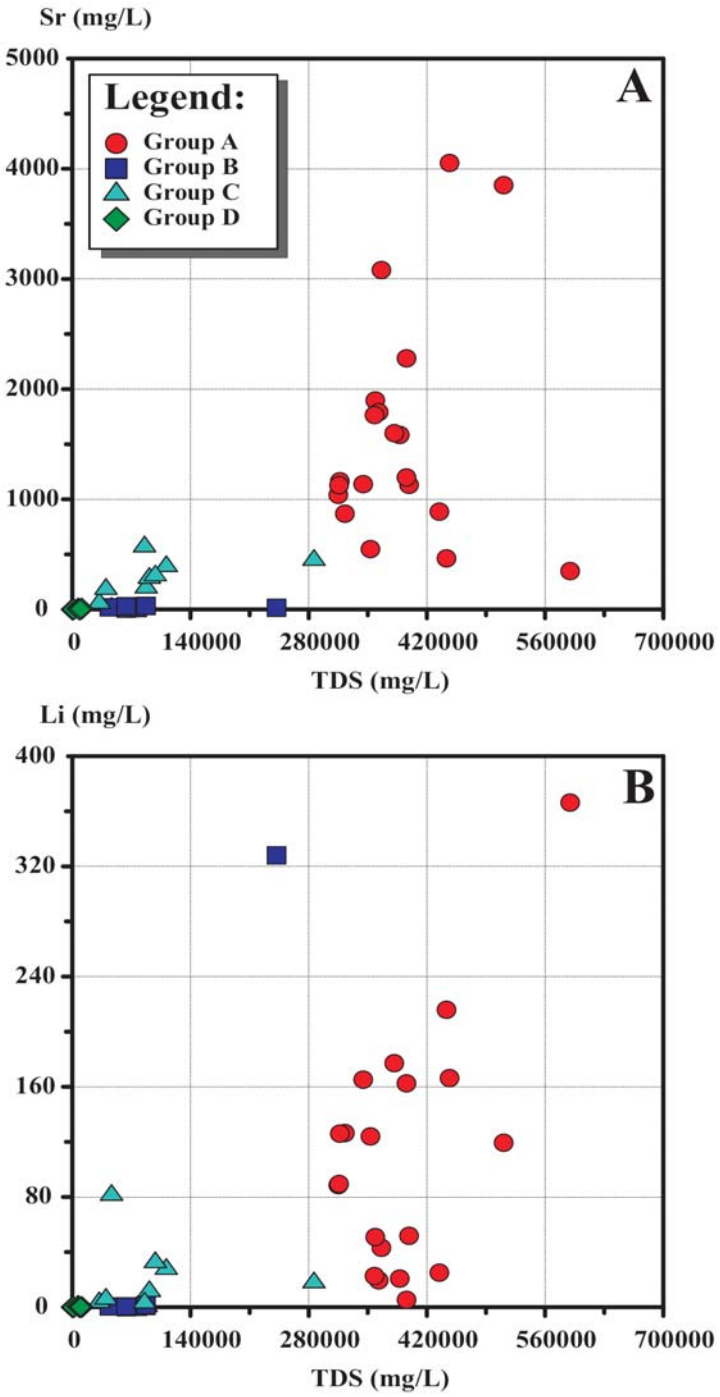

Figure 5.13 (A) Strontium (mg/L) versus TDS (mg/L) and (B) Lithium (mg/L) versus TDS (mg/L) of the Siberian Platform. Group A (Ca-Cl) samples show elevated Sr and Li contents in comparison with the other three groups.

5.7.2 Interpretation based on the isotopes of ^{18}O and ^{2}H

The $\delta^{2}H$ versus $\delta^{18}O$ values of the four groups of samples are presented in Table 5.1. Figure 5.14 illustrates the behaviour of seawater isotopic compositions ($\delta^{2}H$ and $\delta^{18}O$) during evaporation as proposed by Holser (1979). During the early phases of evaporation of seawater the lighter isotopes are preferentially removed from solution and the residual seawater becomes enriched in the heavier isotopes (^{18}O and ^{2}H). Isotopic analysis of an evaporating marine salt pan by Holser (1979) indicated that progressive enrichment of the heavier isotopes does not continue indefinitely, but that the trajectory hooks around as shown in Figure 5.14 at an evaporation degree of 4 fold. During progressive evaporation the relative amount of water tied up in hydration spheres around cations increases. Isotope exchange between this water, the unbound water, water molecules leaving the liquid-air interface, and atmospheric water vapour may be the cause of the hook-shaped trajectory (Holser, 1979). The shape and the extent of the hook very probably depend on local humidity, temperature, average wind speeds, and other climatic variables (Knauth and Beeunas, 1986). The evaporation hook-shaped curve of Holser (1979) was extrapolated by Knauth and Beeunas (1986) to demonstrate to x45 degree of evaporation. Halite precipitation begins at about x11 (Knauth and Beeunas, 1986). Additional processes such as hydrothermal activities (e.g. mixing with geothermal waters) and high temperature water-rock interaction could be important in sedimentary basins as they would cause enrichment of the ^{18}O content of the water. For example, Sheppard (1986) reported that the $\delta^{18}O$ signature enrichments and shifts

to the right of the GMWL are predominantly caused by isotopic exchange with ^{18}O-rich sedimentary minerals such as carbonates.

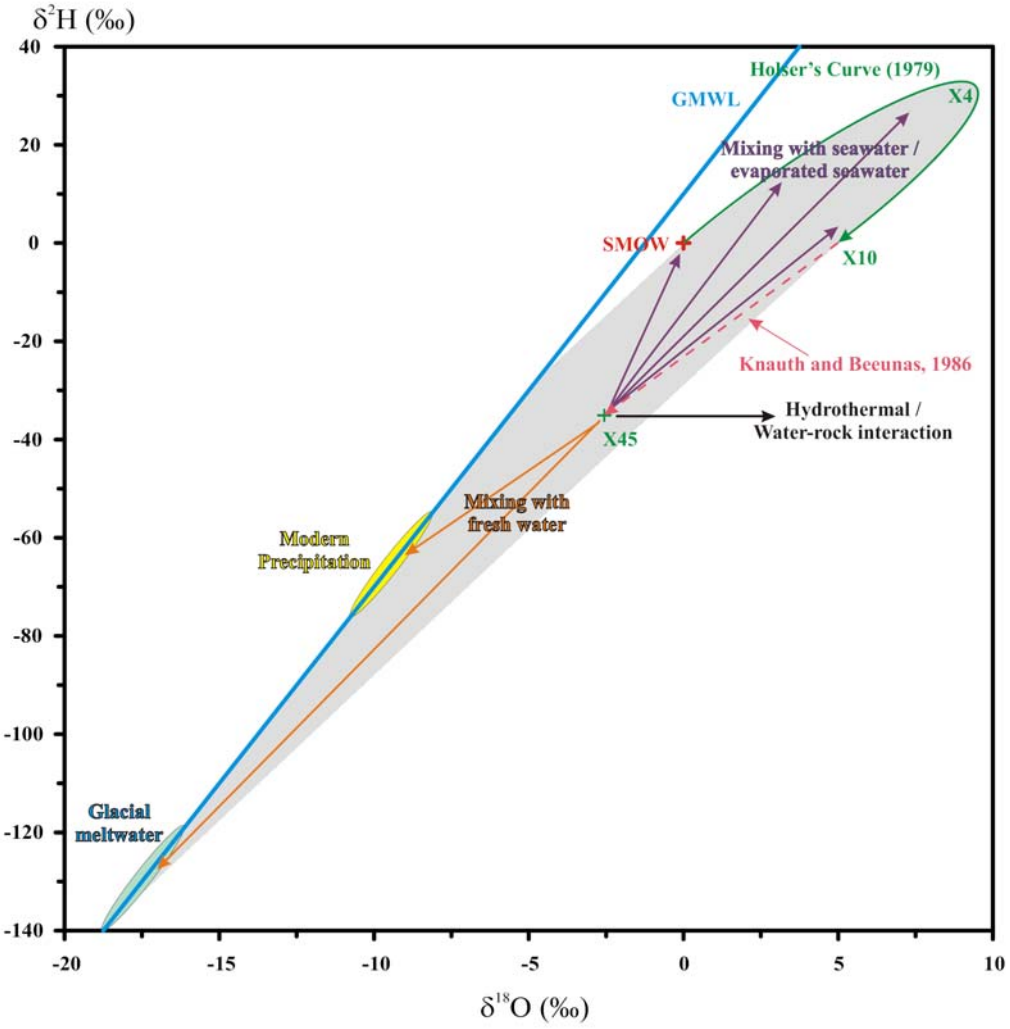

Figure 5.14 The different possible end members and processes that control the oxygen and hydrogen isotopic compositions of the southern Ontario and Michigan formation waters. Seawater (SMOW), different degrees of seawater evaporation, modern precipitation, and glacial melt-water are the main end-members. Mixing between various end members, seawater evaporation, hydrothermal activities, and water-rock interactions are the major processes. The shaded area represents the mixing area between the main end members. The Figure contains the seawater evaporation curve by Holser (1979) and indicates some evaporation degrees (x4 and x10). It contains also the extrapolated evaporation point at 45 fold of evaporation (x45) extrapolated by Knauth and Beeunas (1986).

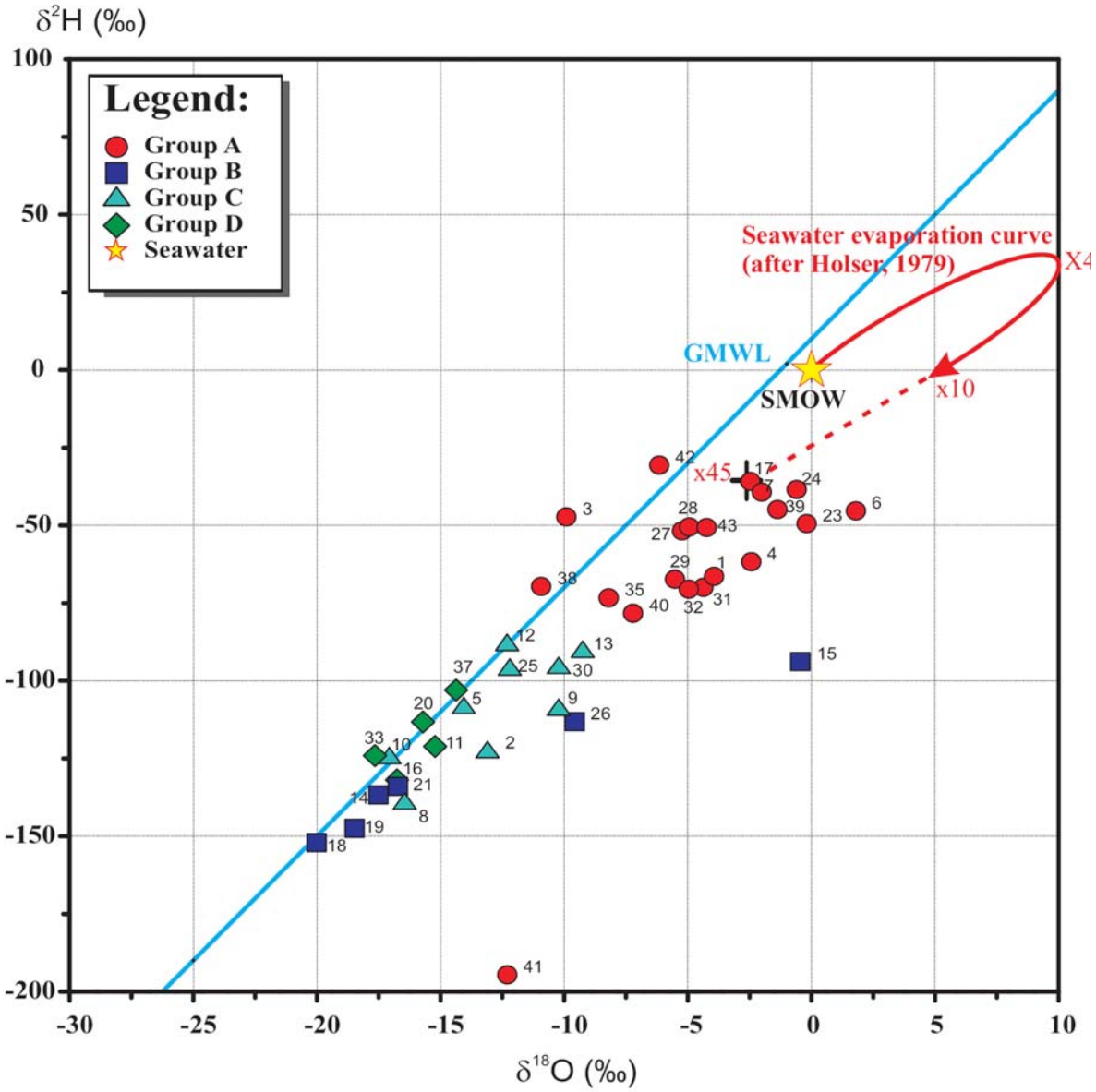

Figure 5.15 Stable isotopic composition (δ^2H and $\delta^{18}O$) of water samples from the Siberian Platform compared to the Global Meteoric Water Line (GWML). Group A (Ca-Cl) samples are characterized by enriched δ^2H and $\delta^{18}O$ values relative to the results from the other groups. The Figure contains the seawater evaporation curve by Holser (1979) and indicates some evaporation degrees (x4 and x10). It contains also the extrapolated evaporation point at 45 fold of evaporation (x45) extrapolated by Knauth and Beeunas (1986).

The $\delta^{18}O$ compositions are enriched in marine carbonates by 29 ‰ relative to the water they precipitated from at ambient temperature, however, the equilibrium between carbonate and water is reduced to only 8 ‰ at 250°C (Clark and Fritz, 1997). Therefore, at high temperature water-rock interaction processes, the ^{18}O of formation waters tends to get enriched and that of carbonates tends to get depleted. Figure 5.14, illustrates also few mixing scenario between the following end members; 1) Seawater (SMOW), 2) saline waters of different degrees of seawater evaporation, 3) modern precipitation, and 4) glacial melt-water. The shaded area represents the mixing area between the main end members.

Figure 5.15 shows the $\delta^{2}H$ versus $\delta^{18}O$ values of the four groups of samples. The different water groups are not distinguished from each other based solely on their chemical composition; they are also distinguishable based on isotopic characteristics. The O and H stable isotope signatures of group A samples are the most enriched in comparison to the other groups and they fall to the right of the GMWL and along a possible evaporation line. Holser (1979) estimated the behaviour of $\delta^{2}H$ versus $\delta^{18}O$ of seawater during evaporation. The comparison between the $\delta^{2}H$ and $\delta^{18}O$ of these samples (Figure 5.15) and the diagram in Figure 5.14, indicates that group A brines underwent extensive evaporation that exceeds a 45-fold increase in seawater concentration. This lends support to evaporation as the major evolutionary process that affected the original water. It is also in agreement with the assumption made earlier based on the TDS and Br concentrations that these samples experienced evaporation of 30–128 times. Although these samples cluster together, they also show some variation in their isotopic characteristics, which is consistent with what is

observed through their chemical composition. This is probably due to the large geographic distances that these samples cover resulting in various degrees of evaporation at the time of formation. Furthermore, the enriched $\delta^{18}O$ values of some of the samples could be due to different depositional climates (e.g. temperature and humidity) that would affect the shape of the hook or could be due to high temperature water-rock interaction which in line with interpretation made earlier to explain the high concentrations of Ca in these brines.

Five of the seven group B samples fall on the GMWL indicating that these samples did not experience significant evaporation and suggesting that the origin of these samples is probably fresh meteoric waters that were impacted by the salt deposits. This is consistent with the sample depth (Figure 5.9) where infiltration of fresh water is feasible. The $\delta^{2}H$ versus $\delta^{18}O$ values of group B samples are the most depleted of all samples and their signatures are very different from group A signatures. They are typical of recharge under cold climate conditions and they are within the range of $\delta^{2}H$ versus $\delta^{18}O$ (-165 ‰ to -110 ‰ and -20 ‰ to -15 ‰, respectively) of lakes, rivers and precipitation in the northern part of the Siberian Platform (Alexeev and Alexeeva, 2003). Generally, group B brines are more depleted than the isotopic signatures of shallower samples found in group D samples from the same geographic area, which might imply that these waters were recharged at colder climatic conditions. The isotopic differences, along with the chemical differences discussed previously, indicate that groups A and B are representative of two different types of brines from two different processes and sources. One of the two samples deviating from the GMWL and showing enriched values for $\delta^{2}H$ versus $\delta^{18}O$ (-113 ‰ and -9.6 ‰, respectively) is from Lake

Mohsogoloh (sample #15). The enrichment in both stable isotopes is explained by the evaporation effect on lake water. The other sample that showed some deviation from the GMWL is sample #26, which was sampled from a 500 m borehole in a dolomite aquifer. This specific sample, besides being enriched in $\delta^{2}H$ versus $\delta^{18}O$ (-94 ‰ and -0.5 ‰, respectively), has the highest pH value of all samples (8.4). It has the lowest water temperature (-1°C) of this group and the most enriched $\delta^{37}Cl$ (+1.54 ‰) value of all samples. The enrichment in $\delta^{2}H$ versus $\delta^{18}O$ can be explained by evaporation. The enriched $\delta^{37}Cl$ value is greater that any reported $\delta^{37}Cl$ values for evaporites (-0.5 ‰ to +1 ‰) in the literature (Kaufmann et al., 1984; Eggenkamp and Schuiling, 1995; Eggenkamp et al., 1995; Eastoe et al., 1999; Eastoe and Peryt, 1999; Eastoe et a., 2001; Stewart and Spivack, 2004). Although the presence of evaporites outside this range is possible, this enriched $\delta^{37}Cl$ value is not easily explained simply by halite dissolution. Long term permafrost impact cannot explain this as well, as permafrost would normally cause the three isotopic composition ($\delta^{2}H$, $\delta^{18}O$ and $\delta^{37}Cl$) to get depleted in the residual (Zhang and Frape, 2003) which the opposite to what is observed in this case. It is probably more reasonable to assume that the groundwaters represented by this specific sample were impacted by other processes in combination with halite dissolution, such as water–rock interaction with some minerals that were enriched in $\delta^{37}Cl$.

Group C samples either fall on the GMWL or to the right of the GMWL on possible evaporation lines. The location of these samples on the $\delta^{2}H$ versus $\delta^{18}O$ plot is intermediate between group A and group B samples, with a tendency to be closer to group B samples. This might suggest that the waters involved in the dissolution of halite that produced group B

brines or similar waters were involved in evolving group C brines. This observation is consistent with the discussion on the chemical data and further supports the assumption that these samples are the probable result of dilution of evaporated seawater brines such as group A with less saline waters (e.g. fresh waters). In fact, the $\delta^{2}H$ and $\delta^{18}O$ suggest that the dilution was with fresh waters and not seawaters which cannot be differentiated based on the illustration of the data in Figure 5.8 and Figure 5.12. The $\delta^{2}H$ and $\delta^{18}O$ of group D samples are within the local precipitation range. All samples in group D fall on or just below the GMWL, suggesting that these samples do represent local meteoric waters in each of the areas.

5.7.3 Additional information to be learned from ^{37}Cl and ^{81}Br isotopes

The Cl and Br stable isotope results of group A samples show narrow variations (Figure 5.16). The $\delta^{37}Cl$ values fall between -0.67 ‰ and +0.04 ‰ (range of 0.71 ‰) and the $\delta^{81}Br$ values are between -0.31 ‰ and +0.27 ‰ (range of 0.58 ‰). The relatively narrow variation of these two isotopes might suggest that the $\delta^{37}Cl$ and $\delta^{81}Br$ signatures of the original source waters are within the isotopic ranges obtained. The small variations would be due to the large geographical area over which the samples occur or to post depositional evolution(s) that affected the composition of the waters. Although the variations for both isotopes are not large, they are significant enough to show that they are the result of various degrees of evolution or mixing, which is consistent with the assumptions made earlier based on chemical composition and traditional isotopes ($\delta^{2}H$ and $\delta^{18}O$).

Four samples (#17, #23, #24 and #42) of group A were obtained from the crystalline basement (AR-PR) from two different sites (II and V) (Figure 5.1). These samples have some isotopic signatures ($\delta^{2}H$, $\delta^{18}O$, $\delta^{37}Cl$ and $\delta^{81}Br$) that are characteristic of crystalline type brines (Frape et al., 2004). A careful examination of the isotopic values of the 4 brines shows some small discrepancies. Sample #42 has $\delta^{2}H$ and $\delta^{18}O$ values that plot above (to the left of) the GMWL while the other three samples plot below (to the right of) the GMWL unlike crystalline shield brines. Values above the GMWL are not uncommon in crystalline type brines (Fritz and Frape, 1982; Frape et al., 2004). This is most likely due to hydration processes and the formation of clay minerals that affected the isotopic signature and enriched both $\delta^{2}H$ and $\delta^{18}O$ values (Fritz and Frape, 1982). The isotopic signatures of these group A basement brines, unlike typical crystalline brine signatures, may be more representative of Cambrian sedimentary formation fluids that have penetrated the underlying rocks. The $\delta^{37}Cl$ and $\delta^{81}Br$ values of these four brines are very close to those reported for Canadian Shield brines (Shouakar-Stash et al., 2005a). It is worth noting here that sample #42 shows the most depletion of $\delta^{37}Cl$ and $\delta^{81}Br$ compared to all other samples (Figure 5.16), as well as a significant isotopic shift for ^{18}O (Figure 5.15). It is hypothesized that hydration and long term water–rock interactions between brines and crystalline rocks have modified the Cl and Br stable isotope signatures in these samples. This coincidence between $\delta^{2}H$ and $\delta^{18}O$ values plotting above the GMWL and the $\delta^{37}Cl$ and $\delta^{81}Br$ values that are more depleted is also observed in sample #3. This might suggest some common geochemical process that alters $\delta^{2}H$ and $\delta^{18}O$ as well as $\delta^{37}Cl$ and $\delta^{81}Br$ values.

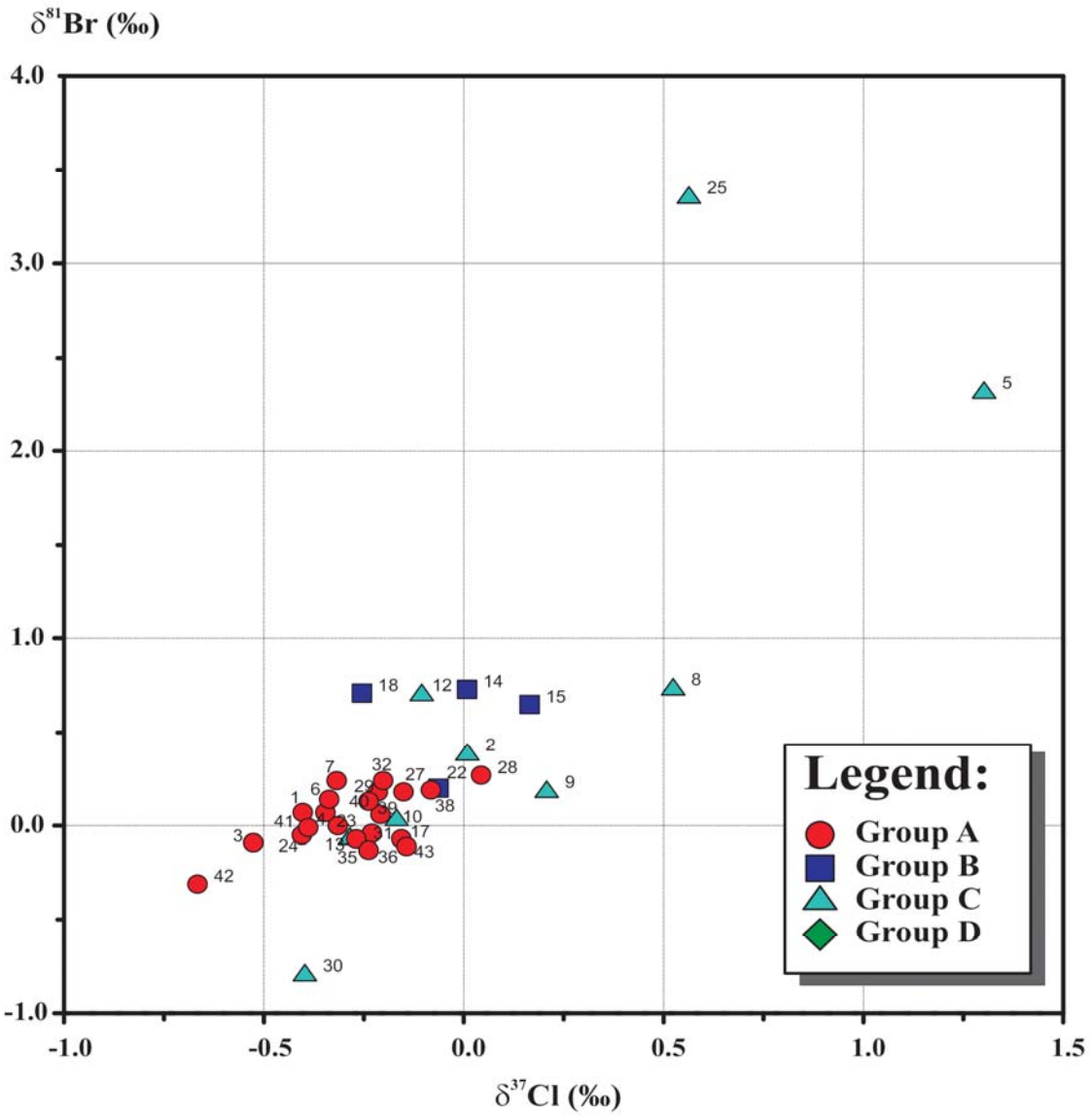

Figure 5.16 The $\delta^{37}Cl$ (‰) - $\delta^{81}Br$ (‰) relationship for the Siberian Platform samples. Group C samples show the widest spread of both $\delta^{37}Cl$ and $\delta^{81}Br$ values. These $\delta^{81}Br$ values demonstrated an increased range (-0.8 ‰ to +3.35 ‰) natural samples.

The $\delta^{37}Cl$ values of group B samples range between -0.25 ‰ and +1.54 ‰; however, four of the samples fall within a narrow range, -0.25 ‰ and +0.17 ‰ (Figure 5.16). These values

are consistent with and within the reported range for halite (-0.9 ‰ and +1.2 ‰) (Kaufmann et al., 1984; Eggenkamp and Schuiling, 1995; Eggenkamp et al., 1995; Liu et al., 1997; Eastoe et al., 19991; Eastoe and Peryt, 1999; Eastoe et al., 2001; Stewart and Spivack, 2004; Eastoe et al., 2007). The δ^{81}Br values range between +0.20 ‰ and +0.73 ‰. The δ^{81}Br values of this group are generally more enriched than group A samples. The relatively small variation of these two isotopes suggests that the processes that affected these samples were limited to halite dissolution and evaporation. From the chemical composition and the isotopic characteristics of the samples of this group, it is concluded that halite dissolution as a result of recharge of a ^{2}H and ^{18}O depleted colder climate water is the major process in creating these saline waters. This assumes that isotopic alteration of Br stable isotopes during halite dissolution is not a major fractionation process and therefore that the δ^{81}Br signature of halite deposits in the study area are probably similar to those of δ^{81}Br values obtained from group B brine samples (+0.20 ‰ and +0.73 ‰). However, these signatures are probably enriched in comparison to the original brines that deposited the halite. One might expect that during the precipitation of halite, more heavy bromine isotopes would be incorporated in the halite lattice (structurally bonded), which will cause an isotopic fractionation of bromine isotopes between bromide ions in the halite lattice and bromide ions in the residual brine. Because of the very small partition coefficient of bromide between halite and solution, this will not cause any measurable fractionation to the brine. Nonetheless, this hypothesis needs to be taken with caution, because, the amount of bromide that exists in halite as fluid inclusions and/or pore water is even higher than that structurally bonded. Trapped bromide as fluid inclusion is most

likely not affected by any fractionation and is probably isotopically representative of the original brines that formed the halite. Therefore, the isotopic signature of the trapped pore waters and or fluid inclusions will most likely mask the isotopic signature of the structurally bonded bromide and the bulk bromine isotopic signature of the halite deposits can be representative of that of the original brine.

The $\delta^{37}Cl$ values of group C samples range between -0.40 ‰ and +1.30 (Figure 5.16) and their $\delta^{81}Br$ values have the greatest range of all samples collected (-0.80 ‰ to +3.35 ‰) (Figure 5.16). The combination of these results (Figure 5.16) strongly dismisses the simple mixing scenario discussed above between group A and group B (e.g., Figures. 5.10, 5.12, and 5.15). A more complex scenario for brine evolution needs to be considered. Figure 5.17 illustrates sample depth versus $\delta^{37}Cl$ and $\delta^{81}Br$ signatures. Two positive correlations between depth and both $\delta^{37}Cl$ and $\delta^{81}Br$ are observed in group C samples. More fractionation is observed for the shallower samples. The larger range of $\delta^{81}Br$ signatures of shallow samples compared to deeper samples was also observed in the Michigan samples (Figure 4.12, Chapter 4). These fractionations are probably due to surficial processes (e.g. biological activities or reduction/oxidation processes), especially that shallow samples are characterized by enriched isotopic values. For example, oxidation processes are reported to cause large isotopic fractionations (Coleman et al., 2003; Böhlke et al., 2005), where the residual is isotopically enriched. High temperature water-rock interaction cannot be used to explain the highly enriched $\delta^{37}Cl$ and $\delta^{81}Br$ compositions of samples #5 and #25 and their $\delta^{18}O$ values do not support this mechanism as well. Similarly the permafrost freezing mechanism is not

considered as this process is expected to cause depletion and not enrichment to these two isotopic vales along with the $\delta^{18}O$ value (Zhang and Frape, 2003).

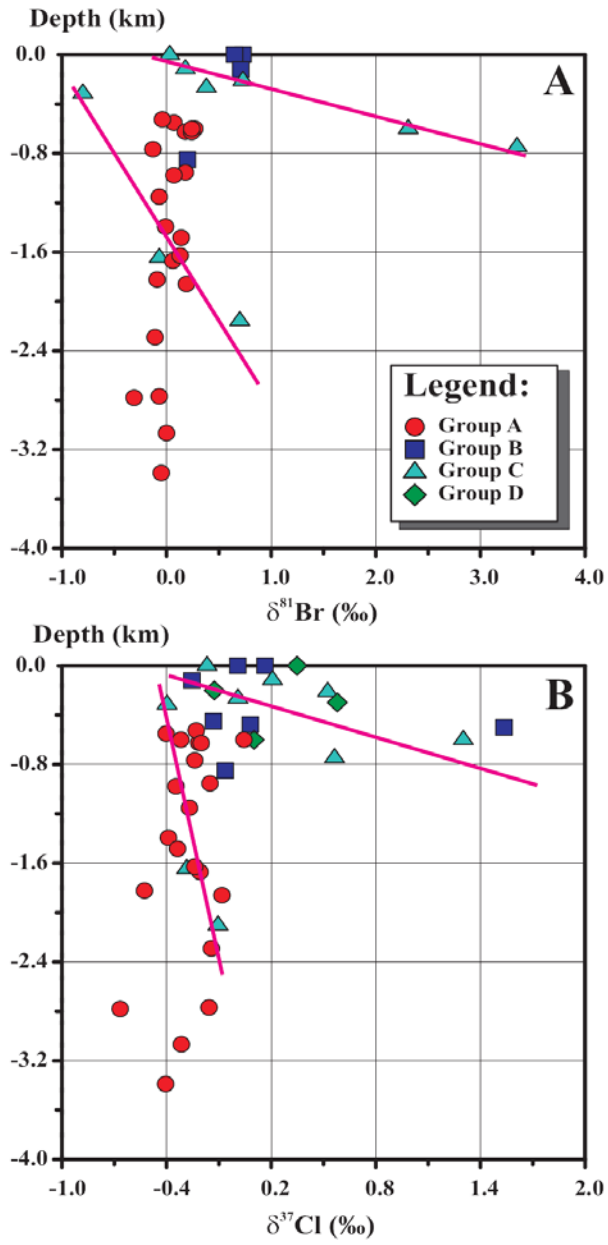

Figure 5.17 (A) Depth (km) versus $\delta^{81}Br$ (‰) and (B) depth (km) versus $\delta^{37}Cl$ of the Siberian Platform samples. Group C samples show the most diverse range for both isotopes. Enrichment trends of both isotopes with depth of group C are also indicated.

Sample # 12 is different from the rest of the samples of group C. It has a high TDS value (286,000 mg/L) and relatively high Sr and Li contents. Furthermore, it has a $\delta^{37}Cl$ value that is within the range of the group A samples. This shows a probable connection to group A type samples, however, the low Br/Cl ratio (Figure 5.11) suggest that this sample was modified by halite dissolution. This interpretation sounds reasonable when considering chemical and isotopic data except for the relatively $\delta^{81}Br$ enriched value (0.70 ‰) of this sample relative to the range of $\delta^{81}Br$ values of group A samples (-0.31 ‰ and +0.27 ‰). Therefore, the most likely origin of this sample is a group A member that was heavily modified by halite dissolution which is supported by the high Na content (see Figure 5.12).

Samples #2 and #9, are probably mixtures between group A type waters and meteoric fresh waters. Their chemical data (e.g. their relatively high Sr and Li contents and their Na and Cl content (Figure 5.12)) and their $\delta^{2}H$ and $\delta^{18}O$ values (relatively depleted values that indicate a meteoric origin) would support this conclusion. This is further supported by the small shift of these samples outside the group A range. This is reasonable given the fact that the chlorine and bromine content in meteoric waters is relatively low in comparison to those in brines and hence the isotopic values of both Cl and Br would be controlled by the brine.

Sample # 10 (spring water) is probably a similar scenario to that of sample # 2 and #9; however the higher Na content than Ca in this sample in comparison to the other two samples (#2 and #9) suggest another component to the equation, which is halite dissolution. The meteoric component is evident by the relatively depleted $\delta^{2}H$ and $\delta^{18}O$ values (-124.9 ‰ and -17.07 ‰, respectively). The relatively high Li and Sr contents (Table 5.1) are in support of a

group A component and the high Cl content and low Br/Cl ratio are evident for the third component (halite dissolution). The near zero $\delta^{37}Cl$ and $\delta^{81}Br$ values of this sample, that are similar to group A samples are very much in favour of this, because in the case of such a combination between all three components, the isotopic signature of group A would be the dominant.

The evolution of sample # 13 is probably similar to that of the above sample #10, although the halite component seems to be higher (higher Na concentration in comparison to Ca concentration). However, the Br/Cl does not support this and actually suggests the opposite. Its $\delta^{2}H$ and $\delta^{18}O$ values and their deviation below the GMWL line, suggests an evaporation process and much smaller meteoric water component. A clear conclusion is not easy to draw and this could be due to the quality of this sample (charge balance ~13.8).

Sample # 5 and # 25 that are characterized by the two most enriched samples in both chlorine and bromine isotopes and are most likely the results of a complex scenario of evolution that is beyond halite dissolution or mixing. The depleted $\delta^{2}H$ and $\delta^{18}O$ values of these two samples are an indication of meteoric water origin. Their position near the GMWL suggests that they did not experience any degree of evaporation. The relatively high Br/Cl values (~0.015) of these two samples are an indication of a lack of halite contribution. This is also evident by their deviation from the Na:Cl (1:1) line. Their Sr and Li content are probably indicative of some group A component. However, their $\delta^{37}Cl$ and $\delta^{81}Br$ values suggest that a mixing between the different end-members discussed so far will not produce such enriched values. Diffusion is expected to cause depletion not enrichment to the low concentration end

(Kaufmann et al., 1988). Therefore, diffusion cannot be responsible for these isotopically enriched values. Furthermore, due to the larger relative difference in mass between the chlorine isotopes, diffusion is expected to cause more fractionation to the chlorine isotopes relative to the bromine isotopes. The larger fractionation in the bromine isotopes of these samples relative to the chlorine isotopes lends support to the elimination of diffusion as the responsible mechanism of the evolution of these waters. The physical process that can be responsible for enrichment is ion filtration (Hanshaw and Coplen, 1973; Fritz and Marine, 1983; Phillips and Bentley, 1987), however, it is not known at this stage if ion filtration is expected to cause larger fraction for bromine isotopes in comparison to chlorine isotopes. Because of the smaller relative difference in mass between the bromine isotopes, one would expect less fractionation between the bromine isotopes, with respect to that of chlorine isotopes, during ion filtration. Therefore, although there is no enough evidence to support ion filtration as the responsible mechanism for the evolution of these waters, the isotopic enrichments suggests ion filtration as one of the potential evolutionary processes that affected these waters.

All of the chemical and isotopic data of sample # 8, including $\delta^{37}Cl$ and $\delta^{81}Br$ suggest that this sample has experienced the same evolutionary process, however with different mixing ratios. The lower TDS values and the depleted $\delta^{2}H$ and $\delta^{18}O$ values of this sample strongly suggest a larger fresh water component.

The $\delta^{37}Cl$ values of group D samples range between -0.13 ‰ and +0.58 ‰ (Table 5.1). They tend to be more positive than the deeper samples and are typical of most shallow

groundwaters reported in the literature (Kaufmann et al., 1984; Desaulniers et al., 1986; Hendry et al., 2000; Frape et al., 2004; Stewart and Spivack, 2004). These samples were not analyzed for $\delta^{81}Br$ due to the very low Br content and small sample volumes.

Figure 5.18 shows the $\delta^{37}Cl$ and $\delta^{81}Br$ values obtained from group A samples based on the geological section from which they were sampled to determine if there is any relationship between the isotopic signatures of the two isotopes and the stratigraphy in group A, as these samples represent paleoseawater. The majority of group A samples are either Archaean–Proterozoic crystalline brines or Early Cambrian sedimentary brines. However, there are some samples that are associated with Early to Middle, Middle, and Middle to Late Cambrian formations. The $\delta^{37}Cl$ and $\delta^{81}Br$ values of the Archaean–Proterozoic crystalline brines range between -0.67 ‰ and -0.16 ‰ and between -0.31 ‰ and 0 ‰, respectively. This group is characterized by the most depleted range in both isotopes. The Early Cambrian sedimentary brines $\delta^{37}Cl$ values range between -0.53 ‰ and +0.04 ‰ and their $\delta^{81}Br$ values range between -0.11 ‰ and +0.27‰. The $\delta^{37}Cl$ and $\delta^{81}Br$ values of the Early to Middle, Middle, and Middle to Late Cambrian formation waters fall within the range for the Early Cambrian brines. This suggests that all of the Cambrian sedimentary brines have a common origin.

5.8 Conclusions

The water samples collected from the Siberian Platform were examined and classified into four different groups (A, B, C and D) based on their chemical composition. Group A samples

are deep (>1000m), Ca–Cl type formation waters that are characterized by high TDS (> 300,000 mg/L). The $\delta^{2}H$ versus $\delta^{18}O$ values of group A samples range between -78 ‰ and -31 ‰; and between -10.9 ‰ and +1.8 ‰, respectively and their $\delta^{37}Cl$ and $\delta^{81}Br$ values range between -0.67 ‰ and +0.04 ‰; and between -0.31 ‰ and +0.27 ‰, respectively. Based on their chemical composition and isotopic signatures they are determined to be residual brines of evaporated paleoseawaters.

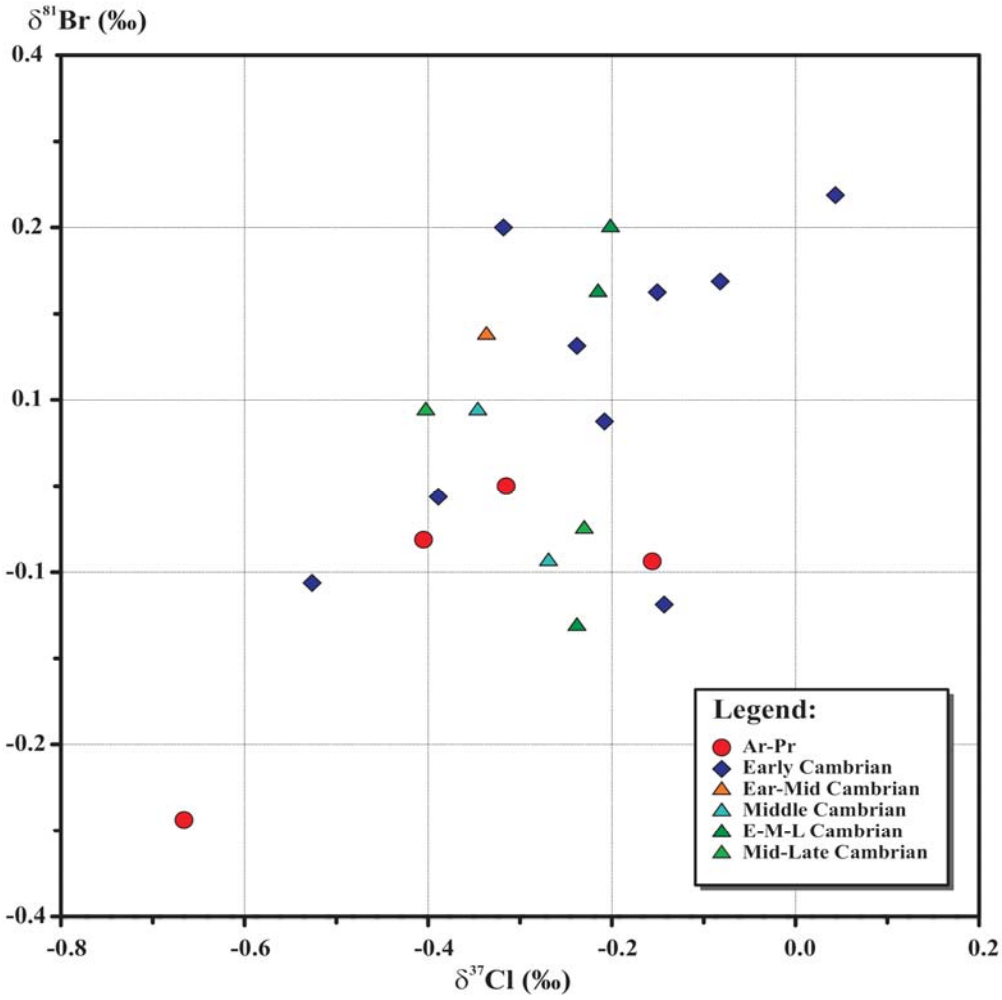

Figure 5.18 $\delta^{37}Cl$ (‰) – $\delta^{81}Br$ (‰) relationship of group A samples of the Siberian Platform according to the geological sections from which they were sampled.

Group B samples are Na–Cl type waters that occur at shallower depths (0–1000 m) and their TDS values range between 44,000 mg/L and 242,000 mg/L. The $\delta^{2}H$ versus $\delta^{18}O$ values of group B samples range between -152 ‰ and -94 ‰; and between -20 ‰ and -0.5 ‰, respectively. The $\delta^{37}Cl$ and $\delta^{81}Br$ values of this group of samples range between -0.25 ‰ and +1.54 ‰; and between -0.25 ‰ and +0.17 ‰, respectively. The chemical and isotopic data obtained for group B samples indicate that these samples are derived from halite dissolution, most likely as a result of recharge in a colder climate, possibly Pleistocene derived water.

Group C samples are not characterized as one primary water type. However the majority of these samples are either Na–Ca–Cl or Na–Cl type waters. Samples are from various depths ranging from 100 to 2100 metres and are characterized by high TDS values between 32,000 mg/L and 286,000 mg/L. The $\delta^{2}H$ and $\delta^{18}O$ of group C samples range between -140 ‰ and -89 ‰; and between -17.1‰ and -9.3 ‰, respectively. The $\delta^{37}Cl$ and $\delta^{81}Br$ values of these samples range between -0.40 ‰ and +1.30 ‰; and between -0.40 ‰ and +0.56 ‰, respectively. The chemical compositions and isotopic signatures of this group of samples showed differences so that data interpretation could not lead to a definite brine source. However, the available data suggest that these samples were produced via a number of scenarios that involved several end members such as meteoric water, group A brines (paleoseawater), and also some geochemical evolutionary processes such as halite dissolution, biological activities and/or ion filtration. All or some of these processes and end members probably played in producing these waters (group C) with their chemical and isotopic unique characteristics.

Group D samples represent fresh and brackish waters in the area and are not characterized by one specific water type. They are either surface waters or from shallow wells. They are characterized by low TDS values that range between 318 mg/L and 11200 mg/L. The $\delta^{2}H$ and $\delta^{18}O$ of group D samples range between -132 ‰ and -103 ‰; and between -17.7 ‰ and -14.4 ‰, respectively, and are local meteoric in origin. The $\delta^{37}Cl$ values of these samples range between -0.13 ‰ and +0.58 ‰.

The Br stable isotope results obtained from this study are very similar for most samples (-0.30 ‰ to +0.75 ‰), but a few samples from group C extend the known isotopic range between -0.80 ‰ and +3.35 ‰. This variation is wider than previously reported results (0.00 ‰ to +1.80 ‰) for Br stable isotopes of natural samples (Eggenkamp and Coleman, 2000; Shouakar-Stash et al., 2005a). The Archaean–Proterozoic crystalline brines were found to have $\delta^{37}Cl$ values that range between -0.67 ‰ and -0.16 ‰ and $\delta^{81}Br$ values that range between -0.31 ‰ and 0 ‰, while the Early Cambrian sedimentary brines have $\delta^{37}Cl$ values that range between -0.53 ‰ and +0.04 ‰ and $\delta^{81}Br$ values range between -0.11 ‰ and +0.27 ‰. There is a slight enrichment in values with decreasing age and/or depth of sample which may be due to seawater variation with time or long term diagenetic processes.

The variation of Br stable isotopes observed in this study suggests two things: (1) different water types may have different Br stable isotope signatures, i.e., they are originally different, and (2) different geochemical processes may affect the Br stable isotopes of the waters differently and cause significant fractionations.

CHAPTER 6

BROMINE AND CHLORINE ISOTOPES IN SEDIMENTARY FORMATION WATERS FROM THE WILLISTON BASIN (CANADA AND USA)

6.1 Introduction

The examination and investigation of the origin of saline waters in sedimentary basins began in the late 1800s (e.g. Hunt, 1879). In the last 60 years several well referenced studies investigated the origin and the evolution of formation waters in many sedimentary basins around the world and enriched our understanding of these systems (Bredhoeft et al., 1963; White et al., 1963; Davis, 1964; Clayton et al., 1966; Rittenhouse, 1967; Hitchon and Friedman, 1969; Collins, 1975; Graf, 1982; Hanor, 1983; Kharaka and Carothers, 1986; Carpenter, 1978; Carpenter and Trout, 1978; McCaffery et al., 1987; McNutt et al., 1987; Knauth, 1988; Long et al., 1988; Lowry et al., 1988; Connolly et al., 1990; Siegel, 1990; Dollar et al. 1991; Siegel, 1991; Siegel et al., 1991; Stueber and Walter, 1991; Kaufmann et al. 1993; Wilson and Long, 1993; Davisson and Criss, 1996; Hitchon, 1996; Kesler et al., 1996; Martini et al., 1998; Worden et al., 1999; Iampen and Rostron, 2000; Husain et al., 2004; Kharaka and Hanor, 2004; Hanor and McIntosh, 2006; McIntosh and Walter, 2006).

These studies were carried out to provide important information concerning the chemical and isotopic compositions of basinal fluids related to geochemical, hydrologic, thermal, and tectonic evolution of the Earth's crust (Kharaka and Hanor, 2004). These processes were summarized by Kharaka and Hanor (2004) as the following:

"1) generation, transport, accumulation, and production of petroleum; 2) chemical aspects of mineral diagenesis, including dissolution, precipitation, and the alteration of sediment porosity and permeability; 3) transport and precipitation of copper, uranium, and especially lead and zinc in sediment-hosted Mississippi-Valley-type ore deposits; 4) tectonic deformation; 5) transport of thermal energy for geothermal and geopressured–geothermal systems; and 6) interaction, movement, and ultimate fate of large quantities of liquid hazardous wastes injected into the subsurface (Hanor et al., 1988; Kharaka and Thordsen, 1992; Tuncay et al., 2000)."

The origin of the formation waters in the Williston Basin has been investigated in the past by several researchers (e.g. Downey, 1986; Downey and Dinwiddie, 1988; Wittrup and Kyser, 1990; Chipley and Kyser, 1991; Busby et al., 1995; Bachu and Hitchon, 1996; Hitchon, 1996; Benn and Rostron, 1998; Grasby and Betcher, 2000; Iampen and Rostron, 2000; Rostron and Holmden, 2003). For example, Hitchon (1996) evaluated formation water samples from 15 different stratigraphic units and concluded that halite and anhydrite in the Middle Devonian Prairie aquiclude has strongly influenced the composition of aquifers above and below. He also recognized the influx of freshwater and the consequent dissolution of halite in the Prairie aquiclude. More recently, Iampen and Rostron (2000) studied these brines

and concluded that the fluids are made up of three chemically distinct waters ($CaSO_4$ saline waters, Na–Ca–Cl brine and Na–Cl brine). They proposed that the two end member brines are ancient evaporated seawater and a fluid resulting from halite dissolution.

The objectives of this study are: 1) to better understand the geochemistry and the evolution of formation waters in the Williston basin by using the available chemical data and the stable isotopes ^{18}O and ^{2}H, and 2) to determine the $\delta^{37}Cl$ and $\delta^{81}Br$ compositions of these brines and examine the usefulness of these isotopic parameters to better understand the system and investigate the effect of different evolutionary processes on the isotopes.

6.2 Study Area

The Williston Basin is a sub-circular Phanerozoic intracratonic sedimentary basin (Figure 6.1) located in the middle of the North American continent. It is part of the Northern Great Plains, centered in north-western North Dakota and extends into Saskatchewan and Manitoba in Canada and Montana and South Dakota in the USA (Figure 6.1). The Williston Basin is approximately 800 km in diameter and covers approximately 518,000 km^2 (Fuller, 1961). It extends from approximately 98.50° W to 108.50° W longitudes and 45.00° N to 51.50° N latitudes (Brown and Brown, 1987).

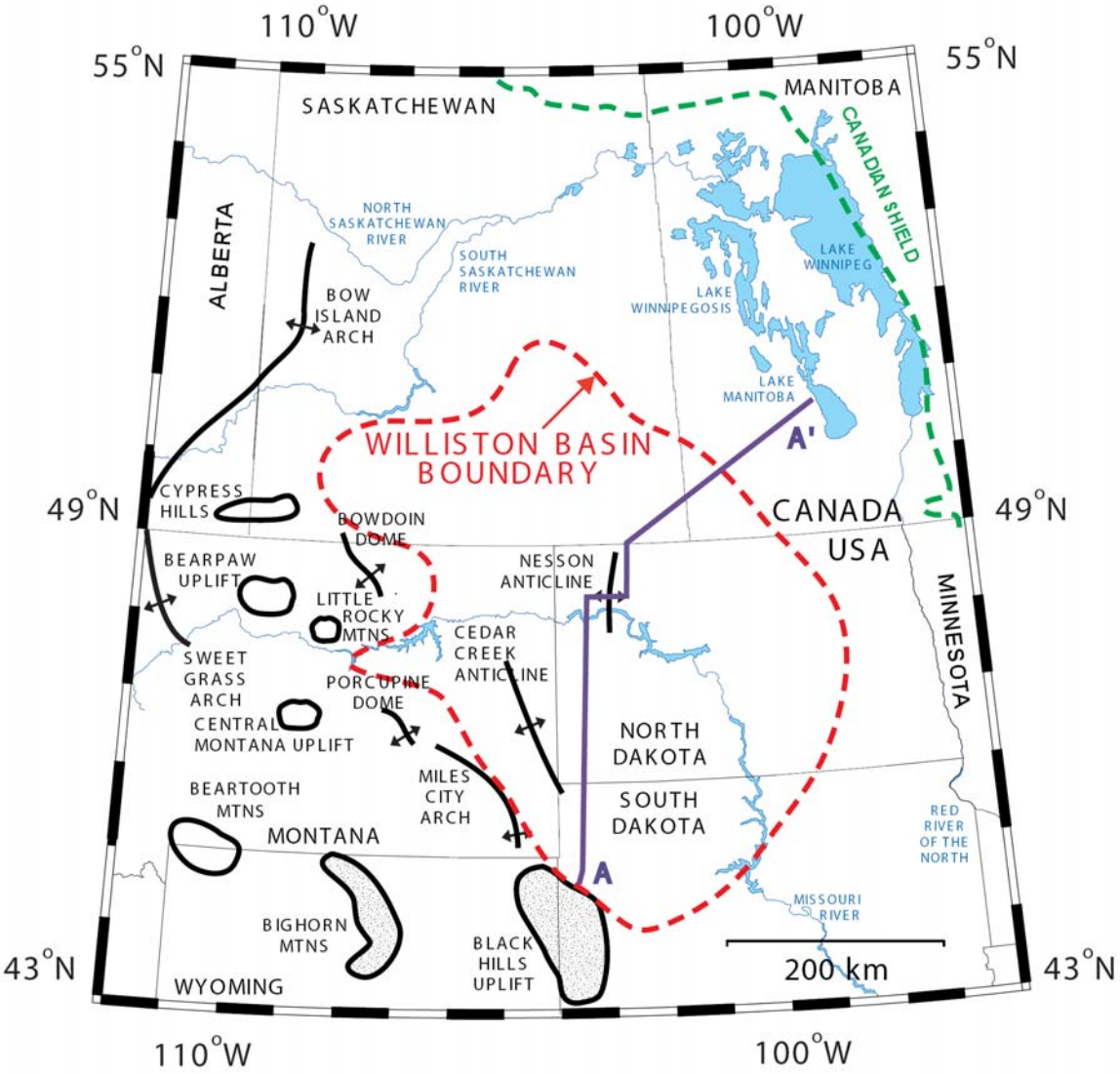

Figure 6.1 Significant physiographic features of the Williston Basin (boundary after Laird, 1952), modified from Iampen and Rostron, 2000. The location of cross-section A to A' (Figure 6.2) is shown. The green dashed line signifies the limit of the Canadian Shield. Shaded uplifts signify major recharge areas.

However, the focus of this study is mainly the central part of the Basin extending from 102.50° W to 105.00° W longitudes and 46.50° N to 49.50° N latitudes. It is separated from the Alberta Basin by the Sweetgrass Arch and the Bow Island Arch (Hitchon, 1996). The basin is bounded on the west and southwest by a series of Tertiary age uplifts (Sloss, 1987) and bounded on the east by the erosional edge on the Precambrian Canadian Shield. Major physiographic features in the western part of the study area include the Bighorn Mountains, the Laramie Mountains, Hartville uplift, the Big Snowy Mountains, and the Black Hills uplift. In the east, the study area is characterized by the broad, flat, lake plain formed by glacial Lake Agassiz in the north-eastern part of North Dakota and the Canadian Prairie Provinces (Downey, 1986).

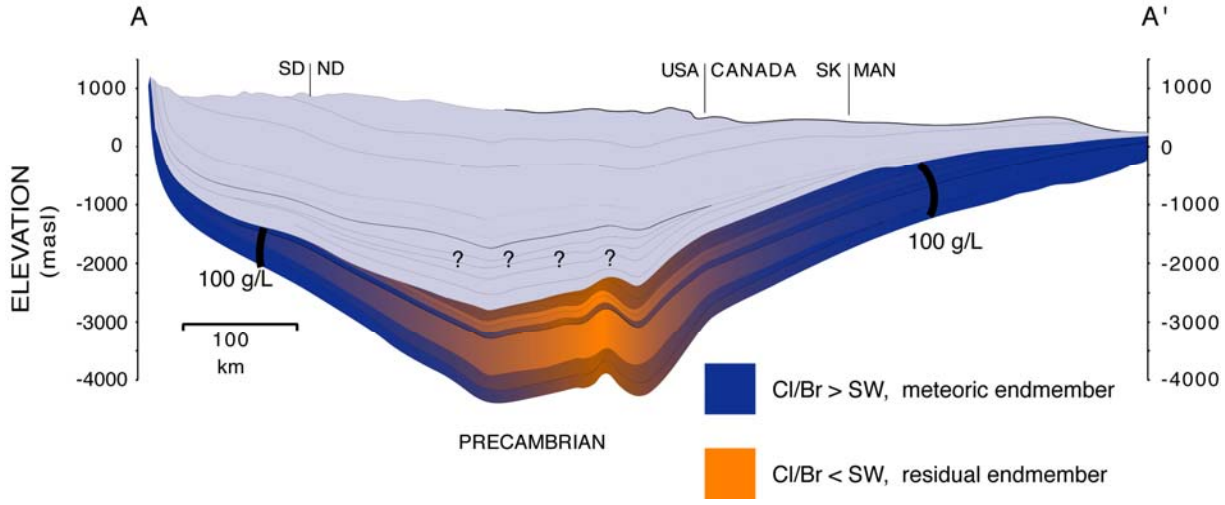

Figure 6.2 Cross-section A-A' in Figure 6.1 of the Williston Basin. It also shows the position (coloured in orange) of the highly concentrated formation waters in the central part of the basin (after Iampen, 2003).

6.3 Geology

The Williston Basin is a Phanerozoic basin, filled with sedimentary rocks of predominantly marine origin (Gerhard et al., 1982; Ahern and Mrkvicka, 1984; Obermajer et al., 2000). Historically, the geologic environment of the study area was that of a stable shelf margin throughout most of the Paleozoic. Periods of transgression and regression occurred when seas advanced from west to east in response to mountain-building activity of the Antler Orogeny to the west (Sandberg, 1962; Sandberg and Poole, 1977). Phanerozoic successions of this region overlie parts of the North American Craton (Precambrian basement) and contain significant petroleum provinces and mineral deposits (e.g., Podruski et al., 1987). The North American Central Plains Conductivity Anomaly (NACPCA) is located under the Williston Basin and extends north and south beyond the basin. The NACPCA is characterized by basal heat flow which is ~20 % higher than elsewhere in the basin (Jones and Craven, 1990; Jones and Savage, 1986).

A relatively complete sedimentary rock section of Late Cambrian through Tertiary age ranges from more than 5 km thick in the deepest part of the structural basin (north-western North Dakota) to less complete sedimentary sections on the western border of the basin (eastern Montana) (Downey, 1986; Osadetz et al., 1992). These deposits thin to the northeast where the rocks outcrop on the Canadian Shield in Manitoba. The main focus of this study will be the Cambrian to Mississippian strata (Figure 6.3) which comprise the lower three sequences of the Williston Basin: 1) The lower clastic, Middle Cambrian to Early

Ordovician, Sauk sequence strata, that overlies the basement and were deposited on the early Paleozoic western North American passive margin (Bond and Kominz, 1984; LeFever et al., 1987; Ricketts, 1989); 2) the Tippecanoe sequence of Middle Ordovician clastics and Late Ordovician and Silurian carbonates which are linked to the eastern North American epeiric seaway (Osadetz and Haidl, 1989); 3) the Devonian-Mississippian Kaskaskia sequence is important successions for petroleum source rocks and are mainly bituminous lime mudstones and shales (Edie, 1958; Meijer Drees, 1994; Osadetz and Snowdon, 1995).

6.4 Hydrostratigraphy

The Cambrian to Mississippian strata examined in this study were divided into eighteen hydrostratigraphic units (Figure 6.4) that were defined based on subsurface lithologies, estimates of rock hydraulic properties, and inferences regarding the regional flow system elsewhere in the basin as discussed by Downey (1986) and Iampen and Rostron (2000). Aquifers are predominantly clastic or carbonate in composition and aquitards include shale, evaporites and cemented breccias. Both aquifers and aquitards are locally and laterally discontinuous (Iampen and Rostron, 2000, Rostron and Khan, 2005).

The relatively high permeability clastics of the Deadwood Formation and the Winnipeg Formation have been grouped into the Cambro-Ordovician Aquifer. Separating these lower clastics from overlying sequences, the upper Winnipeg Formation shale member represents a less permeable cap referred to as the Winnipeg Aquitard. Next, the Yeoman Formation

limestones and dolomites are considered an aquifer. The evaporite units in the Herald Formation are referred to as the Herald Aquitard. The Upper Ordovician to Lower Silurian limestones and dolomites are called the Ordo-Silurian Aquifer. The Ordo-Silurian Aquifer is separated from the aquifers higher in sequence by the low permeability Ashern Formation shales comprising the Ashern Aquitard. Porous dolomite and reef deposits of the Winnipegosis Formation are referred to as the Winnipegosis Aquifer. The Winnipegosis Aquifer is capped by the Prairie Formation evaporites that form the Prairie Aquitard. The Manitoba aquifer overlies the Prairie Aquitard and it consists of the relatively permeable dolomites of the Dawson Bay and Souris River Formations. The upper part of the Souris River Formation, which contains more anhydrite, and is less permeable, forms the Souris River Aquitard. The permeable Limestones and dolostones units of the Duperow Formation are called the Duperow Aquifer. The Ireton Aquitard overlies the Duperow Aquifer and consists of thin units of shale. The porous Birdbear Formation limestones form the Birdbear Aquifer. The lower shale units of the Bakken Formation are designated as the Lower Bakken Aquitard. The more permeable sandy portion of the Bakken Formation represents the upper-most aquifer of the section and it is referred to as the Bakken Aquifer. Finally, the upper Bakken Shale caps the section with a low permeability unit called the Upper Bakken Aquitard (Iampen, 2003). The limestone Lodgepole Formation and Mission Canyon Formation that contain the Frobisher Member are considered an aquifer. This is capped by marine evaporites of the Charles Formation.

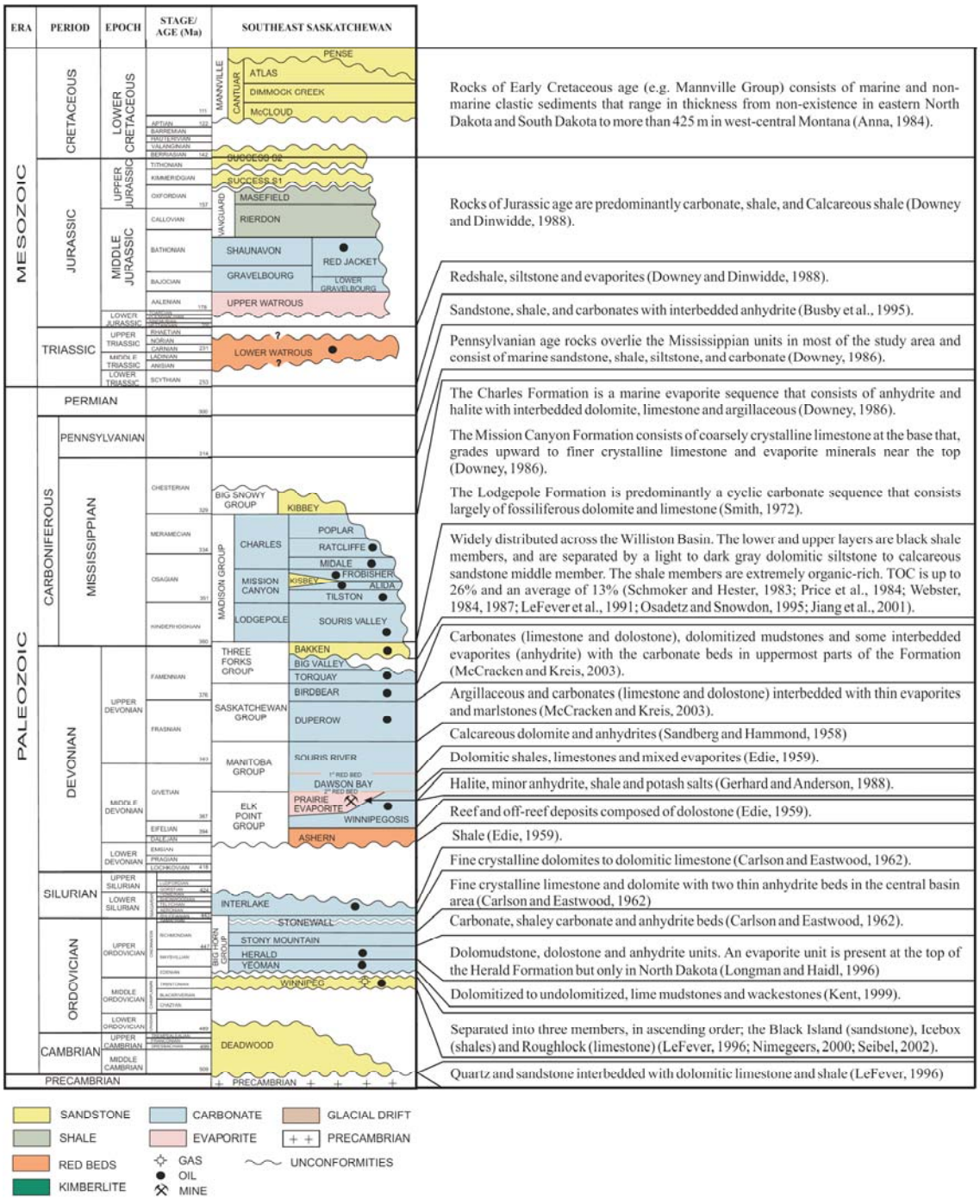

Figure 6.3 The Cambrian to Early Cretaceous stratigraphic units of the Williston Basin (modified from the new Saskatchewan Stratigraphic Correlation Chart, 2004) (Saskatchewan Industry and Resources, 2004) (http://www.ir.gov.sk.ca/).

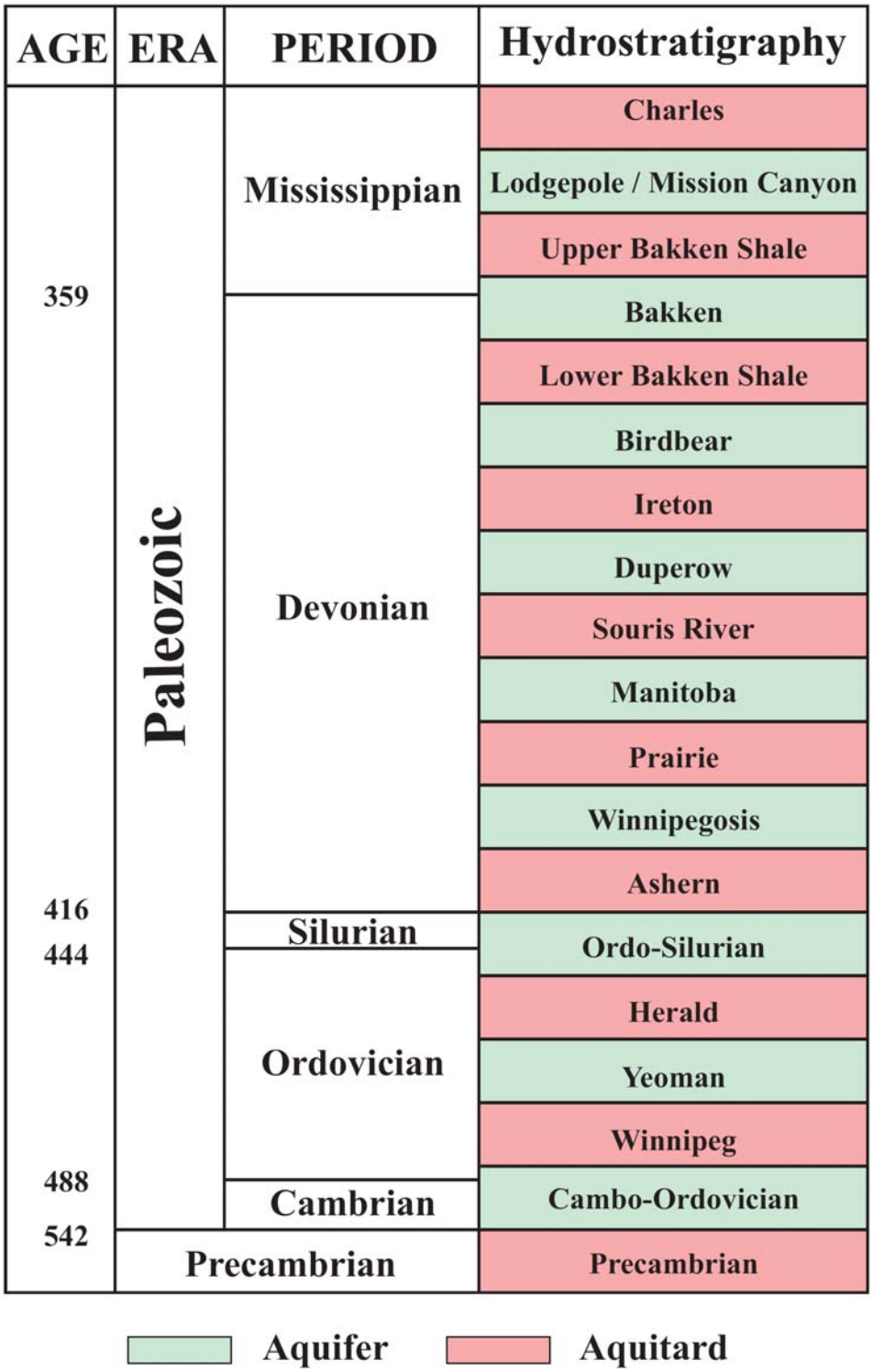

Figure 6.4 A simplified sketch of the Cambrian to Mississippian hydrostratigraphic units of the Williston Basin.

6.5 Hydrogeology

The hydrogeology and hydrochemistry of the Williston basin have been widely studied by several researchers (e.g. Downey, 1984; Anna, 1986; Downey, 1986; van Everdingen, 1986; Downey and Dinwiddie, 1988; Busby et al., 1995; Bachu and Hitchon, 1996; Benn and Rostron, 1998). The present hydrodynamic regime in the Williston Basin is thought to have developed in response to the Laramide Orogeny on the western margin of North America 50 to 40 million years ago(Bachu and Hitchon, 1996). This tectonic regime caused uplifts in Montana and South Dakota including the Black Hills, Bighorn Mountains, Beartooth Mountains and Little Rocky Mountains. The groundwater flow system in the Williston basin is one of the best examples of a large-scale confined aquifer system in the world (Rostron and Holmden, 2003) with a flow system extending for almost 1000 km from recharge to discharge areas (van Everdingen, 1986). The regional groundwater system receives recharge from the highland areas along the Rocky Mountains in Montana and Wyoming, and from the Black Hills of South Dakota in the USA. Generally water flows from the recharge areas through and around the Williston Basin and then north-eastward toward discharge areas in eastern North Dakota (Lake Agassiz), eastern South Dakota in the USA and the provinces of Manitoba and Saskatchewan in Canada (Downey and Dinwiddie, 1988; Bachu and Hitchon, 1996). The Precambrian basement forms the lower boundary of the hydrologic system. Elevation differences between recharge and discharge areas of more than 1000 m provide the driving force for fluid flow (Iampen and Rostron, 2000).

Virtually all eastward flowing streams draining the highland area lose part of their flow as they cross the aquifer outcrop (Swenson 1968; Wyoming State Engineer's Office, 1974). Although available surface-water data indicate that large quantities of water enter the aquifers along the outcrop areas in the western highlands, not all of this water recharges the deep, regional flow system and moves to the eastern discharge area (Downey, 1984).

Geological structure is an important control of the rate and direction of water movement in the bedrock aquifer system in the northern Great Plains (Downey, 1984; Anna, 1986). Anna (1986) suggested that tensional features, oriented east-west and northeast-southwest, enhance secondary porosity or permeability and become partial conduits for groundwater flow, while compressional features, oriented generally northwest-southeast, decrease porosity or permeability and become efficient barriers or partial barriers to groundwater flow. For example, the flow path from recharge areas in Montana are also limited by the Cedar Creek anticline and flow is channelled north of the Cedar Creek anticline (Downey, 1984). This makes the Cedar Creek anticline a natural geological barrier that deflects the groundwater flow south and north around the central part of the Williston Basin, minimizing, if not totally blocking recharge to the central part of the Basin.

Downey (1986) and a more recent study conducted by Grasby and Betcher (2000) suggested that the present-day flow system of the Williston Basin was different in the past. Grasby and Betcher (2000) suggested that the continental ice sheet that was sitting over the outcrop belt in southern Manitoba during the Pleistocene glaciation would have provided sufficient hydrologic head to cause the flow system of the Williston Basin to reverse during

that period (1.8 million years – 10,000 years). Furthermore, they suggested that the present-day flow system of the Williston Basin is likely to still be re-establishing to the new boundary conditions set by the removal of the ice sheet. However, Downey (1986) suggested that the present recharge areas in the highland areas remained to serve as a recharge area during these glaciations as they were not affected by the continental glaciations.

6.6 Sampling and Analysis

The formation water samples examined in this chapter were collected as part of the on-going Williston Basin brine-sampling program by Rostron between 1997 and 2005. Formation waters were collected from producing oil wells with high water cuts (>50% Water-Oil Ratio (WOR)). Care was taken to avoid oil fields subjected to enhanced recovery practices (water-flooding). Oil-water emulsions were sampled at the wellhead in 12 L pre-cleaned plastic jugs. The water fraction was passed through a 0.45μm PES filter and then aliquoted for field tests and laboratory analyses including temperature, density, pH, alkalinity, major and minor ions, and ^{18}O, ^{2}H, ^{37}Cl, ^{81}Br and $^{87}Sr/^{86}Sr$ stable isotopes.

Most major and minor cations were analyzed using Inductively Coupled Plasma Atomic Emission Spectroscopy (ICP-AES) at a commercial Laboratory in Edmonton. Compositions of Na, Cl, Br, Sr and I were determined by Neutron Activation Analysis (NAA). Major, minor ions and some of the $^{87}Sr/^{86}Sr$ isotopes were analyzed at the University of Alberta.

^{18}O and ^{2}H stable isotopes were analyzed at the University of Saskatchewan. Both $\delta^{18}O$ and $\delta^{2}H$ measurements were performed on a Continuous Flow Isotope Ratio Mass Spectrometry (CF-IRMS) on CO_2 and H_2 gases, respectively. The $\delta^{37}Cl$, $\delta^{81}Br$ and some of the $^{87}Sr/^{86}Sr$ isotopes were analyzed at the University of Waterloo. The $\delta^{37}Cl$ analyses were performed on methyl chloride (CH_3Cl) gas using an IRMS following the procedure described in Eggenkamp (1994) and Shouakar-Stash et al., (2005b). The $\delta^{81}Br$ analyses were performed on methyl bromide (CH_3Br) gas using a CF-IRMS following the procedure described in Shouakar-Stash et al., (2005a). The strontium isotopes were determined on a Thermal Ionization Mass Spectrometry (TIMS) (Triton, Thermo Finnigan). The analytical precisions for the ^{18}O, ^{2}H, ^{37}Cl and ^{81}Br isotopes are 0.14 ‰, 2.3 ‰, 0.1 ‰ and 0.1 ‰, respectively.

6.7 Chemical Compositions

The geochemical data including major and minor cations and anion compositions of the Williston Basin formation water samples are presented in Table C.1. Samples were collected at various depths ranging from ~1 km to more than ~4 km (Table C.1). Figure 6.5 illustrates the sampling location of the samples examined in this study. The majority of the formation waters are characterized by high TDS ranging between 100,000 mg/L and 550,000 mg/L. Only six formation waters from this study (mainly Mississippian) are found to be characterized by low TDS values (TDS < 30,000 mg/L). The vast majority of highly concentrated formation waters (TDS > 100,000 mg/L) are Na-type waters (Na-Cl or Na-Ca-

Cl) with few exceptions (eight samples) that are Ca-type waters (Ca-Na-Cl or Ca-Cl) from the Late Devonian and Late Ordovician formations. The formation waters that are characterized by low TDS composition are of different water types (Na-Cl-HCO_3, Na-Cl-SO_4, Na-K-Cl-SO_4, and Na-Cl).

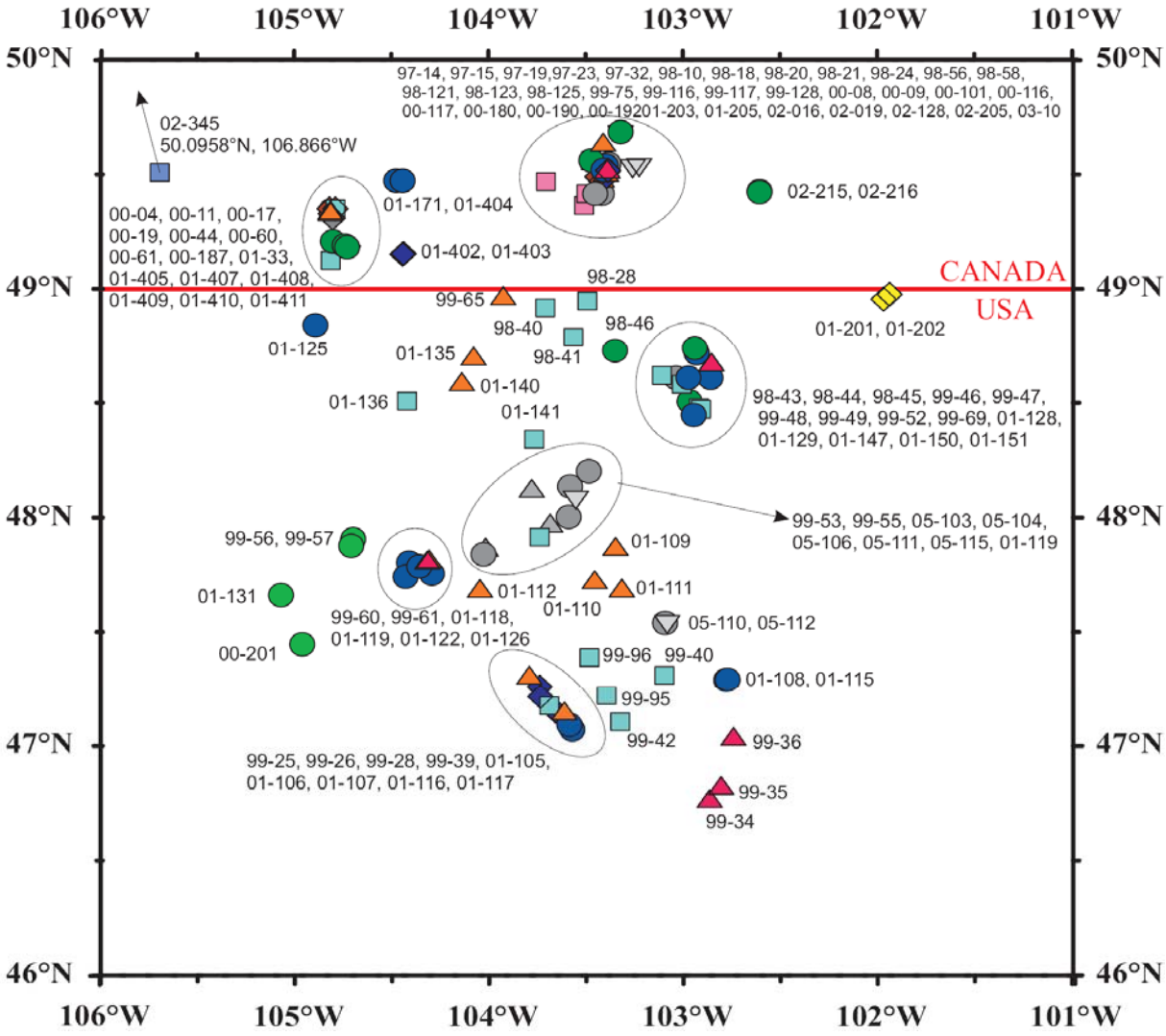

Figure 6.5 Sample locations of the Williston Basin formation waters.

Numerous evolutionary processes have been proposed to explain the high TDS of such sedimentary formation waters, including 1) the evaporation of seawater (e.g. Carpenter, 1978; Kharaka et al., 1987); 2) the dissolution of halite or other evaporites such as potash or gypsum (e.g. Rittenhouse 1967; Land and Prezbindowski 1981; Hitchon, 1996); 3) membrane filtration (Bredehoeft et al., 1963; Berry, 1969; Kharaka and Berry, 1973; Graf, 1982); 4) concentration and metamorphism of waters at great depths assisted by high temperatures and pressures (Chebotarev, 1955; Krotova, 1958; Pinneker and Lomonosov, 1964); and/or 5) freezing of water or hydration of silicates (clays) with the resulting concentration of solutes (Hanor, 1987).

The sediments comprising the Paleozoic rocks in the Williston Basin were deposited predominantly in shallow inland seas during the Cambrian to Mississippian. Deposition of carbonate, sulphate and halite would require salinity values greater than the salinity of seawater (McCaffrey et al., 1987; Gerhard and Anderson, 1988). Therefore, the resulting highly concentrated brines may have been incorporated in the sediments during the sedimentation (i.e. evaporated paleoseawater).

The relationship between Br and TDS contents and also between Br and other cations and anions such as Ca, Mg, K, Cl and SO_4 has been used routinely to divide formation waters into groups and determine their origin and/or interpret the evolutionary processes (Valyaskho, 1956; Braitsch and Hermann, 1963; Rittenhouse, 1967; Carpenter, 1978; Carpenter and Trout, 1978; Frape et al., 2004; Kharaka and Hanor, 2004). Figure 6.6 illustrates the logarithmic relationship between Cl (mg/L) and Br (mg/L) contents of seawater during

evaporation. The figure illustrates the initial precipitation point of evaporite mineral phases as reported by Matray (1988). Figure 6.6 also shows some mixing scenarios between several end members (e.g. evaporated seawater, seawater, fresh water). Further it shows the affect of dissolving halite by different fluids such as seawater and brines. These different scenarios were examined and reported previously (e.g. Rittenhouse, 1967; Carpenter, 1978; Kharaka and Hanor, 2004).

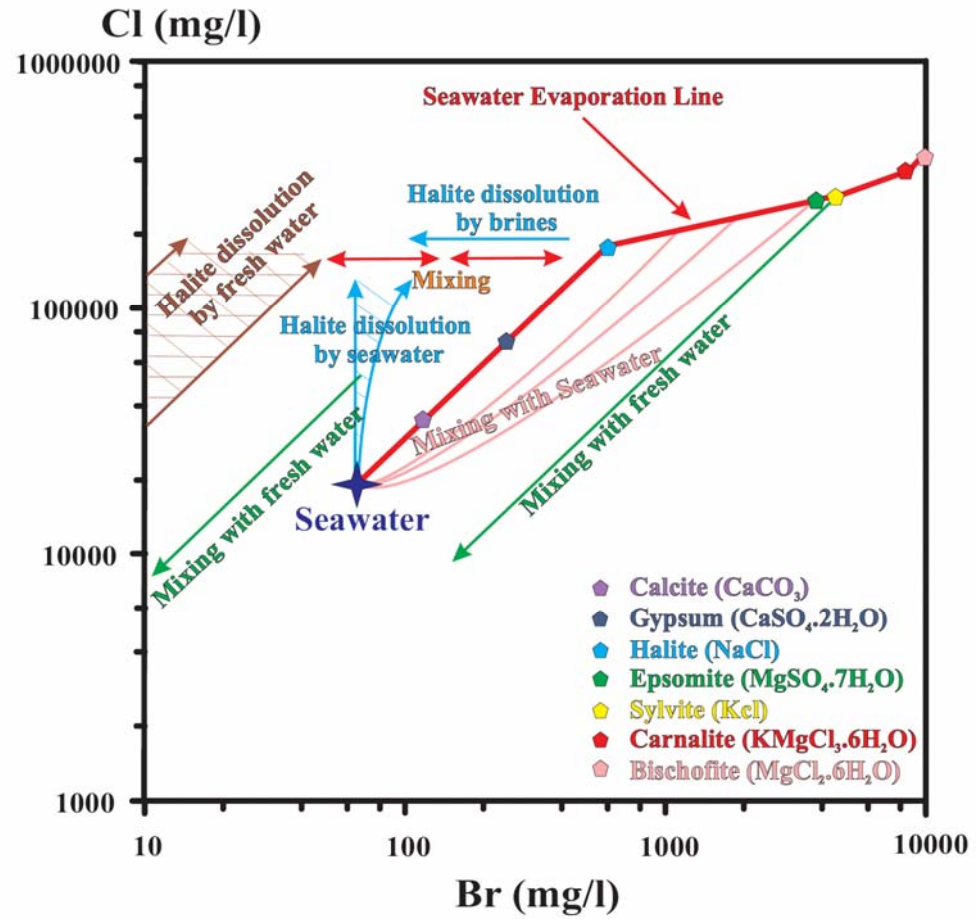

Figure 6.6 A logarithmic plot of the concentration trends of chloride versus bromide during the evaporation of seawater showing the initial precipitation point of evaporite mineral phases (after Matray, 1984). Also shows some of the possible mixing scenarios after Rittenhouse (1967) with different halite dissolution products and different end member waters (Carpenter, 1978).

6.7.1 Grouping by Water Types

In this study, the samples were grouped according to their water type. The Cl (mg/L) and Br (mg/L) contents of the Williston Basin formation waters were plotted on a logarithmic graph (Figure 6.7) and compared to the evaporation lie of modern seawater to determine their origin(s) and/or the effect of evolutionary processes.

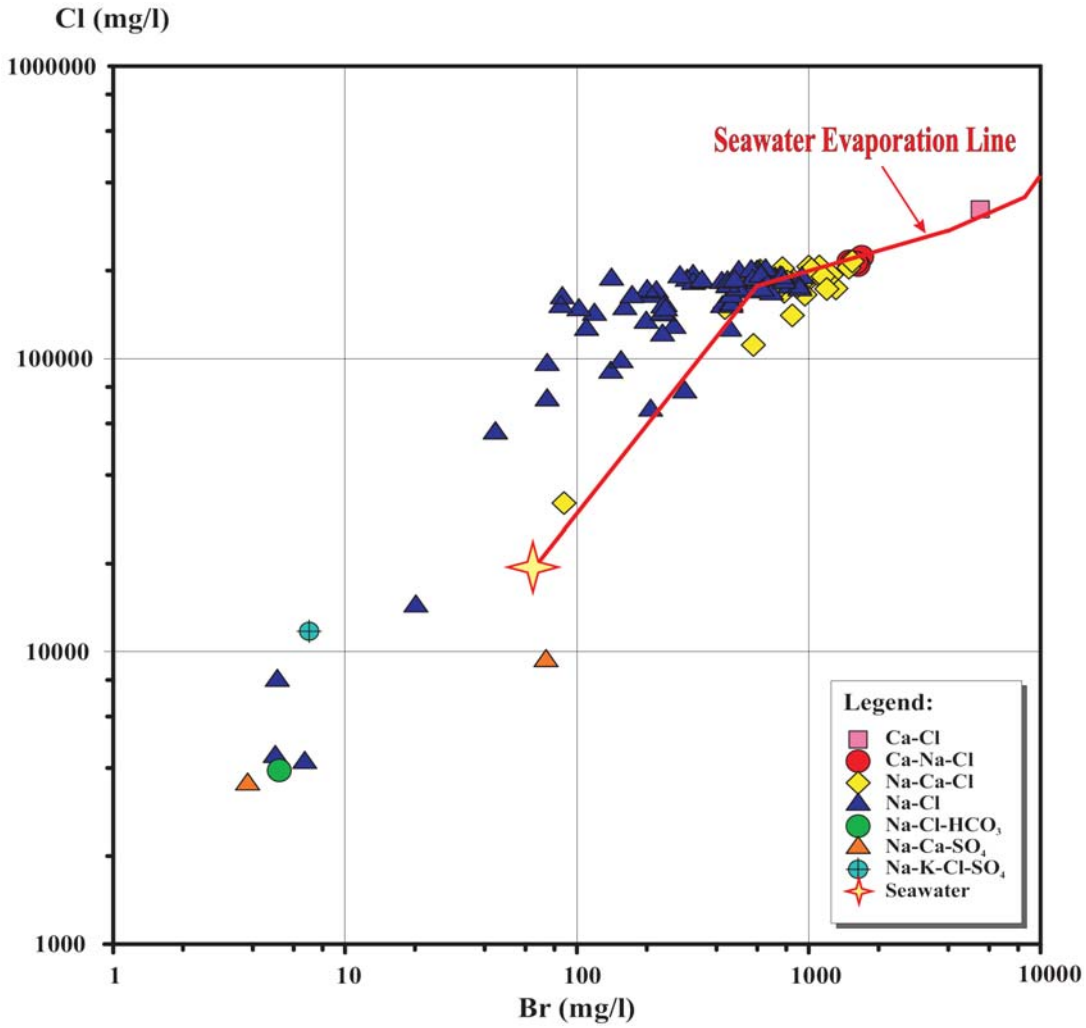

Figure 6.7 A logarithmic plot of Cl (mg/L) versus Br (mg/L) of the different water types of the Williston Basin formation waters. The plot also illustrates the seawater evaporation line.

The results show that all Ca-Cl and Ca-Na-Cl type waters plot on the evaporation line while only some of the Na-type waters (Na-Ca-Cl and Na-Cl) plot on the evaporation line. More than half of the Na-type waters, especially the Na-Cl type waters, plot off the seawater evaporation line. The other three water types (Na-Cl-HCO_3, Na-Cl-SO_4, and Na-K-Cl-SO_4) plot far from the seawater evaporation line and below the seawater point. The plot suggests that several end member fluids are present in the Williston Basin. Based on the diagram (i.e. the Cl and the Br contents) the Ca-Cl and Ca-Na-Cl type waters are the result of evaporated seawater and they are the least affected by dilution afterward (i.e. mixing with seawater or fresh water). The Na-Cl type waters were either produced by seawater evaporation or by halite dissolution by seawater or meteoric waters. The high Br contents in these formation waters suggest that they were mixed with highly concentrated brines (e.g. generated from seawater evaporation such as the Ca-type brines). The bromine content in various evaporites such as halite and sylvite range between 68 ppm and 260 ppm (Valyaskho, 1956; Holser, 1979), which means that formation waters originating from halite dissolution by meteoric waters should be characterized by Br contents in the range between 24 and 93 mg/L at saturation (Rittenhouse, 1967), while formation waters originating from halite dissolution by seawater should be characterized by Br contents in the range between 90 and 150 mg/L at saturation (Rittenhouse, 1967) when considering a solubility of 359 g/L for halite. The majority of the Na-Cl type waters examined in this study are characterized by Br contents that are higher than that range, which imply that these formation waters are not simply produced by halite dissolution by meteoric waters or seawater. Although, halite dissolution by seawater would produce formation waters that are characterized by higher Br content (70-

105 mg/L). It is necessary to consider mixing with highly concentrated end member brine that is Br-rich, in order to explain the high Br content Na-Cl type waters. Another possible mechanism that can explain the Br enrichment is several stages of halite dissolution and re-crystallization which would increase the Br content in the brine and decrease it in the mineral phase (Land and Prezbindowski, 1981; Hanor, 1987).

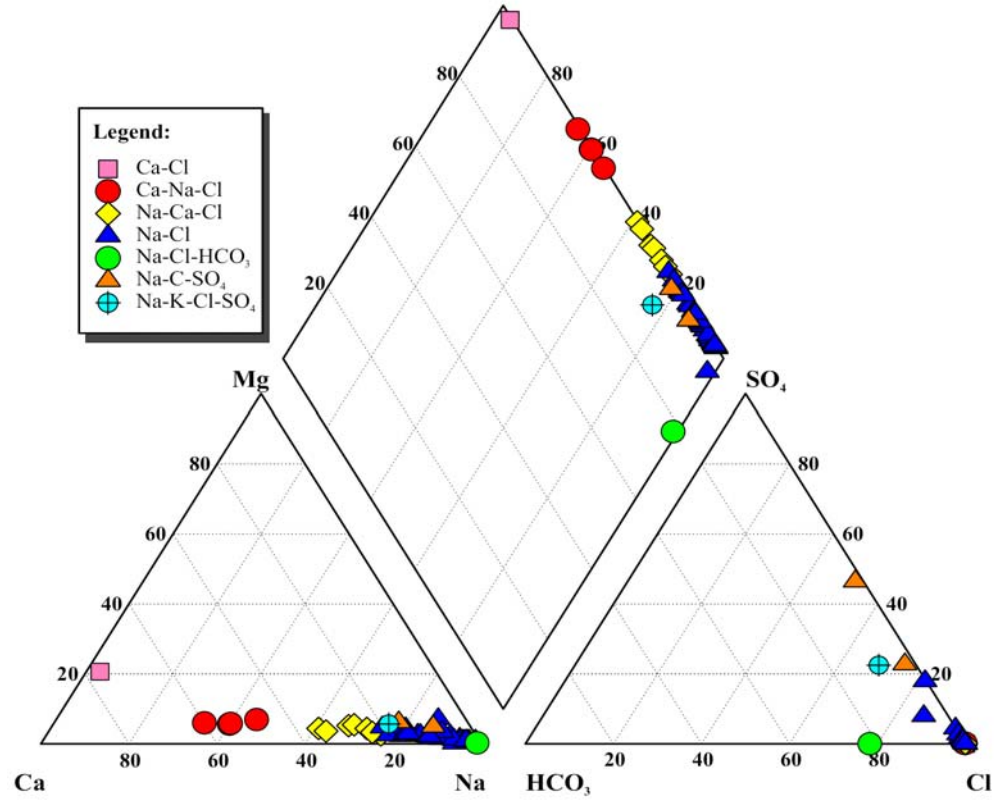

Figure 6.8 Piper diagram of the Williston Basin formation waters grouped based on their water types.

The Na-Ca-Cl type waters fall between the Ca-Na-Cl and Na-Cl type waters, and they seem to be produced by mixing between the other two water types. Some of the Na-Ca-Cl type waters that plot below the seawater evaporation line imply mixing with seawater and/or

with meteoric water. The low TDS waters are characterized by low Cl and Br contents and are affected by meteoric waters. The Piper diagram (Figure 6.8) also illustrates the separation between the three main water types and shows the position of the Na-Ca-Cl type waters between the Ca-Na-Cl and Na-Cl type waters with the tendency of being closer to the Na-Cl type waters.

Further support for the origin of these samples can be found by comparing the Cl/Br (molar) versus Na/Br (molar) of these samples (Figure 6.9). Martini et al. (1998) used the Na-Cl-Br systematic of formation waters (Cl/Br versus Na/Br) to identify solute sources and determine the effects of dilution by Br-depleted sources such as meteoric waters and halite dissolution. Seawater plots just above the 1:1 (Cl/Br : Na/Br) line, where Cl/Br and Na/Br for seawater are 169 and 292, respectively. This diagram shows that almost all Ca-type waters are the result of residual seawater as they plot below the seawater mark (Na/Br < seawater and Cl/Br < seawater). Most of the Na-Ca-Cl formation waters also plot below the seawater mark, suggesting a residual seawater origin. Some of the Na-Ca-Cl plot above the seawater mark (Na/Br > seawater and Cl/Br > seawater), which implies mixing with Na-Cl waters. Most of the Na-Cl type formation waters plot above the seawater mark, which suggests halite dissolution as the origin of these formation waters or at least a significant impact from halite dissolution. Some of the Na-Cl type formation waters plot below the seawater mark (Figure 6.9) and that implies that these samples are residual seawater or they might result from mixing between halite dissolution formation waters and the seawater residual Ca-type formation waters.

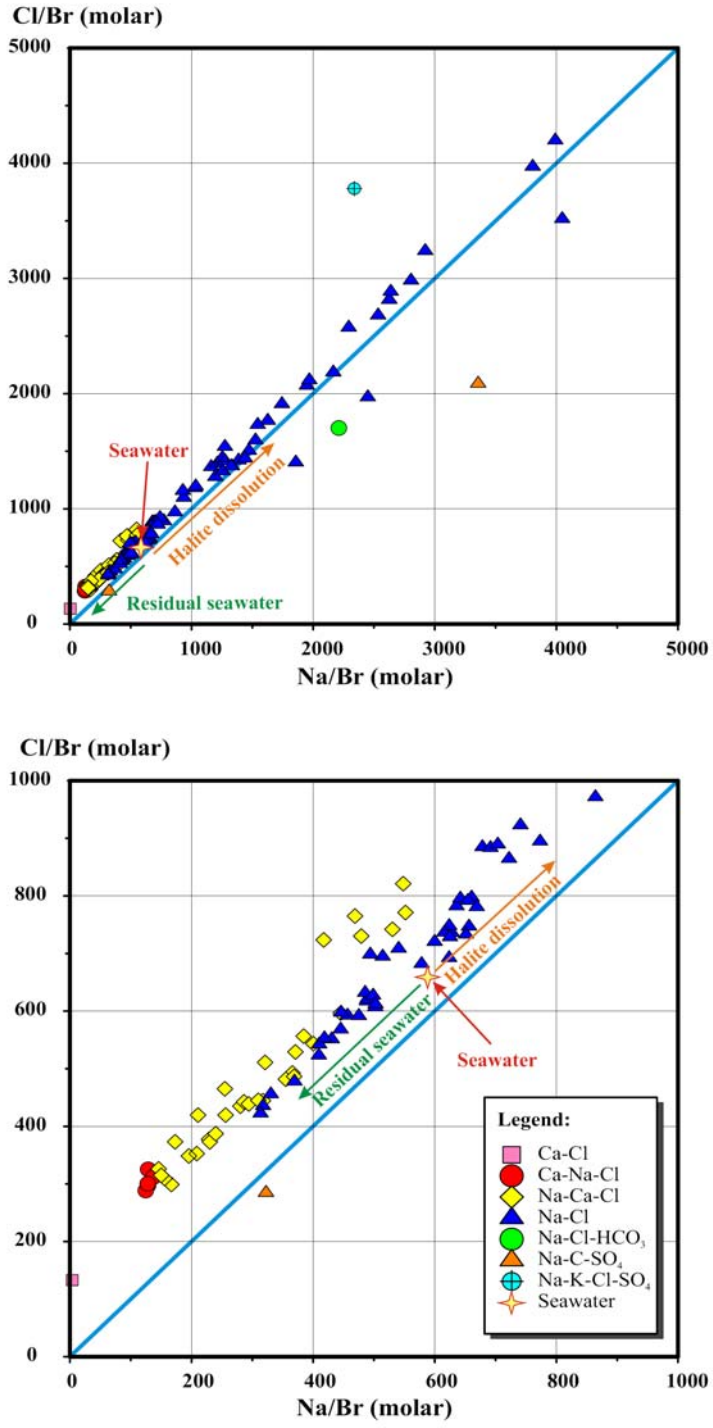

Figure 6.9 The relationship between Cl/Br (molar) versus Na/Br (molar) of the Williston Basin formation waters grouped based on their water types.

Figure 6.10 show the concentrations of major ions and TDS (mg/L) contents versus Br (mg/L) concentrations of the different water types obtained from this study. These chemical data are compared to the changes in major ions during seawater evaporation and consequent precipitation of some minerals such as $CaSO_4$ and NaCl. The plots in Figure 6.10 shows that almost all water types show a large excess in Ca and a large deficit in SO_4 content where Ca-type waters are the most deviated from the seawater evaporation trends. These plots also show that K and Mg are characterized by a positive trend versus Br where they follow the seawater evaporation trend, however, all formation waters show an excess in K and a deficit in Mg. The Na (mg/L) versus Br (mg/L) plot shows that most Ca-type waters are characterized by a Na-deficit, while Na-type waters show a Na-excess.

The chemical characteristics of the formation waters especially when compared to the seawater evaporation trend strongly suggest at least three end members (evaporated paleoseawater, halite dissolution brines that involved fresh water or seawater, and meteoric waters). It also shows mixing products between these end members. Although the deviations of some of these ions (especially Ca, Na and SO_4) from the seawater evaporation trends does not support the presence of an evaporated paleoseawater component (end member) this is still supported by other ions such as Cl and Br and TDS composition as well. In fact, the majority of sedimentary formation waters described in the literature have chemistries that vary considerably from what would be expected of evaporated seawater. During the diagenetic evolution of the brines, calcium and strontium concentrations increase by up to an order of magnitude compared to evaporated seawater, while magnesium and potassium concentrations

may decrease by as much as an order of magnitude (Kharaka and Hanor 2004). There are several water-rock interaction processes that can account for these changes of the major ions. For example, the loss of Na and gain of Ca can be attributed to ion exchange between the water and the host rock. As mention earlier, dolomitization is another mechanism that can account for the loss of Mg and gain of Ca. During the dolomitization process calcite (limestone) ($CaCO_3$) reacts with Mg to form dolomite, which results in the release of Ca to solution and loss of Mg from the solution.

The excess in K is probably due to the involvement of sylvite (KCl) dissolution or high temperature water-rock interaction with feldspar-rich sediments and this is supported by the enriched $\delta^{18}O$ composition of these formation waters. The large deficit of SO_4 can be attributed to SO_4 reduction or to gypsum and anhydrite precipitation.

Alternatively, Lowenstein et al. (2003) have suggested that $CaCl_2$ brines present in most sedimentary basins inherited their compositions and salinities from evaporated paleoseawater that were rich in calcium and depleted in sulphate relative to modern day seawater (e.g. during the Silurian and Devonian). However, Hanor and McIntosh (2006) emphasized that the compositions of typical brines hosted by Silurian and Devonian-aged formations from the Illinois and Michigan basins do not show the same compositional trends of progressively evaporated $CaCl_2$-rich seawater.

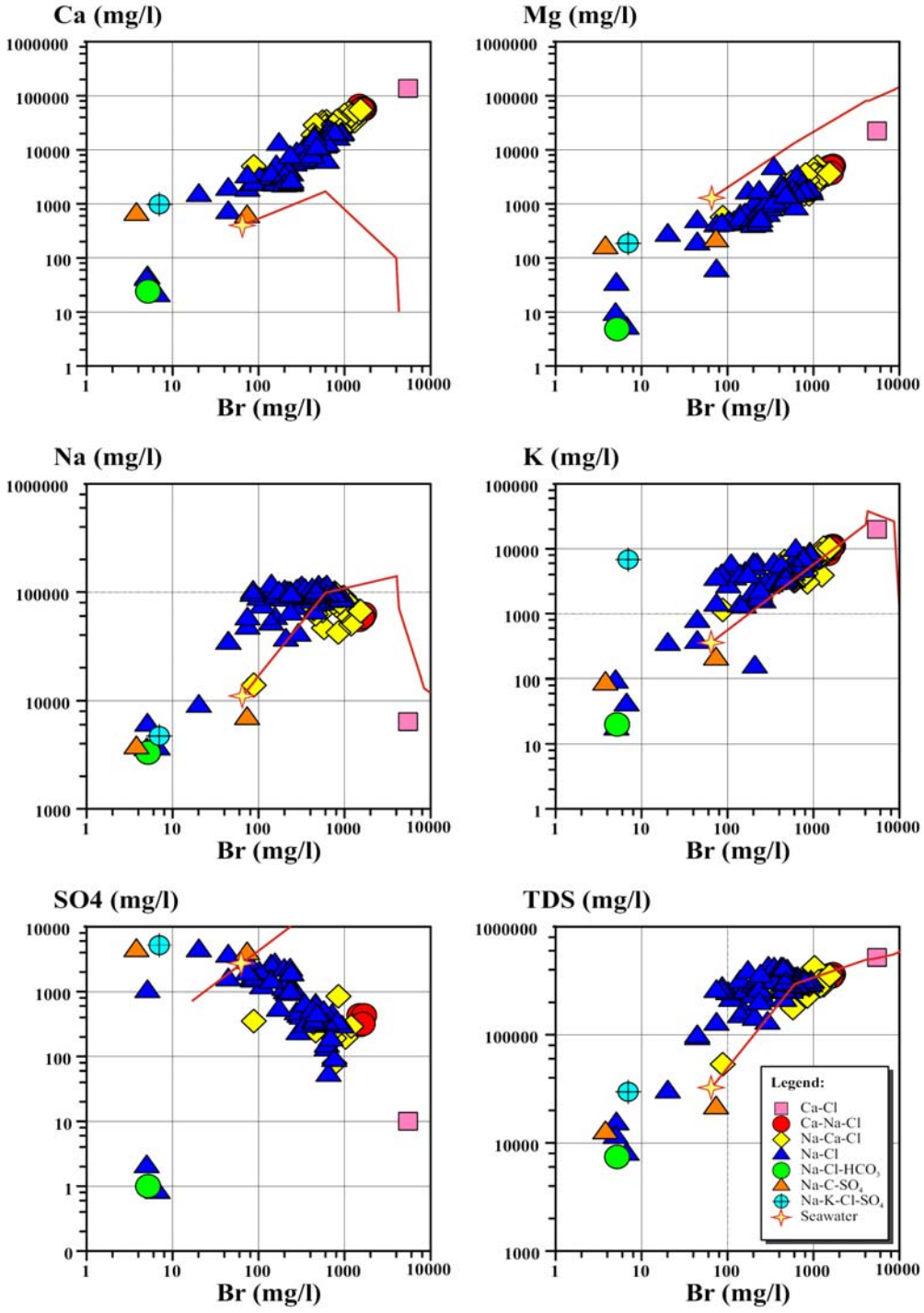

Figure 6.10 The relationship between major cations and anions concentrations (mg/L) versus Br (mg/L) of the Williston Basin formation waters grouped based on their water types. The figures show the changes of concentrations during seawater evaporation.

6.7.2 Grouping by the Stratigraphic Units

Figure 6.11 (A) illustrates the relationship between Cl and Br concentrations of the Williston Basin formation waters based on the stratigraphic unites from which they were sampled. A comparison of the Cl and Br concentrations of the formation waters against the seawater evaporation line shows that less than half of the samples fall on the evaporation line. The plot does not show different "clusters" for the different formation waters based on the stratigraphic units from which they were sampled. Figure 6.11 (B) shows that the Mannville Group formation waters are mainly of fresh water origin with low Cl and Br contents. A couple of samples from the Mississippian units are also characterized by low Cl and Br contents, suggesting a strong fresh water impact on these samples. In general, the Cl and Br contents of the formation waters from the Mississippian stratigraphic units show large variations. Samples that fall on the seawater evaporation line are probably the least affected by halite dissolution and dilution, while the samples that plot to the left of the seawater evaporation line are the most affected by both halite dissolution and dilution. Figure 6.11 (C) demonstrates the position of the formation waters from the different Devonian stratigraphic units. The plot shows that these formation waters unlike the Mississippian formation waters plot to the right as well as to the left of the seawater evaporation line. The Cl and Br contents vary over a large range which is a reflection of the involvement of almost all end members in their evolution. Some of the Duperow formation waters are the most evolved on the seawater evaporation line. The plot does not show any specific characteristic for the formation waters

from the different Devonian units (i.e. formation waters from different stratigraphic units are not chemically unique).

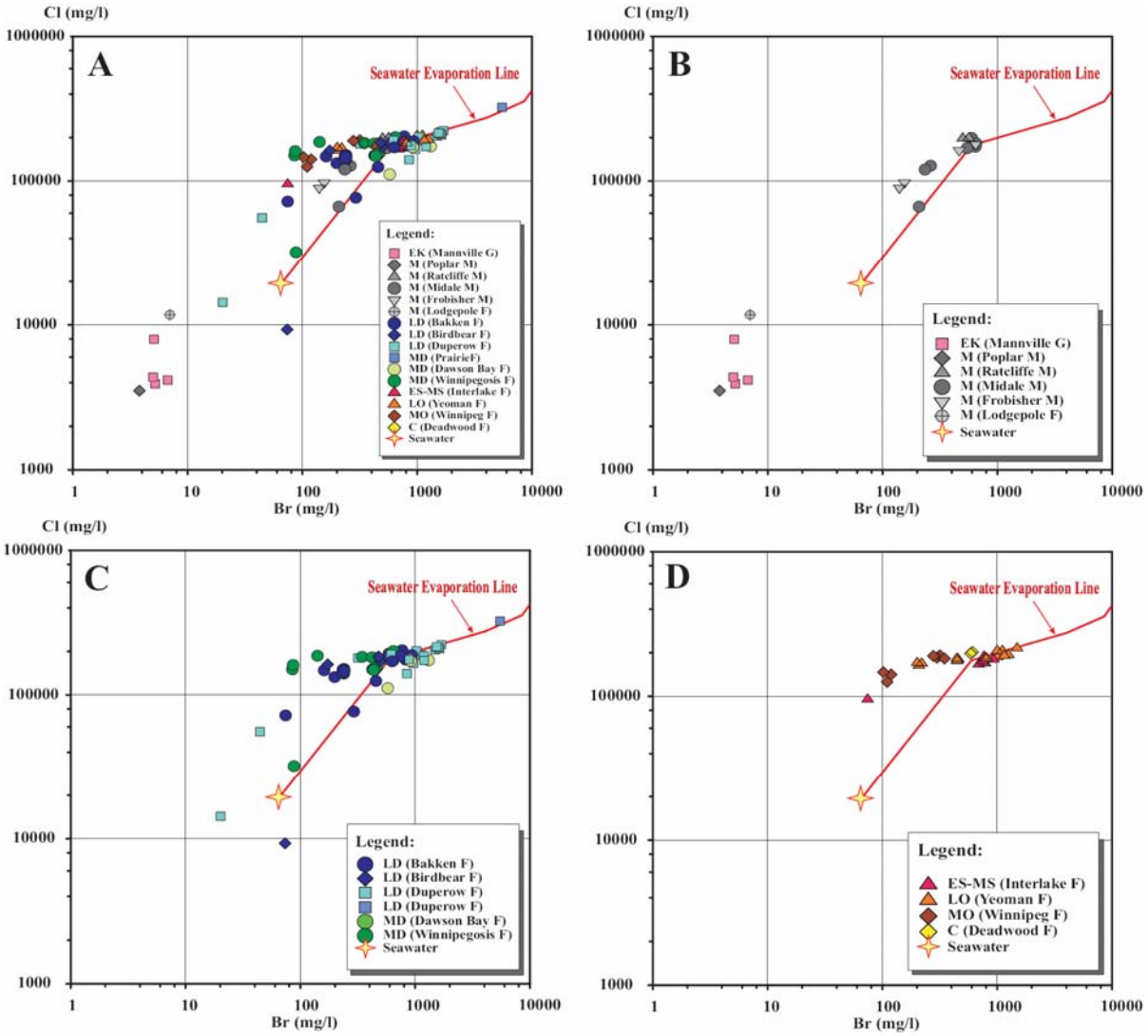

Figure 6.11 Logarithmic plot of Cl (mg/L) versus Br (mg/L) of the Williston Basin formation waters based on the stratigraphic units from which they were sampled. A) All units. B) Early Cretaceous and Mississippian stratigraphic units. C) Devonian stratigraphic units. D) Silurian, Ordovician and Cambrian stratigraphic units. These plots illustrate also the seawater evaporation line.

Figure 6.11 (D) shows the Cl and Br concentrations of the Silurian, Ordovician and Cambrian formation waters. These formation waters are the least affected by dilution in comparison to the other fluids from younger formations discussed above. All Interlake Formation brines plot on the seawater evaporation line except for one sample which shows both the impact of halite dissolution and dilution. The Late Ordovician Yeoman Formation brines are the most evolved on the seawater evaporation line. None of the Middle Ordovician Winnipeg Formation brines plot on the seawater evaporation line and they show the impact of halite dissolution. The two Cambrian brines analyzed in this study plot very close to the seawater evaporation line, suggesting minimal impact of halite dissolution.

Further support to the finding discussed above can be seen in Figure C.1 (Na (meq/L) versus Cl (meq/L)) and Figure C.2 (Ca/Na (mmol) versus TDS (mg/L)) available in Appendix C.

In summary, the geochemical data examined in this study suggests that the Williston Basin formation waters are of several origins (i.e. end members) and that they are the result of various evolutionary process that include evaporation, evaporite dissolution, mixing and water-rock interaction. The proposed end members are: 1) residual paleoseawater that were highly concentrated by evaporation during the deposition of several mineral phases; 2) evaporite dissolution formation waters that involved seawater or meteoric water or both; 3) meteoric water; 4) paleoseawaters. Mixing between these end members along with water-rock interaction (e.g. ion exchange) are some of the evolutionary processes that are involved in the evolution of these formation waters. All formation waters from older (deeper)

stratigraphic units are generally highly concentrated in comparison to formation waters from younger stratigraphic units that are characterized by larger range of TDS compositions. This is due to minimal dilution by meteoric water in the deeper formations in comparison to the younger formations.

These findings disagree with some of the early studies that suggested evaporite (halite and anhydrite in the Middle Devonian Prairie) dissolution as the only or at least the main mechanism responsible for the Williston Basin formation waters (e.g. Wittrup and Kyser, 1990; Busby et al., 1995; Hitchon, 1996), or Clayton et al. (1966) who argued that formation waters in general are dominantly of meteoric water origin and not of seawater origin. However, these findings agree with the finding of a more recent study by Iampen and Rostron (2000) who concluded that the formation waters in the Williston Basin are of at least three origins (residual seawater, halite dissolution and fresh waters) and the mixing between these end members.

6.8 Isotopic Compositions

6.8.1 $\delta^{18}O$ and $\delta^{2}H$ Compositions

During the early phases of the evaporation of seawater the lighter isotopes are preferentially removed from solution and the residual seawater becomes enriched in the heavier isotopes (^{18}O and ^{2}H). Isotopic analysis of an evaporating marine salt pan by Holser (1979) indicated that progressive enrichment of heavier isotopes does not continue indefinitely, but that the trajectory hooks around as shown in Figure 6.12 at an evaporation degree of 4 fold.

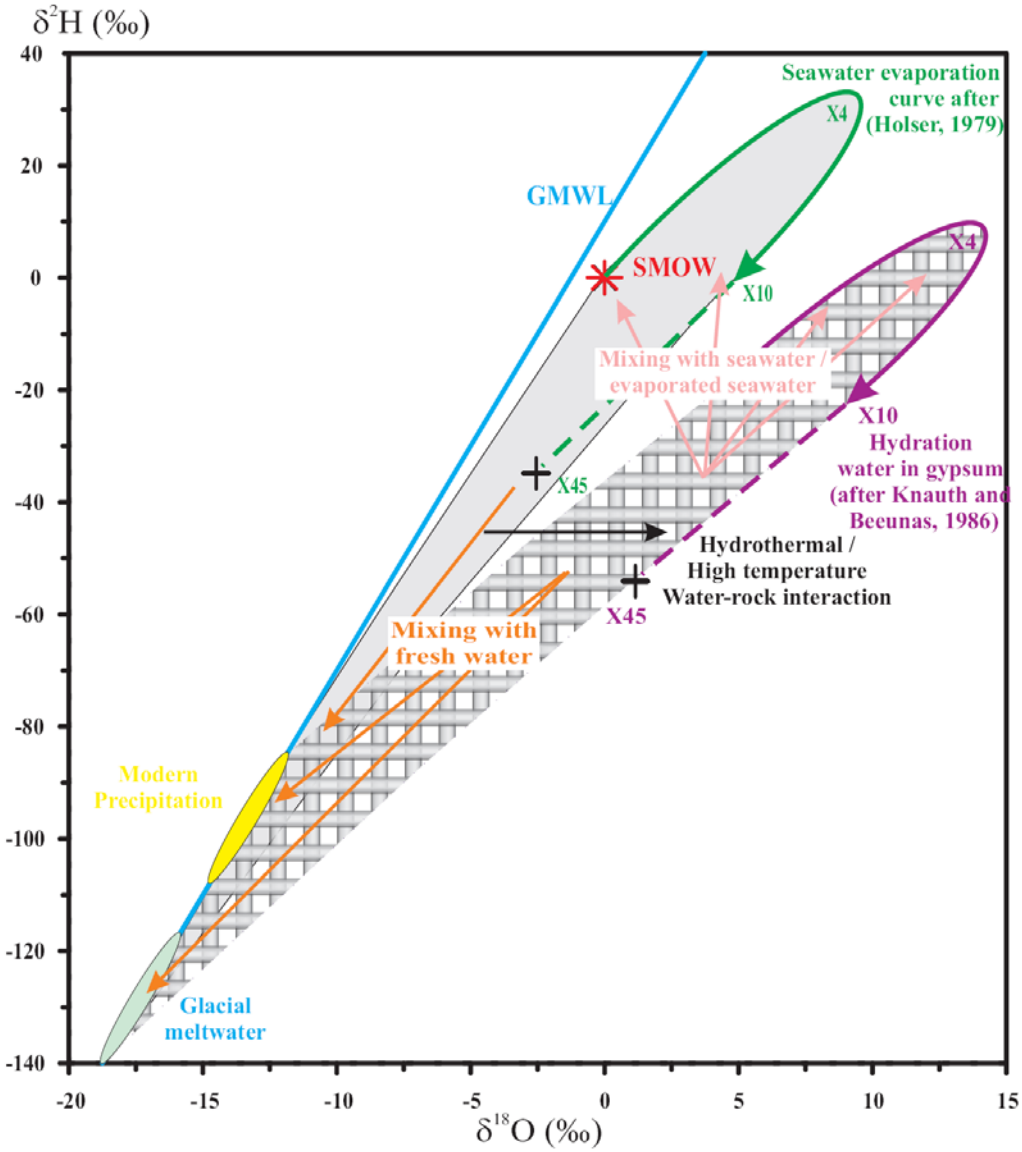

Figure 6.12 The different possible end members and processes that control the oxygen and hydrogen isotopic compositions of the Williston Basin formation waters. Seawater (SMOW), different degrees of seawater evaporation, modern precipitation, and glacial melt-water are the main end members. Mixing between various end members, seawater evaporation, hydrothermal activities, and high temperature water-rock interactions are the major processes. The shaded area represents the mixing area between the main end members. The area filled with bars represents the mixing area between end members after high temperature water rock interaction that enriched the $\delta^{18}O$ signatures. The Figure contains the seawater evaporation curve by Holser (1979) and the extrapolation by Knauth and Beeunas (1986). It contains also the hydration water in gypsum (after Knauth and Beeunas, 1986).

During progressive evaporation the relative amount of water tied up in hydration spheres around cations increases. Isotope exchange between this water, the unbound water, water molecules leaving the liquid-air interface, and atmospheric water vapour may be the cause of the hook-shaped trajectory (Holser, 1979). The shape and the extent of the hook depend on local humidity, temperature, average wind speeds, and other climatic variables (Knauth and Beeunas, 1986). In Figure 6.12, the behaviour of hydrogen and oxygen isotopes during the evaporation of seawater is illustrated by the hook-shape curve presented by Holser (1979). The degrees of evaporation (x4 and x10) are also indicated on the curve as proposed by Holser (1979). The Figure also contains the x45 degree of evaporation as extrapolated by (Knauth and Beeunas, 1986). The halite precipitation begins at about x11 and continues to about x65 (Knauth and Beeunas, 1986). Figure 6.12 shows the gypsum hydration curve as proposed by Knauth and Beeunas, 1986). This curve represents the hydration water in gypsum precipitated during the evaporation of seawater. This water is enriched in ^{18}O and ^{2}H by 4 ‰ and 20 ‰, respectively for the water they precipitated from (Sofer, 1978). However, the stability of gypsum depends greatly on temperature (Hardie, 1967). At temperature above 50°C, gypsum losses it's two water molecules and transforms into anhydrite. Consequently, this changes the isotopic signature of the formation waters by shifting the $\delta^{18}O$ toward more enriched value. Further processes that might cause ^{18}O enrichment are hydrothermal activities (e.g. mixing with geothermal waters) and high temperature water-rock interaction. For example, Sheppard (1986) reported that the $\delta^{18}O$ signature enrichments and shifts to the right of the GMWL are predominantly due to isotopic exchange with ^{18}O-rich sedimentary

minerals such as carbonates. The $\delta^{18}O$ compositions are enriched in marine carbonates by 29 ‰ relative to the water they precipitated from at ambient temperature, however, the equilibrium between carbonate and water is reduced to only 8 ‰ at 250°C (Clark and Fritz, 1997). Therefore, at high temperature water-rock interaction processes the ^{18}O of formation waters tends to get enriched and that of carbonates tends to get depleted. Figure 6.12, also illustrates a few mixing scenarios between the following end members; 1) Seawater (SMOW), 2) saline waters of different degrees of seawater evaporation, 3) modern precipitation, and 3) glacial melt-water.

The $\delta^{2}H$ versus $\delta^{18}O$ values of the formation waters from the Williston Basin are presented in Table 6.1 and illustrated in Figure 6.13 based on water type and in Figure 6.14 based on the stratigraphic units from which they were sampled. The stable isotopic compositions ($\delta^{2}H$ versus $\delta^{18}O$) of the majority of waters are typical of sedimentary basin brines in that they are enriched in ^{18}O relative to modern day meteoric water, plotting to the right of the GMWL (Figure 6.13). However, unlike the Michigan Basin formation waters (Chapter 4), the majority of the highly concentrated formation waters are characterized by more enriched oxygen isotopic compositions than that of seawater (VSMOW = 0 ‰).

Figure 6.13 shows that the majority of the formation waters of this study plot to the right of the GMWL and fall on a line that looks like an evaporation line, but which is most likely a mixing line. The formation waters fit perfectly in the mixing area (filled in bars) between the hydration water hook trajectory and meteoric waters illustrated in Figure 6.12. The Ca-Cl type fluids plot in an evolved position on the seawater evaporation hook passed the 45x mark

along with a shift toward more positive $\delta^{18}O$ values. This agrees very well with the chemistry of this sample and the projection of the sample on the seawater evaporation line [Cl (mg/L) versus Br (mg/L)] in Figure 6.7, where it plots in a highly evolved position.

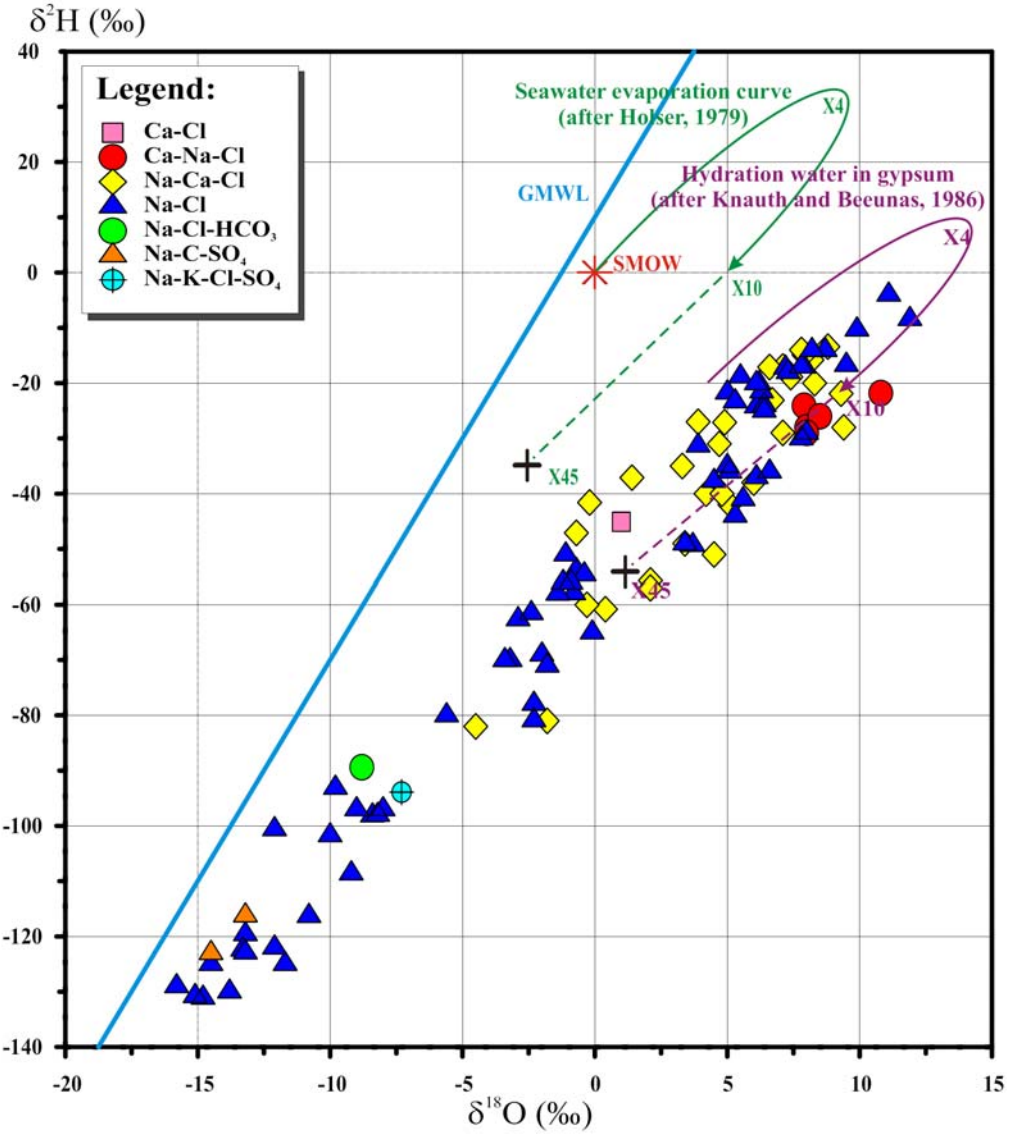

Figure 6.13 δ^2H_{VSMOW} (‰) versus $\delta^{18}O_{VSMOW}$ (‰) of Williston Basin formation waters grouped based on their water types.

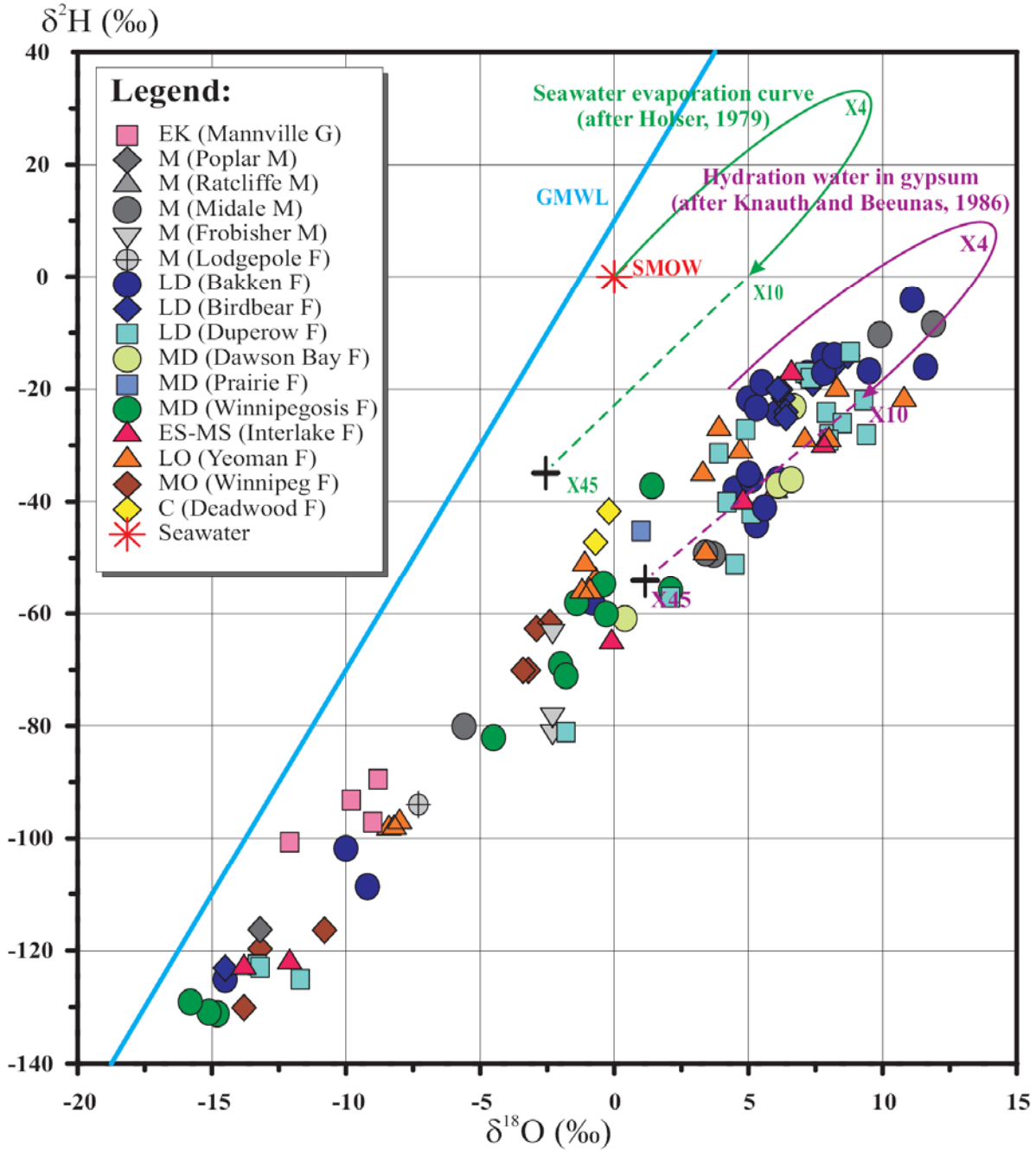

Figure 6.14 $\delta^{2}H_{VSMOW}$ (‰) versus $\delta^{18}O_{VSMOW}$ (‰) of Williston Basin formation waters grouped based on the stratigraphic units from which they were sampled.

Table 6.1 Isotopic compositions of the Williston Basin formation waters. Formation waters are from different stratigraphic units (Early Cretaceous to Cambrian). Sample numbers are per Iampen, 2003 and Jensen, 2007.

No.	Sample ID	$\delta^{18}O$ ‰ (VSMOW)	$\delta^{2}H$ ‰ (VSMOW)	$^{87}Sr/^{86}Sr$	$\delta^{37}Cl$ ‰ (SMOC)		$\delta^{81}Br$ ‰ (SMOB)	
					Aver	Stdv	Aver	Stdv
Early Cretaceous (Mannville Group)								
1	99-116	-9.0	-97	0.70803	-1.01	0.04		
2	00-101	-9.8	-93.1	0.70831	-0.91	0.15		
3	01-205	-12.1	-100.6		0.16	0.09		
4	02-128	-8.8	-89.4		-0.72	0.17		
Mississippian (Madison Group)								
5	01-128	11.9	-8.4	0.70809	-0.06	0.02	0.26	0.09
6	01-129	9.9	-10.3	0.70805	-0.05	0.06	0.13	0.12
Mississippian (Poplar Member)								
7	01-033	-13.2	-116.2		-0.10	0.08		
Mississippian (Ratcliffe Member)								
8	05-106			0.70807	-0.19	0.05	0.04	0.07
9	05-109			0.70802	-0.25	0.09	-0.39	0.07
10	05-111				-0.11	0.05	-0.19	0.09
Mississippian (Midale Member)								
11	99-117	3.4	-49	0.70807	0.19	0.10		
12	00-180	3.7	-49	0.70810	0.05	0.03	0.30	0.08
13	00-190	-5.6	-80	0.70800	0.97	0.05	0.45	0.06
14	05-103			0.70813	-0.20	0.01	0.50	0.08
15	05-104			0.70831	-0.27	0.06	0.45	0.05
16	05-110				-0.22	0.13	0.71	0.12
17	05-115				-0.20	0.07	0.69	0.12
18	05-117				-0.16	0.08	0.68	0.08
Mississippian (Frobisher Member)								
19	00-116	-2.3	-81	0.70810	-0.01	0.11	0.63	0.08
20	00-117	-2.3	-78	0.70800	0.01	0.06	0.67	0.11
21	02-019	-2.3	-63		-0.09			
22	05-112				-0.02	0.07	0.70	0.10
23	05-119				-0.03	0.01	0.36	0.06
Mississippian (Lodgepole Formation)								
24	00-04	-7.3	-93.9		-0.31	0.06		
Late Devonian (Bakken Formation)								
25	97-23	5.6	-41	0.70956	0.20	0.08	1.67	0.04
26	98-20	5.1	-36	0.71084	0.31		1.93	0.06
27	98-21	5.0	-35	0.70842	0.18	0.07	1.45	0.02
28	98-43	7.8	-17		0.26		1.41	0.11
29	98-56	5.3	-44	0.71097	0.74	0.12	1.95	0.06
30	99-48	8.2	-14	0.70851	0.09	0.04	0.97	0.11

Table 6.1 Continued

No.	Sample ID	$\delta^{18}O$ ‰ (VSMOW)	$\delta^{2}H$ ‰ (VSMOW)	$^{87}Sr/^{86}Sr$	$\delta^{37}Cl$ ‰ (SMOC)		$\delta^{81}Br$ ‰ (SMOB)	
31	99-69	11.1	-4		0.82	0.14	0.54	0.11
32	01-108	5.0	-22	0.71004	0.33	0.06	2.77	0.12
33	01-115	5.5	-19	0.71012	0.30	0.02	2.52	0.09
34	01-116	7.8	-14	0.71038	0.47	0.08	2.45	0.10
35	01-117	7.2	-17	0.71027	0.58	0.08	2.11	0.05
36	01-118	9.5	-17		-0.07	0.04	0.72	0.04
37	01-119	-0.8	-58	0.71037	0.27		2.03	0.11
38	01-122	11.6	-16		-0.15	0.04	0.38	0.09
39	01-125	-9.2	-109		0.44	0.15	0.39	0.08
40	01-126	-10.0	-102	0.71028	0.15		2.14	0.11
41	01-150	6.1	-24		-0.15	0.07	0.20	0.06
42	01-171	-14.5	-125	0.70976	0.39	0.09	1.29	0.07
43	01-404	5.3	-23	0.71234	-0.08	0.10	0.86	0.15
44	02-016	6.1	-36		0.31	0.11		
45	02-205	4.5	-38		0.43		1.89	0.05
Late Devonian (Birdbear Formation)								
46	97-14	6.1	-20	0.70866	0.00	0.01		
47	97-32				0.38			
48	98-18	6.2	-20		0.18	0.01		
49	98-125	6.4	-25		0.13	0.04		
50	99-25	8.7	-14	0.70934	-0.15	0.08	1.01	0.09
51	01-105	7.9	-15	0.70931	-0.18	0.05	0.91	0.07
52	01-106	8.2	-16	0.70926	-0.18	0.08	0.75	0.10
53	01-107	7.4	-19	0.70925	-0.15	0.02	0.86	0.08
54	01-402	6.4	-24	0.70888	0.28	0.05		
55	01-403	6.3	-22	0.70895	0.15	0.02		
56	01-405	-14.5	-123	0.70836	0.37	0.09		
Late Devonian (Duperow Formation)								
57	98-28	7.1	-17	0.70863	-0.05	0.14	1.24	0.06
58	98-40	7.9	-17		0.05	0.13	0.52	0.11
59	98-41	7.3	-18		0.03	0.11	0.50	0.11
60	98-123	4.2	-40		0.08	0.12	0.35	0.05
61	99-26	5.1	-42	0.70850	-0.27	0.13	0.43	0.11
62	99-40	9.4	-28	0.70873	-0.19	0.13	0.44	0.06
63	99-42	4.5	-51	0.70852	-0.36	0.12	0.13	0.04
64	99-46	2.1	-57		-0.17	0.00	0.38	0.11
65	99-47	-1.8	-81		-0.12		0.33	0.08
66	99-49	8.0	-28	0.70838	-0.25	0.01	0.18	0.12
67	99-52	8.5	-26	0.70839	-0.42	0.05	0.29	0.11
68	99-53	8.0	-29		-0.29	0.14	0.48	0.12
69	99-95	8.8	-13		-0.23	0.15	1.00	0.09
70	99-96	9.3	-22	0.70867	-0.28	0.08	0.30	0.08
71	00-17	-13.3	-122		0.41	0.13		
72	00-44	-13.2	-123		0.49	0.08		
73	00-61	-11.7	-125		0.16	0.05		

Table6.1 Continued

No.	Sample ID	$\delta^{18}O$ ‰ (VSMOW)	$\delta^{2}H$ ‰ (VSMOW)	$^{87}Sr/^{86}Sr$	$\delta^{37}Cl$ ‰ (SMOC)		$\delta^{81}Br$ ‰ (SMOB)	
74	01-136	4.9	-27	0.70831	0.01	0.05	0.57	0.08
75	01-141	7.9	-24	0.70840	-0.27		0.36	0.07
76	01-203	3.9	-31		0.82	0.13		
77	02-345	1.0	-45	0.70828	-0.21	0.16	0.22	0.01
Middle Devonian (Dawson Bay Formation)								
78	99-56	6.1	-37	0.70998	0.06	0.08	0.00	0.11
79	99-57	6.6	-36	0.71014	-0.16	0.13	-0.27	0.06
80	00-201	0.4	-61		-0.02	0.13	0.12	0.06
81	01-131	6.7	-23		-0.14	0.13	0.18	0.08
Middle Devonian (Winnipegosis Formation)								
82	98-45	-0.3	-60	0.70946	-0.06	0.09	-0.09	0.08
83	98-46	-4.5	-82		-0.41		0.10	0.09
84	98-58	-2.0	-69		-0.32	0.02		
85	99-75	-1.8	-71	0.70994	-0.38	0.13	0.18	0.10
86	01-147	1.4	-37	0.70945	-0.32	0.05	0.20	0.13
87	01-151	2.1	-56	0.70901	-0.37	0.10	-0.42	0.12
88	01-407	-14.8	-131	0.71203	0.09	0.06	0.52	0.08
89	01-408	-15.1	-131	0.71201	0.06	0.03	0.53	0.07
90	01-411	-15.8	-129	0.70892	-0.01	0.06		
91	02-215	-1.4	-58		-0.36		0.28	0.09
92	02-216	-0.4	-55		-0.46		0.38	0.13
Early to Middle Silurian (Interlake Formation)								
93	98-44	9.5	49		-0.24	0.06		
94	98-121	-12.1	-122		-0.02	0.05		
95	99-34	4.8	-40		-0.25	0.16	-0.35	0.08
96	99-35	6.0	-38	0.70917	-0.16	0.09	0.36	0.12
97	99-36	-0.1	-65	0.70878	-0.10	0.03	0.30	0.12
98	99-55	6.6	-31	0.70828	-0.09	0.07	0.39	0.10
99	99-61	7.8	-30	0.70954	0.16	0.01	0.34	0.06
100	03-010	-13.80	-123		0.36	0.10		
Late Ordovician (Yeoman Formation)								
101	97-15	-1.2	-56	0.70994	-0.44	0.00		
102	97-19	-0.9	-56	0.70988	-0.29	0.13		
103	99-28	7.1	-29	0.71004	-0.66	0.04	-1.5	0.08
104	99-39	8.3	-20		-0.23	0.06	0.45	0.05
105	99-60	8.0	-29		0.07	0.08	0.28	0.05
106	99-65	3.4	-49		-0.45	0.13	-0.88	0.07
107	99-128	-1.1	-51		-0.14	0.02		
108	00-187	-8.4	-98		-0.28	0.07	0.12	0.11
109	00-192	-0.7	-54		-0.19			
110	01-109	7.1	85	0.71409	-0.39		-1.29	0.06
111	01-110	10.8	-22	0.70942	-0.39	0.01	-1.07	0.09
112	01-111	7.1	121	0.70899	-0.45		-1.34	0.09

Table 6.1 Continued

No.	Sample ID	$\delta^{18}O$ ‰ (VSMOW)	$\delta^{2}H$ ‰ (VSMOW)	$^{87}Sr/^{86}Sr$	$\delta^{37}Cl$ ‰ (SMOC)		$\delta^{81}Br$ ‰ (SMOB)	
113	01-112	4.7	-31	0.71127	-0.73	0.11	-1.43	0.09
114	01-135	3.3	-35		-0.41	0.15	-0.93	0.09
115	01-140	3.9	-27		-0.36	0.15	0.29	0.10
116	01-409	-8.0	-97	0.71078	-0.35	0.16	-0.11	0.05
117	01-410	-8.2	-98	0.71040	-0.42	0.07	-0.19	0.11
Middle Ordovician (Winnipeg Formation)								
118	98-10	-3.2	-70	0.71474	0.11	0.00	0.03	0.12
119	98-24	-3.4	-70	0.71521	0.00	0.02	0.00	0.06
120	00-08	-2.4	-61	0.71456	0.06	0.11	0.10	0.09
121	00-09	-2.9	-63	0.71451	-0.01	0.07	0.15	0.10
122	00-11	-13.2	-120		-0.09	0.02		
123	00-19	-10.8	-116		0.01	0.07		
124	00-60	-13.8	-130		0.15	0.03		
Cambrian (Deadwood Formation)								
125	01-201	-0.2	-42	0.72159	-0.05	0.00	0.09	0.04
126	01-202	-0.7	-47	0.72103	-0.04	0.10	-1.41	0.09

All of the Ca-Na-Cl type waters and the majority of the Na-Ca-Cl type waters are characterized by $\delta^{2}H$ value between 0 ‰ and -40 ‰ (i.e. between x10 and x45 fold enrichment). This is in agreement with the conclusion drawn from the chemistry of these samples that they were evaporated beyond the start of halite precipitation. The shift of the $\delta^{18}O$ values of these samples toward more positive values is mostly likely due to processes such as gypsum hydration and water-rock interaction with ^{18}O-rich sedimentary minerals such as carbonates as a result of elevated temperatures (Sheppard, 1986). This water-rock interaction scenario is supported by the presence of the North American Central Plains Conductivity Anomaly (NACPCA) under the entire Williston Basin from the North-South direction that is characterized by basal heat flow (Jones and Craven, 1990; Jones and Savage, 1986). This is also supported by the presence of anhydrite in almost all stratigraphic units in

the Williston Basin (see the geology section). Some of the Na-Ca-Cl type waters are characterized by depleted δ^2H and $\delta^{18}O$ values, suggesting dilution with meteoric waters. These same water samples are deviated from the seawater evaporation line in Figure 6.7. This shows agreement and support between the chemical and isotopic data.

The Na-Cl type waters show the largest variation in δ^2H and $\delta^{18}O$ values of all water types. This large variation is a reflection of the presence of more than one end member and various degrees of mixing between the end members. All of the samples that are characterized by enriched δ^2H (-40 ‰ to 0 ‰) are also characterized by high TDS compositions (TDS ~ 300,000 mg/L). They also plot on the seawater evaporation line in Figure 6.7. This lends support to the conclusion that these samples were evolved by seawater evaporation. The rest of the Na-Cl type water samples that are characterized by depleted δ^2H and $\delta^{18}O$ values (along the mixing trend with the fresh water) are in agreement with the dilutions observed from their chemistry. Water samples that plot the farthest from the seawater evaporation line (Figure 6.7) plot the farthest on the mixing line between the highly concentrated brines and the modern precipitation toward the modern precipitation area (Figure 6.12 and Figure 6.13).

The last three water types (Na-Cl-HCO_3, Na-Cl-SO_4, Na-K-Cl-SO_4) that are characterized by low TDS compositions are characterized by depleted δ^2H and $\delta^{18}O$ and plot close to modern precipitation and melt-water in the area. This is in agreement with the chemistry that suggests a fresh meteoric water origin for these samples.

In general, the δ^2H and $\delta^{18}O$ compositions of the different water types, suggests seawater evaporated component as one of the end members and modern precipitation and melt water as

the other end members. The samples show mixing between these two end members. All of the Ca-type waters are not affected by dilution which is in agreement with the chemistry of these samples. The largest variations of δ^2H and $\delta^{18}O$ values observed in Na-type waters suggest that meteoric waters were involved in the halite dissolution and not seawaters. The highly depleted δ^2H and $\delta^{18}O$ values observed in some of the samples indicate melt-water components. Grasby and Betcher (2000) investigated the possibility of a Pleistocene recharge of the Williston Basin and they concluded that a significant influx of fresh water into the Williston Basin took place along the outcrop belt in southern and central Manitoba during Pleistocene glaciation.

Figure 6.14 demonstrates the δ^2H and $\delta^{18}O$ signatures based on the stratigraphic unit of origin. Formation waters from most stratigraphic units are characterized by a large range of isotopic values. However, some of the stratigraphic units are characterized mainly by enriched δ^2H and $\delta^{18}O$ (e.g. Bakken and Duperow). This suggests that brines from these formations are relatively unaffected by fresh water dilution and this is in agreement with findings from the chemistry section. Brines from the Winnipegosis Formation and Winnipeg Formation seem to be affected by fresh water, which is in agreement with the previous findings (see Figure 6.7, all of these samples plot off the seawater evaporation line). All of the Early Cretaceous formation waters are highly affected by fresh water.

In summary, the δ^2H and $\delta^{18}O$ of the formation waters from the different stratigraphic units are characterized by large variations. The enriched $\delta^{18}O$ values indicate high temperature water interactions. The infiltration and mixing with fresh waters (e.g. precipitation and glacial

melt-water) is observed, especially in the shallower formations. Brines that are characterized by enriched isotopic values are located in the central part of the basin and the brines that show isotopic depletions are normally further away from the centre of the basin.

6.8.2 $\delta^{37}Cl$ and $\delta^{81}Br$ Compositions

6.8.2.1 $\delta^{37}Cl$ and $\delta^{81}Br$ Compositions Based on Water Types

The $\delta^{37}Cl$ and $\delta^{81}Br$ compositions of the Williston Basin formation waters are presented in Table 6.1. They are also illustrated in Figure 6.15 based on their water types. In general, the different formation water types show large variations in both isotopes, especially in bromine stable isotope compositions. The $\delta^{37}Cl$ and $\delta^{81}Br$ compositions vary from -1.01 ‰ to +0.97 ‰, and from -1.5 ‰ to +2.77 ‰, respectively. However the majority of the samples fall in a smaller range (between -0.50‰ and +0.25 ‰ for $\delta^{37}Cl$ and between -0.5 ‰ and +1.0 ‰ for $\delta^{81}Br$). The Ca-type waters are characterized by the smallest variations for both isotopes and they also tend to be depleted in both isotopes relative to the Na-Cl type waters that are generally more enriched in both isotopes.

Figure 6.15 demonstrates a possible relationship (positive) between $\delta^{37}Cl$ and $\delta^{81}Br$ of the Williston Basin formation waters. The regression of all data points can be presented by line (A) in Figure 6.15 and the relationship can be expressed by the following equation:

$$\delta^{81}Br = 1.841 \times \delta^{37}Cl + 0.582 \qquad (R^2 = 0.659)$$

When applying the regression after omitting four data points that are deviated from the trend, the relationship can be presented by line (B) in Figure 6.15 and the relationship can be expressed by the following equation:

$$\delta^{81}Br = 2.537 \times \delta^{37}Cl + 0.725 \qquad (R^2 = 0.797)$$

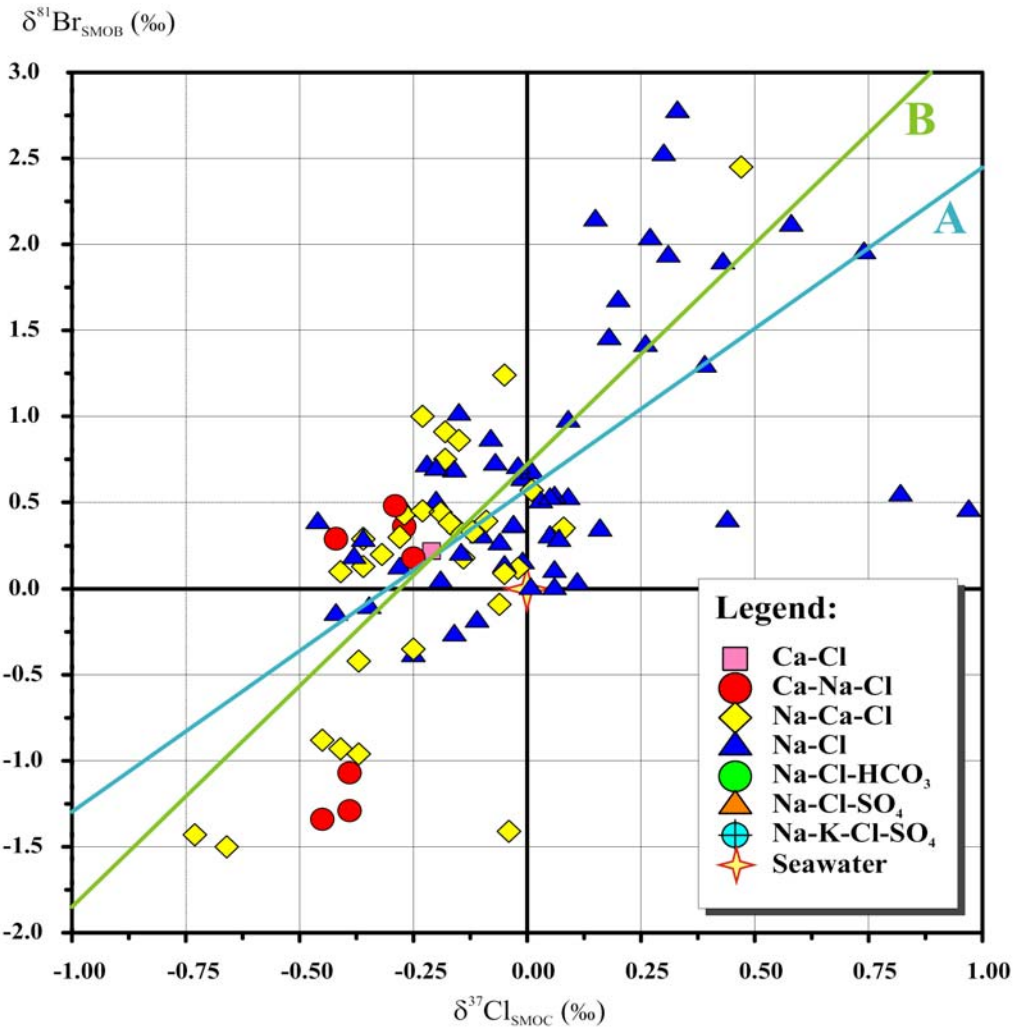

Figure 6.15 $\delta^{81}Br_{SMOB}$ (‰) versus $\delta^{37}Cl_{SMOC}$ (‰) of Williston Basin formation waters grouped based on their water types. The plot demonstrates a possible relationship (positive) between $\delta^{37}Cl$ and $\delta^{81}Br$ of the Williston Basin formation waters. Line (A) is expressed by all data points, while line (B) represents the relationship after omitting four data points.

The Na-Cl type waters show the largest variation in chlorine stable isotope compositions of all water types. Based on the evaluation of the chemistry and hydrogen and oxygen isotopic compositions of these samples, it was determined that these formation waters were evolved from halite dissolution by fresh waters and mixing with evaporated seawater residuals. The chlorine isotopic compositions of these brines fall within the reported range of chlorine isotopes (-0.9 ‰ and +1.2 ‰) for evaporites in the literature (Kaufmann et al., 1984; Eggenkamp and Schuiling, 1995; Eggenkamp et al., 1995; Liu et al., 1997; Eastoe et al., 1999; Eastoe and Peryt, 1999; Eastoe et al., 2001; Stewart and Spivack, 2004; Eastoe et al., 2007). This large variation in the chlorine isotopic compositions is a reflection of the complex evolution of these brines. It is either due to the involvement of different evaporite bodies with different isotopic compositions, various degrees of mixing between the different end members (i.e. Ca-type brines and Na-type brines), or various degrees of other evolutionary processes (e.g. water-rock interaction). Regardless of the processes involved in the evolution of these brines, these Na-type brines are mainly characterized by positive bromine isotopic values. In summary, separation of isotopic compositions based on water types is not identified.

Figure 6.16 illustrates the relationship between the isotopic compositions ($\delta^{37}Cl$ and $\delta^{81}Br$) and the concentrations of Sr and Li. Generally, the formation waters investigated in this study are characterized by high concentrations of both Sr and Li. These concentrations, especially for Ca-type waters and Na-Ca-Cl type waters are much higher than what is expected from seawater evaporation. Such high concentrations of Sr and Li are found in brines from other

sedimentary basins (Heier and Billings, 1969; Collins, 1975; Kharaka and Hanor, 2004). Kharaka and Hanor (2004) suggested that during the diagenetic evolution of the brines, calcium and strontium concentrations increase by up to an order of magnitude compared to evaporated seawater. Therefore, these highly concentrated Sr and Li values lend support to an extensive water-rock interaction as one of the processes in brine evolution. However, since there is no relationship between the increase of these elements and the isotopic composition of the brines, one can assume that the isotopic variations are not due to water-rock interaction or at least water-rock interaction does not cause a significant isotopic fractionation and cannot be responsible for the large range of values for these isotopes for $\delta^{37}Cl$ and $\delta^{81}Br$. This favours the second scenario that implies that the isotopic variations are mainly due to the original fluids that were isotopically different rather than being altered due to diagenetic processes that evolved the brines, such as water-rock interaction.

6.8.2.2 $\delta^{37}Cl$ and $\delta^{81}Br$ Compositions Based on Stratigraphic Units

Figure 6.17 demonstrates the $\delta^{37}Cl$ and $\delta^{81}Br$ signatures of the Williston Basin formation waters based on stratigraphic units. The $\delta^{37}Cl$ and $\delta^{81}Br$ ranges for the different stratigraphic units are presented in Table C.2 (Appendix C). The results show that the formation waters from some of the stratigraphic units (e.g. Bakken and Yeoman) are characterized by very distinctive $\delta^{37}Cl$ and $\delta^{81}Br$ compositions. For example, the brines sampled from the Bakken Formation are generally enriched in both isotopes with few exceptions. The Yeoman Formation brines are generally characterized by depleted $\delta^{37}Cl$ and $\delta^{81}Br$ compositions. The

formation waters from other units are concentrated in a smaller range ($\delta^{37}Cl$: between -0.50 ‰ and +0.20 ‰; and $\delta^{81}Br$: between -0.5 ‰ and +1.0‰) (Figure 6.17). However, brines from specific stratigraphic units seem to group together.

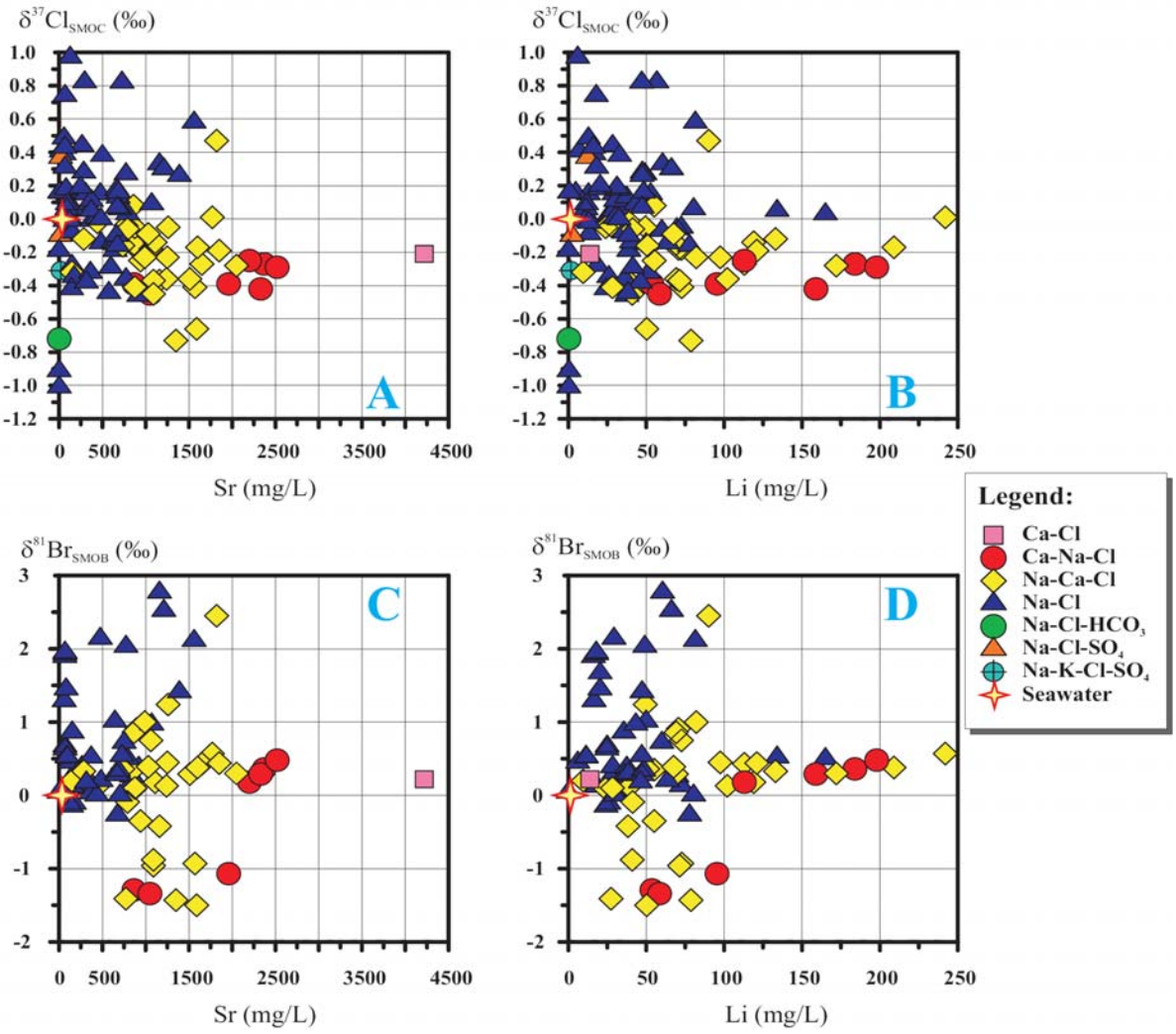

Figure 6.16 Plots A, B, C and D are $\delta^{37}Cl_{SMOC}$ (‰) versus Sr (mg/L) and Li (mg/L) and $\delta^{81}Br_{SMOB}$ (‰) versus Sr (mg/L) and Li (mg/L), respectively of the Williston Basin formation waters grouped based on their water types.

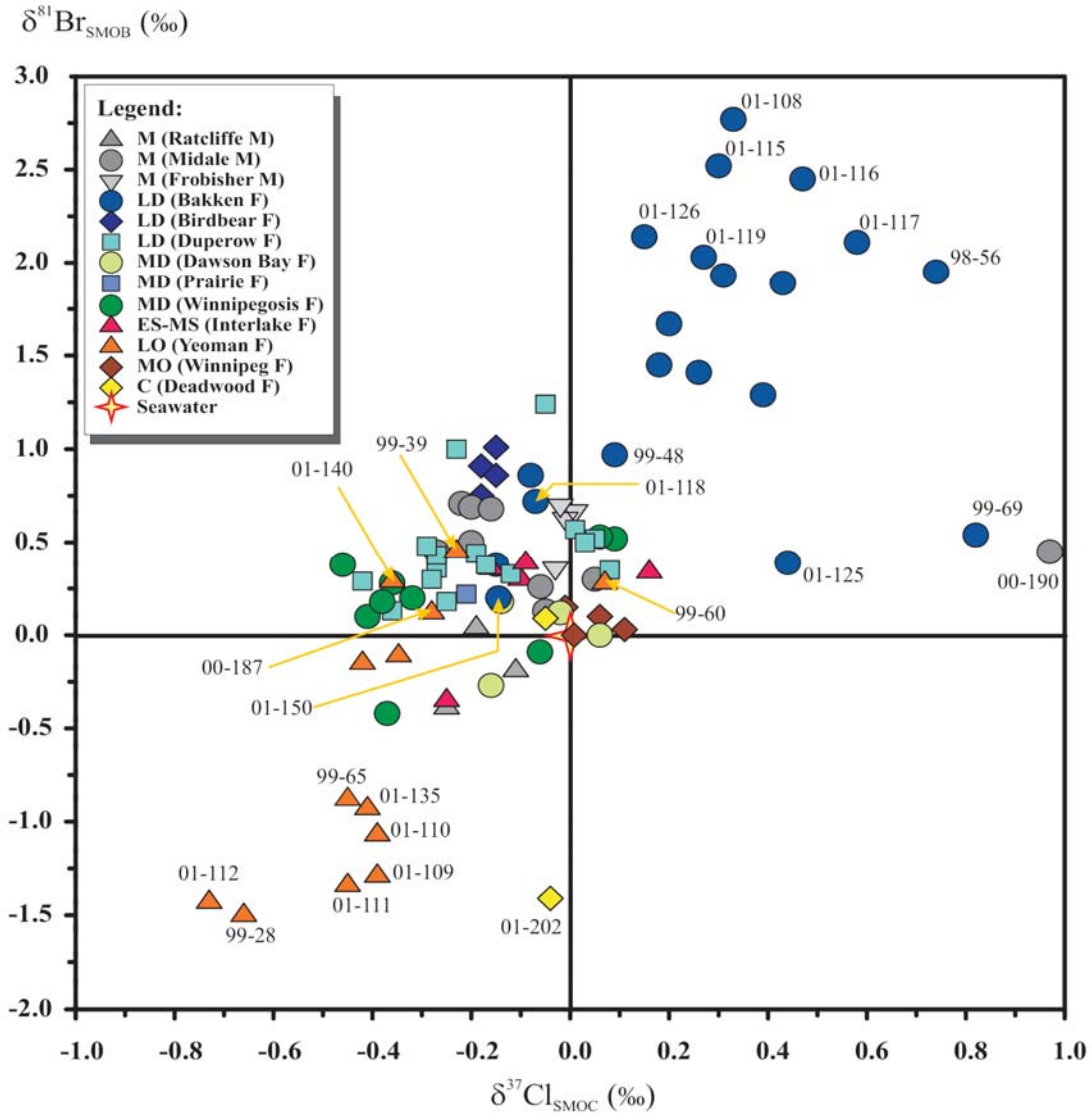

Figure 6.17 $\delta^{81}Br_{SMOB}$ (‰) versus $\delta^{37}Cl_{SMOC}$ (‰) of the Williston Basin formation waters grouped based on the stratigraphic units they were sampled from. The samples that were discussed in the text are labelled.

Figure 6.18 illustrates two plots: a) $\delta^{81}Br$ (‰) versus TDS (mg/L) and b) $\delta^{37}Cl$ (‰) versus TDS (mg/L). Three formations (Duperow, Bakken and Yeoman) are characterized by a large number of samples and also distinctive isotopic values.

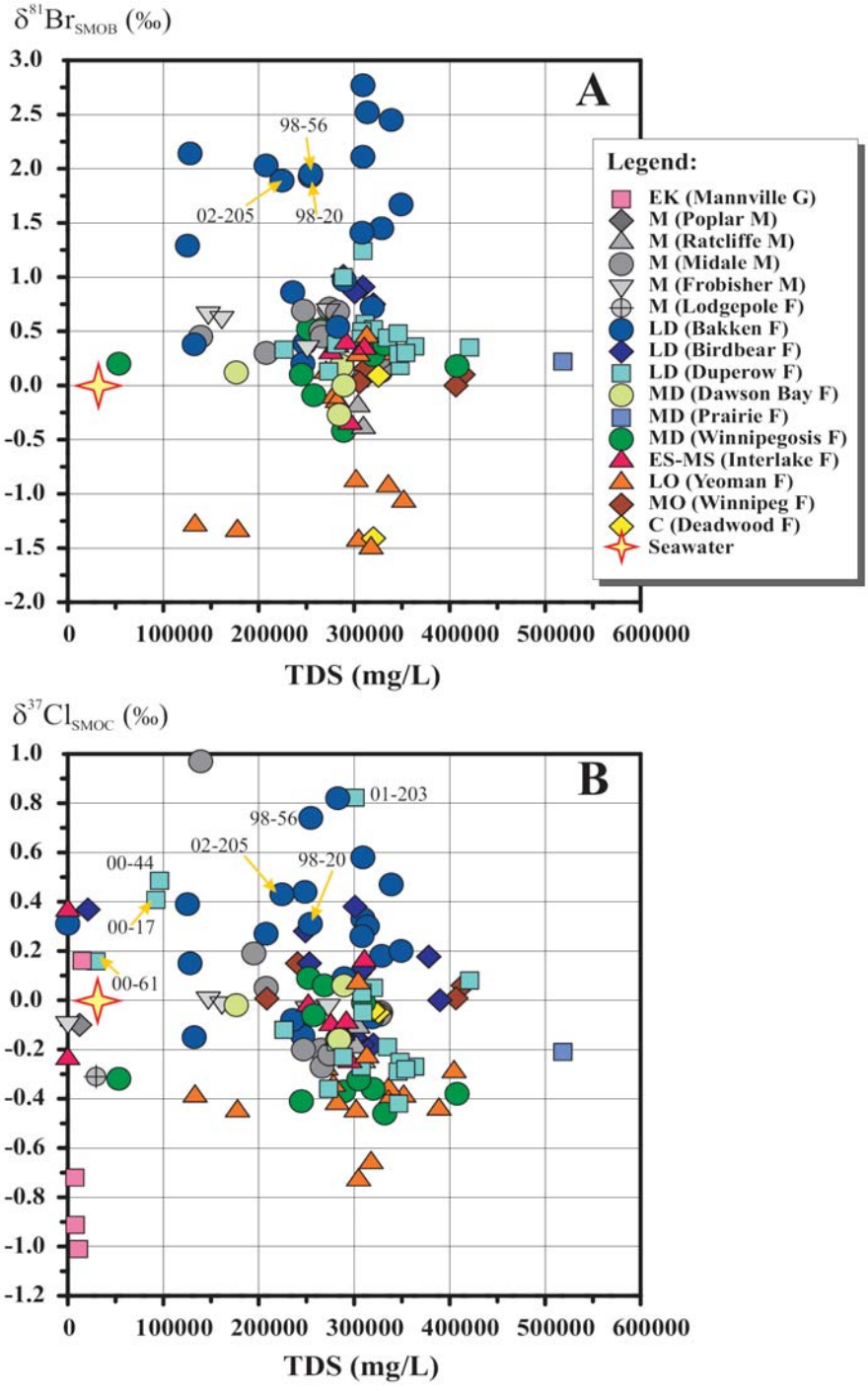

Figure 6.18 A) $\delta^{81}Br_{SMOB}$ (‰) versus TDS (mg/L) and B) $\delta^{37}Cl_{SMOC}$ (‰) versus TDS (mg/L) of the Williston Basin formation waters grouped based on the stratigraphic units they were sampled from. The samples that were discussed in the text are labelled.

The Duperow Formation brines are mainly characterized by a large range of TDS compositions that vary between 220,000 mg/L and 421,000 mg/L and modest isotopic variations ($\delta^{37}Cl$ and $\delta^{81}Br$). Most of the Duperow Formation brines that are characterized by depleted isotopic values are Ca-type waters while most of the Na-type waters are characterized by more enriched isotopic values. Based on the chemical compositions of the Duperow brines discussed previously which suggest that these samples are mainly of marine origin (evaporated paleoseawater) and by assuming that the isotopic values of the ocean ($\delta^{37}Cl$ = 0 ‰ and $\delta^{81}Br$ = 0 ‰) does not change, then the residual brines produced by halite precipitation should be slightly more negative in their $\delta^{37}Cl$ (Eggenkamp, 1994). Eggenkamp (1994) suggested that halite precipitation can cause as much as 0.26 ‰ fractionation. Since the Ca-type waters are characterized by slightly more depleted $\delta^{37}Cl$ values in comparison to the Na-type waters, then the evolutionary processes (e.g. high temperature water-rock interaction) that forms the Ca-type brines causes a slight isotopic fractionation that produces more depleted isotopic values. However, these fractionations seem to be very minimal. The enriched $\delta^{18}O$ values (Figure 6.13) and the elevated Ca, Sr and Li contents (Table C.1, Appendix C) of these brines are evidence of water-rock interaction. This suggests that processes such as water-rock interaction at elevated temperatures do not cause large chlorine isotopic fractionation. The small bromine isotopic range also suggests very minimal fractionation due to high-temperature water-rock interaction.

Three of the Duperow Formation samples (00-17, 00-44 and 00-61; Figure 6.18) that are characterized by enriched $\delta^{37}Cl$ (> 0.2 ‰) are characterized also by low TDS values. This

can be explained by the mixing with less saline waters that are isotopically enriched. The dilution with less saline waters and possibly the involvement of halite dissolution can be seen in Figure 6.11. It is worth noting that these samples were collected from the north-western edges of the Williston Basin, away from the central part.

The enriched $\delta^{37}Cl$ value (0.82 ‰) of sample (01-203; Figure 6.18) from the Duperow Formation, while maintaining high TDS (~300,000 mg/L) composition can be explained only by extensive mixing with a highly concentrated brine that is isotopically more enriched than the Duperow Formation brines such as brines from the overlying Birdbear Formation or Bakken Formation that are characterized by isotopically enriched brines.

The Bakken Formation brines are characterized by the largest isotopic variations of both isotopes (^{37}Cl and ^{81}Br) (Figure 6.17) and also by a large variation in their TDS compositions (~ 120,000 mg/L to ~ 350,000 mg/L) (Figure 6.18). The results of these brines show the following observations:

1) All of the brines sampled from the Bakken Formation are Na-type waters and all samples show positive isotopic values for $\delta^{81}Br$ (Figure 6.18). Most of the samples are characterized by positive $\delta^{37}Cl$ values (Figure 6.18). All of the brines (01-108, 01-115, 01-116 and 01-117; Figure 6.17) that are characterized by highly enriched $\delta^{81}Br$ values (>2 ‰) have Br concentrations greater than 700 mg/L and fall on the seawater evaporation line (figure 6.11). This suggests that these signatures belong to an evaporated paleoseawater. Generally, the elevated Br content of the Bakken samples (ranging between 74 and 934 mg/L with an average of 459 mg/L) and also the position of most of these samples on the seawater

evaporation line in Figure 6.11 lend support to the involvement of evaporated paleoseawater brines in this group of samples.

2) Two samples (01-119 and 01-126; Figure 6.17) that underwent dilution (decrease in TDS) were collected from the western edges of the Basin and away from the center. These samples are characterized by depleted $\delta^{18}O$ and $\delta^{2}H$ values suggesting fresh water component. These two samples maintained enriched chlorine and bromine isotopic values. This suggests that these samples experienced simple mixing with fresh water, where minimal chlorine and bromine isotopic changes are expected as the brine isotopic signature would dominate.

3) Three samples (98-20, 98-56 and 02-205; Figure 6.17) show some dilution based on their low TDS values (Figure 6.18) and also show halite dissolution (Figure 6.11). Their $\delta^{18}O$ and $\delta^{2}H$ values (Table 6.1) supports dilution. These samples were collected from the northern edges of the Basin. These three samples are characterized by enriched $\delta^{81}Br$ (~ 2 ‰) and $\delta^{37}Cl$ values (~ 0.5 ‰). The involvement of halite dissolution has a small effect on the $\delta^{81}Br$ signatures and that is expected as the Br contribution from the halite is small in comparison to that of the brine and hence the isotopic signature of the brine is expected to dominate. On the other hand the variation of the $\delta^{37}Cl$ values of these samples is an indication of the involvement of different evaporites or different degrees of mixing with the halite dissolution waters.

4) Samples (e.g. 99-48, 01-118, and 01-150; Figure 6.17) that are characterized by depleted $\delta^{81}Br$ and $\delta^{37}Cl$ values (< 1.0 ‰ and < 0.2 ‰, respectively) and in the same time

characterized by high TDS compositions (~ 300,000 mg/L) are believed to be produced by mixing with other formation waters that are isotopically light (depleted). This is supported by the enriched $\delta^{18}O$ and $\delta^{2}H$ compositions of these brines (Figure 6.13 and Table 6.1) and also by their position on the seawater evaporation line (i.e. high Br concentrations) (Figure 6.11). This implies that, although the highly concentrated brines that plot on the seawater evaporation line seem chemically similar they are not isotopically similar. This might lead to the suggestion that the Williston Basin contains two or more brines (evaporated paleoseawater) that are isotopically different.

5) Samples (99-69 and 01-125; Figure 6.17) are characterized by depleted $\delta^{81}Br$ and enriched $\delta^{37}Cl$ compositions. These samples are believed to have a more complex scenario than just mixing between two different brines. The $\delta^{81}Br$ values are inherited from the mixing with different brines (e.g. brines from the Duperow Formation), however, the $\delta^{37}Cl$ signatures are most likely due to dissolution of evaporites with enriched $\delta^{37}Cl$ signatures. Sample 99-69 is very concentrated and enriched in both ^{18}O and ^{2}H. This supports the idea of evaporite dissolution being the mechanism that enriched $\delta^{37}Cl$ and most likely did not change the $\delta^{81}Br$. On the other hand sample 01-125, suffered dilution as well as evaporite dissolution. These two samples are from two different locations. Sample 99-69 was sampled from the eastern parts of the basin while sample 01-125 was sampled from the western parts of the basin. This could mean that the evaporites involved in dissolutions are isotopically different.

The brines collected from the Yeoman Formation are characterized by the most depleted isotopic ($\delta^{81}Br$ and $\delta^{37}Cl$) values of all formation waters. Similar to what was observed in the

Bakken Formation brines, the brines of the Yeoman Formation are characterized by variable TDS concentration (~ 120,000 mg/L to ~ 350,000 mg/L) and dilution does not seem to affect the isotopic (δ^{81}Br and δ^{37}Cl) signatures as the isotopic signatures of the brines dominates. In general, the following observations can be extracted from these brines:

1) Brines (99-28, 01-109, 111 and 01-112; Figure 6.17) with the most depleted δ^{81}Br and δ^{37}Cl are from the central part of the basin. These brines plot on the seawater evaporation line suggesting a paleoseawater origin and the δ^{18}O and δ^{2}H values also support this idea. This suggests that these represent an end member that is depleted in both ^{81}Br and ^{37}Cl.

2) Three samples (99-65, 01-110 and 01-135; Figure 6.17) were found to have relatively less depleted signatures in comparison to the previous four samples. These brines are believed to be mixtures between two types of brines that are isotopically different. The mixing between two different brines is supported by the high TDS compositions of these brines. Although all of these brines fall on the seawater evaporation line, they plot apart and their δ^{18}O and δ^{2}H values vary also, indicating that these samples experienced different degrees of mixing.

3) A group of samples (e.g. 99-39, 99-60, 00-187, 01-140; Figure 6.17) from the Yeoman Formation brines are characterized by δ^{81}Br and δ^{37}Cl values that are enriched in comparison with the two previous groups. These brines are most likely affected by extreme mixing with other formation waters. For example, it could be mixing with brines from the overlaying Interlake Formation. The Interlake Formation brines are characterized by near zero δ^{81}Br

signatures and by slightly negative $\delta^{37}Cl$ signatures. Although the Cl and Br concentrations of these samples (Figure 6.11) suggest that these samples were affected by halite dissolution. It is highly unlikely that this large shift in the $\delta^{81}Br$ is due to the halite dissolution, due to the low Br content in halite.

The $\delta^{81}Br$ and $\delta^{37}Cl$ signatures of the Williston Basin brines suggest the existence of several different brine types that are "isotopically distinct". Some of the major processes such as dilution with meteoric waters were found to affect the isotopic signatures in a minimal way. Mixing between different types of brines was found to exist which suggest cross-formational flow or hydraulic connection. Mixing between the different brines affects the isotopic compositions and these isotopic compositions can be used to determine the dominant brine and might be also used to calculate mixing ratios. In general, halite dissolution or evaporite dissolution processes affects the chlorine isotopic signatures more than the bromine isotopic signatures. Further comparisons between the $\delta^{81}Br$ and $\delta^{37}Cl$ compositions and other parameters will be discussed below to evaluate the effect of various processes on these two isotopes.

Figure 6.19 illustrates two plots: a) $\delta^{81}Br$ (‰) versus Ca/Na (mmol/L) and b) $\delta^{37}Cl$ (‰) versus Ca/Na (mmol/L). In general, these two plots show that brines with high Ca/Na ratios (i.e. high Ca contents) are characterized by depleted isotopic ($\delta^{81}Br$ and $\delta^{37}Cl$) values. However, these two properties do not seem to be related. Because formation waters from both, the Duperow and the Yeoman formations are characterized by high Ca/Na ratios, they are isotopically distinct, especially their $\delta^{81}Br$ signatures. This implies that the isotopic

signatures are not inherited from the mechanisms that evolved Ca-rich brines such as water-rock interaction processes (e.g. ion exchange, albitization and dolomitization), or isotopic changes due to these processes is minimal.

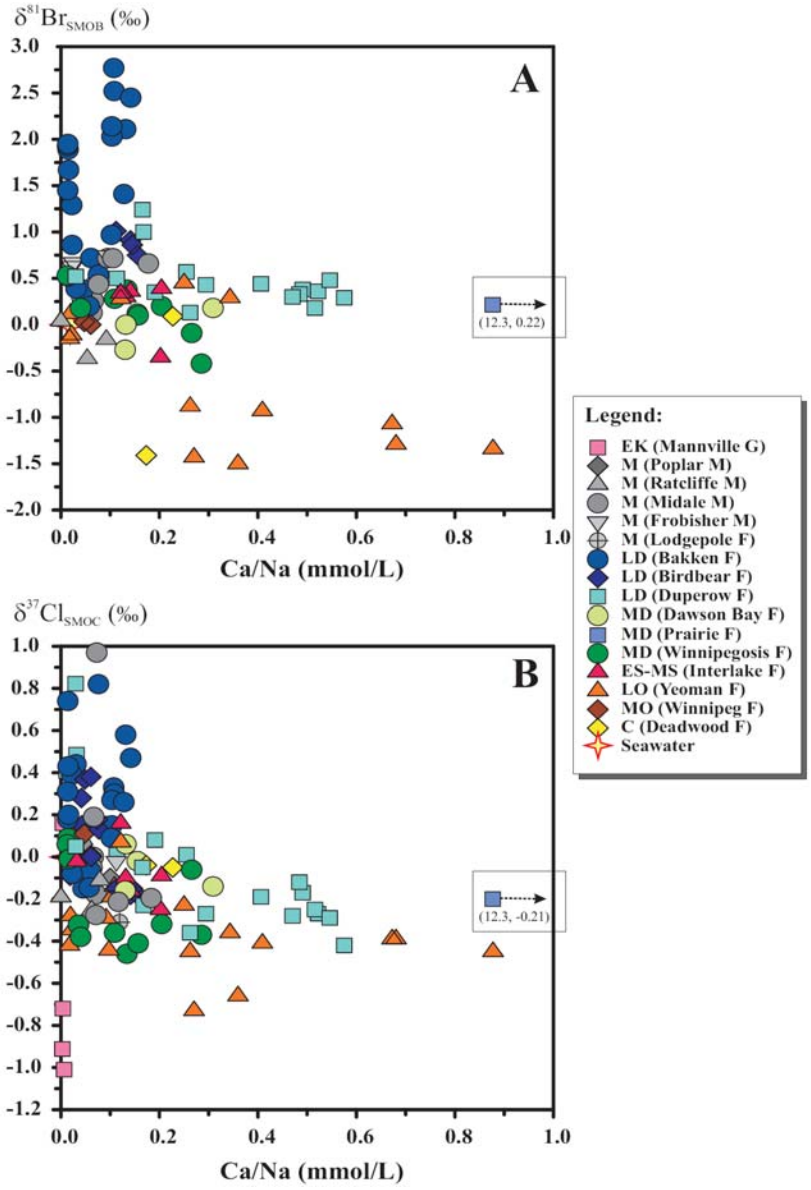

Figure 6.19 A) $\delta^{81}Br_{SMOB}$ (‰) versus Ca/Na (mmol/L) and B) $\delta^{37}Cl_{SMOC}$ (‰) versus Ca/Na (mmol/L) of the Williston Basin formation waters grouped based on stratigraphic units.

In general, the results and the observations made from this study do not support significant isotopic fractionation of chlorine and bromine in the brine due to water-rock interaction processes. However, these results do not imply that these processes do not cause some fractionation.

Furthermore, the two plots illustrated in Figure 6.10 ($\delta^{81}Br$ versus $\delta^{18}O$ and $\delta^{37}Cl$ versus $\delta^{18}O$) show the wide isotopic variations ($\delta^{81}Br$ and $\delta^{37}Cl$) of the brines from different formations (e.g. Bakken, Duperow and Yeoman) that are characterized by $\delta^{18}O$ signatures between 5 ‰ and 10 ‰ (i.e. high temperature water-rock interaction).

Several other plots (Figures C.3, C.4 and C.5) that show the relationship of $\delta^{81}Br$ and $\delta^{37}Cl$ signatures versus Mg (mg/L), temperature (°C) and pH values are illustrated in Appendix C.

Diffusion and ion filtration processes that can cause isotopic fractionations (Campbell, 1985; Desaulniers et al., 1986; Coleman et al., 2001; Lavastre et al., 2005; Hesse et al., 2006) are among the numerous evolutionary processes that are proposed to explain brines in sedimentary basins (Bredehoeft et al., 1963; Berry, 1969; Kharaka and Berry, 1973; Graf, 1982). However, these two processes cannot explain the isotopic variations found in the Williston Basin. For example, the brines found in the Bakken Formation which is a sandstone unit between two shale layers is characterized by highly enriched values of $\delta^{81}Br$ and $\delta^{37}Cl$. This is the opposite of what one should expect from an ion filtration process where the residual brine is expected to become isotopically depleted.

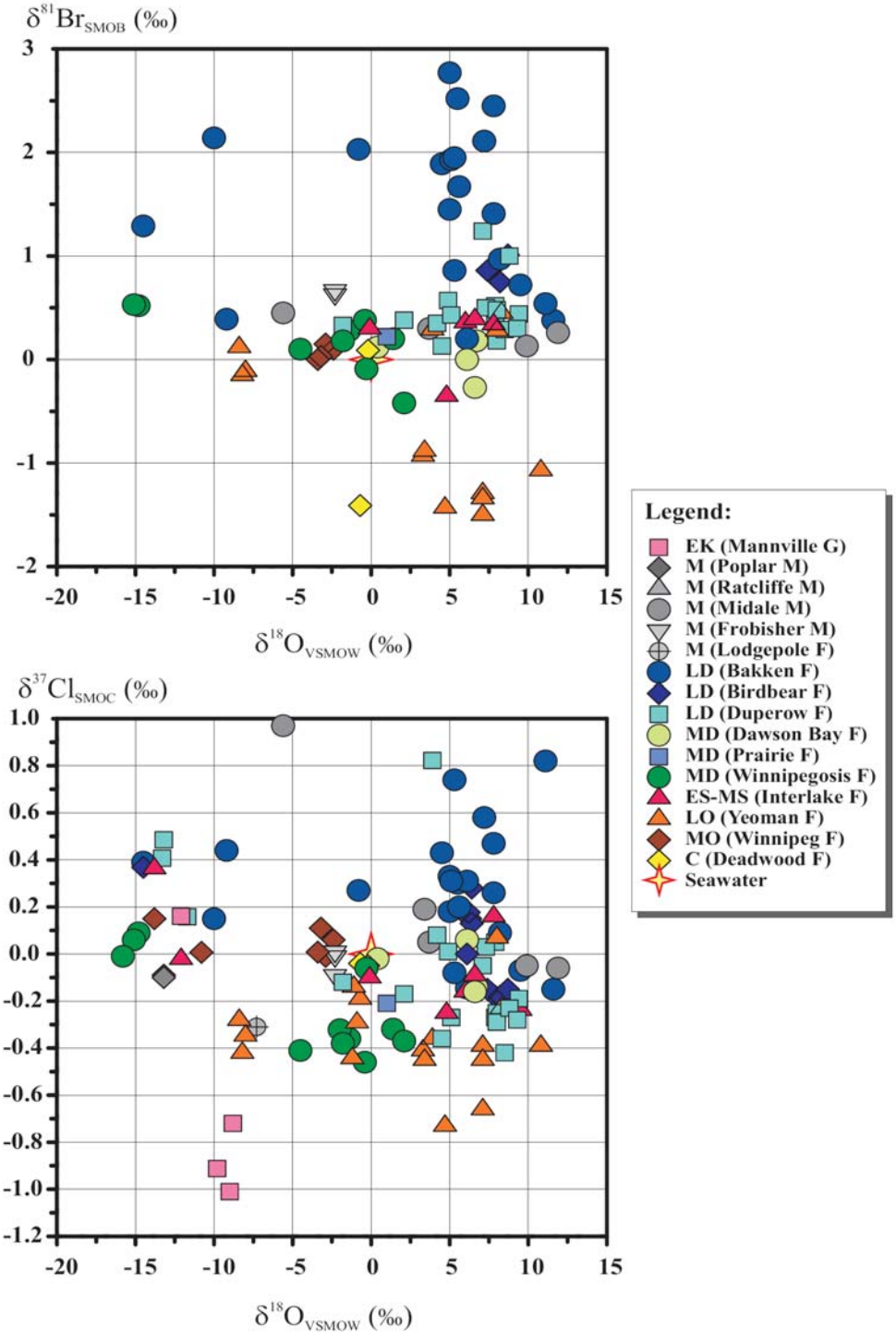

Figure 6.20 A) $\delta^{81}Br_{SMOB}$ (‰) versus $\delta^{18}O_{VSMOW}$ (‰) and B) $\delta^{37}Cl_{SMOC}$ (‰) versus $\delta^{18}O_{VSMOW}$ (‰) of the Williston Basin formation waters grouped based on stratigraphic units.

Since most of the diagenetic processes that can be responsible for evolving these brines such as evaporation, halite dissolution, water-rock interaction, diffusion and/or ion filtration cannot explain the isotopic variations ($\delta^{81}Br$ and $\delta^{37}Cl$) found in the basin and since some of the units show distinct isotopic signatures (e.g. Bakken and Yeoman), then these isotopic variations could be connate reflecting the isotopic signatures of the original paleoseawaters. Figure 6.21 illustrates the $\delta^{81}Br$ and $\delta^{37}Cl$ signatures of the formation waters versus the age of the stratigraphic units they were obtained from. This diagram illustrates the isotopic ranges of both elements ($\delta^{81}Br$ and $\delta^{37}Cl$) of all formation waters that were examined in this study from each stratigraphic unit. The diagram illustrates also a possible temporal variation of the seawater constructed by the average isotopic values of the brines of each stratigraphic unit versus the age of the unit. Although, both isotopes ($\delta^{81}Br$ and $\delta^{37}Cl$) provided similar curves that suggest a systematic temporal variation of seawater, the temporal variations for the $\delta^{81}Br$ values are more pronounced in comparison to the variations in the $\delta^{37}Cl$ values. Several lines of evidence support the hypothesis of temporal variation of the isotopic ($\delta^{81}Br$ and $\delta^{37}Cl$) composition of seawater. The first one is the large isotopic variations of the Williston Basin brines that is not easy to explain by the diagenitic processes as discussed earlier. The second is the agreement between the temporal variation found in this study from the bromine and chlorine isotopes with the well-defined temporal variation of seawater strontium isotopic signatures ($^{87}Sr/^{86}Sr$) (Burke et al., 1982).

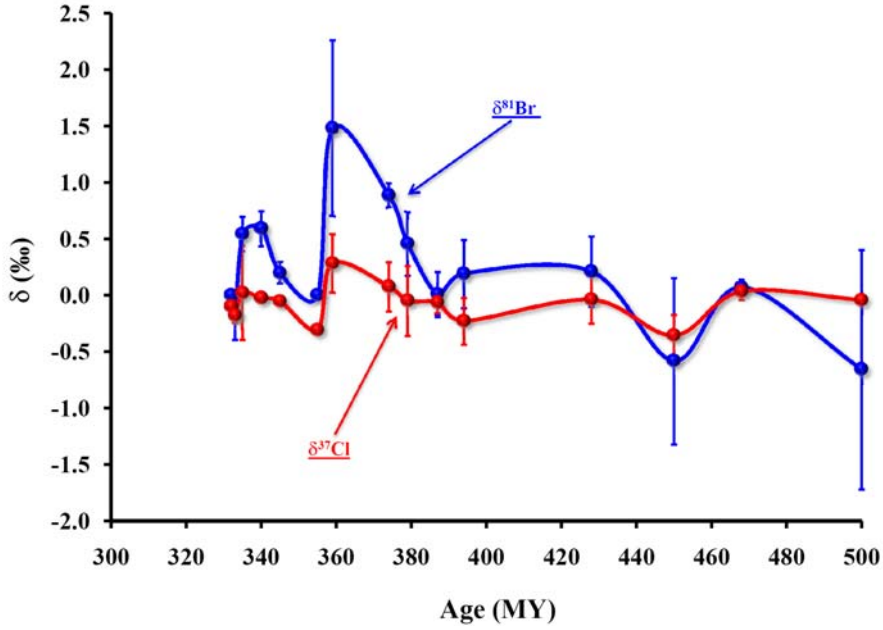

Figure 6.21 $\delta^{81}Br_{SMOB}$ (‰) and $\delta^{37}Cl_{SMOC}$ (‰) versus Age (MY) of the Williston Basin formation waters (Mississippian – Cambrian) The bars represent the isotopic ranges in each specific formation, and the dotes represent the average isotopic values of these stratigraphic units.

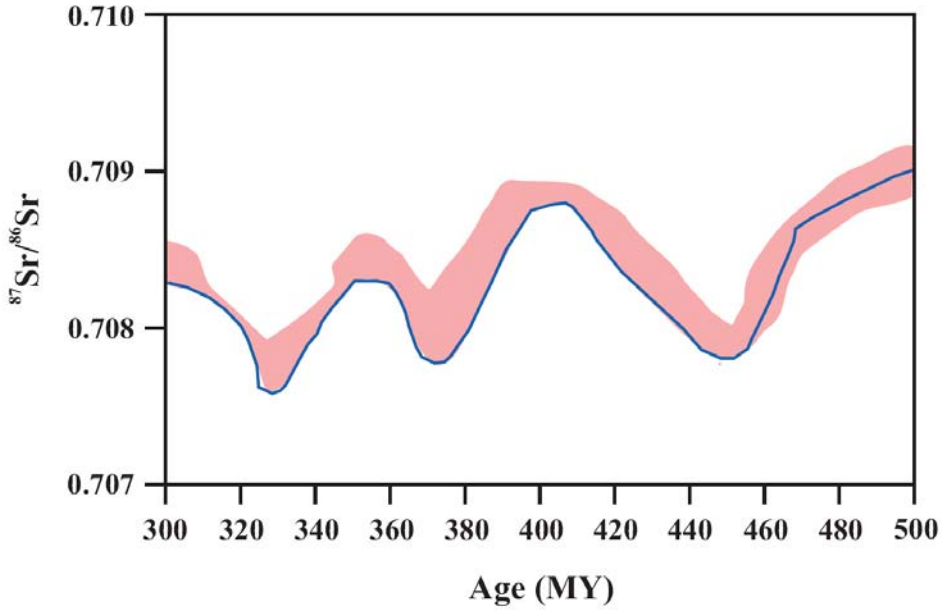

Figure 6.22 The $^{87}Sr/^{86}Sr$ temporal variation of seawater (blue line) (redrawn from Burke et al., 1982). The pink band represents the range of isotopic variations.

The comparison between the $^{87}Sr/^{86}Sr$ seawater curve (Figure 6.22) and the two curves produced by the $\delta^{81}Br$ and $\delta^{37}Cl$ data of the Williston Basin illustrate good agreement between these curves during the period between the Mississippian and the Cambrian. All isotopes follow the same pattern of isotopic enrichment or depletion (e.g. the isotopic enrichment during the Late Devonian and the isotopic depletion during the Late Ordovician). The third is the reasonable agreement with the $\delta^{34}S$ seawater curve (Figure 6.23) produced by Claypool et al. (1972) and discussed later in more detail (Holser, 1977; Claypool et al., 1980). There is good agreement in the depletion of the $\delta^{34}S$ signature of seawater during the Middle Devonian and the following sharp rise (enrichment) of the $\delta^{34}S$ signature during the Late Devonian period. Furthermore, it agrees with the depletion of the $\delta^{34}S$ in the Late Ordovician Period reported by Fox and Videtich (1997) in their revision of the seawater $\delta^{34}S$ curve (Figure 6.23). These variations agree with the isotopic and organo-geochemical study on the Phanerozoic sediments of the Williston Basin conducted by Arneth (1984). Arneth (1984) concluded from his study that the $\delta^{13}C$ compositions of the carbonates, total organic and bitumen of the rocks from the Ordovician (Red River) to be the most depleted of all old rocks (Cambrian – Mississippian) and he also reported the Bakken (reported as Mississippian in his paper) to be characterized by the most enriched $\delta^{13}C$ values in all three materials (carbonates, total organic and bitumen).

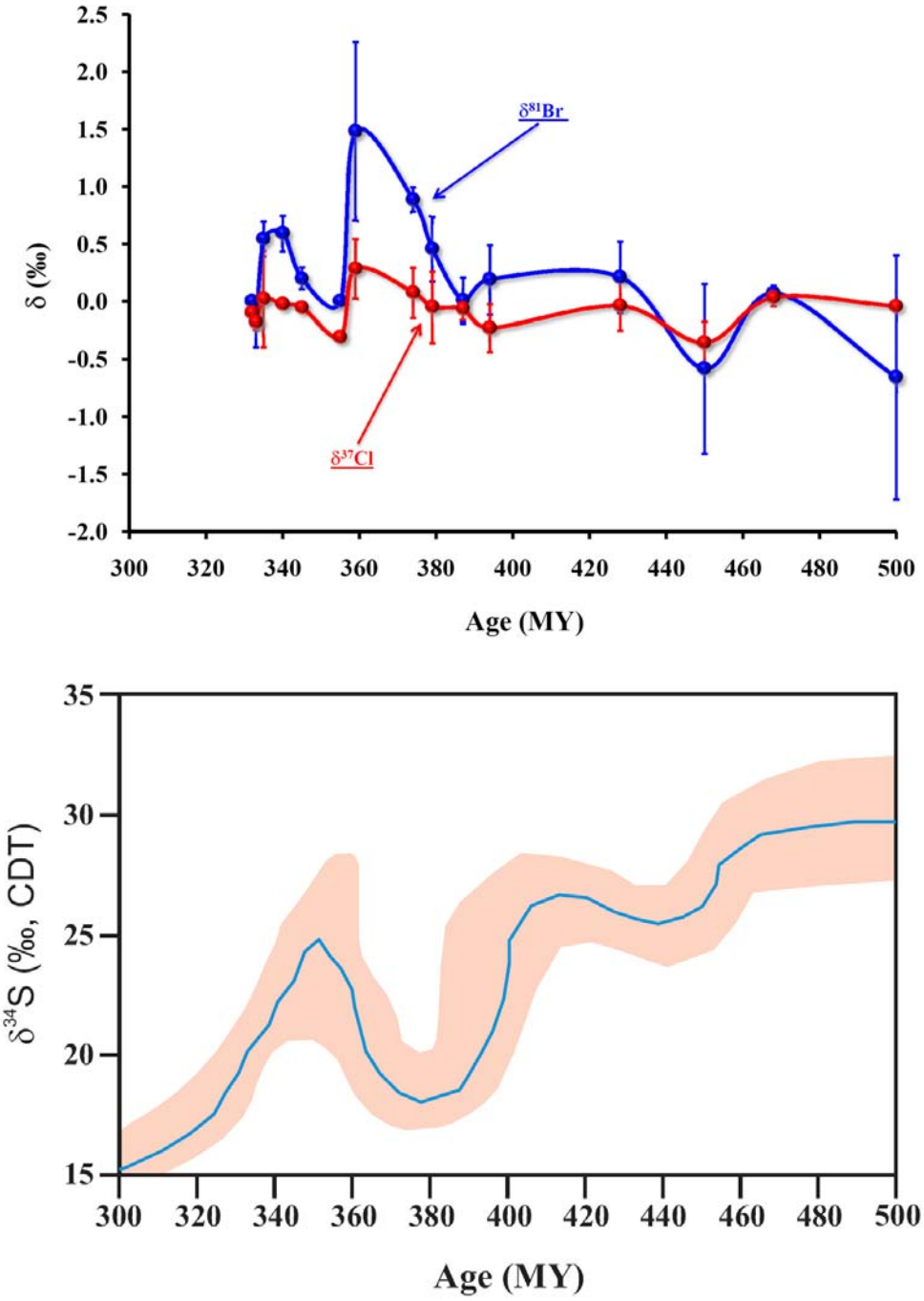

Figure 6.23 The seawater $\delta^{34}S$ (‰ CDT) curve (blue) of marine sulphates redrawing after Claypool et al. (1980). The pink band represents uncertainty limit estimates on either side of the curve. Above plot is the $\delta^{81}Br_{SMOB}$ (‰) and $\delta^{37}Cl_{SMOC}$ (‰) versus Age (MY) of the Williston Basin formation waters

In summary, the comparison of the $\delta^{81}Br$ and $\delta^{37}Cl$ variations of seawater with both the $^{87}Sr/^{86}Sr$ and the $\delta^{34}S$ variations of seawater over the geologic period from the Mississippian through Cambrian, show good agreement but with different intensities. This in turn suggests a systematic link between the causes of these variations of all the isotopes but in the same time, the different intensities suggests either different responses to the causes, additional factors that affects the isotopes of one element but not the others or both. These coincidences support the hypothesis of $\delta^{81}Br$ and $\delta^{37}Cl$ seawater variations.

Some of the data obtained during this study (Table 6.1) were eliminated, in order to obtain a better demonstration of the temporal variation of the seawater $\delta^{81}Br$ and $\delta^{37}Cl$ signatures. Samples that fall under the following criteria were eliminated: 1) samples with TDS values less than 200,000 mg/L, 2) samples that show dilution with fresh water (see Figure 6.11), 3) samples that show halite dissolution (see Figure 6.9 and Figure 6.11), 4) samples that were collected outside the area from 102.50° W to 104.00° W longitudes and 46.50° N to 49.00° N latitudes. Two more samples (99-69; Bakken and 01-202; Deadwood) were eliminated due to their deviation from the positive relationship between $\delta^{81}Br$ and $\delta^{37}Cl$ as presented in Figure (6.17). The exceptions were samples from Dawson Bay Formation, Winnipeg Formation and Deadwood Formation that qualified for the first three points but failed the last criteria. These samples were considered because all samples from these three formations were collected from outside the area specified in point 4. Generally, most of the remaining samples fall on the seawater evaporation line as illustrated in Figure (6.11) or in close proximity. The main objective of the elimination process is to minimize the isotopic variations due to mixing,

dilution and halite dissolution and examine only the highly concentrated formation waters from the very central part of the Williston Basin. This in turn will better represent the paleoseawaters from the various end members. The new seawater curves of both $\delta^{81}Br$ and $\delta^{37}Cl$ are illustrated in Figure (6.26). These two curves show the same pattern observed in Figure (6.23), however, the intensities of the variations (isotopic enrichments and depletions) are more pronounced and better defined. It is worth noting that the analytical error bars are smaller than the symbols on Figure (6.26). This suggests that the variations observed, even, for the chlorine isotopes are significant.

Figure (6.27) illustrates the $\delta^{81}Br$ versus $\delta^{37}Cl$ signatures of the Williston Basin formation waters that were used to construct the seawater curves in Figure (6.26). Figure (6.27) demonstrates a positive relationship between $\delta^{37}Cl$ and $\delta^{81}Br$ that is better defined from the one previously proposed in Figure 6.15. The regression of all data points can be presented by line (C) in Figure 6.25 and the relationship can be expressed by the following equation:

$$\delta^{81}Br = 2.841 \times \delta^{37}Cl + 0.780 \ (R^2 = 0.802)$$

Since the two curves produced in Figure 6.24, follow the Sr seawater curve (Figure 6.22), one would expect a positive relationship between both $\delta^{81}Br$ and $\delta^{37}Cl$ and $^{87}Sr/^{86}Sr$ of these formation waters. Typically, the strontium isotopic composition of formations waters has shown great potential as a means of identifying sources of strontium in formation waters, the degree of water–rock interaction, and the degree of mixing along regional fluid flow paths (e.g., Armstrong et al., 1998, McNutt, 2000).

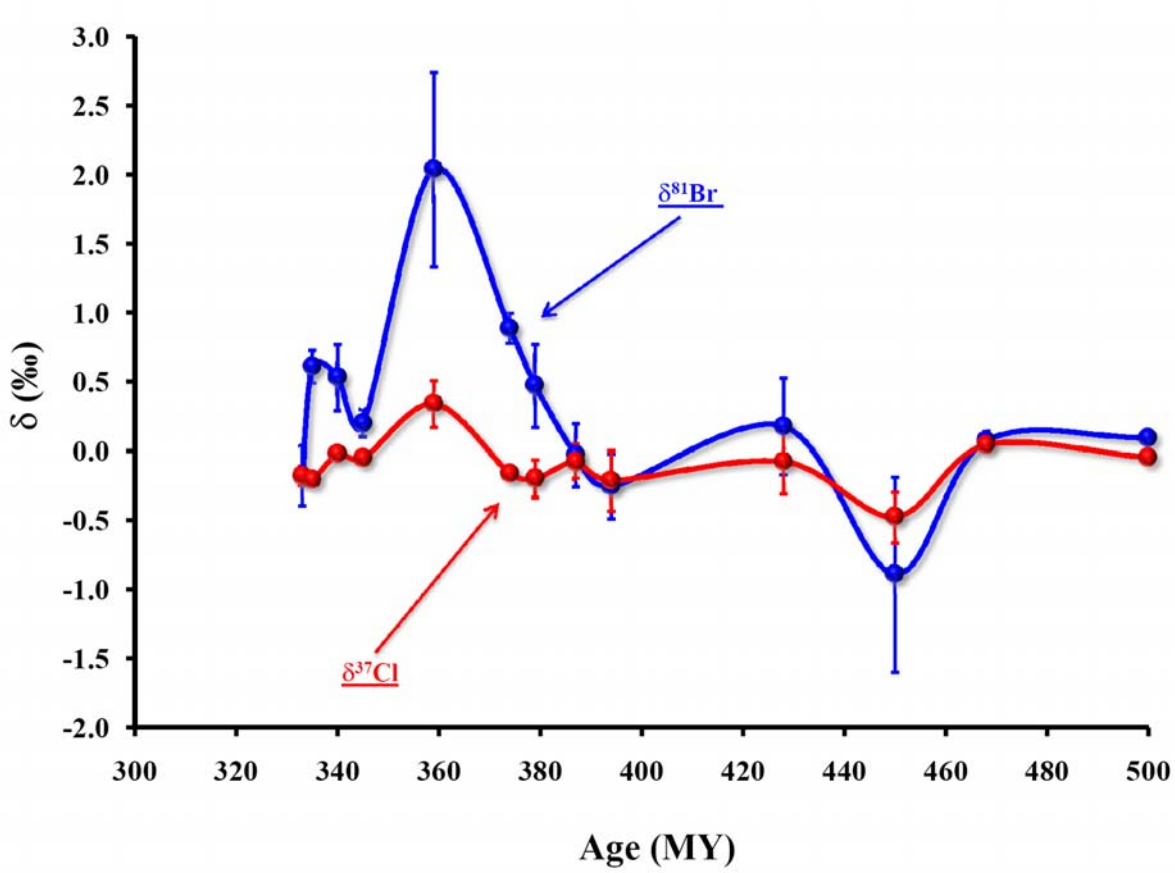

Figure 6.24 $\delta^{81}Br_{SMOB}$ (‰) and $\delta^{37}Cl_{SMOC}$ (‰) versus Age (MY) of the Williston Basin formation waters (Mississippian – Cambrian) after eliminating samples with TDS vales less than 200,000 mg/L, samples that suffered dilution or halite dissolution and samples that were collected outside the area from 102.50° W to 104.00° W longitudes and 46.50° N to 49.00° N latitudes. The bars represent the isotopic ranges in each specific formation, and the dotes represent the average isotopic values of these stratigraphic units.

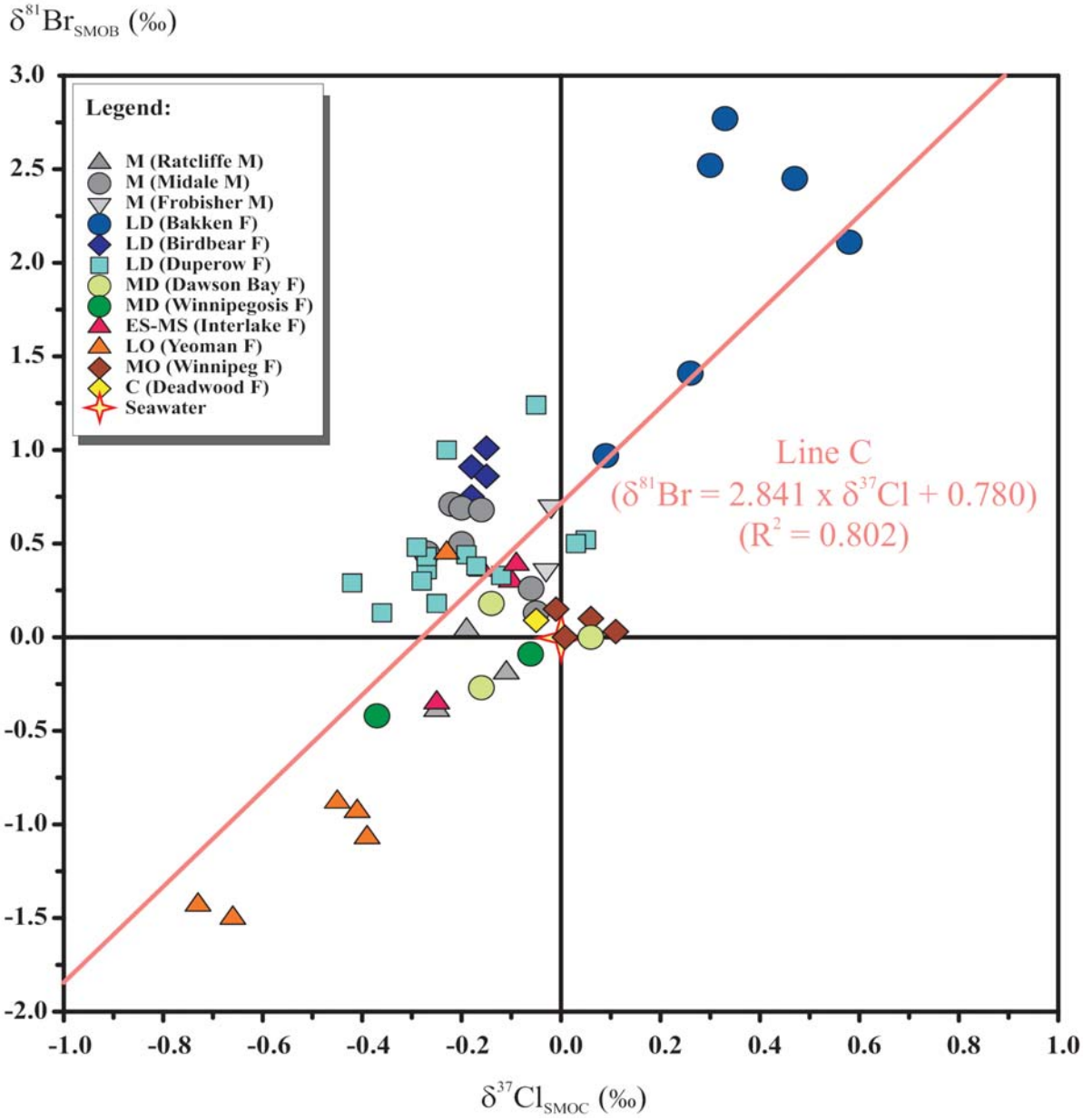

Figure 6.25 $\delta^{81}Br_{SMOB}$ (‰) versus $\delta^{37}Cl_{SMOC}$ (‰) of the Williston Basin formation waters (Mississippian – Cambrian) from the central part of the basin (after eliminating some samples) (see the text and Figure 6.27 for more details).

A detailed review of strontium isotopic behaviour in formation waters with emphasis on water–rock interaction is explained in McNutt (2000). The strontium isotopic composition of geological materials is expressed as the ratio of $^{87}Sr/^{86}Sr$. The $^{87}Sr/^{86}Sr$ ratios of the world's oceans have varied from 0.7065 to 0.7092 during the Phanerozoic (Burke et al., 1982) as the result of variations in the relative rates of input of ^{87}Sr-enriched strontium from continental weathering and ^{87}Sr-depleted strontium from mantle sources. The $^{87}Sr/^{86}Sr$ signatures of the Williston Basin formation waters are presented in Table 6.2. In general, the $^{87}Sr/^{86}Sr$ values fall between 0.708 and 0.722. These values confirm the marine origin of these formation waters and they show a radiogenic component in some of the samples. Typically, when a brine has a signature within that range, then it is permissible to consider a marine isotopic signature. However, when the isotopic values fall outside that range, one must consider other factors to explain the values such as water-rock interaction processes (Frape et al., 2004). Figure 6.26 illustrates the relationship between: a) $\delta^{81}Br$ and $^{87}Sr/^{86}Sr$ and b) $\delta^{37}Cl$ and $^{87}Sr/^{86}Sr$. These two plots do not show any clear relationship between the various isotopes. This means that although a positive correlation between $\delta^{81}Br$ and $\delta^{37}Cl$ signatures of the brines and the $^{87}Sr/^{86}Sr$ signatures of the rocks from the same age is possible, a correlation might not be possible when compared with the $^{87}Sr/^{86}Sr$ signatures of the brines. This is because of the sensitivity of the $^{87}Sr/^{86}Sr$ toward water-rock interaction processes and these brines showed high degrees of water-rock interaction as discussed earlier (e.g. the highly enriched $\delta^{18}O$ and highly elevated Sr and Li contents of these samples).

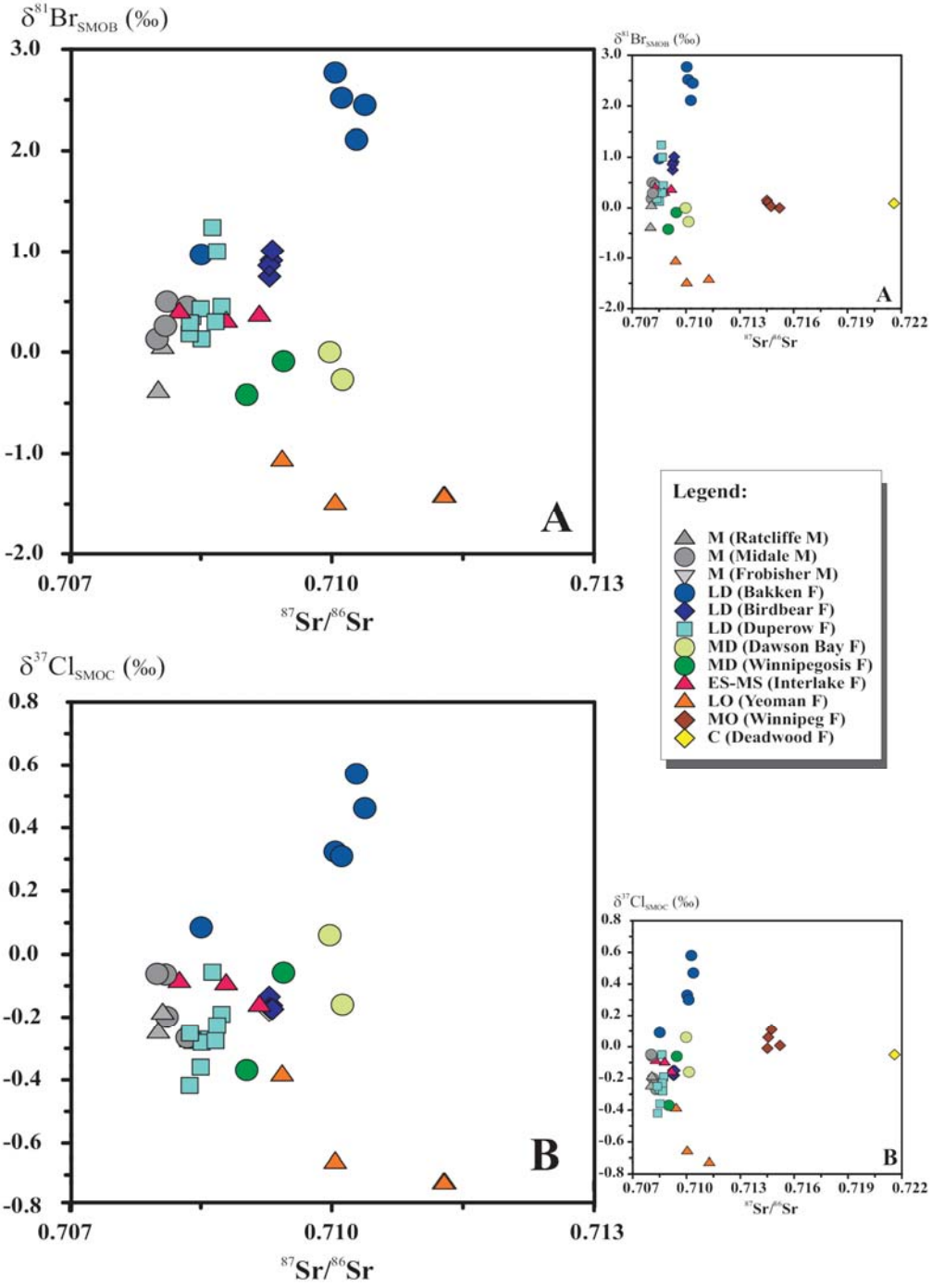

Figure 6.26 A) $\delta^{81}Br_{SMOB}$ (‰) versus $^{87}Sr/^{86}Sr$ and B) $\delta^{37}Cl_{SMOC}$ (‰) versus $^{87}Sr/^{86}Sr$ of the Williston Basin formation waters from the central part of the basin.

Generally, most formation waters in this study are characterized by more enriched values in comparison to the $^{87}Sr/^{86}Sr$ values of the stratigraphic units they were sampled from. Typically, formation waters in sedimentary basins containing Paleozoic strata have $^{87}Sr/^{86}Sr$ ratios that are more enriched than seawater values of the depositional age of the current host sediment (Connolly et al., 1990; Kharaka and Hanor, 2004). This enrichment is usually, attributed to the release of strontium from the alteration of silicates, albitization and feldspar dissolution (Stueber et al., 1993). Although, no correlation is observed in Figure 6.26, this figure shows samples with similar $^{87}Sr/^{86}Sr$ ratios to have totally different $\delta^{81}Br$ and $\delta^{37}Cl$ signatures (e.g. Bakken, Dawson Bay and Yeoman) and vice versa (e.g Deadwood, Winnipeg and Dawson Bay). This implies that the evolutionary processes that affect these different isotopes are not exactly the same, although some common factors are possible.

Figure 6.27 illustrates the relationship between: a) $\delta^{81}Br$ and Sr and b) $\delta^{37}Cl$ and Sr. These two plots show three possible paleoseawater end member that are isotopically distinct. The three end members are labeled A, B and C (Figure 6.27). The first end member (A) is isotopically enriched in both isotopes ($\delta^{81}Br$ and $\delta^{37}Cl$) and located in the Bakken Formation (Late Devonian), the second end member (B) is characterized by near zero isotopic signatures from the Duperow Formation (Middle Devonian), and the third one (C) is isotopically depleted in both isotopes ($\delta^{81}Br$ and $\delta^{37}Cl$) and located in the Yeoman Formation (Late Ordovician). Whether the rest of the formation waters from the other stratigraphic units (e.g. Dawson Bay, Winnipegosis and Winnipeg) are also end members that happen to be isotopically similar or simply the product of mixing between these three end members is not

clear from these plots. The co-existence of different brines that are isotopically distinct is previously reported (Eastoe and Guilbert, 1992). Eastoe and Guilbert (1992) conducted a study on three different basins and they concluded that formation waters from three different basins have bimodal distribution of $\delta^{37}Cl$, with one fluid being characterized by an isotopic value near -0.8 ‰ and the other near 0 ‰.

In summary, the $\delta^{81}Br$ and $\delta^{37}Cl$ signatures of the formation waters present in the central part of the Williston Basin suggests multiple end members located in different stratigraphic units. The isotopic variations of these two elements agree well with the $^{87}Sr/^{86}Sr$ seawater variation during the same period and reasonably with the seawater variation of the $\delta^{34}S$. Furthermore, the presence of multiple sources of brines is in line with the presence of different types and sources of oil in the Williston Basin (e.g. Williams, 1974; Osadetz et al., 1992; Osadetz et al., 1994; Kirk et al., 1998; Obermajer et al., 2000; Jiang and Li, 2002; Smith and Bend, 2004). For example, Smith and Bend (2004) indicated that oils found in the Winnipeg and Red River formations are distinct and originate from two separate sources, despite their close stratigraphic proximity.

Although the cause of the temporal variations of these two isotopes is not one of the objectives of this study, a few observations will be addressed below.

If changes in the chlorine and bromine input did occur, and the isotopic signatures of the various contributors are different, then seawater isotopic signatures varied over time as well. Kovalevich et al (1998) concluded from their work on inclusions in primary bedded halite from many evaporite formations of northern Pangaea that the chemical composition of

marine brines was oscillating significantly between the Na-K-Mg-Ca-Cl type and the Na-K-Mg-Cl-SO_4 type during the Phanerozoic. They attributed these changes as corresponding to the chemical evolution of the Phanerozoic Ocean.

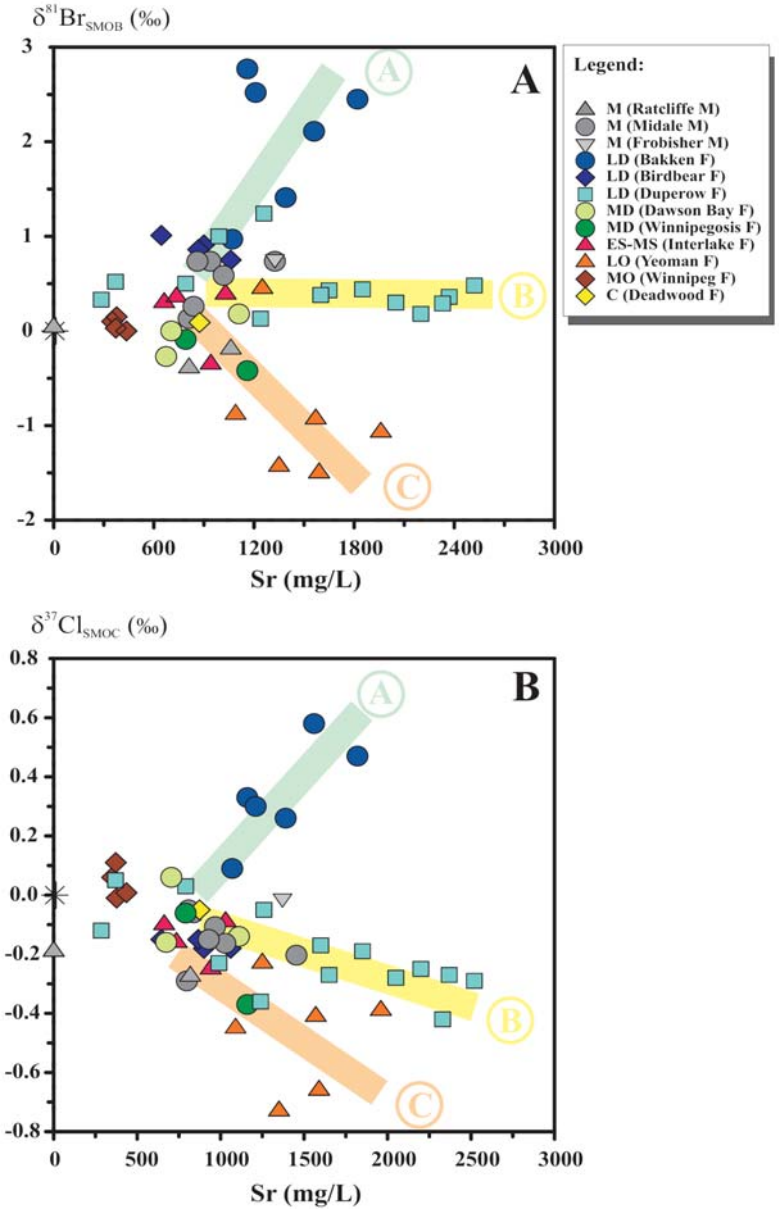

Figure 6.27 A) $\delta^{81}Br_{SMOB}$ (‰) versus Sr (mg/L) and B) $\delta^{37}Cl_{SMOC}$ (‰) versus Sr (mg/L) of the Williston Basin formation waters from the central part of the basin.

Similar to the explanation presented to explain the variation of the $^{87}Sr/^{86}Sr$ signature of the seawater (Burke et al., 1982), one can suggest that both chlorine and bromine isotopic signatures of the seawater are controlled by the input of these two elements (weathering and mantle degassing through various volcanic activities including seafloor spreading regions).

The agreement between the behaviour of Sr, Br and Cl isotopes during the Late Ordovician Period might suggest a common source. Since the contribution of mantle sources is put forward to explain the depleted $^{87}Sr/^{86}Sr$ values during the Late Ordovician, it is reasonable to suggest that the depleted $\delta^{37}Cl$ and $\delta^{81}Br$ signature of seawater at the same time period may be due to the same source (i.e. mantle sources). Several lines of evidence seem to support this suggestion. The mantle is the main reservoir of both chlorine and bromine as 98.2 % and 98.9% of these two elements in the Earth are present in the mantle (Table 1.1 and Table 1.2; Chapter 1). Rubey (1951) argued that that there is more chloride (and other elements such as sodium, magnesium and potassium) in the ocean than can be accounted for by weathering of igneous rocks in the crust. In fact, both chloride and bromide are classified as excess volatile (i.e. a constituent of seawater that cannot be accounted for by rock weathering). Volcanic eruptions are prolific sources of HCl and they are suggested to be the strongest single source of Br in the atmosphere (Graedel and Keene, 1996; Bobrowski et al., 2003; Aiuppa et al., 2005). Schilling et al. (1978) calculated that Cl and Br associated with the lithosphere formation and hotspot activity are outgassed rather than recycled. Furthermore, they reported that geological time integrated rate of Cl and Br transfer from the mantle is comparable with masses of Cl and Br in the surface reservoir. They hypothesized that the Cl and Br in surface

reservoir has accumulated throughout the geologic time by volcanic processes. They also argued that it is reasonable to assume that the rate of crustal production during the geologic time was proportional to the rate of heat production from natural radioactivity within the Earth which implies that the degassing of Cl and Br by the volcanic activities was higher (almost twice as the present). Because most of these volcanic gases are highly soluble gases they are quickly dissolved in the ocean or deposited at the surface (Brown et al., 1989; Graedel and Keene, 1996). Several isotopic studies suggested negative values of chlorine stable isotopes for mantle derived Cl materials. Due to the kinetics of isotope fractionation, the gaseous sublimation products will probably have a lower $\delta^{37}Cl$ than solid residue. For example, Eggenkamp and Schuiling (1995) reported negative chlorine isotope values of $PbCl_2$ and sal ammoniac minerals that formed from the condensation of volcanic gas compounds. Eggenkamp and Koster van Gross (1997) reported depleted chlorine isotope values (-0.8 and 0.1 ‰) of primary carbonatites. Willmore et al., (2002) explained the enriched $\delta^{37}Cl$ values of the Bushveld Complex in South Africa by few possible scenarios including the degassing of light chlorine isotopes during subduction, leaving heavy chlorine to be degassed at a deeper level that subsequently metasomatize and partially melted the mantle wedge. Subduction recycling of oceanic crust and mantle releases was suggested to be responsible for the depleted chlorine isotopic signatures reported from active (Ransom et al., 1995) and passive (Hesse et al., 2006) margins. Hesse et al. (2006) also suggested that mantle chlorine-degassing might release a dominantly isotopically depleted chlorine gas. The Late Ordovician concluded with a massive glaciation, where glaciers grew in and around the south

polar region of Gondwanaland and as the Period came to a close, the glacial event reached a climax. This lends support to the increase of the mantle contribution by limiting the continental weathering input due to the glaciation. Therefore, it is reasonable to assume that the depletion of chlorine and bromine isotopes in the Late Ordovician is due to the increase of contribution of mantle derived Cl and Br.

Although it is logical to attribute the highly enriched isotopic values found in the Bakken Formation to an increase of the continental weathering, this cannot be the only reason. The sharp rise in the Bakken Formation (Figure 6.24) is proportionally greater than the change observed for $^{87}Sr/^{86}Sr$. Furthermore, the $\delta^{37}Cl$ and $\delta^{81}Br$ signatures of the formation waters in Figure 6.27 do not fall on a perfectly straight line, which means that the isotopic variations are not due to only two end members (two input source). For example the Bakken Formation brines show larger enrichment values for bromine isotopes versus chlorine isotope values when compared to the Yeoman Formation brines. This implies that other factors played a role in this enrichment aside from the input (the different sources), such as depositional conditions.

Smith and Bustin (1998) suggested that the organic-rich (up to 35% TOC) Bakken Formation had accumulated in response to both increased productivity and enhanced preservation that resulted from unique palaeogeographic, palaeoceanographic and palaeoclimatic conditions. They proposed a pattern of estuarine-like marine circulation between the Williston Basin and open-ocean conditions at the western craton edge of North America. Surface water discharged from the basin was replaced by nutrient-rich deeper water

sourced from the equatorial undercurrent in the Pacific Basin. This nutrient-rich water enhanced the productivity and led to a high rate of organic sedimentation and the development of anoxic bottom water on the basin floor. These depositional conditions might have played a role in the isotopic enrichment of both Br and Cl isotopes by extensive biological activity. These activities could affect the bromine isotopes by a larger scale in comparison to the chlorine isotopes because of the different redox behaviour of Br (much easier to oxidize), different behaviour in biological processes (easier to incorporate in organic compounds by organisms) (Eggenkamp and Coleman, 1998). The presence of similar organic-rich deposits across the North American interior during the Late Devonian, suggests that these conditions were not restricted to the Williston Basin, but were probably worldwide. In order to explain the sharp rise of the seawater $\delta^{34}S$, Holser (1977) suggested that the brine generated by evaporite deposition was initially stored in deep areas of a Mediterranean basin like system, where the precipitation of pyrite produced highly enriched $\delta^{34}S$ brine. Later a catastrophic mixing of the brine and the surface ocean caused by the destruction of the basin that stored the highly enriched $\delta^{34}S$ brine is put forward to explain the enriched $\delta^{34}S$ distributed world-wide during this period. Therefore, a similar catastrophic scenario could be responsible for mixing the isotopically enriched water that was produced by the biological activities were lighter isotopes were preferentially removed from the water into organic matter or released as gases.

It is worth noting that both major shifts for chlorine and bromine isotopes in the Late Ordovician and Late Devonian were concurrent with two of the five major mass extinctions

on Earth. Both, the Late Ordovician and Late Devonian mass extinctions were attributed to climate condition changing and massive glacial events (Kump, 2004). Widespread anoxia has also been invoked to explain the Late Devonian mass extinction (e.g., Joachimski and Buggisch, 1993, Kump, 2004). These extinctions were accompanied with rises and dips of several isotopic signatures including ($\delta^{34}S$, $\delta^{13}C$, $^{87}Sr/^{86}Sr$, $\delta^{37}Cl$ and $\delta^{81}Br$). Although it is not conclusive, some of the isotope results suggest different environmental conditions during these two mass extinctions. This might suggest that glaciation cannot explain both events and that widespread anoxia is a more favoured explanation for the Late Devonian event.

6.9 Conclusions

The majority of the formation waters are characterized by high TDS compositions ranging between (100,000 mg/L and 550,000 mg/L). The vast majority of highly concentrated formation waters (TDS > 100,000 mg/L) are Na-type waters (Na-Cl or Na-Ca-Cl) with few exceptions that are Ca-type waters (Ca-Na-Cl or Ca-Cl).

The geochemical data examined in this study suggests that the Williston Basin formation waters are of several origins (i.e. end members) and that they are the result of various evolutionary process that include evaporation, evaporite dissolution, mixing and water-rock interaction. The proposed end members are: 1) residual paleoseawater that were highly concentrated; 2) evaporite dissolution formation waters; 3) meteoric water; and 4) seawater. Mixing between these end members along with water-rock interaction (e.g. ion exchange) are

some of the evolutionary processes that are involved in the evolution of these formation waters. Generally, all formation waters from older (deeper) stratigraphic units are highly concentrated in comparison to formation waters from younger stratigraphic units that are characterized by larger range of TDS compositions due to greater dilution effects on the younger (shallower) formations.

The $\delta^{2}H$ and $\delta^{18}O$ of the formation waters from the different stratigraphic units are characterized by large variations. The infiltration of fresh waters (e.g. precipitation and glacial melt-water) is evident, especially in the shallower formations. Brines that are characterized by enriched isotopic values are located in the central part of the basin and the brines that show isotopic depletions are normally further away from the centre of the basin.

The $\delta^{37}Cl$ and $\delta^{81}Br$ signatures of the Williston Basin formation waters show large variations in both isotopes, especially in the bromine stable isotopes. The $\delta^{81}Br$ and $\delta^{37}Cl$ signatures of the Williston Basin brines suggest the existence of several different brines that are isotopically distinct. Mixing between different types of brines was found to exist which suggest cross-formational flow or hydraulic connection. In general, halite dissolution or evaporite dissolution processes affects chlorine isotopic signatures more than the bromine isotopic signatures.

The relatively wide range of $\delta^{37}Cl$ and $\delta^{81}Br$ of the formation waters suggests that evaporated paleoseawater and halite dissolution cannot be considered as the origin of these brines, unless the ocean isotopic signatures were variable over geologic time. Although precipitation, dissolution, diffusion and ion filtration are possible mechanisms for isotopic

fractionation, they cannot be reasonable factors to cause the observed isotopic variability. The $\delta^{81}Br$ and $\delta^{37}Cl$ signatures of the formation waters present in the central part of the Williston Basin suggests multiple end members located in different stratigraphic units. A seawater temporal curve for $\delta^{81}Br$ and $\delta^{37}Cl$ was proposed, where $\delta^{81}Br$ show larger variations than $\delta^{37}Cl$. The isotopic variations of these two elements agree very well with $^{87}Sr/^{86}Sr$ seawater variation during the same period and reasonably with the seawater variation of $\delta^{34}S$.

The $^{87}Sr/^{86}Sr$ signatures of the Williston Basin formation waters fall between 0.708 and 0.722. These values confirm the marine origin of these formation waters and they show a radiogenic component in some of the samples as well.

The relationship between both $\delta^{81}Br$ and $\delta^{37}Cl$ versus Sr illustrates the presence of at least three possible paleoseawater end member that are isotopically distinct. The three end members are defined as (A) which is isotopically enriched in both isotopes ($\delta^{81}Br$ and $\delta^{37}Cl$) and located in the Bakken Formation (Late Devonian), (B) which is characterized by near zero isotopic signatures from the Duperow Formation (Middle Devonian), (C) that is isotopically depleted in both isotopes ($\delta^{81}Br$ and $\delta^{37}Cl$) and located in the Yeoman Formation (Late Ordovician). Whether the rest of the formation waters from the other stratigraphic units (e.g. Dawson Bay, Winnipegosis and Winnipeg) are also end members that happen to be isotopically similar or simply the product of mixing between these three end members is not clear from the data.

Two major sources of input for chlorine and bromine to the ocean are proposed; 1) continental weathering which is isotopically enriched and 2) mantle degassing that is isotopically depleted.

An increase of the mantle contribution of Cl and Br to the seawater and a decrease of the continental weathering input due to a glacial event was proposed to explain the isotopic dip of both δ^{81}Br and δ^{37}Cl during the Late Ordovician. On the other hand, an anoxic seawater and biological activity were proposed to explain the sharp rise in the δ^{81}Br and δ^{37}Cl values during the Late Devonian Period.

In general, this finding has very important implications in different disciplines. These two isotopes can be used in drawing preliminary conclusions about the origin and the evolutionary processes involved in evolving formation waters and also to distinguish different brines (end members). Further, they can also be employed in assessing hydrogeological dynamic of sedimentary basins in different studies (e.g. nuclear waste storage and petroleum exploration). They can be used as "fingerprinting" tools in investigating mine leakage issues and mixing scenarios. Moreover, they might aid in understanding and resolving some of the scientific controversies in the earth's history.

CHAPTER 7

SUMMARY

This thesis consists of two parts: a technical part comprising of chapters two and three, and an application part in chapters four, five and six.

7.1 Analytical Advances

Two new analytical methodologies were developed based on the Continuous Flow (CF) technology by means of Isotope Ratio Mass Spectrometry (IRMS). The CF-IRMS was coupled with a GC system and an autosampler in order to combine both online separation and mass spectrometric analysis in one automated step. The analyses in these two methodologies were carried out on halide gases (methyl chloride and methyl bromide) and showed excellent results (chapters 2 and 3). These analytical methodologies are much faster (16 minutes) than the classical off-line techniques and allow smaller sample sizes; they are also more cost-effective.

The first methodology involved the analysis of chlorine stable isotopes in water samples. This new technique uses samples as small as 0.2 mg of AgCl (1.4 μmol of Cl^-). The internal precision using pure CH_3Cl gas is less than ±0.04 ‰ (±STDV). The external precision using

seawater standard is less than ±0.07 ‰ (±STDV) for n = 12. This precision is better than that achieved by any previous methods.

The second methodology was developed for bromine stable isotope in waters. The bromine stable isotope analysis by CF-IRMS technology gave excellent results with high precision. The internal precision using pure CH_3Br gas is better than ±0.03 ‰ (±STDV); the external precision with the seawater standard used at Waterloo is better than ±0.06 ‰ (±STDV) for *n* = 12. This new technique measures samples as small as 0.2 mg of AgBr (1 μmol of Br^-). The precision is very important when dealing with small variations in isotopic range and the small size requirement is highly important for samples with very low concentrations of bromide.

The bromine stable isotope values obtained during the development of this methodology extended the known range of isotopic variation of stable bromine isotopes and showed promising results that lead to the further investigation of bromine isotopes in various sedimentary environments as illustrated in chapters four, five and six. The CF-IRMS methodologies developed during the course of this thesis will enhance the application of both chlorine and bromine stable isotope in more research areas and will allow the use of this analysis in studies where chlorine and bromine contents are small and precision is important.

7.2 The Evaluation of Chlorine and Bromine Isotopes in Sedimentary Basins

The analytical methodologies developed during this thesis were employed to determine $\delta^{37}Cl$ and $\delta^{81}Br$ isotopic signatures in three sedimentary environments (the southern Ontario and

Michigan Paleozoic sedimentary sequences, the Siberian Platform and the Williston Basin). The results obtained from the bromine stable isotopes analysis demonstrated a range between -1.50 ‰ and +3.35 ‰ relative to SMOB. This range extended the isotopic variation of bromine isotopes reported for formation water in the literature.

The $\delta^{37}Cl$ and $\delta^{81}Br$ values of the brines from the Middle Silurian carbonate sequence of Michigan and southern Ontario and brines from the Lower Silurian sandstone formations of the Appalachian basin are very distinct. The brines from the Lower Silurian sandstone formations are enriched in both isotopes relative to the brines from the Middle Silurian carbonate formations. Similarly, the brines collected from the Ordovician formations illustrated different $\delta^{37}Cl$ and $\delta^{81}Br$ signatures. In both cases (Ordovician and Silurian) formation waters from the central areas of the Michigan Basin are characterized by more depleted isotopic signature in comparison with the formation waters from the marginal areas. This indicates that the formation waters in these stratigraphic units are either of different origins or they experienced different evolutionary processes and/or mixed with different intrusive or allochthonous fluids that altered their isotopic signatures during mixing.

The projection of Cl and Br composition on the seawater evaporation line (Figure 4.7) suggests that the origin of these brines is evaporated paleoseawaters. However, dilution with less saline waters (e.g. seawater and/or freshwater) is also evident. The contribution of halite dissolution is minor and it is restricted to marginal areas. Generally, the degree of dilution and halite impact increases with distance from the central part of the basin and towards the

marginal areas. As well, the $\delta^{2}H$ and $\delta^{18}O$ compositions of these fluids confirms the proposed end member and mixing scenarios as was concluded from the geochemical data.

Although the chemical parameters and also the $\delta^{18}O$ and $\delta^{2}H$ show some similarities and overlaps between various samples, the $\delta^{37}Cl$ and $\delta^{81}Br$ shows some distinctive differences between the samples from northwest of the Algonquin Arch and those from southeast of the Algonquin Arch. All of the brines collected from the northwest of the Algonquin Arch are characterized by depleted isotopic values in comparison with the isotopic values from the brines collected from southeast of the Arch. The $\delta^{81}Br$ signatures of the two brines show a complete separation in isotopic signatures with no overlaps or mixing, unlike the $\delta^{37}Cl$ values that show some overlap between the two groups. One of the scenarios that can be put forward is that the Arch forms a water divide, where sediments southeast of the Arch are dominated by Appalachian Basin formation waters, and the sediments located northwest of the Arch are dominated by the Michigan Basin formation waters. The fact that formation waters from either side of the Arch are isotopically (^{37}Cl and ^{81}Br) distinct strongly suggests that the evolutionary processes that affected the waters are very different, which is in agreement with previous studies that investigated geochemistry and origin of natural gases in southern Ontario (Barker and Pollock, 1984) and suggested that natural gas formation and accumulation in the two basins (Appalachian and Michigan) proceeded under different conditions and sources. Further in-depth investigation and understanding of the behaviour of these isotopes under different conditions are necessary to answer that question and to better understand the system.

The Siberian Platform formation waters were classified into four different groups based on their chemical compositions. The two main water types found are Ca-Cl and Na-Cl type waters. The $\delta^{37}Cl$ and $\delta^{81}Br$ values of the Ca-Cl type brines range between -0.67 ‰ and +0.04 ‰; and between -0.31 ‰ and +0.27 ‰, respectively. These brines are from depths below 1000 m and characterized by high TDS (> 300,000 mg/L). Their $\delta^{2}H$ versus $\delta^{18}O$ values of this group of samples range between -78 ‰ and -31 ‰ and between -10.9 ‰ and +1.8 ‰, respectively. Based on their chemical composition and isotopic signatures, it is postulated that they are residual brines of evaporated paleoseawaters.

The $\delta^{37}Cl$ and $\delta^{81}Br$ values of the Na-Cl type fluids range between -0.25 ‰ and +1.54 ‰ and between -0.25 ‰ and +0.17 ‰, respectively. These waters occur at shallower depths (0–1000 m) and their TDS values range between 44,000 mg/L and 242,000 mg/L. The $\delta^{2}H$ versus $\delta^{18}O$ values of this group of samples range between -152 ‰ and -94 ‰ and between -20 ‰ and -0.5 ‰, respectively. The chemical and isotopic data indicate that these samples are derived from halite dissolution, most likely as a result of recharge in a colder climate, possibly Pleistocene derived water.

The $\delta^{37}Cl$ and $\delta^{81}Br$ values of the third group of waters range between -0.40 ‰ and +1.30 ‰ and between -0.40 ‰ and +0.56 ‰, respectively. The waters of this group are characterized by Na–Ca–Cl and Na–Cl type waters. These samples were collected from various depths ranging from 100 to 2100 metres. They are characterized by high TDS values between 32,000 mg/L and 286,000 mg/L and their $\delta^{2}H$ and $\delta^{18}O$ values range between -140 ‰ and -89 ‰ and between -17.1‰ and -9.3 ‰, respectively. The chemical compositions and

isotopic signatures did not show any obvious trends that could lead to a definite brine source. However, the available data suggest that these samples were produced via a number of scenarios that involved several end members such as meteoric water, evaporated paleoseawater brines, and also some geochemical evolutionary processes such as mixing, halite dissolution, biological activities and/or ion filtration.

The Archaean–Proterozoic crystalline brines were found to have $\delta^{37}Cl$ values that range between -0.67 ‰ and -0.16 ‰ and $\delta^{81}Br$ values that range between -0.31 ‰ and 0 ‰, while the Early Cambrian sedimentary brines have $\delta^{37}Cl$ values that range between -0.53 ‰ and +0.04 ‰ and $\delta^{81}Br$ values range between -0.11 ‰ and +0.27 ‰. The variation of Br stable isotopes observed in this study can imply two things: (1) different water types may have different Br stable isotope signatures, i.e., they are originally different, and (2) different geochemical processes may affect the Br stable isotopes of the waters differently and cause significant fractionations.

Generally, larger isotopic variations are observed in shallower samples, which is also consistent with samples from the southern Ontario Paleozoic sequences. This suggests that surficial processes could be responsible for isotopic fractionations that led to these larger variations. The $\delta^{81}Br$ and $\delta^{37}Cl$ signatures of the brines from the various sedimentary sequences investigated in this study including the Siberian Platform revealed a general positive trend between $\delta^{81}Br$ and $\delta^{37}Cl$ values, where an enrichment of $\delta^{81}Br$ is coupled by an enrichment of $\delta^{37}Cl$. This is also observed in the formation waters from the southern Ontario Paleozoic sequences and the Williston Basin.

The relationship between both $\delta^{81}Br$ and $\delta^{37}Cl$ versus Sr of the Williston Basin showed that at least three evaporated paleoseawater end members that are isotopically distinct are present in the Williston Basin. The three end members are: A) isotopically enriched in both isotopes ($\delta^{81}Br$ and $\delta^{37}Cl$) and located in the Bakken Formation; B) characterized by near zero isotopic signatures from the Duperow Formation; and C) isotopically depleted in both isotopes ($\delta^{81}Br$ and $\delta^{37}Cl$) and located in the Yeoman Formation. Whether the rest of the formation waters from the other stratigraphic units (e.g. Dawson Bay, Winnipegosis and Winnipeg) are also end members that happen to be isotopically similar or simply the product of mixing between these three end members is not clear from the data.

The geochemical data examined in this study suggests that the Williston Basin formation waters are of several origins (i.e. end members) and that they are the result of various evolutionary processes that include evaporation, evaporite dissolution, mixing and water-rock interaction. The proposed end members are: 1) residual evaporated; 2) evaporite dissolution formation waters; 3) meteoric water; and 4) seawater. Mixing between these end members along with water-rock interaction (e.g. ion exchange) are some of the evolutionary processes that are involved in the evolution of these formation waters. The enriched $\delta^{18}O$ of these formation waters is an indication of an elevated temperature water-rock interaction. The infiltration of fresh waters (e.g. precipitation and glacial melt-water) is also evident by the $\delta^{2}H$ and $\delta^{18}O$ values.

Unless the ocean isotopic signatures were variable over geologic time, it is difficult to explain the relatively wide ranges of $\delta^{37}Cl$ and $\delta^{81}Br$ of the formation waters found in the

Williston Basin. Although precipitation, dissolution, diffusion and ion filtration are possible mechanisms for isotopic fractionation, they are not reasonable factors to cause the observed ranges. The $\delta^{81}Br$ and $\delta^{37}Cl$ signatures of the formation waters found in the central part of the Williston Basin showed that several end members are present in different stratigraphic units. Based on the findings of this study, a seawater temporal curve for $\delta^{81}Br$ and $\delta^{37}Cl$ was proposed with more pronounced variation of $\delta^{81}Br$ observed in comparison to the variation of $\delta^{37}Cl$. The isotopic variations of these two elements agree very well with $^{87}Sr/^{86}Sr$ seawater variation during the same period and agree reasonably with the seawater variation of the $\delta^{34}S$.

Two major sources of input for chlorine and bromine to the ocean are proposed: 1) continental weathering (isotopically enriched) and 2) mantle sources (isotopically depleted). An increase of the mantle contribution of Cl and Br to the seawater and a decrease of the continental weathering input due to a glacial event was proposed to explain the isotopic dip of both $\delta^{81}Br$ and $\delta^{37}Cl$ during the Late Ordovician. On the other hand, an anoxic seawater and biological activity were proposed to explain the sharp rise in the $\delta^{81}Br$ and $\delta^{37}Cl$ values during the Late Devonian Period.

In general, this new range of isotopic variation of bromine stable isotopes has very important implications in different disciplines. The of bromine and chlorine stable isotopes can be useful in drawing preliminary conclusions about the origin and the evolutionary processes involved in evolving formation waters and also in distinguishing different brines (end members). This will consequently help improve our understanding of the hydrogeological behaviour of sedimentary basins and crystalline shield areas as well. This

knowledge can be very crucial in assessing the hydrogeological dynamic and the hydraulic connection between different geological units in sedimentary basins, and, accordingly, its application in various diverse fields such as nuclear waste storage and petroleum exploration. They can be also employed in as "fingerprinting" tools in mine leakage investigations. Furthermore, they can be useful in studying mixing scenarios and determining mixing ratios. Moreover, they might aid in understanding and resolving some of the scientific controversies in the earth's history.

7.3 Recommendations

Based on the outcome results of this thesis, it is important to further investigate and examine the systematic of Br stable isotopes in nature and during geochemical and physical processes which might unfold broad applications of these isotopes in various disciplines. A number of experiments are needed in order to understand the behaviour of bromine stable isotopes during different chemical and physical process. The following list provides a number of recommended experiments that should be considered and carried out in rder to understand their effect on bromine stable isotopes:

1. The effect of evaporation.
2. The effect of dissolution and precipitation of various evaporites, especially halite.
3. The effect of diffusion.

4. The effect of ion filtration.
5. The effect of water-rock interaction on both formation waters and host rock.
6. The effect of freezing.
7. The effect of oxidation and reduction reactions.

It is also necessary to investigate the bromine stable isotope compositions from various different natural materials such as different types of rocks and minerals and also waters from different environments such as near volcanic sites, subduction zones, Sabkhat and wetlands. It is also recommended to explore the bromine stable isotopes in natural and synthetic organic compounds.

REFERENCES

Ahern, J.L. and Mrkvicka, S.R., 1984. A mechanical and thermal model for the evolution of the Williston Basin. Tectonics. vol. 3, no.1, 79-102.

Alexeev, S.V., 2000. The cryogenesis of groundwater and rocks as exemplified by the Daldyn-Alakit region of Western Yakutia. Novosibirsk, Publ. SPC UIGGM SB RAS, 119pp.

Alexeev, S.V. and Alexeeva, L.P., 2002. Ground ice in the sedimentary rocks and kimberlites of Yakutia, Russia. Permafrost Periglacial Proc. 13, 53–59.

Alexeev, S.V. and Alexeeva, L.P., 2003. Hydrogeochemistry of the permafrost zone in the central part of the Yakutian diamond bearing province, Russia. Hydrogeology Journal. vol. 11, 574–581.

Aiuppa, A., Federico, C., Franco, A., Giudice, G., Gurrieri, S., Inguaggiato, S., Liuzzo, M., McGonigle, A.J.S. and Valenza, M. 2005. Emission of bromine and iodine from Mount Etna volcano. Geochemistry Geophysics Geosystems G^3. vol. 6, no. 8, 1-8.

Anders, E. and Ebihara, M., 1982. Solar-system abundances of the elements. Geochimica et Comochimica Acta. vol. 46, 2363-2380.

Anna, L.O, 1986. Geologic framework of the ground-water system in Jurassic and Cretaceous rocks in the Northern Great Plains, in parts of Montana, North Dakota, South Dakota and Wyoming – Regional Aquifer-System Analysis. U.S. Geological Survey Professional Paper 1402-B. 35pp.

Armstrong, S.C., Sturchio, N.C., and Hendry, M.J., 1998. Strontium isotopic evidence on the chemical evolution of pore waters in the Milk River aquifer, Alberta, Canada. Applied Geochemistry. vol. 13, 463-475.

Arneth, J.-D., 1984. Stable isotope and orgao-geochemical studies on Phanerozoic sediments of the Williston Basin, North America. Isotope Geoscience. vol. 2, 113-140.

Aston, F.W., 1919. The constitution of elements. Nature. vol. 104, 393.

Aston, F.W., 1920. The mass-spectra of chemical elements (Part 2). Philosophical Magazine. vol. 40, 628-634.

Bachu, S. and Hitchon, B., 1996. Regional-scale flow of formation waters in the Williston Basin, American Association of Petroleum Geologists Bulletin. vol. 80, 248-264.

Balobaev, V.T., Pavlov, A.V. and Perlshtein, G.Z., 1983. Thermal–physical researches of cryolithozone of Siberia. Nauka, Novosibirsk, 22–34. (in Russian).

Banks, D. A., Green, R., Cliff, R. A. and Yardley, B. W. D., 2000. Chlorine isotopes in fluid inclusions: Determination of the origins of salinity in magmatic fluids. Geochimica et Cosmochimica Acta. vol. 64, No. 10, 1785-1789.

Barker, J.F. and S. J. Pollock, S.J., 1984. The Geochemistry and Origin of Natural Gases in southern Ontario. Bulletin of Canadian Petroleum Geology. vol. 32, No. 3, 313-326.

Bassett, D., Chetland, J., Kyte, A. B., Marsdon, H. M., Roberts, P. N., Summers, W. N., Watkins, D. and Wylde, L. E., 1988. Introductory Review. In: Bromine Compounds, Chemistry and Applications; Price, D., Iddon, B. and Wakefield, B. J., (Eds.). Elsevier, Amsterdam. 1-120.

Begley, I. S. and Scrimgeour, C. M., 1996. On-line reduction of H_2O for δ^2H and $\delta^{18}O$ measurement by continuous-flow isotope ratio mass spectrometry. Rapid Communications in Mass Spectrometry. vol. 10, 969-973.

Beneteau, K. M., Aravena, R., Frape, S. K., 1999. Isotopic characterization of chlorinated solvents – laboratory and field results. Organic Geochemistry. vol. 30, 739-753.

Benn, A.A., and Rostron, B.J., 1998. Regional hydrochemistry of Cambrian to Devonian aquifers in the Williston Basin, Canada–U.S.A. In: Christopher, J.E., Gilboy, C.E, Paterson, D.F., Bend, S.L. (Eds.), Eighth International Williston Basin Symposium. Saskatchewan Geological Society, Regina. vol. 13, 238-246.

Berner, E.K. and Berner, R.A., 1987. The Global Water Cycle: Geochemistry and Environment. Prentice Hall, Englewood Cliffs, New Jersey. 397 pp.

Berry, F.A.F, 1969. Relative factors influencing membrane filtration effects in geologic environments. Chemical geology. vol. 4, 295-301.

Blewett, J. P., 1936. Mass spectrograph analysis of bromine. Physical Review. vol. 49, 900-903.

Bloom, Y., Aravena, R., Hunkeler, D., Edwards, E. and Frape, S. K., 2000. Carbon isotope fractionation during microbial dechlorination of trichloroethene, cis-1,2-dichloroethene, and vinyl chloride: implications for assessment of natural attenuation. Journal of Environmental Science and Technology, vol. 34, 2768-2772.

Bobrowski, N., Hönninger, G., Galle, B., and Platt, U., 2003, Detection of bromine monoxide from a volcanic plume, Nature. vol. 423, 273-276.

Böhlke, J.K., Sturchio, N.C., Gu, B., Horita, J., Brown, G.M., Jackson, W.A., Batista, J. and Hatzinger, P.B., 2005. Perchlorate isotope forensics. Analytical Chemistry, vol. 77, 7838-7842.

Bolton, T.E., 1957. Silurian Stratigraphy and paleontology of the Niagara Escarpment in Ontario; Geological Survey of Canada, Memoir 289, 145pp.

Bond, G.C. and Kominz, M.A., 1984. Construction of tectonic subsidence curves for the early Paleozoic miogeocline, southern Canadian Rocky Mountains– implications for

subsidence mechanisms, age of breakup and crustal thinning. Geological Society of America Bulletin. vol. 95, 155-173.

Bonifacie, M., Charlou, J.L., Jendrzejewski, N., Aginier, P. and Donval, J.P., 2005. Chlorine isotopic compositions of high temperature hydrothermal vent fluids over ridge axes. Chemical Geology. vol. 221, 279-288.

Bonifacie, M., Jendrzejewski, N., Agriner, P., Coleman, M. and Javoy, M., 2006. The global chlorine cycle: Cl isotope constraints. In: Goldschmidt Conference Abstracts 2006. Geochimica et Comochimica Acta. A78.

Borisov, V.N., 1976. Underground chemical discharge in the central part of the Tungussky artesian basin. In: Proceddings of the VIII Conference of Ground Water Siberia and Far East. Irkutsk-Ulan-Dde. 100-101.

Brand WA., 1996. High precision isotope ratio monitoring techniques in mass spectrometry. Journal of Mass Spectrometry. vol. 31, 225-235.

Braitsch, O. and Hermann, A.G., 1963. Zur Geochemie des broms in salinaren sedimenten. Teil I: Experimentelle bestimmung der Br-verteilung in verschiedenen natürlichen salzsystemen. Geochimica et Cosmochimica Acta. vol. 27, 361-391.

Bredehoeft, J.D., Blyth, C.R., White, W.A. and Maxey, G.B., 1963. Possible mechanism for concentration of brines in subsurface formations. American Association of Petroleum Geologists Bulletin. vol. 47, 257-269.

Brown, D. and Brown, D., 1987. Wrench style deformation and paleostructural influence on sedimentation in and around a cratonic basin. In: Longman, M., (Ed.), Williston Basin - Anatomy of a cratonic oil province, Rocky Mountain Association of Geologists, 57-70.

Brown, J., Colling, A, Park, D., Phillips, J., Rothery, D. and Wright, J., 1989. Seawater: Its composition, properties and behavior In: Bearman, G. (ed.). The Open University, S330, vol. 2. Pergamon Press. 165pp.

Budai, J.M. and Wilson, J.L., 1991. Diagenetic history of the Trenton and Black River Formations in the Michigan Basin. In: Catacosinos, P.A. and Daiels, P.A., Jr., (eds.); Early sedimentary evolution of the Michigan Basin: Geological Society of America Special Paper 256, 73-88.

Burke, W.H., Denison, R.E., Hetherington, E.A., Koepnick, R.B., Nelson, H.F. and Otto, J.B., 1982. Variation of seawater $^{87}Sr/^{86}Sr$ throughout Phanerozoic time. Geology. vol. 10, 516-519.

Busby, J.F., Kimball, B.A., Downey, J.S. and Peter, K.D., 1995. Geochemistry of water in aquifers and confining units of the Northern Great Plains in parts of Montana, North Dakota, South Dakota, and Wyoming – Regional Aquifer-System Analysis. U.S. Geological Survey Professional Paper 1402-F. 146pp.

Cameron, A. E. and Lippet, E. L., Jr., 1955. Isotopic composition of bromine in nature. vol. 121, 136-137.

Campbell, D.J., 1985. Fractionation of stable chlorine isotopes during transport through semipermeable membranes. Master thesis, The University of Arizona, AZ, USA. 103pp.

Carlson, C.G. and Eastwood, W.P., 1962. Upper Ordovician and Silurian rocks of North Dakota. North Dakota Geological Survey Bulletin. vol. 38, 52pp.

Carpenter, A.B., 1978. Origin and chemical evolution of brines in sedimentary basins. Oklahoma Geological Survey Circular. vol. 79, 60-77.

Carpenter, A.B. and Trout, M., 1978. Geochemistry of bromide-rich brines of the Dead Sea and southern Arkansas. Oklahoma Geological Survey Circular. vol. 79, 78-88.

Carter, T.R., Trevail, R.A. and Easton, R.M., 1996. Basement controls on some hydrocarbon traps in southern Ontario, Canada. In: Pluijm, B. A. and Catacosinos, P.A. (eds.); Basement and basins of North America. Geol. Soc. America Spec. Paper 308, 95-107.

Catanzaro, E.J., Murphy, T.J., Garner, E.L. and Shields, W.R., 1964. Absolute isotopic abundance ratio and the atomic weight of bromine. Journal of Research of Natural Bureau of Standards, Section A. vol. 68A, 593-599.

Cercone, K.R., 1988. Evapourative sea-level drawdown in the Silurian Michigan basin. Geology. vol. 16, 387-390.

Chebotarev, I.I., 1955. Metamorphism of natural waters in the crust of weathering - part 3. Geochimica et Cosmochimica Acta. vol. 8, 198-212.

Chester, R., 2000. Marine Geochemistry, 2nd Edition. Blackwell Science, Oxford.

Chipley, D. and Kyser, T.K., 1991. Large scale fluid movement in the Western Canadian Sedimentary Basin as recorded by fluid inclusions in evaporites. In: Christopher, J.E. and Haidl, F.M. (Eds.), Sixth International Williston Basin Symposium, (Saskatchewan Geological Society, Regina, Saskatchewan), 265-269.

Clark, I. and Fritz, P., 1997. Environmental Isotopes in Hydrogeology. CRC Press, Boca Raton, FL. 328pp.

Claypool, G.E., Holser, W.T., Kaplan, I.R., Sakai, H., and Zak., I., 1972. Sulfur and oxygen isotope geochemistry of evaporite sulfates. Geological Society of America. vol. 4, 473.

Claypool G.E., Holser W.T., Kaplan I.R., Sakai H. and Zak I., 1980. The age curves of sulfur and oxygen isotopes in marine sulfate and their mutual interpretation. Chemical Geology. vol. 28, 199-260.

Clayton R.N., Friedman I., Graf D.L., Mayeda T.K., Meets W.F., and Shimp N.F., 1966. The origin of saline formation waters: I. Isotopic composition. J. Geophys. Res. vol. 71, 3869-3882.

Cloutier, V., 1994. Stable isotopes of chlorine as indicators of the source and migrational paths of the solutes within glacial deposits and bedrock formations, Lambton County, southwestern Ontario. MSc thesis, University of Waterloo, Waterloo, Ontario, Canada. 131pp.

Coleman, M.L., Ader, M., Chaudhuri, S. and Coates, J.D., 2003. Microbial isotopic fractionation of perchlorate chlorine. Applied Environmental Microbiology. vol. 69, 4997-5000.

Coleman, M.L., Eggenkamp, H.G.M. and Aranyossy, J.F., 2001. Chlorine stable isotope characterization of solute transport in mudrocks, ANDRA. Actes des Jounées Scientifique: EDP Sciences, France, 155-175.

Coleman, M.L., Shepherd, T.J., Durham, J.J., Rouse, J.E. and Moore, G.R., 1982. Reduction of water with Zinc for hydrogen isotope analysis. Analytical Chemistry, vol. 54, 993-995.

Collins, A.G., 1975. Geochemistry of oilfield brines: Elsevier Scientific Publishing Company, Amsterdam, 496pp.

Coniglio, M., Zheng, Q. and Carter, T.R., 2003. Dolomitization and recrystallization of middle Silurian reefs and platformal carbonates of the Guelph Formation, Michigan Basin, southwestern Ontario. Bulletin of Canadian Petroleum Geology. vol. 51, No. 2, 177-199.

Connolly C.A., Walter L.M., Baadsgaard H., and Longstaffe F.J., 1990. Origin and evolution of formation waters, Alberta Basin, Western Canada Sedimentary Basin: II. Isotope systematics and fluid mixing. Applied Geochemistry. vol. 5, 397-413.

CRC Handbook of Chemistry and Physics, 2005. Lide, D.R., (ed.), Norman E. Holden in CRC Handbook of Chemistry and Physics, 85th Edition, online version. CRC Press. Boca Raton, Florida (2005). Section 11, Table of the Isotopes.

Curie, I., 1921. Sur le poids atomique du chloe dans quelques minéraux. CR Acad Sci (Paris). vol. 172, 1025-1028.

Das, N., Horita, J. And Holland, H. D., 1990. Chemistry of fluid inclusions in halite from the Salina Group of the Michigan Basin: Implications for Late Silurian seawater and the origin of sedimentary brines. Geochimica et Cosmochimica Acta. vol. 54, 319-327.

Davis S.N., 1964. The chemistry of saline waters by R. A. Krieger. Discussion. Ground Water. vol. 2, 51.

Davisson, M.L. and Criss, R.E., 1996. Na–Ca–Cl relations in basinal fluids. Geochimica et Cosmochimica Acta. vol. 60, 2743-2752.

Dechan, M., 1886. Detection and estimation of iodine, bromine and chlorine. Journal of Chemical Society. vol. 49, 682-685.

De Laeter, J.R., Böhlke, J.K., De Bièvre, P., Hidaka, H., Peiser, H.S., Rosman, K.J.R. and Taylor, P.D.P., 2003. Atomic weights of the elements: Review 2000 (**IUPAC** Technical Report). International Union of Pure and Applied Chemistry – Inorganic Chemistry

Division Commission on Isotopic Abundances and Atomic Weights. Pure Applied Chemistry. vol. 75, No. 6, 683-800.

Desaulniers, D.E., Kaufmann, R.S., Cherry, J.A., and Bentley, H.W., 1986. ^{37}Cl-^{35}Cl variations in a diffusion-controlled groundwater system. Geochimimica Cosmochimica Acta. vol. 50, 1757-1764.

Dollar, P.S., 1988. Geochemistry of formation waters, southwestern Ontario, Canada and southern Michigan, U.S.A. – Implications for origin and evolution. MSc thesis. University of Waterloo, Waterloo, Ontario, Canada. 129pp.

Dollar, P.S., Frape, S.K. and McNutt, R.H., 1991. Geochemistry of Formation Waters, Southwestern Ontario, Canada and Southern Michigan U.S.A.: Implications for Origin and Evolution, Ontario Geoscience Research Grant Program, Grant No. 249; Ontario Geological Survey, Open File Report 5743, 72pp.

Downey, J.S. 1984. Hydrodynamics of the Williston Basin in the northern Great Plains. In: Jorgensen, D.G., Signor, D.C. (eds.,); Geohydrology of the Dakota Aquifer (Proceedings of the first C.V. Theis Conferences on the Geohydrology, Lincoln, Nebraska). The National Water Well Association, Ohio. 93-98.

Downey, J.S. 1986, Geohydrology of bedrock aquifers in the Northern Great Plains in parts of Montana, North Dakota, South Dakota, and Wyoming - Regional Aquifer-System Analysis. U.S. Geological Survey Professional Paper 1402-E. 87pp.

Downey, J.S. and Dinwiddie, G.A., 1988. The regional aquifer system underlying the Northern Great Plains in parts of Montana, North Dakota, South Dakota and Wyoming-Summary – Regional Aquifer-System Analysis. U.S. Geological Survey Professional Paper 1402-A. 63pp.

Downs, A. J. and Adams, C. J., 1975. The Chemistry of Chlorine, Bromine, Iodine, and Astatine, Pergamon Press. Great Britain. 1594pp.

Drenzek, N. J., Tarr, C. H., Eglinton, T. I., Heraty, L. J., Sturchio, N. C., Shiner, V. J. and Reddy, C. M. 2002. Stable chlorine and carbon isotopic compositions of selected semi-volatile organochlorine compounds. Organic Geochemistry. vol. 33, 437-444.

Drever, J.I., 1988. The Geochemistry of Natural waters. Prentice Hall, Inc., Englewood Clifs, New Jersey, USA. 437pp.

Drimmie, R. J. and Frape, S. K., 1996. Stable Chlorine Isotopes in Sediment Pore Waters of Lake Ontario and Lake Erie. In: Proceedings of a Symposium on Isotopes in Water Resources Management, vol. 1, IAEA: Vienna (IAEA-SM-366/17), 141-155.

Eastoe, C.J. and Guilbert, J.M., 1992. Stable chlorine isotopes in hydrothermal processes. Geochimica et Cosmochimica Acta. vol. 56, 4247-4255.

Eastoe, C. J., Guilbert J. M. and Kaufmann, R. S., 1989. Preliminary evidence for fractionation of stable chlorine isotopes in ore-forming hydrothermal systems. Geology. vol. 17, 285-288.

Eastoe, C.J., Long, A., Land, L.S. and Kyle, J.R., 2001. Stable chlorine isotopes in halite and brine from the Gulf Coast Basin: Brine genesis and evolution. Chemical Geology. vol. 176, 343-360.

Eastoe, C.J., Long, A. and Knauth, L.P., 1999. Stable chlorine isotopes in the Palo Duro Basin, Texas: Evidence for preservation of Permian evaporite brines. Geochimica et Cosmochimica Acta. vol. 63, 1375-1382.

Eastoe, C.J. and Peryt, T., 1999. Multiple sources of chloride in Badenian evaporites, Carpathian Mountains: Stable chlorine isotope evidence. Terra Nova. vol. 11, 118-123.

Eastoe, C.J., Peryt, T.M., Petrychenko, O. Y. and Geisler-Cussey, D., 2007. Stable chlorine isotopes in Phanerozoic evaporites. Applied Geochemistry. vol. 22, 575-588.

Eberts, S. M. and George, L. L. 2000. Regional ground-water flow and geochemistry in the midwestern basins and arches aquifer system in parts of Indiana, Ohio, Michigan, and Illinois. In: Regional Aquifer-System Analysis—Midwestern Basins and Arches. US Geological Survey Professional Paper 1423-C. 103pp.

Edie, R.W., 1958. Mississippian Sedimentation and oil fields in south-eastern Saskatchewan. American Association of Petroleum Geologists Bulletin. vol. 42, no. 1, 94-126.

Edie, R.W., 1959. Middle Devonian sedimentation and oil possibilities, central Saskatchewan, Canada. American Association of Petroleum Geologists Bulletin. vol. 43, no. 5, 1026-1057.

Eggenkamp, H.G.M., 1994. The geochemistry of chlorine isotopes. Ph.D. Thesis. University of Utrecht, The Netherlands. 150pp.

Eggenkamp, H.G.M. and Coleman, M.L., 1998. Heterogeneity of formation waters within and between oil fields by halogen isotopes. In: Arehart, G.B. and Hulston, J.R. (eds.,); 9th International Symposium on Water-Rock Interaction, New Zealand. Balkema, Rotterdam. 309-312.

Eggenkamp, H.G.M. and Coleman, M.L., 2000. Rediscovery of classical methods and their application to the measurement of stable bromine isotopes in natural samples. Chemical Geology. vol. 167, 393-402.

Eggenkamp, H.G.M., and Koster van Groos, A.F., 1997. Chlorine stable isotopes in carbonatites: evidence for isotopic heterogeneity in the mantle. Chemical Geology. vol. 140, 137-143.

Eggenkamp, H.G.M., Kreulen, R. and Koster van Groos, A.F., 1995. Chlorine stable isotope fractionation in evapourates. Geochimica et Cosmochimica Acta. vol. 59, 5169-5175.

Eggenkamp, H.G.M. and Schuiling, R.D., 1995. $\delta^{37}Cl$ variations in selected minerals; a possible tool for exploration. Journal of Geochemical Exploration. vol. 55, 249-255.

Environmental Chemistry: (http://environmentalchemistry.com/yogi/chemistry/)

Epstein, S. and Mayeda, T.K., 1953. Variation of the ^{18}O content of waters from natural sources. Geochimica et Cosmochimica Acta. vol. 4, 213-224.

Farquhar, R.M., Haynes, S.J., Mostaghel, M.A., Tworo, A.G., Macqueen, R.W. and Fletcher, I.R., 1987. Lead isotope ratios in Niagara Escarpment rocks and galenas: implications for primary and secondary sulphide deposition. Can. J. Earth Sci. vol. 24, 1625-1633.

Fisher, D.W., 1954. Stratigraphy of the Medinan Group, New York and Ontario; Bulletin of the American Association of Petroleum Geologist, vol. 38, 1979-1996.

Fisher, J.H., and Barratt, M.W., 1985. Exploration in Ordovician of central Michigan Basin. Bulletin of the American Association of Petroleum Geologist, vol. 69, 2065-2076.

Fox, J.S. and Videtich, P.E., 1997. Revised estimate of $\delta^{34}S$ for marine sulfates from the Upper Ordovician: data from the Williston Basin, North Dakota, U.S.A. Applied Geochemistry. vol. 12, 97-103.

Frape, S.K., Blyth, A., Blomqvist, R., McNutt, R.H. andGascoyne, M., 2004. Deep Fluids in the continents; II. Crystalline Rocks. In: Drever, J.I. (Ed.), Surface and Ground Water, Weathering and Soils. In: Treatise on Geochemistry, vol. 5. Elsevier, 541-580.

Frape, S. K., Bryant, G., Blomqvist, R. and Ruskeeniemi, T., 1996. Evidence from Stable Chlorine Isotopes for Multiple Sources of Chloride in Groundwaters from Crystalline Shield Environments. In: Proceedings of a Symposium on Isotopes in Water Resources Management, vol. 1, IAEA: Vienna (IAEA-SM-336/24), 19-31.

Frape, S.K., Shouakar-Stash, O., Pačes, T. and Stotler, R., 2007. Geochemical and isotopic characteristics of the waters from crystalline and sedimentary structures of the Bohemian Massif. In: Bullen, T. (ed.,); 12th International Symposium on Water Rock Interaction. vol. 1, 727-733.

Freeze, A. and Cherry, J., 1979. Groundwater, Prentice Hall, Inc., Englewood Cliffs, NJ. 604pp.

Friedheim, C., Meyer, R. J., 1892. Über die quantitative Trennung und Bestimmung von Chlor, Brom und Jod. Z. Anorg. Chemie. vol. 1, 407–422.

Fritz, P. and Frape, S.K., 1982. Saline groundwaters in the Canadian Shield – A first overview. Chemical Geology. vol. 36, 179-190.

Fritz, S.J. and Marine, I.W., 1983. Experimental support for a predictive osmotic model of clay membranes. Geochimica et Cosmochimica Acta. vol. 47, 1515-1522.

Fuller, J.G., 1961. Ordovician and contiguous formations in North Dakota, South Dakota, Montana and adjoining areas of Canada and the United States. AAPG Bulletin vol. 45, 1334-1364.

Gardner, W.C., 1974. Middle Devonian Stratigraphy and depositional environments in the Michigan Basin: Michigan Basin Geological Society Special Papers No. l, 133pp.

Geology and gas-petroleum-bearing prospects of the Tungusskaya syneclise and its framing, 1968. Moscow, Nedra, 260pp.

Gerhard, L.C., and Anderson, S.B., 1988, The Williston Basin - Sedimentary cover - North American Craton - U.S.. Geological Society of America, Chapter 9, Geology of North America, D-2, 221-242.

Gerhard, L.C., Anderson, S.B., Carlson, C., and LeFever, J., 1982, Geological development, origin, and energy and mineral resources of the Williston Basin, North Dakota. American Association of Petroleum Geologists, Bulletin, vol. 66, no. 8, p. 989-1,020.

Gifford, S., Bentley, H.W. and Graham, D.L., 1985. Chlorine isotopes as environmental tracers in Columbia River basalt groundwaters. Proceedings of the 17th International Congress I.A.H.. Hydrogeology of rocks of low permeability. vol. 17, 417-429.

Gleditsch, E. and Sandahl, B., 1922. Radioactiveité sur le poids atomique de chlore dans un mineral ancient, l'apatede Balme. C.R. Acad Sci. Paris. vol. 174, 746-748.

Godon, A., Jendrzejewski, A., Eggenkamp, H.G.M., Banks, D.A., Ader, M., Coleman, M.L. and Pineau, F., 2004. A cross-calibration of chlorine isotopic measurements and suitability of seawater as the international reference material. Chemical Geology. vol. 207, 1-12.

Graedel, T.E. and Keene, W.C., 1996. The budget and cycle of Earth's natural chlorine. Pure & Applied Chemistry. vol. 68, No. 9, 1689-1697.

Graf, D.L., 1982. Chemical osmosis and the origin of subsurface brines. Geochimica et Cosmochimica Acta. vol. 46, 1431-1448.

Graham, R.P., MacNamara, J., Crocker, I.H. and MacFarlene, R.B., 1951. The isotopic constitution of germanium. Canadian Journal of Chemistry. vol. 29, 89-102.

Grasby, S.E., Betcher, R., 2000. Pleistocene recharge and flow reversal in the Williston Basin, central North America. Journal of Geochemical Exploration. vol. 69-70, 403-407.

Hanor, J.S., 1983. Fifty years of development of thought on the origin and evolution of subsurface sedimentary brines. In: Evolution and the Earth Sciences Advances in the Past Half-century; ed. S. J. Boardman. Kendall/Hunt, Dubuque, 99–111.

Hanor, J.S., 1987. Origin and migration of subsurface sedimentary brines. Short course No. 21. Society for Sedimentary Geology (SEPM), Tulsa, OK, USA. 247pp.

Hanor, J.S. and McIntosh, J.C., 2006. Are secular variations in seawater chemistry reflected in the compositions of basinal brines?. Journal of Geochemical Exploration. vol. 89, 153-156.

Hanor, J.S., Kharaka, Y.K., and Land L.S., 1988. Geochemistry of waters in deep sedimentary basins. Geology. vol. 16, 560-561.

Hanratty, D.E., 1996. Isotopic and Hydrogeochemical evaluation of the low regime at the Redland south quarry pit in Dundas, Ontario. BSc thesis, University of Waterloo, Waterloo, Canada. 32pp.

Hanshaw, B.B. and Coplen, T. 1973. Ultrafiltration by a compacted clay membrane - II. Sodium ion exclusion at various ionic strengths. Geochimica et Cosmochimica Acta. vol. 37, 2311-2327.

Harben, P.W. and Kužvart, M., 1996. Industrial minerals - A global geology. Industrial Minerals Information Ltd., Metal Bulletin PLC, London, UK. 462pp.

Harkins, W.D. and Stone, S.B., 1926. The isotopic composition and atomic weight of chlorine from meteorites and from minerals of non-marine origin. Journal of the American Chemical Society. vol. 48, 938-949.

Hardie, L.A., 1967. The gypsum-anhydrite equilibrium at one atmosphere pressure. American Mineralogist. vol. 52, no. 1-2, 171-200.

Haynes, S.J. and Mostaghel, M.A., 1979. Formation temperature of fluorite in the Lockport dolomite in the upper New York State as indicated by fluid inclusion studies - with a discussion of heat sources - A discussion. Economic Geology. vol. 74, 154-165.

Heier, K.S. and Billings, G.K., 1970. Lithium. In: Wedephohl, K.H. (ed.), Handbook of Geochemistry. vol. II, Springer-Verlag, Berlin.

Hendry, M.J., Wassenaar, L.I., and Kotzer, T., 2000. Chloride and chlorine isotopes (^{35}Cl, ^{36}Cl, ^{37}Cl) as tracers of solute migration in a clay-rich aquitard system. Water Resources Research. vol. 36, 285-296.

Heraty, L. J., Fuller, M. E., Huang, L., Abrajano, T. Jr. and Sturchio, N. C. 1999. Isotopic fractionation of carbon and chlorine by microbial degradation of dichloromethane. Organic Geochemistry. vol. 30, 793-799.

Hesse, R. Egeberg, P.K. and Frape, S.K., 2006. Chlorine stable isotope ratios as advection rates in a submarine implication for hydrate concentration. Geofluids. vol. 6, 1-7.

Hesse, R., Frape, S. K., Egeberg, P. K. and Matsumoto, R., 2000. Stable Isotope Studies (Cl, O and H) of Interstitial Waters From Site 997, Blake Ridge Gas Hydrate Field, West Atlantic. Proceedings of the Ocean Drilling Program. Scientific Results. , Paul CK, Matsumoto R, Wallace PJ, Dillon WP (eds). vol. 164, 129-137.

Hewitt, D.F., 1971. The Niagara Escarpment; Ontario Department of Mines, Industrial Mineral Report, No. 35, 71pp.

Hill, J. W. and Fry A., 1962. Chlorine Isotope Effects in the Reactions of Benzyl and Substituted Benzyl Chlorides with Various Nucleophiles Journal of American Chemical Society. vol. 84, 2763-2769.

Hitchon B., 1996. Rapid evaluation of the hydrochemistry of a sedimentary basin using only standard' formation water analysis: example from the Canadian portion of the Williston Basin. Applied Geochemistry. vol. 11, 789-795.

Hitchon, B. and Friedman, I., 1969. Geochemistry and origin of formation waters in the western Canada sedimentary basin: I. Stable isotopes of hydrogen and oxygen. Geochimica et Cosmochimica Acta. vol. 33, 1321-1349.

Hoaglund III, J.R., Kolak, J.J., Long, D.T. and Larson, G.J., 2004. Analysis of modern and Pleistocene hydrologic exchange between Saginaw Bay (Lake Huron) and the Saginaw Lowlands area. Geol. Soc. Am. Bull. 116 (1/2), 3–15.

Hobbs, MY., Frape, S.K., Shouakar-Stash, O. and Kennell, L., 2008. Hydrogeochemical synthesis for south western Ontario. Technical Report No: TR-xx, Nuclear Waste Management Organization. *(In progress).*

Hoefs, J., 2004. Stable isotope Geochemistry. 5th Edition. Sringer, Germany. 244pp.

Hoering T.C. and Parker, P. L., 1961. The geochemistry of the stable isotopes of chlorine. Geochimica et Cosmochimica Acta. vol. 23, 186-199.

Holmstrand, H., Andersson, P. and Gustafsson, Ö., 2004. Chlorine isotope analysis of submicromole organochlorine samples by sealed tube combustion and thermal ionization mass spectrometry. Analytical Chemistry. vol. 76, 2326-2342.

Holser, W.T., 1977. Catastrophic chemical events in the history of the ocean. Nature. vol. 267, 403-408.

Holser, W.T., 1979. Trace elements and isotopes in evaporites. In: Burns, R.G. (Ed.), Reviews in Mineralogy, In: Marine Minerals, vol. 6. Mineralogical Society of America, Washington, DC, 295-346.

Holt, B.D., Heraty, L. J. and Sturchio, N. C., 2001. Extraction of chlorinated aliphatic hydrocarbons from groundwater at micromolar concentrations for isotopic analysis of chlorine. Environmental Pollution. vol. 113, 263-269.

Holt, B.D., Sturchio, N. C., Abrajano, T. A. and Heraty, L. J. 1997. Conversion of chlorinated volatile organic compounds to carbon dioxide and methyl chloride for isotopic analysis of carbon and chlorine. Journal of Analytical Chemistry, vol. 69, 2727-2733.

Huang, L., Sturchio, N. C., Abrajano, T., Heraty, L. J. and Holt, B. D. 1999. Carbon and chlorine isotope fractionation of chlorinated aliphatic hydrocarbons by evaporation. Journal of Organic Geochemistry, vol. 30, 777-785.

Hunkeler, D., Aravena, R., 2000. Determination of compound-specific carbon isotope ratios of chlorinated Methanes, Ethenes, and Ethanes in aqueous samples. Journal of Environmental science and technology, vol. 34, 2839-2844.

Hunkeler, D. and Aravena, R. and Butler, B.J., 1999. Monitoring Microbial Dechlorination of tetrachloroethene (PCE) in groundwater using compound-specific stable carbon isotope ratios: Microcosm and field studies. Journal of Environmental science and technology, vol. 33, 2733-2738.

Hunt, T.S., 1879. Chemical and Geological Essays. Osgood and Company, Boston. (Cited in Kharaka and Hanor, 2004)

Husain, M.M. 1996. Origin and persistence of Pleistocene and Holocene water in a regional clayey aquitard and underlying aquifer in part of southwestern Ontario. Ph.D. thesis, University of Waterloo, Waterloo, Ontario, Canada. 336pp.

Husain, M.M., Cherry, J.A. and Frape, S.K., 2004. The persistence of a large stagnation zone in a developed regional aquifer, southwestern Ontario. Canadian Geotechnical Journal. vol. 41, 943-958.

Iampen, H.T., 2003. The genesis and evolution of pre-Mississippian brines in the Williston Basin, Canada-U.S.A. MSc Thesis. University of Alberta. 124pp.

Iampen, H.T. and Rostron, B.J., 2000. Hydrogeochemistry of pre-Mississippian brines, Williston Basin, Canada–USA. Journal of Geochemical Exploration. vol. 69-70, 29-35.

Jendrzejewski, N., Eggenkamp, H. G. H. and Coleman, M. L. 1997. Sequential Determination of Chlorine and Carbon Isotopic Composition in Single Microlitre Samples of Chlorinated Solvents. Analytical Chemistry. vol. 69, 4259-4266.

Jensen, G.K.S., 2007. Fluid flow geochemistry of the Mississippian aquifers in the Williston Basin, Canada-U.S.A. MSc Thesis. University of Alberta. 123pp.

Jensen, G.K.S., Rostron, B.J., Duke, M.J.M., and Holmden, C., 2006. Chemical profiles of formation waters from potash mine shafts, Saskatchewan; *in* Summary of Investigations 2006, Volume 1, Saskatchewan Geological Survey, Sask. Industry Resources, Misc. Rep. 2006-4.1, CD-ROM, Paper A-7, 8pp.

Jiang, C. and Li, M., 2002. Bakken/Madison petroleum systems in the Canadian Williston Basin. Part 3: geochemical evidence for significant Bakken-derived oils in Madison Group reservoirs. Organic Geochemistry. vol. 33, 761-787.

Jiang, C., Li, M., Osadetz, K.G., Snowdon, L.R., Obermajer, M. and Fowler, M.G., 2001. Bakken/Madison petroleum systems in the Canadian Williston Basin. Part 2: molecular markers diagnostic of Bakken and Lodgepole source rocks. Organic Geochemistry vol. 32, 1037–1054.

Joachimski M.M. and Buggisch W., 1993. Anoxic events in the late Frasnian—causes of the Frasnian–Famennian faunal crisis. Geology. vol. 21, 675-678.

Johnson, M.D., Armstrong, D.K., Sanford, B.V., Telford, P.G. and Rutka, M.A., 1992. Paleozoic and Mesozoic Geology in Ontario; In: Geology of Ontario; Ontario Geological Survey, Special Volume 4, Part 2. Ministry of Northern Development and Mines. Chapter 20, 907-1008.

Jones, A.G. and Craven, J.A., 1990. The North American Central Plains conductivity anomaly and its correlation with gravity, magnetic, seismic, and heat flow data in Saskatchewan, Canada. Physics of the Earth and Planetary Interiors. vol. 60 169-194.

Jones, A.G. and Savage, P.J., 1986. North American Central Plains conductivity anomaly goes east. Geophysical Research Letters. vol. 13, no. 7, 685-688.

Kaufmann, R.S., 1984. Chlorine in ground water: Stable isotope distribution. PhD Dissertation, University of Arizona, Tucson, AZ, USA. 137pp.

Kaufmann, R. S., 1989. Equilibrium exchange models for chlorine stable isotope fractionation in high temperature environments. In: Miles, D.L. (ed.,); 6th International Symposium on Water-Rock Interaction, Malvern, UK. Balkema, Rotterdam. 365-368.

Kaufmann, R. S. and Arnórsson, S., 1986. $^{37}Cl/^{35}Cl$ Ratios in Icelandic Geothermal Waters. In: 5th International Symposium on Water-Rock Interactions. Orkustofnun, Reykjavik, Iceland. 325-328.

Kaufmann, R., Frape, S. K., Fritz, P. and Bentley, H., 1987. Chlorine stable isotope composition of Canadian Shield brines. Geological Association of Canada Special Paper 33. 89-93.

Kaufmann, R.S., Frape, S.K., McNutt, R. and Eastoe, C., 1993. Chlorine stable isotope distribution of Michigan Basin formation waters. Applied Geochemistry. vol. 8, 403–407.

Kaufmann, R.S., Long, A., Bentley, H. and Davis, S., 1984. Natural chlorine isotope variations. Nature. vol. 309, 338-340.

Kaufmann, R.S., Long, A. and Campbell, D.J., 1988. Chlorine isotope distribution in formation waters, Texas and Louisiana. American Association of Petroleum Geologists Bulletin. vol. 72, 839-844.

Kaufmann, R. S., McNutt, R., Frape, S. K. and Eastoe, C. 1992. Chlorine stable isotope distribution of Michigan Basin and Canadian Shield formation waters. In: Kharaka, Y.K. and Maest, A.S. (eds., International Symposium on); 7th International Symposium on Water-Rock Interaction, Park City, Utah, USA. Balkema, Rotterdam, Brookfield. vol. 2, 943-946.

Kent, D.M., 1999. Geology of Ordovician Winnipeg and Red River Rocks Southeast Saskatchewan. Canadian Society of Petroleum Geologists Short Course Notes, 1-32.

Kesler S. E., Martini A. M., Appold M. S., Walter L. M., Huston T. J., and Furman F.C., 1996. Na-C-Br systematics of fluid inclusions from Mississippi Valley type deposits,

Appalachian Basin: constraints on solute origin and migration paths. Geochimica et Cosmochimica Acta. vol. 60, 225-233.

Kharaka, Y.K. and Berry, F.A.F., 1973. Simultaneous flow of water and solutes through geological membranes-I. Experimental investigation. Geochimica et Cosmochimica Acta. vol. 37, 2577-2603.

Kharaka Y.K. and Carothers W.W., 1986. Oxygen and hydrogen isotope geochemistry of deep basin brines, Chapter 2. In: Handbook of Environmental Isotope Geochemistry (eds. Fritz, P. and Fontes, J. Ch.). Elsevier, Amsterdam, vol. II, 305-360.

Kharaka, Y.K. and Hanor, J.S., 2004. Deep Fluids in the continents; II. Sedimentary Basins. In: Drever, J.I. (Ed.), Surface and Ground Water, Weathering and Soils, In: Treatise on Geochemistry, vol. 5. Elsevier, 499-540.

Kharaka, Y.K., Maest, A.S., Carothers, W.W., Law, L.M., Lamothe, P.J. and Fries, T.L., 1987. Geochemistry of metal rich brines from central Mississippi Salt Dome Basin, USA. Applied Geochemistry. vol. 2, 543-561.

Kharaka, Y.K. and Thordsen J.J., 1992. Stable isotope geochemistry and origin of water in sedimentary basins. In: Isotope Signatures and Sedimentary Records (eds. N. Clauer and S. Chaudhuri). Springer, Berlin, 411–466.

Kirk, M.L., Osadetz, G., Yao, H., Obermajer, M., Fowler, M.G., Snowdon, L.R. and Christensen, R., 1998. Unusual crude oils in the Canadian Williston Basin, southeastern Saskatchewan. Organic Geochemistry. vol. 28, 477-488.

Klimovsky, I.V. and Gotovcev, S.P., 1994. The cryolithozone of the Yakutian diamond-bearing province. Nauka, Novosibirsk. 167pp.

Knauth L.P., 1988. Origin and mixing history of brines, Palo Duro Basin Texas, USA. Applied Geochemistry. vol. 3, 455-479.

Knauth, L.P., 1998. Salinity history of the Earth's early ocean. Nature. vol. 395, 554-555.

Knauth, L.P. and Beeunas, M.A., 1986. Isotope geochemistry of fluid inclusions in Permian halite with implications for the isotopic history of ocean water and the origin of saline formation waters. Geochimica et Cosmochimica Acta. vol. 50, 4l9-433.

Kovalevich, V.M., Peryt, T.M. and Petrichenko, O.I., 1998. Secular variations in seawater chemistry during the Phanerozoic as indicated by brine inclusions in halite. The Journal of Geology. vol. 106, 695-712.

Kraynov, S.R. and Ryzhenko, B.N., 1997. Origin of chloride groundwater and brines in crystalline massifs; evidence from thermodynamic modeling of geochemical processes in water–granite systems. Geochemistry. vol. 10, 1035–1057 (in Russian).

Krotova, V.A., 1958. Conditions of formation of calcium chloride waters in Siberia. Petrol. Geol. vol. 2, 545-552.

Kump, L.R., 2004. The Geochemistry of Mass Extinction. In: Drever, J.I. (Ed.), Surface and Ground Water, Weathering and Soils, In: Treatise on Geochemistry, Elsevier. vol. 7, 351-367.

Land, L.S., 1987. The major-ion chemistry of saline brines in sedimentary basins. In: Banavar, J.R., Koplik, J, and Winkler, K.W. (Eds.); Proceedings of the 2nd international Symposium on the Physics and Chemistry of Porous Media. 160-179.

Land, L.S. and Prezbindowski, D.R., 1981. The origin and evolution of saline formation water, Lower Cretaceous carbonates, south-central Texas, USA. Journal of Hydrology. vol. 54, 51-74.

Langvard, T. 1954. Separation of Chlorine Isotopes by Ion-exchange Chromatrography. Acta Chemica Scandinavica. vol. 8, no. 3, 526-527.

Laird, W.M., 1952. Geology of the Williston Basin in North Dakota. World Petroleum, vol. 23, no. 1, 42-44.

Lavastre, V., Jendrzejewski, N., Agrinier, P., Javoy, M. and Evrard, M., 2005. Chlorine transfer out of a very low permeability clay sequence (Paris Basin, France); ^{35}Cl and ^{37}Cl evidence. Geochimica et Cosmochimica Acta. vol. 69, 4949-4961.

LeFever, R.D., 1996. Sedimentology and stratigraphy of the Deadwood-Winnipeg Interval (Cambro-Ordovician), Williston Basin. In: Longman, M.W. and Sonnenfeld, M.D. (Eds), Paleozoic systems of the Rocky Mountain region. Society for Sedimentary Geology, Rocky Mountain Section, United States, 11-28.

LeFever, R.D., Thompson, S.C. and Anderson, D.B., 1987. Earliest Paleozoic history of the Williston Basin in North Dakota. In: Carlson, C.G., Christopher, J.E. (Eds.), Proceedings of the fifth International Williston Basin Symposium. Special Publication 9. Saskatchewan Geological Society, Regina, SK, Canada, 22-36.

LeFever,J.A.,Martiniuk,C.D., Dancsok, E.F.R. and Mahnic, P.A.,1991. Petroleum potential of the Middle member, Bakken Formation, Williston Basin. In: Christopher, J.E., Haidl, F.M. (Eds.), The 6th International Williston Basin. Saskatchewan Geological Society Special Publication 11. Regina, Saskatchewan, Canada , 74-94.

Lepin, V.S. and Borisov, V.N., 1979. Calcium genesis in brines of the Siberian platform (according the isotopic strontium data). In: Proc. of Conf. Problems of Regional Hydrogeochemistry, Leningrad, 115–116.

Liberty, B.A., 1969. Paleozoic geology of the Lake Simcoe area, Ontario, Geological Survey of Canada, Memoir 335, 201pp.

Liberty, B.A. and Bolton, T.E., 1971. Paleozoic geology of the Bruce Peninsula area, Ontario, Geological Survey of Canada, Memoir 360, 163pp.

Lico, M.S., Kharaka, Y.K., Carothers, W.W., and Wright, V.A., 1982, Methods for collection and analysis of geopressured geothermal and oil field waters: U.S. Geological Survey Water Supply Paper 2194, 20pp.

Liu, W. G., Xiao, Y. K., Wang, Q. Z., Qi, H. P., Wang, Y. H., Zhou, Y. M. and Shirodkar, P. V. 1997. Chlorine isotopic geochemistry of salt lakes in the Qaidam Basin, China. Chemical Geology. vol. 136, 271-279.

Long, A., Eastoe, C. J., Kaufmann, R. S., Martin, J.G., Wirt, L. and Finley, J.B., 1993. High-Precision measurement of chlorine stable isotope ratios. Geochimica et Cosmochimica Acta. vol. 57, 2907-2912.

Long, D.T., Wilson, T.P., Takacs, M.J. and Rezabek, D.H., 1988. Stable-isotope geochemistry of saline near-surface ground water: East-central Michigan basin. Geological Society of America Bulletin. vol. 100, 1568-1577.

Longman, M.W. and Haidl, F.M., 1996. Cyclic deposition and development of porous dolomites in the Upper Ordovician Red River Formation, Williston Basin. In: Longman, M.W. and Sonnenfeld, M.D. (eds.); Paleozoic Systems of the Rocky Mountain Region. Rocky Mountain Sec, SEPM, 29-46.

Lowenstein, T.K., Hardie, L.A., Timofeeff, M.N. and Demicco, R.V., 2003. Secular variation in seawater chemistry and the origin of calcium chloride basinal brines. Geology. vol. 31, 857-860.

Lowry, R.M., Faure, G., Mullet, D.I. and Jones, L.M., 1988. Interpretation of chemical and isotopic compositions of brines based on mixing and dilution, "Clinton" sandstones, eastern Ohio, U.S.A. Applied Geochemistry. vol. 3, 177-184.

Lyons, W.B., Frape, S.K. and Welch, K.A., 1999. History of McMurdo dry valley lakes, Antarctica, from stable chlorine isotope data. Geology. vol. 27, 527-530.

Lynch, F.L., Mack, L.E. and Land, L.S., 1997. Burial diagenesis of illite/smectite in shales and the origins of authigenic quartz and secondary porosity in sandstones. Geochimica et Cosmochimica Acta. vol. 61, no. 10, 1995-2006.

Magenheim, A. J., Spivack, A. J., Michael, P. J. and Gieskes, J. M., 1995. Chlorine stable isotope composition of the oceanic crust: Implications for Earth's distribution of chlorine. Earth and Planetary Science Letters. vol. 131, 427-432.

Magenheim, A. J., Spivack, A. J., Volpe, C. and Ransom, B., 1994. Precise determination of stable chlorine isotopic ratios in low-concentration natural samples. Geochimica et Cosmochimica Acta. vol. 58, no. 14, 3117-3121.

Markl, G., Musashi, M. and Bucher, K., 1997. Chlorine stable isotope composition of granulites from Lofoten, Norway: implications for the Cl isotopic composition and for the source of Cl enrichment in the lower crust. Earth Planetary Science Letters. vol. 150, 95-102.

Martin, J.-M. and Meybeck, M., 1979. Elemental mass-balance of material carried by major world rivers. Marine Chemistry. vol. 7, 173-206.

Martini, A.M., Walter, L.M., Budai, J.M., Ku, T.C.W., Kaiser, C.J. and Schoel, M., 1998. Genetic and temporal relations between formation waters and biogenic methane: Upper Devonian Antrim Shale, Michigan Basin, USA. Geochimica et Cosmochimica Acta. vol. 62, no. 10, 1699-1720.

Matray J.-M., 1988. Hydrochimie et géochime isotopiques des eaux de réservoir pétrolier du trias et du dogger dans le bassin de Paris. Thése, Université de Paris XI, Paris, 119pp.

Matthews, R.D., 1977. Evaporite cycles and lithofacies in Lucas Formation, Detroit River Group, Devonian, Midland, Michigan, In: Fisher, J.H. (ed.,); Reefs and Evaporites - concepts and epositional models. Amer. Asoc. Petrol. Geol. Studies in Geology. vol. 5, 73-91.

Mazurek, M. 2004. Long-term used nuclear fuel waste management - Geoscientific review of the sedimentary sequence in southern Ontario. Ontario Power Generation, Technical Report TR 04-01, Institute of Geological Sciences, University of Bern, Switzerland. 100pp.

McCaffrey M. A., Lazar B., and Holland H. D., 1987. The evaporation path of sea water and the coprecipitation of Br2 and Kþ with halite. J. Sedim. Petrol. vol. 57, 928-937.

McCracken, A.D. and Kreis, L.K., 2003. A preliminary report of Upper Devonian conodonts from the Birdbear and Duperow formations of southeastern Saskatchewan; *in* Summary of Investigations 2003, Volume 1, Saskatchewan Geological Survey, Sask. Industry Resources, Misc. Rep. 2003-4.1, CD-ROM, Paper A-6, 14pp.

McIntosh, J.C. and Walter, L.M., 2005. Volumetrically significant recharge of Pleistocene glacial meltwaters into epicratonic basins: constraints imposed by solute mass balances. Chemical Geology. vol. 222, 292-309.

McIntosh, J.C. and Walter, L.M., 2006. Paleowaters in Silurian-Devonian carbonate aquifers: Geochemical evolution of groundwater in the Great Lakes region since the Late Pleistocene. Geochimica et Cosmochimica Acta. vol. 70, 2454-2479.

McIntosh, J.C., Walter, L.M. and Martini, A.M., 2002. Pleistocene recharge to midcontinent basins: effects on salinity structure and microbial gas generation. Geochimica et Cosmochimica Acta. vol. 66, 1681-1700.

McIntosh, J.C., Walter, L.M. and Martini, A.M., 2004. Extensive microbial modification of formation water geochemistry: Case study from a Midcontinent sedimentary basin, United States. Geological Society of America Bulletin. vol. 116, 743-759.

McKinney, C.R., McCrea, J.M., Epstein, S., Allen, H.A. and Urey, H.C., 1950. Improvement in mass spectrometers for the measurement of small differences in isotopic abundances ratios. Review of Scientific Instruments. vol. 21, 724-730.

McNutt, R.H., 2000. Strontium isotopes. In: Environmental Tracers in Subsurface Hydrology. (eds. P. Cook and A. L. Herczeg). Kluwer Academic, Boston, 234–260.

McNutt, R.H., Frape, S.K. and Dollar, P., 1987. A strontium, oxygen and hydrogen isotopic composition of brines, Michigan and Appalachian Basins, Ontario and Michigan. Applied Geochemistry. vol. 2, 495-505.

Meybeck., M., 1994. In: Material Fluxes on the Surface of the Earth, National Research Council, National Academy Press, Washington D.C., 61-73.

Meijer Drees, N.C., 1994. Devonian Elk Point Group of the Western Canada Sedimentary Basin (Chapter 10). In: Mossop, G., Shetsen, I. (Compilers), Geological Atlas of the Western Canada Sedimentary Basin. Canadian Society of Petroleum Geologists and Alberta Research Council, Calgary, 129-148.

Morrison, J., Brockwell, T., Merren, T., Fourel, F. and Phillips, A. M. 2001. On-line high-precision stable hydrogen isotopic analyses on nanolitre water samples. Journal of Analytical Chemistry, vol. 73, 3570-3575.

Moser, H. (Ed.), 1977. Jahresbericht 1977. Internal reports of the Institute fur radiohydrometrie GSF Munich, vol. 169, 70–71.

Musashi, M., Markl, G and Kreulen, R., 1998. Stable chlorine-isotope analysis of rock samples: New aspects of chlorine extraction. Analytical Chimica Acta. vol. 362, 261-269.

Nier, A.O., 1947. A mass spectrometer for isotope and gas analysis. Review of Scientific Instruments. vol. 11, 212-216.

Nier, A.O., 1955. Determination of isotopic masses and abundances by mass spectrometry. Science. vol. 121, 737-744.

Nier, A.O. and Hanson, E.E., 1936. A mass-spectrographic analysis of the ions produced in HCL under electron impact. Physical Reviews. vol. 50, 722-726.

Nier, A.O., Ney, E.P. and Ingharm, M.G., 1947. A null method for the comparison of two ion currents in a mass spectrometer. Review of Scientific Instruments. vol. 18, 294.

Nimegeers, A.R. and Qing, H., 2002. Depositional model of the Mississippian Midale Beds, Steelman Field, southeastern Saskatchewan. In: Summary of Investigations 2002, Volume 1, Saskatchewan Geological Survey, Sask. Industry Resources, Misc. Rep. 2002-4.1, CD-ROM, 46-67.

Numata, M., Nakamura, N. and Gamo, T. 2001. Precise measurement of chlorine stable isotopic ratios by thermal ionization mass spectrometry. Geochemical Journal, vol. 35, 89-100.

Obermajer, M., Osadetz, K.G., Fowler, M.G. and Snowdon, L.R., 2000. Light hydrocarbon (gasoline range) parameter refinement of biomarker-based oil-oil correlation studies: an example from Williston Basin. Organic Geochemistry. vol. 31, 959-976.

Ogg, J.G., 2004. Status of Divisions of the International Geologic Time scale. Lethaia. vol. 37, 183-199.

Ontario Geological Survey 1991. Bedrock geology of Ontario, southern sheet. Ontario Geological Survey, map 2544, scale 1:1'000'000.

Osadetz, K.G. and Haidl, F.M., 1989. Tippecanoe sequence: middle Ordovician to lowest Devonian: vestiges of a great epeiric sea. In: Ricketts, B.D. (Ed.), Western Canada Sedimentary Basin: A Case Study. Special Publication - 30. Canadian Society of Petroleum Geologists, Calgary, AB, Canada, 121-137.

Osadetz, K.G. and Snowdon, L.R. 1995. Significant Paleozoic petroleum source rocks, their distribution, richness and thermal maturity in Canadian Williston Basin (southeastern Saskatchewan and southwestern Manitoba). Geological Survey of Canada Bulletin. vol. 487, 60pp.

Osadetz, K.G., Brooks, P.W., and Snowdon, L.R. 1992. Oil families and their sources in Canadian Williston Basin, (southeastern Saskatchewan and southwestern Manitoba). Bulletin of Canadian Petroleum Geology. vol. 40, 254-273.

Osadetz, K.G., Snowdon, L.R., and Brooks, P.W. 1994. Oil families in Canadian Williston Basin southwestern Saskatchewan. Bulletin of Canadian Petroleum Geology. vol. 42, 155-177.

Petroleum and gas geology of the Siberian platform, 1981. Moscow, Nedra, 552pp.

Phillips, F.M. and Bentley, H.W., 1987. Isotopic fractionation during ion filtration: I. Theory. Geochimica et Cosmochimica Acta. vol. 51, 683-695.

Pinneker, E.V., 1966. Brines of the Angara-Lena artesian basin. Moscow, Nauka, 333pp.

Pinneker, E.V., Borisov, N.V., Kustov, U.I., Brandt, S.B. and Dneprovskaya, L.V., 1987. New data about isotope composition of oxygen and hydrogen of brines of the Siberian Platform. Water Resources. vol. 3, 105–115 (in Russian).

Pinneker, Ye.V. and Lomonosov, I.S., 1964. Concentrated brines of Siberian Platform and their counterparts in Asia, Europe, Africa and America. International Geology Review. vol. 10, 431-442.

Podruski, J.A., Barclay, J.E., Hamblin, A.P., Lee, P.J., Osadetz, K.G., Procter, R.M. and Taylor, G.C., 1987. Part I: resource endowment. Conventional Oil Resources of Western Canada (Light and Medium) Geological Survey of Canada, Paper 87-26. Minister of Supply and Services Canada, Ottawa, ON, Canada, 1-125.

Poulson, S, R. and Drever, J, I. 1999. Stable isotopes (C, Cl, and H) fractionation during vapourization of trichloroethylene. Journal of Environmental science and technology, vol. 33, 3689-3694.

Press, F. and Siever, R. 1978. Earth, 2nd ed., W.H. Freeman & Co., San Francisco. 649pp.

Price, L.C., Ging, T., Daws, T., Love, A., Pawlewicz, M., and Anders, D. 1984. Organic metamorphism in the Mississippian-Devonian Bakken Shale, North Dakota portion of the Williston Basin; in Woodward, J., Meissner, F.F., and Clayton, J.L. (eds.), Hydrocarbon Source Rocks of the Greater Rocky Mountain Region. Rocky Mountain Association of Geologist. Denver, Co. 83-134.

Price, D., Iddon, B. and Wakefield, B. J., 1988. Bromine Compounds, Chemistry and Applications. Elsevier, Amsterdam. 422pp.

Ransom, B., Spivack, A. J. and Kastner, M., 1995. Stable Cl isotopes in subduction-zone pore waters. Implications for fluid-rock reactions and the cycling of chlorine. Geology. vol. 23, no. 8, 715-718.

Raven, K.G., Novakowski, K.S., Yager, R.M. and Heystee, R.J. 1992. Supernormal fluid pressures in sedimentary rocks of southern Ontario – western New York State. Can. Geotech. J. 29, 80-93.

Reimann, C. and de Caritat, P., 1988. Chemical Elements in the Environment, Springer-Verlag, Berlin, 88–91.

Ricketts, B.D., 1989. Western Canada Sedimentary Basin: A Case Study. Spec. Publ., vol. 30. Canadian Society of Petroleum Geologists, Calgary, 320pp.

Rittenhouse, G., 1967. Bromine in oil-field waters and its use in determining possibilities of origin of these waters. American Association of Petroleum Geologists Bulletin. vol. 51, 2430-2440.

Rosen, J.B., 1999. Using stable chlorine isotopes and geochemistry to fingerprint anthropogenic salts in groundwater. MSc. thesis, University of Waterloo, Waterloo, Canada. 126pp.

Rostron, B.J. and Holmden, C., 2003. Regional variations in oxygen isotopic compositions in the Yeoman and Duperow aquifers, Williston basin (Canada–USA). Journal of Geochemical Exploration. vol. 78-79, 337-341.

Rostron, B.J., Kelley, L.I., Kreis, L.K., and Holmden, C., 2002. Economic potential of formation brines: Interim results from the Saskatchewan brine sampling program; *in* Summary of Investigations 2002, Volume 2, Saskatchewan Geological Survey, Sask. Industry Resources, Misc. Rep. 2002-4.2, CD-ROM, Paper C-1, 29pp.

Rostron, B.J. and Khan, D.K., 2005. Hydrodynamics and petroleum migration in the Red River Formation, Williston Basin (Canada-USA). In: Abstracts Volume, AAPG/CSPG 2005 Annual Convention, Calgary, Alberta, June 19-22, v. 14, p. A120

Rubey, W., 1951. Geologic history of sea water: an attempt to state the problem. Bulletin of the Geological Society of America. vol. 62, 1111-1148.

Russell, D.J. and Telford, P.G., 1983. Revisions to the stratigraphy of the Upper Ordovician Collingwood Beds of Ontario-A potential oil shale. Canadian Journal of Earth Sciences. vol. 20, 1780-1790.

Rutka, M.A., Cheel, R.J., Middleton, G.V. and Salas, C.J., 1991. The Lower Silurian Whirlpool sandstones; In: Sedimentary and depositional Environments of Silurian Strata of the Niagara Escarpments, Ontario and New York, Geological association of Canada - Mineralogical Association of Canada – Society of Economic Geologists, Joint Annual Meeting, Fieldtrip B4: Guidebook, 27-34.

Sandberg, C.A., 1962. Geology of the Williston Basin, North Dakota, Montana and South Dakota, with reference to subsurface disposal of radioactive wastes. United States Geological Survey Open-File Report TEI-809. 148pp.

Sandberg, C.A. and Hammond, C.R., 1958. Devonian system in Williston Basin and central Montana. American Association of Petroleum Geologists Bulletin. vol. 42, no.10, 2293-2334.

Sandberg, C.A. and Poole, F.G. 1977. Conodont biostratigraphy and depositional complexes of Upper Devonian cratonic-platform and continental shelf rocks in the western United Stastes. In: Murphy, M.A., Berry, W.B.N. and Sandberg, C.A (Eds.,); Western North America-Devonian: University of California at Riverside, Museum Contributions. vol. 4, 144-182.

Sanford, B.V., 1965. Salina salt beds, southwestern Ontario. Geological Survey of Canada. Paper 65-9, 7pp.

Sanford, B.V., 1968. Devonian of Ontario and Michigan; In: International Symposium of the Devonian System, Alberta Society of Petroleum Geologists. vol. 1, 973-999.

Sanford, B.V., 1969. Silurian of southwestern Ontario. Ontario Petroleum Institute, Eighth Annual Conference Proceedings. Technical Paper Number Five, 1-44.

Sanford, B.V., Thompson, F.J. and McFall, G.H., 1985. Plate tectonics - a possible controlling mechanism in the development of hydrocarbon traps in southwestern Ontario. Bull. Can. Petrol. Geol. vol. 33, 52-71.

Sanford, B.V. 1993. St. Lawrence Platform - Geology. In: Stott, D.F. and Aitken, J.D. (eds.); Sedimentary cover of the craton in Canada. Geol. Survey Canada, Geology of Canada, no. 5, 723-786.

Saskatchewan Industry and resources, (http://www.ir.gov.sk.ca), 2004. (Saskatchewan Stratigraphic Correlation Chart, 2004) Government of Saskatchewan, Canada. (http://www.ir.gov.sk.ca/adx/aspx/adxGetMedia.aspx?DocID=3966,3625,3384,5460,2936,Documents&MediaID=8398&Filename=Sask+Strat+Chart.pdf).

Schauble, E.A., Rossman, G.R. and Taylor Jr., H.P., 2003. Theoretical estimates of equilibrium chlorine-isotope fractionations. Geochimica et Cosmochimica Acta. vol. 67, 3267-3281.

Schilling, J.-G., Unni, C.K. and Bender, M.L., 1978. Origin of chlorine and bromine in the oceans. Nature. vol. 273, 631-636.

Schmoker,J.W., Hester,T.C., 1983. Organic carbon in Bakken Formation,United States portion of Williston Basin. Bulletin of American Association of Petroleum Geologists. vol. 67, 2165-2174.

Seibel, C., 2002. An Examination of the Source Rock Potential of the Deadwood and Winnipeg Formations of Southern Saskatchewan. MSc Thesis, University of Regina. Regina, 140pp.

Sheppard, S.M.F., 1986. Characterization and isotopic variations in natural waters. In: Valley, J.W, Taylor, Jr., H.P. and O'Neil, J.R. (eds.); Stable isotopes in high temperature geological processes. Reviews in Mineralology. vol. 16, 165-183.

Sherwood Lollar and Frape 1989. Report on Hydrogeochemical and isotopic investigations at Ontario Hydro UN-2 and OHD-1 Boreholes. Contract # GHED 88-1. 30 pp.

Sherwood Lollar, B., Sleep, B., Witt, M., Klecka, G. M., Harkness, M. and Spivack, J., 2001. Stable carbon isotope evidence for intrinsic bioremediation of tetrachloroethene and trichloroethene at area 6, dover air force base. Journal of Environmental Science and Technology, vol. 35, 261-269.

Shields, W. S., Murphy, T. J., Carner, E.L., and Dibeler, V. H., 1962. Absolute isotopic abundance ratio and the atomic weight of chlorine. Journal of American Chemical Society. vol. 84, 1519-1522.

Shouakar-Stash, O., Alexeev, S.V., Frape, S.K., Alexeeva, L.P. and Drimmie, R.J., 2007. Geochemistry and stable isotopic signatures, including chlorine and bromine Isotopes, of the deep groundwaters of the Siberian Platform, Russia. Applied Geochemistry. vol. 22, 589-605.

Shouakar-Stash, O., Drimmie, R.J., and Frape, S.K., 2005b. Determination of inorganic chlorine stable isotopes by Continuous Flow Isotope Ratio Mass spectrometry. Rapid Communication in Mass Spectrometry. vol. 19, 121-127.

Shouakar-Stash, O., Drimmie, R.J., Morrison, J., Frape, S.K., Heemskerk, A.R. and Mark, W.A., 2000. On-line D/H analysis for water, natural gas and organic solvents by manganese reduction. Analytical Chemistry. vol. 72, 2664-2666.

Shouakar-Stash, O., Drimmie, R.J., Zhang, M., and Frape, S.K., 2006. Compound-specific chlorine isotopes ratio of TCE, PCE and DCE isomers by direct injection using CF-IRM. Applied Geochemistry, vol. 21, 766-781.

Shouakar-Stash, O., Frape, S, K. and Drimmie R, J., 2003. Stable hydrogen, carbon and chlorine isotope measurements of selected chlorinated organic solvents. Journal of Contaminant Hydrology, vol. 60, 211-228.

Shouakar-Stash, O., Frape, S.K. and Drimmie, R.J., 2005a. Determination of bromine stable isotopes using continuous-flow isotope ratio mass spectrometry. Analytical Chemistry. vol. 77, 4027-4033.

Shvartsev, S.L., 1998. Brines in the Siberian Platform: Geochemical and isotopic evidence for water–rock interaction. In: Arehart, G.B. and Hulston, J.R. (eds.,); 9th International Symposium on Water-Rock Interaction, New Zealand. Balkema, Rotterdam. 357-360.

Shvartsev, S.L., 2000. Chemical composition and strontium isotopes in brines of the Tungussky basin connecting with its formation. Geochemistry. vol. 11, 1170–1184.

Sie, P. M. J. and Frape, S. K., 2002. Evaluation of the groundwaters from the Stripa mine using stable chlorine isotopes. Chemical Geology. vol. 182, 565-582.

Siegel, D.I., 1990, Sulfur isotopic evidence for regional recharge of saline water during continental glaciation, north-central United States. Geology. vol. 18, 1054-1056.

Siegel, D.I., 1991, Evidence for dilution of deep, confined groundwater by vertical recharge of isotopically heavey Pleistocene water. Geology. vol. 19, 433-436.

Siegel, D.I. and Mandle, R.J., 1984. Isotopic evidence for glacial meltwater recharge to the Cambrian Ordovician aquifer, north-central United States. Quaternary Res. vol. 22, 328–335.

Siegel, D.I., Szustakowski, R., and Frape, S., 1991, A regional evaluation of brine mixing in the Albion Group (Silurian) sandstones of New York, Pennylvania, and Ohio. Association of Petroleum and Geochemical Explorations Bulletin. vol. 6, 66-78.

Sklash, M., Mason, S, Scott, S. and Pugsley, C., 1986. An investigation of the quantity, quality and sources of groundwater seepage into the St. Clair River near Sarnia, Ontario, Canada. Water Poll. Res. J. Canada. vol. 21, no. 3, 351-367.

Sloss, L.L., 1987. Williston in the family of cratonic basins. In: Longman, M. (Ed), Williston Basin - Anatomy of a cratonic oil province. Rocky Mountain Association of Geologists, 1-8.

Smith, D.L., 1972. Depositional cycles of the Lodgepole Formation (Mississippian) in central Montana. 21st Montana Geological Society Annual Field Conference, Guidebook, 27-36.

Smith, M., and Bend, S., 2004. Geochemical analysis and familial association of Red River and Winnipeg reservoired oils of the Williston Basin, Canada. Organic Geochemistry. vol. 35, 443-452.

Smith, M.G. and Bustin, R.M., 1998. Production and preservation of organic matter during deposition of the Bakken Formation (Late Devonian and Early Mississippian), Williston Basin. Palaeogeography, Palaeoclimatology, Palaeoecology. vol. 142, 185-200.

Sofer, Z., 1978. Isotopic composition of hydration water in gypsum. Geochimica et Cosmochimica Acta. vol. 42, 1141-1149.

Stewart, M.A., Boudreau, A.E. and Spivack, A.J., 1996. Cl isotopes of the Stillwater Complex, Montana, and the formation of high-Cl Bushveld and Stillwater parent liquids during mantle metasomatism by Cl-rich fluids. Eos Trans, AGU 77:F829.

Stewart, M.A. and Spivack, A.J., 2004. The stable-chlorine isotope compositions of natural and anthropogenic materials. In: Johnson, C.M., Beard, B.L., Albare`de, F. (Eds.), Geochemistry of Non-traditional Stable Isotopes. In: Reviews in Mineralogy and Geochemistry vol. 55. Mineralogical Society of America, Washington, DC, 231-254.

Stueber A.M. and Walter L.M., 1991. Origin and chemical evolution of formation waters from Silurian–Devonian strata in the Illinois Basin, USA. Geochimica et Cosmochimica Acta. vol. 55, 309–325.

Stueber, A.M., Walter, L.M., Houston, T.J. and Pushkar, P., 1993. Formation waters from Mississippian-Pennsylvanian reservoirs, Illinois basin, USA: Chemical and isotopic constrains on evolution and migration. Geochimica et Cosmochimica Acta. vol. 57, 763-784.

Sturchio, N.C., Clausen, J.L., Heraty, L.J., Huang, L., Holt, B.D. and Abrajano, T.A. Jr. 1998. Chlorine isotope investigation of natural attenuation of trichloroethene in an aerobic aquifer. Journal of Environmental Science and Technology, vol. 32, 3037-3042.

Swenson, F.A., 1968. New theory of recharge to the artesian basin of the Dakotas. Geological Society of America Bulletin. vol. 79, no.1, 163-182.

Tanaka, N. and Rye, D.M., 1991. Chlorine in the stratosphere, Scientific Correspondence. Nature. vol. 353, 707.

Tanweer, A., and Han, L.-F., 1996. Reduction of microliter amounts of water with manganese for D/H isotope ratio measurement by mass spectrometry. Isotopes Environ. Heath Stud., vol. 32, 97-103.

Taylor, J.W. and Grimsrud, E.P., 1969. Chlorine Isotopic Ratios by Negative Ion Mass Spectrometry. Analytical Chemistry. vol. 41, no. 6, 805-810.

Tectonics, geodynamics and metallogeny of the Sakha Republic (Yakutia) territory, 2001. Moscow, Nauka (Interperiodika), 571pp.

Trevail, R.A., 1990. Cambro-Ordovician shallow water sediments, London area, southwestern Ontario; In: Subsurface Geology of Southwestern Ontario: a core workshop. Ontario Petroleum Institute. American Association of Petroleum Geologists. 1990 Eastern Meeting, 29-50.

Tuncay K., Park A., and Ortoleva P., 2000. Sedimentary basin deformation: an incremental stress approach. Tectonophysics. vol. 323, 77-104.

Uyeno, T.T., Telford, P.G. and Sanford, B.V., 1982. Devonian conodonts and stratigraphy of southwestern Ontario. Geological Survey Canada, Bulletin 332, 45pp.

Valyaskho, M.G., 1956. Geochemistry of bromine in the processes of salt deposition and the use of the bromine content as a genetic and prospecting criterion. Geokhimiya. vol. 6, 570-589.

van Everdingen, R.O., 1968. Studies of formation waters in Western Canada: Geochemistry and hydrodynamics. Canadian Journal of Earth Sciences. vol. 5, 523-543.

van Warmerdam, E. M., Frape, S. K., Aravena, R., Drimmie, R. J., Flatt, H. and Cherry, J. A. 1995. Stable chlorine and carbon isotope measurements of selected chlorinated organic solvents. Journal of Applied Geochemistry. vol. 10, 547-552.

Vengosh, A., Chivas, A. and McCulloch, M. T., 1989. Direct determination of boron and chlorine isotopic compositions in geological materials by negative thermal-ionization mass spectrometry. Chemical Geology (Isotopic Geoscience Section). vol. 79, 333-343.

Volpe, C. and Spivack, A. J. 1994. Stable chlorine isotopic composition of marine aerosol particles in the western Atlantic Ocean. Geophysical Research Letters. vol. 21, no. 12, 1161-1164.

Vugrinovich, R., 1986. Patterns of regional subsurface fluid movement in the Michigan Basin. Michigan Basin Geological Survey. Open-File Report 86-6, 27pp.

Vugrinovich, R. 1987. Regional heat flow variations in the northern Michigan and Lake Superior region determined using the silica heat flow estimator. Journal of Volcanology and Geothermal Research. vol. 34, 15-24.

Vugrinovich, R., 1989. Subsurface temperatures and surface heat flow in the Michigan Basin and their relationships to regional subsurface fluid movement. Marine and Petroleum Geology. vol. 6, 60-70.

Weaver T. R. 1994. Groundwater flow and solute transport in shallow Devonian bedrock formations and overlying Pleistocene units, Lambton County, southwestern Ontario. Ph.D. Thesis, Department of Earth Sciences, University of Waterloo, Waterloo, Ontario, Canada. 401pp.

Weaver, T.R., Frape, S.K. and Cherry, J.A., 1995. Recent cross-formational fluid flow and mixing in the shallow Michigan Basin. Geol. Soc. Am. Bull. vol. 107, no. 6, 697-707.

Webster, R.W., 1987. Petroleum source rocks and Stratigraphy of the Bakken Formation in North Dakota. In: Williston Basin: Anatomy of a Cratonic Oil Province. Rocky Mountain Peterson, J.A., Kent, D.M., Anderson, S.B., Pilatzke, R.H., Longman, M.W. (Eds.), Association of Geologists, Denver, Colo., 269–285.

Webster, R.L. 1984. Petroleum source rocks and stratigraphy of the Bakken Formation in North Dakota; in Woodward, J., Meissner, F.F., and Clayton, J.L. (eds.), Hydrocarbon source rocks of the greater Rocky Mountain region, Rocky Mountain Association of Geologists. Denver, Colorado, 57-81.

Westjohn, D.B. and Weaver, T.L., 1997. Hydrogeologic framework of the Michigan Basin regional aquifer system. In: Regional Aquifer-System Analysis—Michigan Basin Aquifer System. US Geological Survey Professional Paper 1418. 47pp.

White, D.E., Hem, J.D., and Waring, G.A., 1963. Chemical composition of subsurface waters. In: Data of Geochemistry. US Geological Survey Professional Paper 440F. 67pp.

Wieser, M.E., 2006. Atomic weights of the elements 2005 (**IUPAC** Technical Report). International Union of Pure and Applied Chemistry – Inorganic Chemistry Division Commission on Isotopic Abundances and Atomic Weights. Pure Applied Chemistry. vol. 78, no. 11, 2051–2066.

Willey, J. F. and Taylor, J. W., 1978. Capacitive integration to produce high precision isotope ratio measurements on methyl chloride and methyl bromide samples. Analytical Chemistry. vol. 50, 1930-1933.

Williams, D.A., 1991. Paleozoic geology of the Ottawa – St. Lawrence Lowland, soutern Ontario, Ontario Geological Survey. Open File Report 5770, 291pp.

Williams, J.A., 1974. Characterization of oil types in Williston Basin. Bulletin of the American Association of Petroleum Geology. vol. 58, 1243-1252.

Williams, D. and Yuster, P., 1946. Isotopic constitution of Tellurium, Silicon, Tungsten, Molybdenum, and Bromine Physical Review. vol. 69, 556-567.

Willimore, C.C, Boudreau, A.E., Spivack, A.J. and Kruger, F.J., 2002. Halogens of the Bushveld complex, south Africa: d37Cl and Cl/F evidence for hydration melting at the source region in a back-arc setting. Chemical Geology. vol. 182, 503-511.

Wilson, T.P. and Long D.T., 1993a. Geochemistry and isotope chemistry of MichiganBasin brines: Devonian formations. Applied Geochemistry. vol. 8, 81-100.

Wilson, T.P. and Long, D.T., 1993b. Geochemistry and isotope chemistry Ca-Na-Cl brines in Siluriun strata, Michigan Basin, U.S.A. Applied Geochemistry. vol. 8, 507-524.

Wilson, T.R.S. 1975. The major constituents of seawater. In: Chemical Oceanography, vol. 1, 2nd ed. (J. P. Riley, G. Skirrow, eds.). Academic, Orlando, Fla. 365-413.

Winder, C.G. and Sanford, B.V., 1972. Stratigraphy and paleontology of the Paleozoic rocks of southern Ontario. XXIV International Geological Congress. Montreal, Quebec, Excursion A45-C45.

Wittrup, M.B. and Kyser, T.K., 1990. The petrogenesis of brines in Devonian potash deposits of western Canada. Chemical Geology. vol. 82, 103-128.

Worden, R.H., Coleman, M.L., and Matray, J.M., 1999. Basin scale evolution of formation waters: a diagenetic and formation water study of the Triassic Chaunoy Formation, Paris Basin. Geochimica et Cosmochimica Acta. vol. 63, 2513-2528.

Wyoming State Engineer's Office, 1974. Underground water supply in the Madison Limestone. Cheyenne, Wyoming. 117pp.

Xiao, Y. K., Liu, W. G., Qi, H. P. and Zhang, C. G., 1993. A new method for the high precision isotopic measurement of bromine by thermal ionization mass spectrometry. International Journal of Mass Spectrometry and Ion Processes. vol. 123, 117-123.

Xiao, Y., Lu, H., Zhang, C., Wang, Q., Wei, H. Sun, A. and Liu, W., 2002. Major Factors affecting the isotopic measurement of chlorine based on the Cs_2Cl^+ ion by thermal ionization mass spectrometry. Analytical Chemistry. vol. 74, 2458-2464.

Xiao, Y.-K. and Zhang, C.-G. 1992. High precision isotopic measurement of chlorine by thermal ionization mass spectrometry of the Cs_2Cl^+ ion. International Journal of Mass Spectrometry and Ion Processes. vol. 116, 183-192.

Xiao, Y. K., Zhou, Y. M. and Liu, W. G. 1995. Precise Measurement of Chlorine Isotopes Based on Cs_2Cl^+ by Thermal Ionization Mass Spectrometry. Analytical Letters. vol. 28, no. 7, 1295-1304.

Yaron, F., 1966. Bromine manufacture: technology and economic aspects. In: Jolles, Z. E., (Ed.); Bromine and Its Compounds. Ernest Benn Limited, London. 3-42.

Yoshida, M., Takahashi, K. and Yonehara, N., 1971. The fluorine, bromine, and iodine contents of volcanic rocks in Japan. Bulletin of the Chemical Society of Japan. vol. 44, 1844-1850.

Zhang, M. and Frape, S.K., 2003. Permafrost: evaluation of shield groundwater compositions during freezing. Report No: 06819-REP-01200-10098-R00. Ontario Power Generation. Nuclear Waste Management Division, Toronto, Ontario, Canada. 49pp.

Zherebtsova, I.K. and Volkova, N.N., 1966. Experimental study of behavior of trace elements in the process of natural solar evaporation of Black Sea water and Sasyk-Sivash brine. Geochemistry International. vol. 3, 656-670.

Ziegler, K.M., Coleman, M.L. and Howarth, R.J., 2001. Paleohydrodymnamics of fluids in the Brent Group (Oseberg Field, Norwegian North Sea) from chemical and isotopic compositions of formation waters. Applied Geochemistry. vol. 16, 609-632.

Appendix A

A.1 Distribution of Chlorine in Nature

The most recent determination of the primordial abundance of chlorine reported a value of 5240 Cl atom per 10^6 Si atoms (Anders and Ebihara, 1982). Given that silicon is 15 % by weight of the earth (Press and Siever, 1978), which itself weighs 5980 x 10^{24} g, the chlorine content of the Earth is approximately 4.7 x 10^{24} g. Therefore, the chlorine content of the Earth's interior (mantle and core) is that of the Earth's minus that of all other reservoirs, which is approximately 4.61 x 10^{24} g, and accounts for 98.170 % of all of the chlorine content of the Earth.

The amount of chlorine in the form of minerals found in the crust is not equally distributed, but is concentrated in sedimentary salt beds. Ocean derived deposits that contain chloride are dominated by the following minerals: Halite (NaCl), Sylvite (KCl), Carnallite ($MgCl_2.KCl.6H_2O$), Kainite ($MgSO_4.KCl.3H_2O$). These deposits are widely distributed in sedimentary formations around the world. By considering the weight of the crust as 26 x 10^{24} g, then the weight of igneous and metamorphic rocks that makes up almost 95% of the crust is 24.7 x 10^{24} g and the average content of chlorine in igneous rocks to be 270 µg/g (Yoshida et al., 1971), the chlorine content of the crust (igneous and metamorphic) is calculated is 6.67 x 10^{21} g. The chlorine content in the entire crust including sediments is reported by Graedel and Keene (1996) as 60 x 10^{21} g, therefore the chlorine contented in sedimentary rock is

calculated to be approximately 53.33 x 10^{21} g. By considering an average concentration of chlorine in soil as 100 ppm weight, the pedosphere is estimated to contain 24 x 10^{15} g (Graedel and Keene, 1996).

The oceans are the largest natural reservoir for chlorine in the earth's hydrosphere. Out of a total average salinity of about 3.4%, seawater contains approximately 1.9 % chloride. Isolated bodies of water in arid regions are frequently found to have high chloride content; the Great Salt Lake of Utah, for example contains no less than 23% sodium chloride, while the Dead Sea, with a total salinity of more than 30 %, contains about 3.5% calcium chloride, 8.0% sodium chloride and 13% magnesium chloride (Downs and Adams, 1975). With an average volume of about 1370 x 10^6 km^3 (Berner and Berner, 1987) and an average Cl concentration of 19.354 g/kg (Wilson, 1975), the ocean contains approximately 26 x 10^{21} g. The Available evidence suggests that the chlorine content of seawater has remained relatively constant over the past 600 million years, although small fluctuations are expected based on the presence or absence of significant evaporite pans (Berner and Berner, 1987).

Surface waters including lakes and rivers comprise 1.267 x 10^5 km^3 (Berner and Berner, 1987). Whereas, the chloride ion makes up 90% of the total anion content of seawater, it only amount to 2-5% of river waters. The average concentration of non-anthropogenic, dissolved Cl in rivers is about 5.8 mg/L (Meybeck, 1994) and the reservoir content is of the order of 7.35 x 10^{14} g. The groundwater in aquifers and soils comprises about 0.68 % of Earth's water, i.e. 9.5 x 10^6 km^3 (Berner and Berner, 1987), and has a typical chlorine concentration of 40

mg/L (Freeze and Cherry, 1979). The content of chlorine in the groundwater reservoir is thus 380 x 10^{15} g.

The average concentration of Cl in ice is 5 x 10^{-7} M Cl/L (Graedel and Keene, 1996). The current volume of ice on Earth is estimated at 29 x 10^{6} km^3 (Berner and Berner, 1987) and therefore, the estimated chlorine content in the cryosphere is approximately 5.15 x 10^{15} g.

Most volatile chlorine in the atmosphere exists as hydrochloric acid (HCl) and methyl chloride (CH_3Cl) (Berner and Berner, 1987). The average concentration of natural gaseous HCl in the troposphere is about 200 pptv in the boundary layer and ≤ 100 pptv above the boundary layer, while the average concentration of CH_3Cl is constant and about 620 pptv. The chlorine content of these two compounds in the troposphere is estimated at 4.3 x 10^{12} g. The chlorine content of the atmosphere due to sea-salt aerosol varies widely, however the typical concentration measured, is 100 nM/m^3 (Berner and Berner, 1987). The chlorine content in the troposphere due to sea-salt aerosol is estimated to be between 1 and 1.5 x 10^{12} g. The average concentration of chlorine in the stratoshpere is 3 ppbv, most of it from anthropogenic materials. The total content of chlorine in the stratosphere is 0.4 x 10^{12} g (Graedel and Keene, 1996).

A.2 Distribution of Bromine in Nature

The bromine content of the Earth can be calculated based on the most recent determination of the primordial abundance of bromine reported a value of 11.8 Br atom per 10^{6} Si atoms

(Anders and Ebihara, 1982). Given that silicon is 15 % by weight of the Earth (Press and Siever, 1978), which itself weighs 5980 x 10^{18} t, the bromine content of the Earth is approximately 10.585 x 10^{21} g. According to the calculated contents of chlorine and bromine in the Earth the chlorine-to-bromine (Cl/Br) ratio of the Earth is 444.

By considering the average content of Br in igneous rock which makes up over 95 % of the crust as 0.85 μg/g (Yoshida et al., 1971), and taking into account the weight of the crust as 26 x 10^{24} g, the bromine content of the crust is calculated to be 2.21 x 10^{19} g. This gives an average value of 318 for the chlorine-to-bromine (Cl/Br) ratio of the crust.

The oceans are the largest natural reservoir for bromine in the Earth's hydrosphere. The oceans contain approximately 67 mg/L bromide. Isolated bodies such as the Dead Sea have bromide contents that exceeds 5000 mg/L. With an average volume of about 1370 x 10^6 km^3 (Berner and Berner, 1987), the ocean contains approximately 9.18 x 10^{19} g.

Surface waters including lakes and rivers comprises 1.267 x 10^5 km^3 (Berner and Berner, 1987). The average concentration of dissolved Br in rivers is 20 μg/L (Chester, 2000 after Martin and Meybeck, 1979), and thus the Br content in fresh surface waters is 25.34 x 10^{11} g. The bromine content in groundwater in aquifers and soils is calculated by assuming an average Cl/Br of 300 for groundwater (Downs and Adams, 1975) and considering the chlorine content of groundwater, shown in Table 1.1, which is 380 x 10^{15} g. The content of bromine in groundwater reservoir is thus 1.267 x 10^{15} g.

The bromine concentration in the Atmosphere is 7.8×10^{-6} ppm (Schilling et al., 1978) and since the mass of the Earth's atmosphere is 5.1×10^{21} g, then the bromine content in the atmosphere is 3.98×10^{10} g.

The bromine content of the mantle (10.471×10^{21} g) was calculated by subtracting the sum of all reservoirs mentioned above from the total content in Earth.

Appendix B

Table B.1 Geochemical data of formation waters from the southern Ontario and Michigan. Samples were collected from the stratigraphic units shown. (Note: The samples and data presented in this table were compiled from various authors: [1] Dollar, 1988; [2] Walter, Pers. Comm.; [3] Cloutier, 1994; [4] Husain, 1996; [5] Weaver, 1994; [6] Sherwood-Lollar and Frape, 1989)

No.	Author	Sample Name	Rock Type	Depth m	TDS mg/L	Ca mg/L	Na mg/L	Mg mg/L	K mg/L	Sr mg/L
Mississippian (Berea)										
1	[1]	MB-1	Sandstone	746	288600	41100	51200	8760	799	1540
2	[1]	MB-2	Sandstone	760	312900	43600	59400	9160	861	1750
3	[1]	MB-3	Sandstone	738	269400	37800	51000	7500	732	1530
4	[1]	MB-4	Sandstone	737	230100	33000	43500	6320	545	1340
5	[1]	MB-5	Sandstone	728	306500	40900	59600	8060	697	1570
6	[1]	MB-6	Sandstone	723	304500	35100	64300	7080	795	1210
7	[2]	BRENNAN 122	Sandstone		318210	45315	54378	9576	686	1744
8	[2]	CAMPBELL #7	Sandstone		379471	63000	70770	12285	708	2226
9	[2]	CAMPBELL #9	Sandstone		350561	55335	62062	10720	2436	2146
10	[2]	CANNELL #1	Sandstone		349683	41624	86516	9408	627	1663
11	[2]	CARTER	Sandstone		364914	47080	83248	15136	721	2710
12	[2]	JAMES 122	Sandstone		176430	26718	30744	5636	434	1029
13	[2]	NKERN #1	Sandstone		323992	34138	71508	7817	1094	1265
Late Devonian (Kettle Point / Antrim)										
14	[3]	LD-90-3-5	Shale	52	15511	127	5410	120	31	5
15	[3]	DOW-90-3-4	Shale	44	641	8.41	189	0.1	72	0.5
16	[4]	BRP-143	Shale	44	934	39.6	278	14	5	0.8
17	[4]	BRP-151	Shale	46	984	26.5	338	12	9	0.5
18	[2]	SP A2-32	Shale		241262	6770	82600	3590	667	323
19	[2]	WSMC2-10	Shale		205671	7700	63700	4690	487	424
20	[2]	HGR D4-6	Shale		122914	3280	42400	2140	370	221
Late Devonian (Hamilton)										
21	[3]	LD-90-3-4	Shale	68	10415	122	3840	68	29	3
22	[3]	LD-90-3-3	Shale	89	7499	104	2590	59	47	4
23	[3]	LD-90-3-2	Shale	131	12930	200	4230	137	41	14
24	[3]	DOW-90-3-3	Shale	77	10728	164	3760	75	47	3
25	[3]	DOW-90-3-2	Shale	106	19086	367	5940	208	67	8
Middle Devonian (Dundee)										
26	[3]	DOW-90-3-1	Carbonate	142	8380	127	2920	70	48	3
27	[3]	LD-90-3-1	Carbonate	142	4866	92	1510	28.9	136	2
28	[1]	DD-1	Carbonate	108	15940	660	3690	632	85	29
29	[1]	DD-2	Carbonate	97	3260	623	414	83	19	12
30	[1]	DD-3	Carbonate	1131	291500	31500	70600	5410	3030	750
31	[1]	DD-4	Carbonate	1128	292000	40300	56600	6990	3370	1120
32	[5]	PD-COCH	Carbonate		16155	1180	3470	715	91	23
33	[5]	PD-NORTH	Carbonate		22073	1580	4830	898	115	29
34	[5]	PD-RAL	Carbonate		20166	1580	4390	908	117	30
35	[5]	PD-WEST	Carbonate		18399	1400	3870	793	105	26
36	[5]	RA-N	Carbonate		16008	1140	3420	675	85	24
37	[5]	RA-NE	Carbonate		20145	1410	4360	808	105	28
38	[5]	RA-SE	Carbonate		20840	1490	4530	858	111	28
39	[5]	RA-SW	Carbonate		18342	1320	3970	758	100	25
40	[5]	LAI-1	Carbonate		17828	1270	3670	818	103	25
41	[5]	LAI-2	Carbonate		17346	1300	3520	803	102	26
42	[5]	LAI-3	Carbonate		16512	1220	3430	773	107	23
43	[5]	WB-11	Carbonate		10470	736	2100	450	62	51
44	[5]	WB-2	Carbonate		12829	918	2620	593	76	21
45	[5]	WB-7	Carbonate		15334	1100	3090	688	88	22
46	[5]	WB-8	Carbonate		17388	1240	3590	843	111	27
47	[5]	LBH-1	Carbonate		22314	1700	4450	1170	152	32
48	[5]	LBH-2	Carbonate		25194	2000	4950	1320	156	34
49	[5]	LBH-3	Carbonate		24731	1940	4900	1340	169	36
50	[5]	LBH-4	Carbonate		24839	1760	5150	1300	171	36

Table B.1 Continued

No.	Author	Sample Name	Cl mg/L	Br mg/L	SO4 mg/L	HCO3 mg/L	F mg/L	Water Type
Mississippian (Berea)								
1	[1]	MB-1	183800	1340	53	<7	4	Na-Ca-Cl
2	[1]	MB-2	196700	1460	<15	<7	12	Na-Ca-Cl
3	[1]	MB-3	169600	1250	<15	<7	12	Na-Ca-Cl
4	[1]	MB-4	144300	1080	18	<7	10	Na-Ca-Cl
5	[1]	MB-5	194400	1310	<15	<7	9	Na-Ca-Cl
6	[1]	MB-6	194800	1180	66	<7		Na-Ca-Cl
7	[2]	BRENNAN 122	204439	2046	26			Na-Ca-Cl
8	[2]	CAMPBELL #7	228417	2028	38			Ca-Na-Cl
9	[2]	CAMPBELL #9	216104	1738	20			Ca-Na-Cl
10	[2]	CANNELL #1	208313	1460	72			Na-Ca-Cl
11	[2]	CARTER	213993	2000	26			Na-Ca-Cl
12	[2]	JAMES 122	110789	1067	14			Na-Ca-Cl
13	[2]	NKERN #1	206705	1395	70			Na-Ca-Cl
Late Devonian (Kettle Point / Antrim)								
14	[3]	LD-90-3-5	8600	7	1	1210		Na-Cl
15	[3]	DOW-90-3-4	164	0.7	42	164		Na-Cl
16	[4]	BRP-143	393	0.4	10	194		Na-Cl
17	[4]	BRP-151	390	0.3	6	202		Na-Cl
18	[2]	SP A2-32	147000	307	<5	5		Na-Cl
19	[2]	WSMC2-10	128200	454		16		Na-Cl
20	[2]	HGR D4-6	74300	179		24		Na-Cl
Late Devonian (Hamilton)								
21	[3]	LD-90-3-4	5800	5	349	200		Na-Cl
22	[3]	LD-90-3-3	3530	5	783	376		Na-Cl
23	[3]	LD-90-3-2	7260	0	324	724		Na-Cl
24	[3]	DOW-90-3-3	6080	6	379	214		Na-Cl
25	[3]	DOW-90-3-2	11500	21	572	404		Na-Cl
Middle Devonian (Dundee)								
26	[3]	DOW-90-3-1	3880	9	819	504		Na-Cl
27	[3]	LD-90-3-1	793	4	1830	470		Na-SO_4-Cl
28	[1]	DD-1	10000	50	795	293		Na-Cl
29	[1]	DD-2	2000	12	98	<7		Ca-Na-Cl
30	[1]	DD-3	179000	1050	166	<7	17	Na-Ca-Cl
31	[1]	DD-4	182200	1310	150	90	10	Na-Ca-Cl
32	[5]	PD-COCH	8650	58	1700	264		Na-Ca-Mg-Cl
33	[5]	PD-NORTH	12000	91	2200	325		Na-Ca-Cl
34	[5]	PD-RAL	10900	78	2000	158		Na-Ca-Mg-Cl
35	[5]	PD-WEST	9920	82	1940	258		Na-Ca-Mg-Cl
36	[5]	RA-N	8870	62	1380	348		Na-Ca-Mg-Cl
37	[5]	RA-NE	11300	74	1810	499		Na-Ca-Cl
38	[5]	RA-SE	11500	79	1920	320		Na-Ca-Cl
39	[5]	RA-SW	10100	67	1690	308		Na-Ca-Cl
40	[5]	LAI-1	9500	59	1790	589		Na-Mg-Ca-Cl
41	[5]	LAI-2	8980	54	2010	548		Na-Mg-Ca-Cl
42	[5]	LAI-3	8240	44	2110	561		Na-Mg-Ca-Cl
43	[5]	WB-11	5700	43	751	572		Na-Mg-Ca-Cl
44	[5]	WB-2	7190	21	787	599		Na-Mg-Ca-Cl
45	[5]	WB-7	8450	60	1320	512		Na-Mg-Ca-Cl
46	[5]	WB-8	9750	57	1230	536		Na-Mg-Ca-Cl
47	[5]	LBH-1	13200	47	1400	157		Na-Mg-Ca-Cl
48	[5]	LBH-2	14300	86	2340	5		Na-Mg-Ca-Cl
49	[5]	LBH-3	14100	97	2140	5		Na-Mg-Ca-Cl
50	[5]	LBH-4	15000	86	1220	112		Na-Mg-Ca-Cl

Table B.1 Continued

No.	Author	Sample Name	Rock Type	Depth m	TDS mg/L	Ca mg/L	Na mg/L	Mg mg/L	K mg/L	Sr mg/L
Middle Devonian (Detroit River)										
51	[5]	LBO-2	Carbonate		18556	1530	4030	940	131	34
52	[5]	LBO-3	Carbonate		17066	1640	3130	920	125	35
53	[5]	CFN-14	Carbonate		13500	1310	2390	608	85	29
54	[5]	CFN-A	Carbonate		16365	1570	3170	830	123	35
55	[5]	CFN-B	Carbonate		13148	1190	2590	673	98	27
56	[5]	CFN-161	Carbonate		53400	5990	10900	2750	445	100
57	[5]	CFN-C	Carbonate		43912	3830	8690	2430	307	70
58	[5]	CFN-E	Carbonate		43304	4020	8090	2270	288	67
59	[5]	CFS-A	Carbonate		48694	4320	9330	2330	311	70
60	[5]	CFS-B	Carbonate		43805	4240	9700	2270	325	67
61	[5]	CFS-C	Carbonate		43192	3800	8910	2160	309	67
62	[5]	CFS-D	Carbonate		41456	3500	8320	2150	299	67
63	[1]	DR-1	Carbonate	1445	281900	64900	23400	7960	8320	2060
Midddle Silurian (F Salt)										
64	[1]	SF-1	Salt	150	322200	8200	100000	2850	2600	214
65	[1]	SF-2	Salt	150	305900	10300	94500	3100	2780	197
66	[1]	SF-3	Salt	150	304000	9630	94400	3370	2600	158
Middle Silurian (A2 Salt)										
67	[1]	SA2-1	Salt	250	340400	48400	33400	16600	5000	1620
68	[1]	SA2-2	Salt	250	340000	46800	33600	16200	6400	1620
Middle Silurian (A1 Carbonate)										
69	[1]	SA1-1	Carbonate	645	284400	52000	37700	11400	4520	740
70	[1]	SA1-2	Carbonate	649	306400	54700	37900	10900	4760	969
Middle Silurian (Guelph)										
71	[1]	SG-1	Carbonate	354	158800	15000	41200	3780	1430	263
72	[1]	SG-2	Carbonate	448	297600	31300	65500	7770	1880	436
73	[1]	SG-3	Carbonate	553	326800	44500	61300	9000	2740	599
74	[1]	SG-4	Carbonate	614	319800	60300	46600	8250	3040	1220
75	[1]	SG-5	Carbonate	571	300400	29000	70000	8200	2040	449
76	[1]	SG-6	Carbonate	646	297600	53700	42100	9520	3240	744
77	[1]	SG-7	Carbonate	749	334700	66000	42300	8440	3270	1120
78	[1]	SG-8	Carbonate	695	339200	61500	46000	10600	3400	997
79	[1]	SG-9	Carbonate	770	319200	53100	42900	13300	2150	580
80	[1]	SG-10	Carbonate	726	301900	57200	39400	8670	3340	1220
81	[1]	SG-11	Carbonate	518	333300	52600	49900	9500	4840	702
82	[1]	SG-12	Carbonate	597	255000	34700	53200	7080	2390	572
83	[1]	SG-13	Carbonate	670	327000	50200	54800	8230	2810	684
Middle Silurian (Niagaran)										
84	[1]	SN-1	Carbonate	892	330800	62000	40800	8680	6080	1270
85	[1]	SN-2	Carbonate	895	327800	61300	40300	8530	5920	1270
86	[1]	SN-3	Carbonate	1161	359900	73800	24800	17900	8560	2040
87	[1]	SN-4	Carbonate	1272	391700	78500	25300	17900	9280	2170
88	[1]	SN-5	Carbonate	1305	380300	77300	31000	11900	10300	2040
89	[1]	SN-6	Carbonate	1264	397000	79500	25200	15500	9820	2500
90	[1]	SN-7	Carbonate	1010	335300	62900	45300	8550	4320	1160
91	[1]	SN-8	Carbonate	1001	310300	61900	45100	8080	3900	1190
92	[1]	SN-9	Carbonate	713	324100	54900	46000	9600	3560	919
93	[1]	SN-10	Carbonate	717	323100	62600	42600	8530	3370	1060
94	[2]	Cold Srings WH1-29	Carbonate		394620	88643	26275	10176	18285	3661

Table B.1 Continued

No.	Author	Sample Name	Cl mg/L	Br mg/L	SO4 mg/L	HCO3 mg/L	F mg/L	Water Type
Middle Devonian (Detroit River)								
51	[5]	LBO-2	11300	99	448	40		Na-Mg-Ca-Cl
52	[5]	LBO-3	10400	69	630	113		Na-Ca-Mg-Cl
53	[5]	CFN-14	7990	66	796	219		Na-Ca-Mg-Cl
54	[5]	CFN-A	9460	86	916	171		Na-Ca-Mg-Cl
55	[5]	CFN-B	7810	61	398	297		Na-Ca-Mg-Cl
56	[5]	CFN-161	31400	277	1240	328		Na-Ca-Mg-Cl
57	[5]	CFN-C	27400	200	760	221		Na-Mg-Ca-Cl
58	[5]	CFN-E	26800	216	1220	328		Na-Ca-Mg-Cl
59	[5]	CFS-A	30300	294	1390	345		Na-Ca-Mg-Cl
60	[5]	CFS-B	25500	202	1350	148		Na-Ca-Mg-Cl
61	[5]	CFS-C	26600	195	941	206		Na-Ca-Mg-Cl
62	[5]	CFS-D	25700	187	808	421		Na-Mg-Ca-Cl
63	[1]	DR-1	173100	1970	205	258	14	Ca-Na-Cl
Midddle Silurian (F Salt)								
64	[1]	SF-1	207000	587	750			Na-Cl
65	[1]	SF-2	194100	390	510	73		Na-Cl
66	[1]	SF-3	192900	325	595	76		Na-Cl
Middle Silurian (A2 Salt)								
67	[1]	SA2-1	232000	3220	110			Ca-Na-Mg-Cl
68	[1]	SA2-2	232000	3214	106			Ca-Na-Mg-Cl
Middle Silurian (A1 Carbonate)								
69	[1]	SA1-1	176000	1880	167	76		Ca-Na-Cl
70	[1]	SA1-2	195300	1700	193	18		Ca-Na-Cl
Middle Silurian (Guelph)								
71	[1]	SG-1	95500	810	810	127	164	Na-Ca-Cl
72	[1]	SG-2	189100	1390	250	69	8	Na-Ca-Cl
73	[1]	SG-3	206900	1620	127	43		Na-Ca-Cl
74	[1]	SG-4	197800	2510	119	<7		Ca-Na-Cl
75	[1]	SG-5	189100	1390	259	84	8	Na-Ca-Cl
76	[1]	SG-6	186300	1780	227	<7	8	Ca-Na-Cl
77	[1]	SG-7	210900	2440	239	<7	8	Ca-Na-Cl
78	[1]	SG-8	214600	2010	61	<7		Ca-Na-Cl
79	[1]	SG-9	205500	1490	203	<7	8	Ca-Na-Cl
80	[1]	SG-10	189500	2380	172	<7		Ca-Na-Cl
81	[1]	SG-11	213700	1920	170	245		Ca-Na-Cl
82	[1]	SG-12	155200	1510	300	<7	27	Na-Ca-Cl
83	[1]	SG-13	208200	1920	170	77	8	Ca-Na-Cl
Middle Silurian (Niagaran)								
84	[1]	SN-1	209700	2160	79	<7	319	Ca-Na-Cl
85	[1]	SN-2	208500	1880	79	<7	295	Ca-Na-Cl
86	[1]	SN-3	230400	2390	59	<7		Ca-Cl
87	[1]	SN-4	256200	2360	38	<7		Ca-Cl
88	[1]	SN-5	245300	2440	42	<7		Ca-Na-Cl
89	[1]	SN-6	261800	2640	49	<7		Ca-Cl
90	[1]	SN-7	210700	2270	94	<7	8	Ca-Na-Cl
91	[1]	SN-8	187800	2240	105	<7	11	Ca-Na-Cl
92	[1]	SN-9	207100	1970	89	<7		Ca-Na-Cl
93	[1]	SN-10	202500	2320	89	<7	8	Ca-Na-Cl
94	[2]	Cold Srings WH1-29	244975	2570	36			Ca-Cl

Table B.1 Continued

No.	Author	Sample Name	Rock Type	Depth m	TDS mg/L	Ca mg/L	Na mg/L	Mg mg/L	K mg/L	Sr mg/L
Early Silurian (Grimsby/Thorhold)										
95	[1]	STGr-1	Sandstone	431	223900	29000	48100	5980	1000	464
96	[1]	STGr-2	Sandstone	380	258000	36700	51900	7030	1410	611
97	[1]	STGr-3	Sandstone	374	208700	27400	42200	6620	899	463
98	[1]	STGr-4	Sandstone	414	242800	34700	49400	6100	981	536
99	[1]	ST-5	Sandstone	292	232200	30500	44500	5830	1010	490
100	[1]	ST-6	Sandstone	408	231900	33700	45200	6210	1040	544
101	[1]	SGr-7	Sandstone	424	254300	33600	50600	5880	1010	530
102	[1]	SGr-8	Sandstone	426	257400	34200	49500	5840	1130	522
103	[1]	STGr-9	Sandstone	522	282200	42100	49700	7500	1260	697
104	[1]	STGr-10	Sandstone	524	311800	45700	58000	8000	1390	784
105	[1]	SGr-11	Sandstone	512	293500	44600	58700	7700	1450	745
106	[1]	SGr-12	Sandstone	524	191700	26900	38900	5310	878	456
107	[1]	STGr-13	Sandstone	547	229600	31400	45100	5630	877	509
108	[1]	STGr-14	Sandstone	541	325900	47700	58600	8230	1400	883
109	[1]	SGr-15	Sandstone	554	254800	34600	46900	6280	930	564
110	[1]	SGr-16	Sandstone	572	226100	28100	45800	4870	911	452
111	[1]	STGr-17	Sandstone	544	222700	29100	43300	5070	846	483
112	[1]	SGr-18	Sandstone	289	180800	39700	22800	6780	664	347
113	[1]	SGr-19	Sandstone	335	185600	39800	20900	3540	637	358
114	[1]	SGr-20	Sandstone	365	218500	42700	30300	5470	822	481
115	[1]	SGr-21	Sandstone	410	187300	42000	26400	3930	713	426
Early Silurian (Whirlpool)										
116	[1]	SW-1	Sandstone	361	248600	50400	32400	4250	782	489
117	[1]	SW-2	Sandstone	422	231000	47300	29900	3710	763	452
118	[1]	SW-3	Sandstone	422	267500	51100	36400	5500	870	507
119	[1]	SW-4	Sandstone	459	204700	43400	28200	4460	770	420
Late Ordovician (Blue Mountain)										
120	[6]	OHD-1 #15	Carbonate	173	185570	38600	21800	4520	404	702
Middle Ordovician (Trenton)										
121	[1]	OT-1	Carbonate	647	156900	15600	35700	3680	1600	529
122	[1]	OT-2	Carbonate	657	158200	16000	35300	3510	1600	540
123	[1]	OT-3	Carbonate	645	159400	15800	35800	3500	1630	467
124	[1]	OT-4	Carbonate	738	183700	23300	39800	5480	1970	402
125	[1]	OT-5	Carbonate	743	206700	23500	41400	6130	2120	739
126	[1]	OT-6	Carbonate	771	165000	17400	36900	4280	1690	574
127	[1]	OT-7	Carbonate	790	239800	35200	43600	7410	2310	606
128	[1]	OT-8	Carbonate	775	238500	32600	46800	6520	2410	525
129	[1]	OT-9	Carbonate	786	247300	36500	48800	7410	2270	612
130	[1]	OT-10	Carbonate	784	273600	36700	48700	7930	2330	633
131	[1]	OT-11	Carbonate	804	255500	36730	45700	7270	2320	733
132	[1]	OT-12	Carbonate	779	262100	39200	45300	6910	2120	729
133	[1]	OT-13	Carbonate	791	260700	32600	55200	7300	2390	578
134	[1]	OT-14	Carbonate	782	234300	33000	48700	6750	2390	548
135	[1]	OT-15	Carbonate	787	237800	31300	46100	6530	2300	527
136	[1]	OT-16	Carbonate	778	238900	32800	46100	6600	2680	529
137	[1]	OT-17	Carbonate	781	221800	29700	43200	5960	2150	568
138	[1]	OT-18	Carbonate	786	249000	34100	45400	6700	2310	658
139	[1]	OT-19	Carbonate	844	229400	31100	42000	5440	2190	518
140	[1]	OT-20	Carbonate		225000	27200	46500	5170	2080	467
141	[1]	OT-21	Carbonate	854	242700	32500	49700	5960	2070	619
142	[1]	OT-22	Carbonate	1225	195700	21700	41900	4470	3230	493
143	[1]	OT-23	Carbonate	1140	249700	31000	48000	5450	3390	595
144	[1]	OT-24	Carbonate	1247	195300	21800	42300	4270	3130	494
145	[1]	OT-25	Carbonate	1238	184800	18300	40300	3790	3060	447

Table B.1 Continued

No.	Author	Sample Name	Cl mg/L	Br mg/L	SO4 mg/L	HCO3 mg/L	F mg/L	Water Type
Early Silurian (Grimsby/Thorhold)								
95	[1]	STGr-1	137600	1340	385	<7		Na-Ca-Cl
96	[1]	STGr-2	158500	1550	259	<7		Na-Ca-Cl
97	[1]	STGr-3	129400	1260	447	<7		Na-Ca-Cl
98	[1]	STGr-4	149200	1580	320	<7		Na-Ca-Cl
99	[1]	ST-5	148100	1340	413	<7		Na-Ca-Cl
100	[1]	ST-6	143400	1430	339	<7		Na-Ca-Cl
101	[1]	SGr-7	160800	1510	332	<7		Na-Ca-Cl
102	[1]	SGr-8	164300	1540	345	<7		Na-Ca-Cl
103	[1]	STGr-9	179000	1650	272	<7		Na-Ca-Cl
104	[1]	STGr-10	195800	1970	164	<7		Na-Ca-Cl
105	[1]	SGr-11	178300	1870	174	<7		Na-Ca-Cl
106	[1]	SGr-12	117500	1130	657	<7		Na-Ca-Cl
107	[1]	STGr-13	144300	1380	423	<7		Na-Ca-Cl
108	[1]	STGr-14	207000	2010	123	<7		Na-Ca-Cl
109	[1]	SGr-15	163600	1490	404	<7		Na-Ca-Cl
110	[1]	SGr-16	144200	1250	530	<7		Na-Ca-Cl
111	[1]	STGr-17	142200	1260	450	<7		Na-Ca-Cl
112	[1]	SGr-18	109200	755	560	<7		Ca-Na-Cl
113	[1]	SGr-19	119400	694	235	<7		Ca-Na-Cl
114	[1]	SGr-20	137400	920	405	<7		Ca-Na-Cl
115	[1]	SGr-21	112600	855	329	<7		Ca-Na-Cl
Early Silurian (Whirlpool)								
116	[1]	SW-1	158800	1130	320	47	8	Ca-Na-Cl
117	[1]	SW-2	147500	1000	376	60		Ca-Na-Cl
118	[1]	SW-3	171600	1190	375	<7		Ca-Na-Cl
119	[1]	SW-4	126100	920	433	<7		Ca-Na-Cl
Late Ordovician (Blue Mountain)								
120	[6]	OHD-1 #15	118300	1080	120	44		Ca-Na-Cl
Middle Ordovician (Trenton)								
121	[1]	OT-1	98700	578	453	<7	4	Na-Ca-Cl
122	[1]	OT-2	99800	725	742	34		Na-Ca-Cl
123	[1]	OT-3	101100	563	575	<7	5	Na-Ca-Cl
124	[1]	OT-4	111300	832	630	<7	6	Na-Ca-Cl
125	[1]	OT-5	131800	856	152	<7	6	Na-Ca-Cl
126	[1]	OT-6	103200	550	410	58	4	Na-Ca-Cl
127	[1]	OT-7	149500	920	263	17		Na-Ca-Cl
128	[1]	OT-8	148100	1190	353	33		Na-Ca-Cl
129	[1]	OT-9	150500	950	263	<7		Na-Ca-Cl
130	[1]	OT-10	175900	1170	260			Na-Ca-Cl
131	[1]	OT-11	160900	1610	271			Na-Ca-Cl
132	[1]	OT-12	166100	1370	321			Na-Ca-Cl
133	[1]	OT-13	161200	1150	320	32		Na-Ca-Cl
134	[1]	OT-14	141400	1170	358	<7	8	Na-Ca-Cl
135	[1]	OT-15	149500	1120	380	60	8	Na-Ca-Cl
136	[1]	OT-16	148600	1220	347	49	13	Na-Ca-Cl
137	[1]	OT-17	138600	1270	366	<7		Na-Ca-Cl
138	[1]	OT-18	158300	1210	348			Na-Ca-Cl
139	[1]	OT-19	147000	780	393	12		Na-Ca-Cl
140	[1]	OT-20	142300	765	485	45		Na-Ca-Cl
141	[1]	OT-21	150300	1190	335	<7	246	Na-Ca-Cl
142	[1]	OT-22	122700	625	620	49		Na-Ca-Cl
143	[1]	OT-23	159800	1160	327	86		Na-Ca-Cl
144	[1]	OT-24	122000	925	402	66	168	Na-Ca-Cl
145	[1]	OT-25	117600	797	538	90	160	Na-Ca-Cl

Table B.1 Continued

No.	Author	Sample Name	Rock Type	Depth m	TDS mg/L	Ca mg/L	Na mg/L	Mg mg/L	K mg/L	Sr mg/L
Middle Ordovician (Trenton)										
146	[1]	OT-26	Carbonate	1203	188300	19200	41300	4360	3330	490
147	[1]	OT-27	Carbonate	1287	196000	20500	42500	4620	3490	505
148	[1]	OT-28	Carbonate	1299	190700	19800	42000	4320	3460	489
149	[1]	OT-29	Carbonate	1278	190200	21400	41200	4670	3490	512
150	[1]	OT-30	Carbonate	1280	346100	54900	53200	7790	5250	1060
151	[1]	OT-31	Carbonate	1279	218200	23800	46200	5070	3960	564
152	[1]	OT-32	Carbonate	1259	214600	23800	45900	5170	3770	546
153	[1]	OT-33	Carbonate	1289	190700	21600	41900	4110	3890	518
154	[1]	OT-34	Carbonate	1290	209500	22200	44100	4280	3990	550
155	[1]	OT-35	Carbonate	1292	199300	20700	42500	4090	3650	507
156	[1]	OT-36	Carbonate	1292	199400	21400	42500	3960	3770	478
157	[1]	OT-37	Carbonate	1288	199400	20900	43000	4130	3760	508
158	[1]	OT-38	Carbonate	1293	208700	25300	41800	4720	3300	477
159	[1]	OT-39	Carbonate	637	160900	13100	38800	3670	2010	473
160	[1]	OT-40	Carbonate	308	139500	9850	36400	3720	1840	524
161	[1]	OT-41	Carbonate	310	140900	10800	36400	3850	1850	496
162	[1]	OT-42	Carbonate	614	142100	10500	37500	3670	1880	567
163	[6]	UN-2 #13	Carbonate	50	44113	6250	8120	1840	141	277
164	[6]	OHD-1 #13	Carbonate	204	136737	26600	18400	3280	321	515
165	[6]	UN-2 #11	Carbonate	85	101983	15100	17900	4080	271	705
Middle Ordovician (Black River)										
166	[6]	OHD-1 #7	Carbonate	295	297766	58000	37100	7080	636	1210
167	[6]	UN-2 #5	Carbonate	175	251375	36000	40800	11200	709	1130
168	[6]	OHD-1 #5A	Carbonate	326	290235	57800	35700	7100	641	1200
169	[6]	OHD-1 #5B	Carbonate	326	290351	59000	38500	7230	651	1220
170	[6]	OHD-1 #3	Carbonate	353	304086	58500	35100	7150	649	1220
171	[6]	UN-2 #2	Carbonate	210	97385	15000	17400	4090	322	335
172	[6]	UN-2 #4	Carbonate	190	153987	23400	24900	7230	469	488
173	[6]	OHD-1 #2	Sandstone	368	295752	58300	37600	7200	657	1220
Early Ordovician (Prairie du Chien)										
174	[1]	OP-1	Sandstone	3425	325400	68000	26700	7200	14200	2350
175	[2]	LAHAR 1-7	Sandstone		390707	89200	30120	7560	12720	3632
176	[2]	FOSTER 1-21	Sandstone		344142	65250	43500	5568	9483	2906
177	[2]	PRASS 1-12	Sandstone		291389	67600	22702	5744	10600	2848
178	[1]	OP-2	Sandstone	3234	391500	87500	22600	8700	18400	2850
Cambrian										
179	[1]	C-1	Sandstone	1217	279200	47900	41000	6750	1410	1210
180	[1]	C-2	Sandstone	1095	337600	60000	47700	6710	1340	1640
181	[1]	C-3	Sandstone	1097	325600	60200	48500	6680	1330	1690
182	[1]	C-4	Sandstone	1212	306000	57800	49900	7710	1480	1170
183	[1]	C-5	Sandstone	1070	174100	32100	24900	3240	645	1010
184	[1]	C-6	Sandstone	1011	179200	22400	40100	4380	2060	418
185	[1]	C-7	Sandstone	1209	276600	46500	43400	5860	1380	1210
186	[1]	C-8	Sandstone	1264	307400	51200	50800	6510	1810	1320
187	[1]	C-9	Sandstone	1201	301100	52800	45000	7060	1560	1290
188	[1]	C-10	Sandstone	1203	289200	50500	43600	6900	1550	1210
189	[1]	C-11	Sandstone	1149	269900	43600	47700	5340	1570	1130
190	[1]	C-12	Sandstone	1087	288600	53500	42100	5670	1150	1230
191	[1]	C-13	Sandstone	887	305200	54800	44200	7180	937	1210
Precambrian										
192	[6]	OHD-1 #1	Granitic	380	287807	68500	32200	5030	499	1400

Table B.1 Continued

No.	Author	Sample Name	Cl mg/L	Br mg/L	SO4 mg/L	HCO3 mg/L	F mg/L	Water Type
Middle Ordovician (Trenton)								
146	[1]	OT-26	118500	857	256	81	171	Na-Ca-Cl
147	[1]	OT-27	123200	917	312	69	184	Na-Ca-Cl
148	[1]	OT-28	119400	650	622	48	8	Na-Ca-Cl
149	[1]	OT-29	117600	917	418	66	191	Na-Ca-Cl
150	[1]	OT-30	222000	1780	129	95	10	Ca-Na-Cl
151	[1]	OT-31	137300	909	411	73	10	Na-Ca-Cl
152	[1]	OT-32	134100	890	400	61	708	Na-Ca-Cl
153	[1]	OT-33	117500	725	460	57	7	Na-Ca-Cl
154	[1]	OT-34	133000	911	474	71	6	Na-Ca-Cl
155	[1]	OT-35	126400	872	535	96	8	Na-Ca-Cl
156	[1]	OT-36	126100	650	505	48	8	Na-Ca-Cl
157	[1]	OT-37	125700	877	491	75	7	Na-Ca-Cl
158	[1]	OT-38	131800	789	507	<7	7	Na-Ca-Cl
159	[1]	OT-39	101900	510	415	61		Na-Ca-Cl
160	[1]	OT-40	86600	460	66	66		Na-Ca-Cl
161	[1]	OT-41	87000	440	66	137		Na-Ca-Cl
162	[1]	OT-42	87500	460	<15	76		Na-Ca-Cl
163	[6]	UN-2 #13	26975	282	175	53		Na-Ca-Cl
164	[6]	OHD-1 #13	86700	755	125	41		Ca-Na-Cl
165	[6]	UN-2 #11	63050	635	210	32		Na-Ca-Cl
Middle Ordovician (Black River)								
166	[6]	OHD-1 #7	192045	1555	140	<7		Ca-Na-Cl
167	[6]	UN-2 #5	159900	1445	165	26		Ca-Na-Mg-Cl
168	[6]	OHD-1 #5A	186000	1620	145	29		Ca-Na-Cl
169	[6]	OHD-1 #5B	182000	1595	155	<7		Ca-Na-Cl
170	[6]	OHD-1 #3	200500	817	150	<7		Ca-Na-Cl
171	[6]	UN-2 #2	59000	619	575	44		Na-Ca-Cl
172	[6]	UN-2 #4	96000	935	520	45		Ca-Na-Mg-Cl
173	[6]	OHD-1 #2	189000	1620	155	<7		Ca-Na-Cl
Early Ordovician (Prairie du Chien)								
174	[1]	OP-1	205000	1930	63	<7		Ca-Na-Cl
175	[2]	LAHAR 1-7	245673	1719	83			Ca-Cl
176	[2]	FOSTER 1-21	215081	2311	43			Ca-Na-Cl
177	[2]	PRASS 1-12	179576	2229	91			Ca-Cl
178	[1]	OP-2	249700	1780	<30	<7		CaCl
Cambrian								
179	[1]	C-1	179000	1680	277	<7		Ca-Na-Cl
180	[1]	C-2	218700	1420	52	21		Ca-Na-Cl
181	[1]	C-3	205600	1550	47	19		Ca-Na-Cl
182	[1]	C-4	186100	1710	96	<7	11	Ca-Na-Cl
183	[1]	C-5	110100	1110	980	<7		Ca-Na-Cl
184	[1]	C-6	108400	792	645	<7	11	Na-Ca-Cl
185	[1]	C-7	176500	1510	247	<7		Ca-Na-Cl
186	[1]	C-8	193400	2260	134	<7		Ca-Na-Cl
187	[1]	C-9	191800	1450	131	17		Ca-Na-Cl
188	[1]	C-10	183800	1440	169	17		Ca-Na-Cl
189	[1]	C-11	168700	1610	210	<7		Ca-Na-Cl
190	[1]	C-12	183000	1770	138	<7		Ca-Na-Cl
191	[1]	C-13	194900	1835	146	<7		Ca-Na-Cl
Precambrian								
192	[6]	OHD-1 #1	178400	1635	143	<7		Ca-Na-Cl

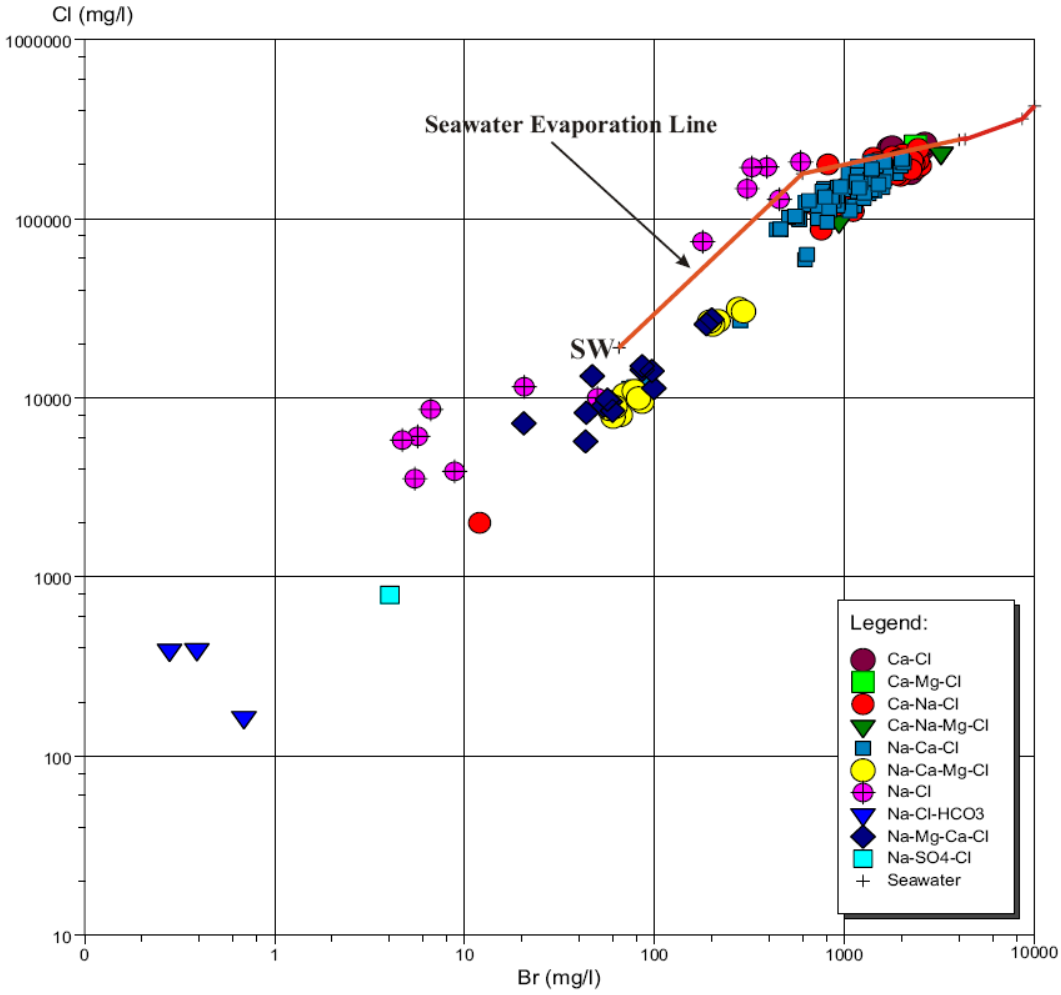

Figure B.1 Logarithmic plot (Cl versus Br) of southern Ontario and Michigan formation waters. Samples were grouped according to their water type.

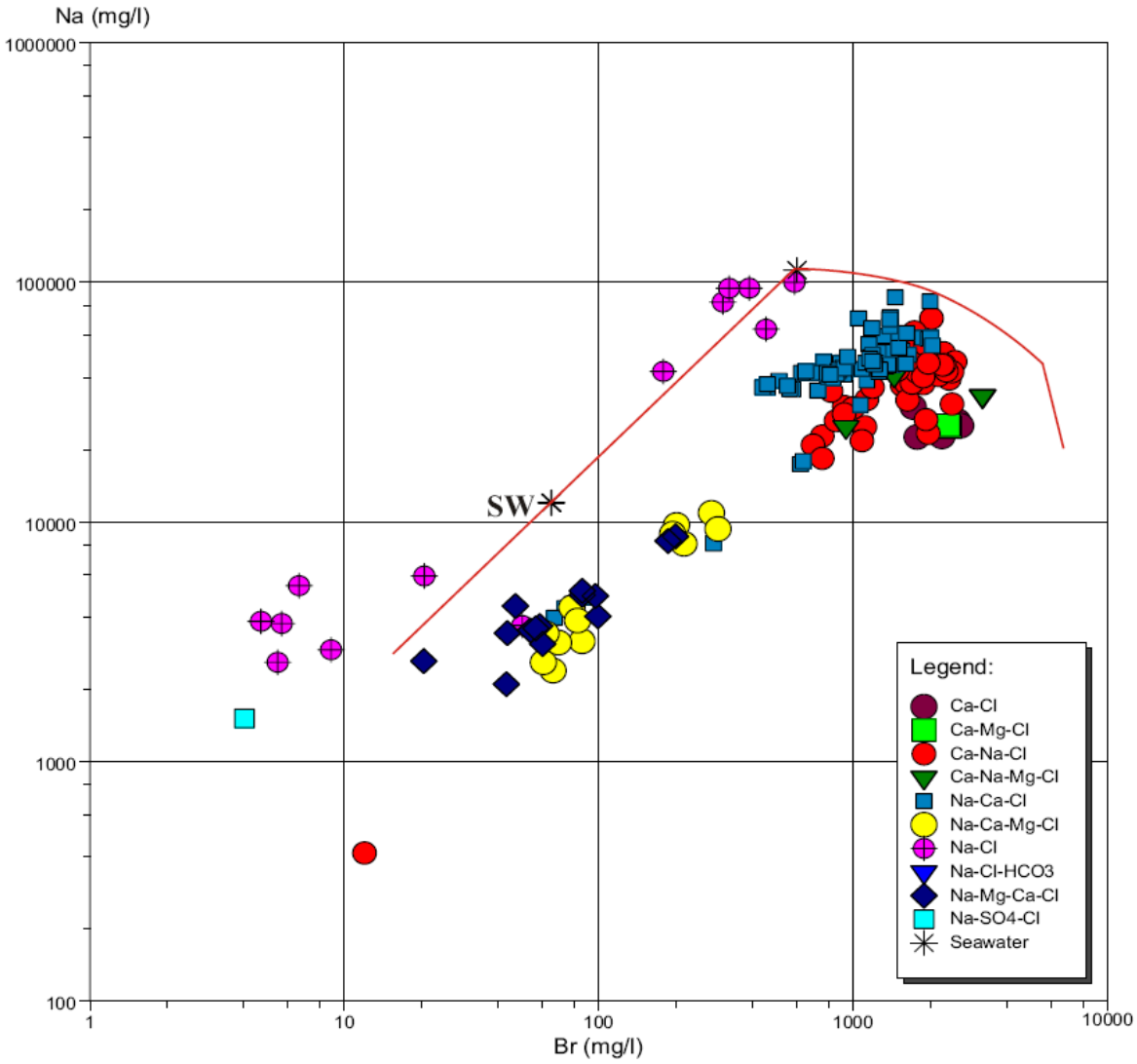

Figure B.2 Na (mg/L) versus Br (mg/L) of the southern Ontario and Michigan samples in comparison to the seawater evaporation line. (after Carpenter, 1978).

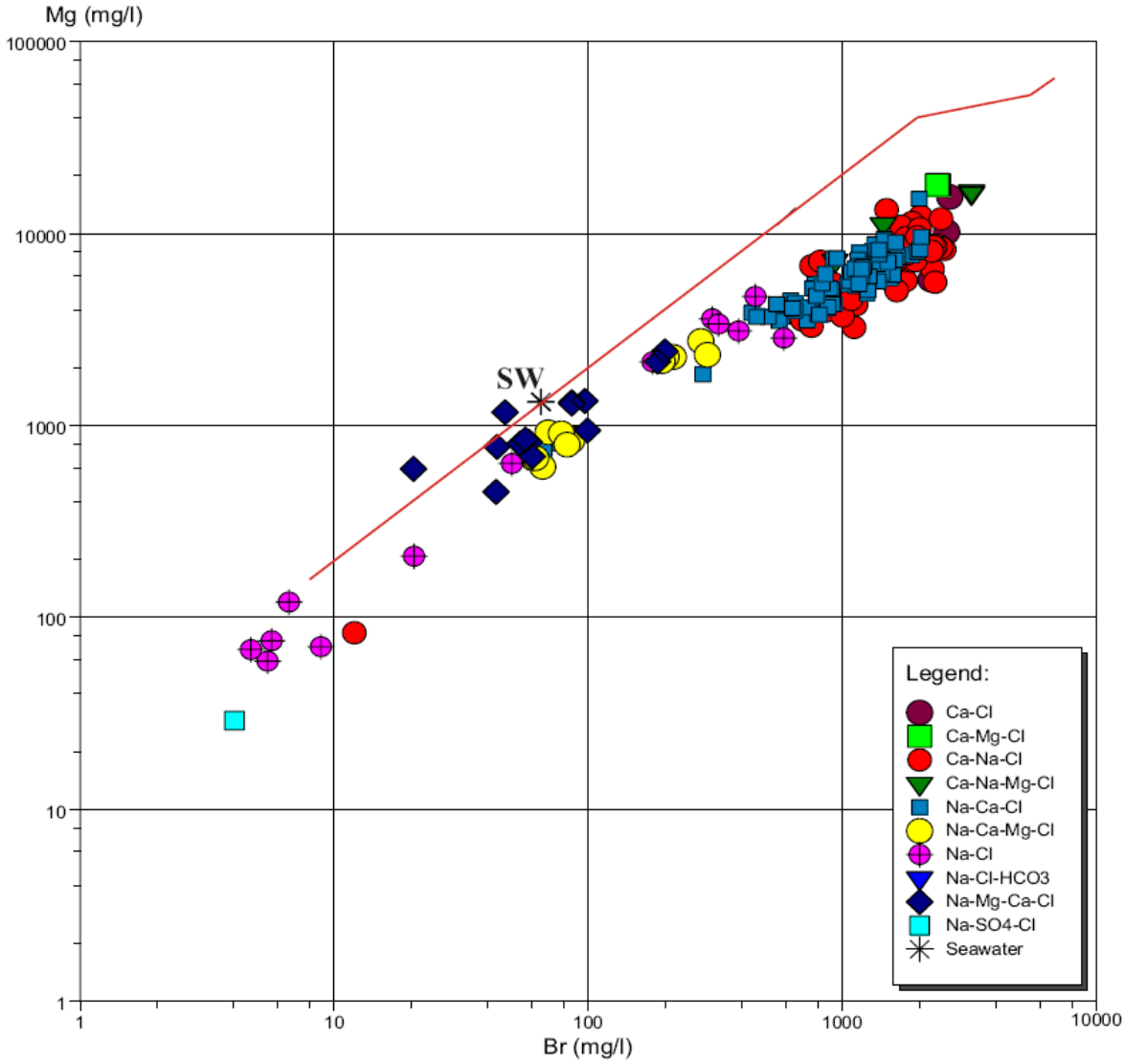

Figure B.3 Mg (mg/L) versus Br (mg/L) of the southern Ontario and Michigan samples in comparison to the seawater evaporation line. (after Carpenter, 1978).

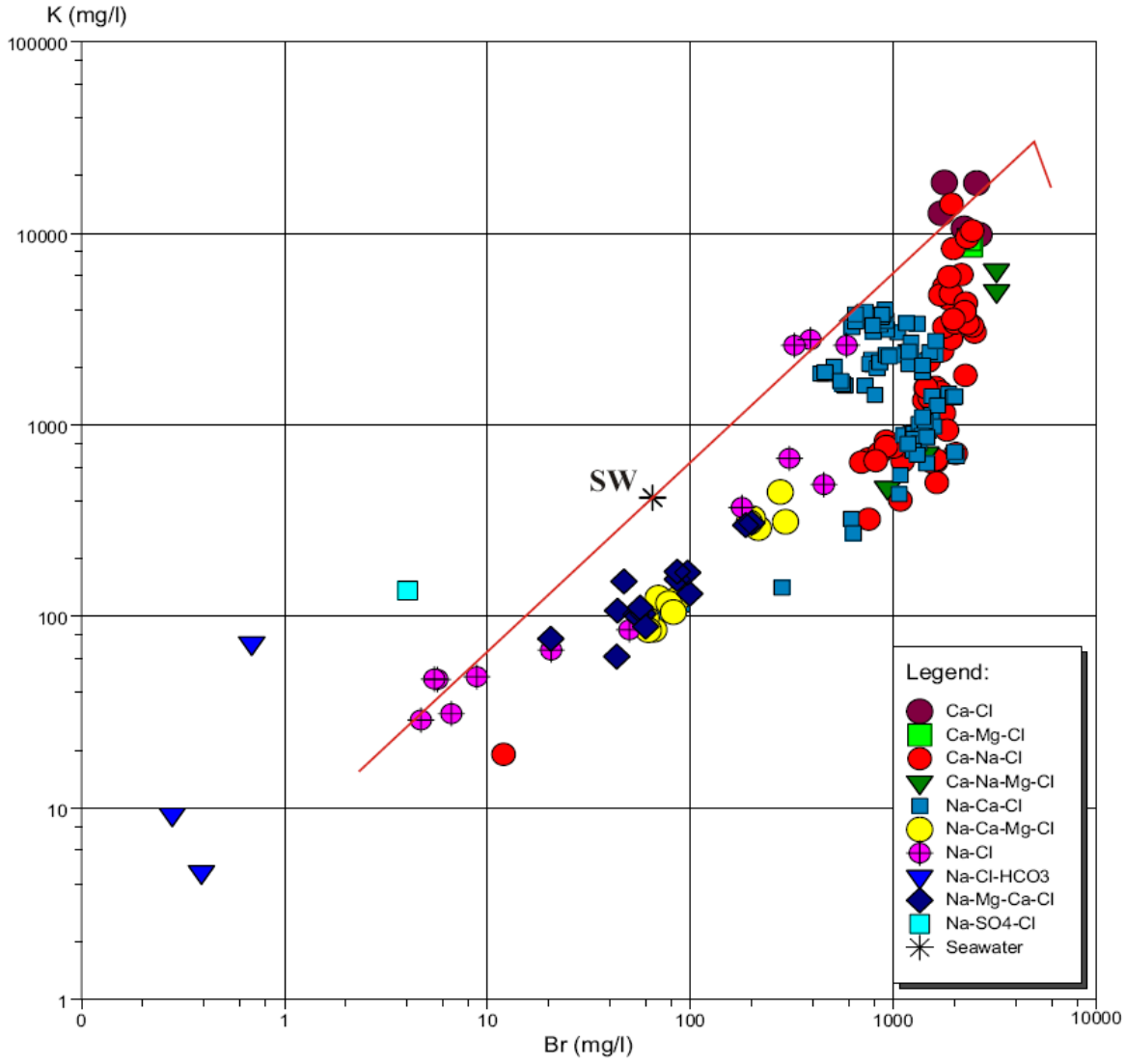

Figure B.4 K (mg/L) versus Br (mg/L) of the southern Ontario and Michigan samples in comparison to the seawater evaporation line. (after Carpenter, 1978).

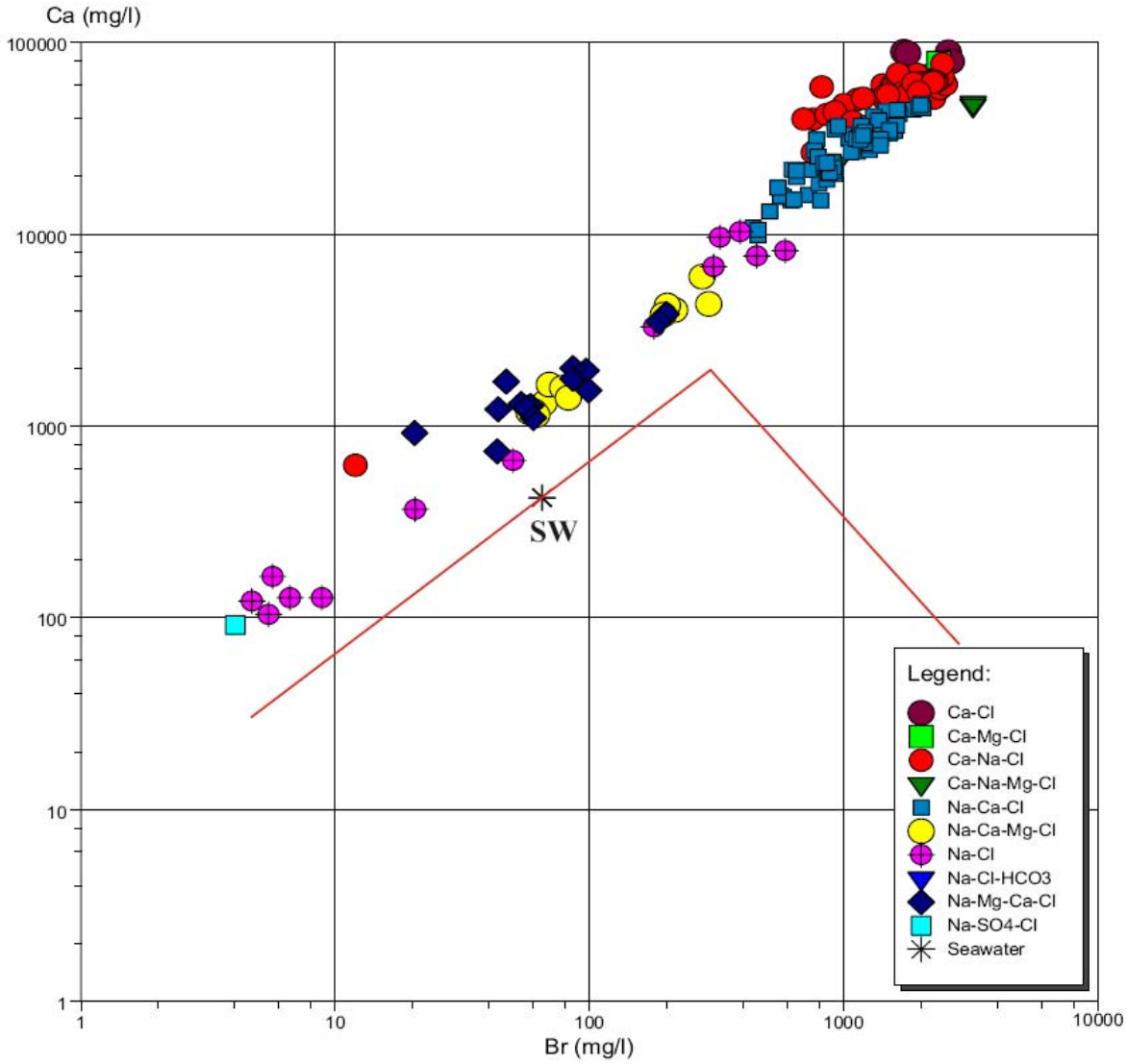

Figure B.5 Ca (mg/L) versus Br (mg/L) of the southern Ontario and Michigan samples in comparison to the seawater evaporation line. (after Carpenter, 1978).

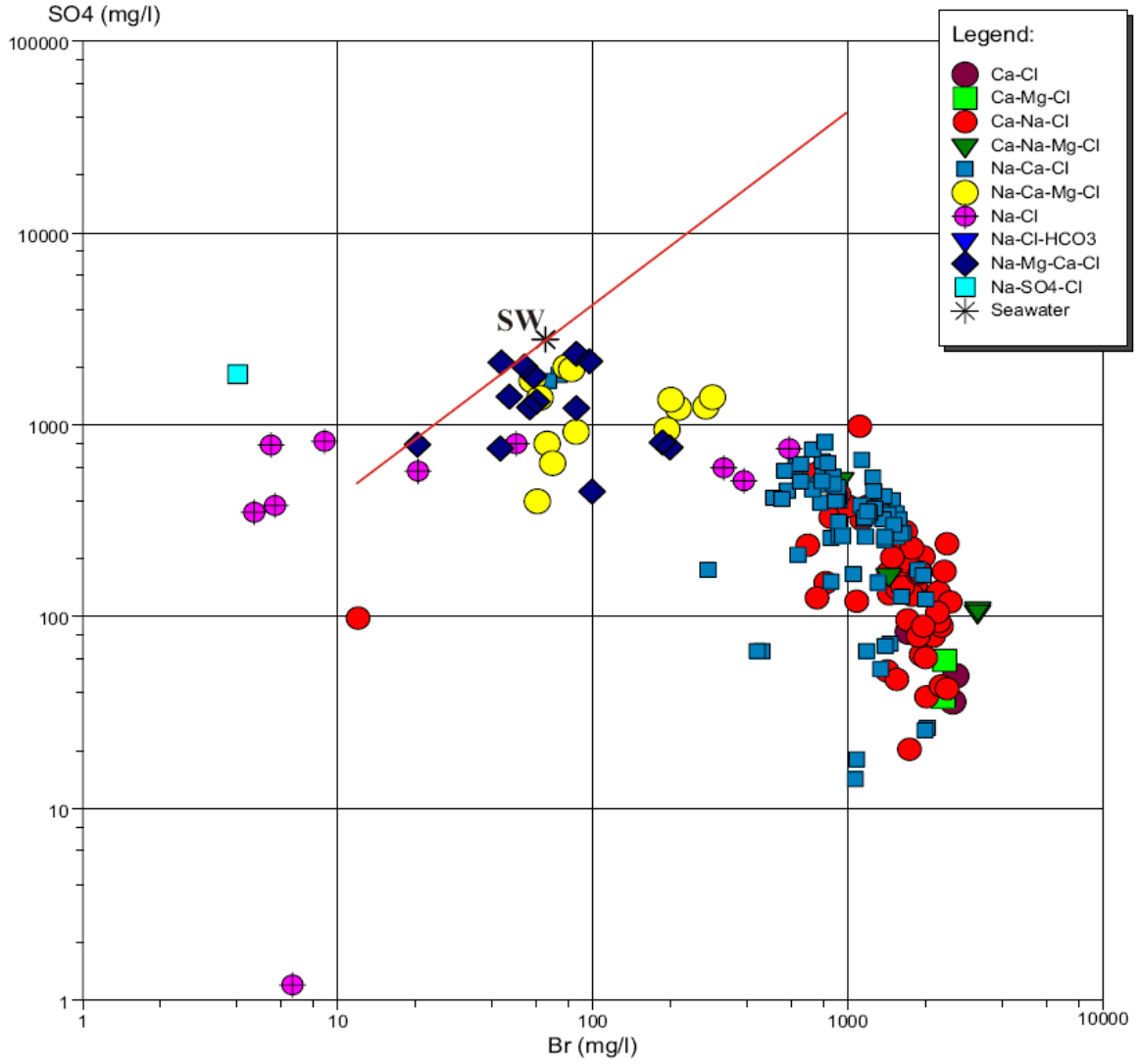

Figure B.6 SO_4 (mg/L) versus Br (mg/L) of the southern Ontario and Michigan samples in comparison to the seawater evaporation line. (after Carpenter, 1978).

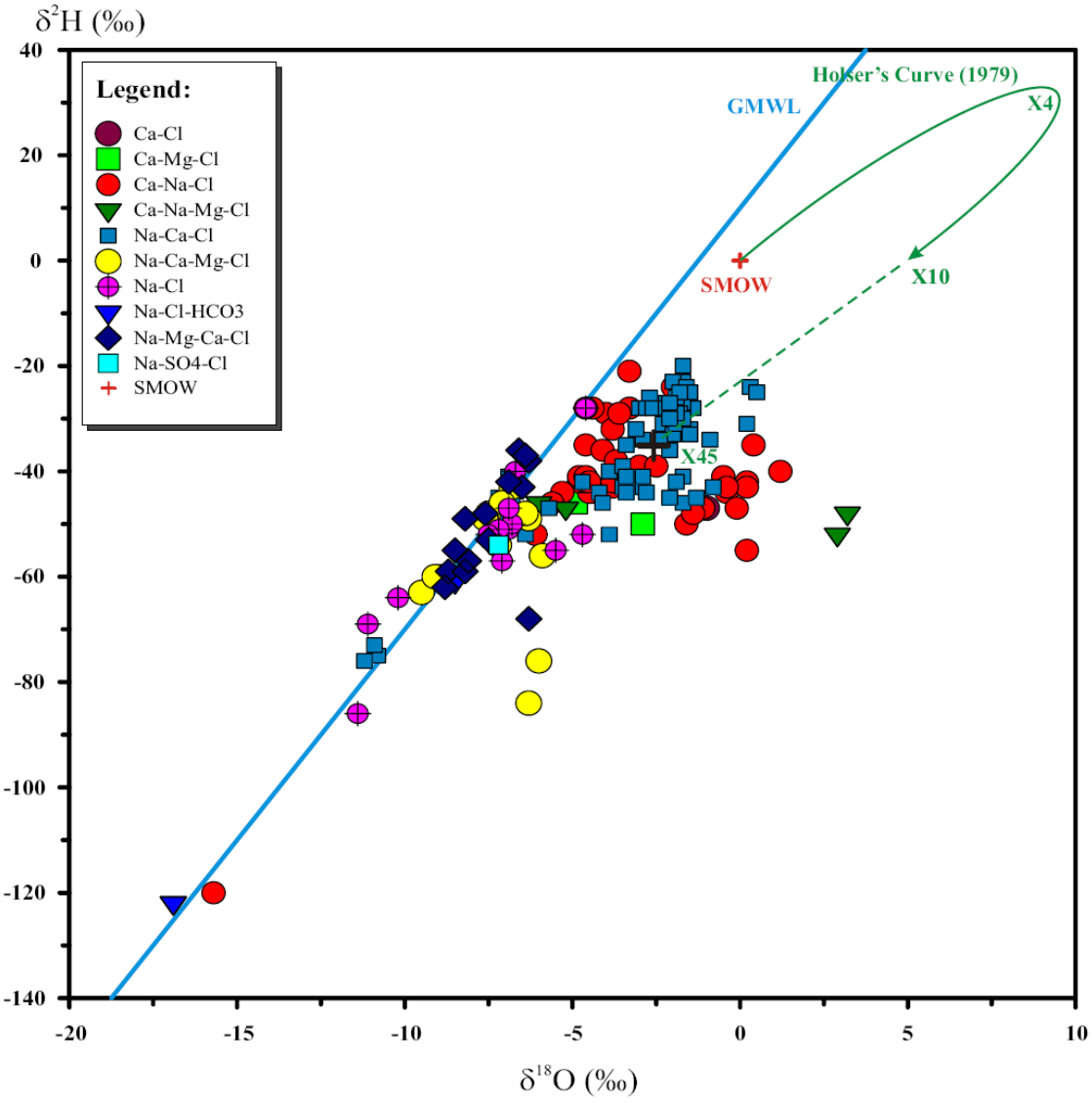

Figure B.7 δ^2H_{VSMOW} (‰) versus $\delta^{18}O_{VSMOW}$ (‰) of all southern Ontario and Michigan formation waters grouped based on their water types.

Table B.2 The isotopic ($\delta^{37}Cl$ and $\delta^{81}Br$) ranges for the formation waters in southern Ontario and Michigan Basin based on the stratigraphic units they were sampled from.

Formation or Group	Variations in $\delta^{37}Cl$ values	Variations in $\delta^{81}Br$ values
Mississippian (Berea)	-0.40 ‰ to +0.10 ‰	
Late Devonian (Kettle Point)	-1.11 ‰ to +1.82 ‰	
Late Devonian (Hamilton)	0.00 ‰ to +0.89 ‰	
Middle Devonian (Dundee)	-0.72 ‰ to +1.25 ‰	-0.21 ‰ to +0.92 ‰
Middle Devonian (Detroit River)	-0.50 ‰ to +0.94 ‰	-0.23 ‰ to +0.63 ‰
Middle Silurian (F Salt)	-0.20 ‰	
Middle Silurian (A-1 Carbonate)	-0.35 ‰	
Middle Silurian (Guelph)	-0.51 ‰ to -0.15 ‰	-0.95 ‰ to -0.61 ‰
Middle Silurian (Niagaran)	-1.04 ‰ to -0.22 ‰	-0.92 ‰ to -0.28 ‰
Early Silurian (Grimsby)	+0.13 ‰ to +0.78 ‰	+0.77 ‰ to +1.74 ‰
Early Silurian (Whirlpool)	+0.60 ‰ to 0.86 ‰	+2.11 ‰ to +2.31 ‰
Late Ordovician (Blue Mountain)	+0.09 ‰	+1.75 ‰
Middle Ordovician (Trenton)	-1.31 ‰ to +0.32 ‰	-0.49 ‰ to +2.15 ‰
Middle Ordovician (Black River)	-0.14 ‰ to +0.32 ‰	+1.18 ‰ to +1.94‰
Middle Ordovician (PDU)	-104 ‰ to -0.18 ‰	-0.73 ‰ to -0.55 ‰
Cambrian	-0.50 ‰ to +0.19 ‰	+0.71 ‰ to +1.51 ‰
Precambrian	+0.30 ‰	

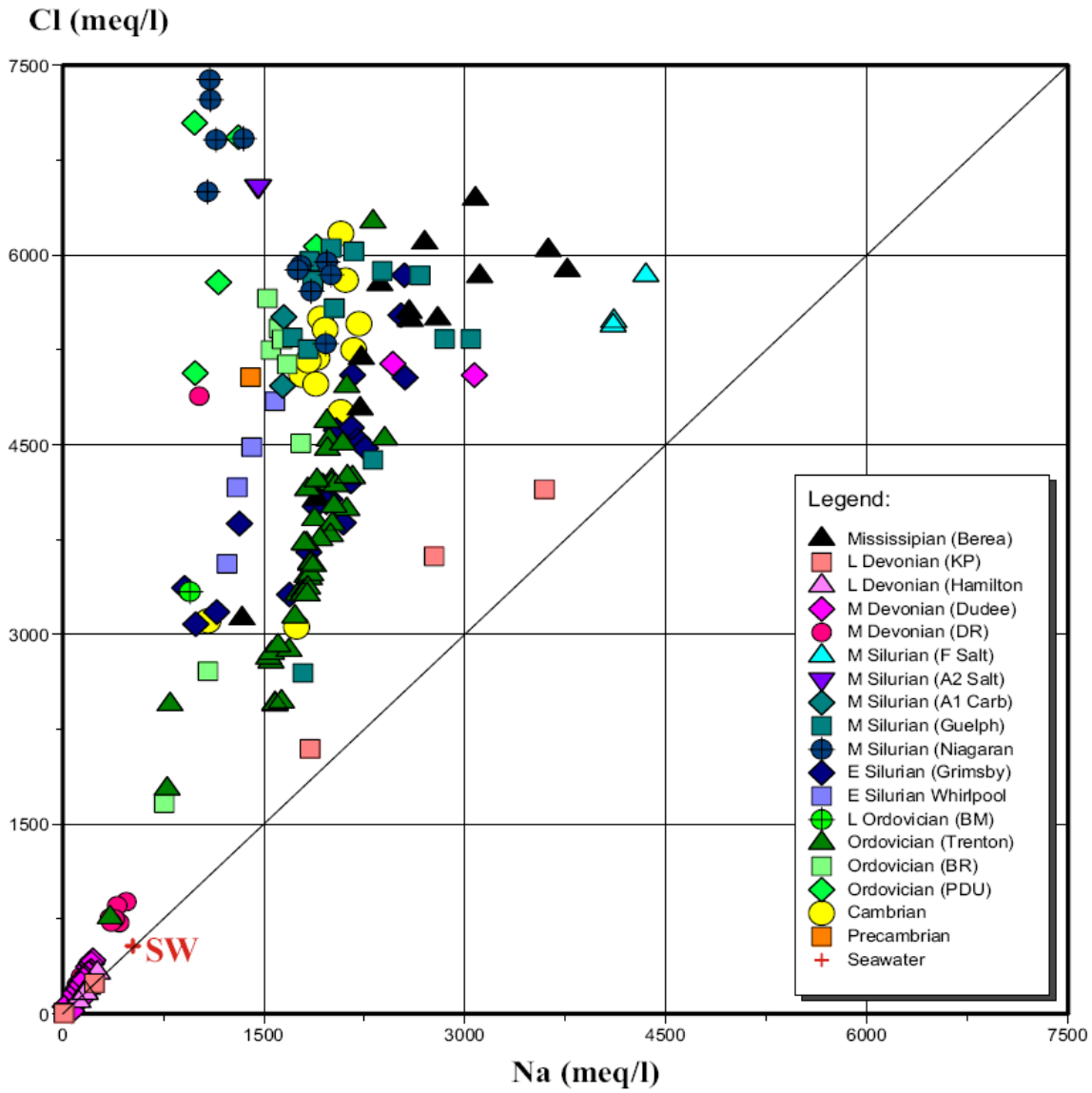

Figure B.8 Na (meq/L) versus Cl (meq/L) of the southern Ontario and Michigan samples based on the stratigraphic units they belonged to. The Na:Cl (1:1 line) expected for the halite dissolution is illustrated also in the plot.

Appendix C

Table C.1 Geochemical data of the Williston Basin formation waters. Formation waters are from different stratigraphic units (Early Cretaceous to Cambrian). (Note: The samples and data presented in this table were compiled from various authors: [1] Rostron et al., 2002; [2] Jensen, 2007; [3] Iampen, 2003; [4] Jensen et al., 2006.)

No.	Sample ID	Author	BH Latitude	BH Longitude	Depth (m)	Temp (°C)	Ph	density	Water Type
Early Cretaceous (Mannville Group)									
1	99-116		49.415539	103.499031	1032	45	7.56	1.0031	Na-Cl
2	00-101		49.363884	103.511909	1046	41	8.17	1.0025	Na-Cl
3	01-205	[1]	49.468548	103.708702	1044	42	7.75	1.0076	Na-Cl
4	02-128		49.415539	103.499031	1032	45	7.75	1.006	Na-Cl-HCO3
Mississippian (Poplar Member)									
5	01-033	[1]	49.309834	104.805626	1587	57	nd	nd	Na-Cl-SO4
Mississippian (Ratcliffe Member)									
6	05-106	[2]	47.962631	103.685886	2856	104	nd	nd	Na-Cl
7	05-109	[2]	47.857765	104.018553	2732	95	6.07	1.2065	Na-Cl
8	05-111	[2]	48.114439	103.781117	2809	98	nd	nd	Na-Cl
Mississippian (Midale Member)									
9	99-117		49.415379	103.455070	1474	61.4	6.35	1.1246	Na-Cl
10	00-180		49.415478	103.421410	1467	61	6.6	1.1265	Na-Cl
11	00-190		49.546276	103.386664	1359	62	7.04	1.0715	Na-Cl
12	01-128	[2]	48.606134	103.017776	2456	89	5.79	1.2015	Na-Cl
13	01-129	[2]	48.602112	103.023225	2453	83	nd	nd	Na-Cl
14	05-103	[2]	48.135740	103.584204	2809	98	nd	nd	Na-Cl
15	05-104	[2]	48.201704	103.487600	2881	106	nd	nd	Na-Cl
16	05-110	[2]	47.540328	103.094908	2879	101	nd	nd	Na-Cl
17	05-115	[2]	48.002414	103.591718	2883	105	nd	nd	Na-Cl
18	05-117	[2]	47.839184	104.029676	2755	104	6.11	nd	Na-Cl
Mississippian (Frobisher Member)									
19	00-116		49.537922	103.261841	1360	54	6.72	1.0995	Na-Cl
20	00-117		49.542480	103.228294	1351	54	6.86	1.0985	Na-Cl
21	02-019		49.684620	103.324142	1255	58	nd	nd	
22	05-112	[2]	47.546827	103.083983	2855	104	nd	nd	Na-Cl
23	05-119	[2]	48.308875	103.554015	2778	99	6.45	nd	Na-Cl
Mississippian (Lodgepole Formation)									
24	00-04	[1]	49.349953	104.821915	1846	56	nd	nd	Na-K-Cl-SO4
Late Devonian (Bakken Formation)									
25	97-23	[3]	49.519096	103.412277	1719	71	6.42	1.16	Na-Cl
26	98-20	[3]	49.521278	103.415405	1718	71	nd	nd	Na-Cl
27	98-21	[3]	49.538319	103.399971	1703	71	nd	nd	Na-Cl
28	98-43	[3]	48.609373	102.861120	2809	98	6.06	nd	Na-Cl
29	98-56	[3]	49.518135	103.411545	1720	71	nd	nd	Na-Cl
30	99-48	[3]	48.609739	102.975285	2822	107	6.01	1.1957	Na-Cl
31	99-69	[3]	48.446634	102.948018	2943	99	6.10	1.1951	Na-Cl
32	01-108		47.290129	102.780465	3303	106	5.98	1.1935	Na-Cl
33	01-115		47.291901	102.773457	3278	103	5.47	1.1951	Na-Cl
34	01-116		47.071580	103.572442	3128	101	5.16	1.212	Na-Ca-Cl
35	01-117		47.092307	103.587434	3135	104	5.13	1.1965	Na-Cl
36	01-118		47.755130	104.294950	3189		nd	nd	Na-Cl
37	01-119		47.803230	104.412840	3189		6.43	1.1435	Na-Cl
38	01-122		47.741770	104.430870	3186		6.35	1.2075	
39	01-125		48.842100	104.894960	2282		6.31	1.16	Na-Cl
40	01-126		47.786710	104.359920	3180		6.8	1.085	Na-Cl
41	01-150		48.717685	102.933323	2699	103	6.42	1.157	Na-Cl
42	01-171	[1]	49.472649	104.478668	1947	62	nd	nd	Na-Cl
43	01-404	[1]	49.147205	104.445717	2227	74	nd	nd	Na-Cl
44	02-016		49.518158	103.412048	1720	71	nd	nd	
45	02-205		49.535255	103.409576	1701	71	6.41	1.1525	Na-Cl

Table C.1 Continued

No.	Sample ID	Author	BH Latitude	BH Longitude	Depth (m)	Temp (°C)	Ph	density	Water Type
Late Devonian (Birdbear Formation)									
46	97-14	[3]	49.517406	103.388321	1790	75	6	1.184	Na-Cl
47	97-32	[3]	49.517406	103.388321	1790	75	nd	nd	Na-Cl
48	98-18	[1]	49.470104	103.421410	1838	75	nd	nd	Na-Cl
49	98-125	[1]	49.470104	103.421410	1838	75	nd	nd	Na-Cl
50	99-25	[3]	47.216217	103.736501	3218	116	6.01	1.1976	Na-Cl
51	01-105		47.151175	103.657314	3258	119	5.63	1.204	Na-Ca-Cl
52	01-106		47.259581	103.739711	3188	116	5.47	1.205	Na-Ca-Cl
53	01-107		47.162280	103.669158	3241	112	5.82	1.168	Na-Ca-Cl
54	01-402	[1]	49.151577	104.446304	2309	78	6.31	1.1545	Na-Cl
55	01-403	[1]	49.154221	104.440437	2317	78	6.2	1.155	Na-Cl
56	01-405	[1]	49.186249	104.726852	2184	71	7.47	1.016	Na-Cl-SO4
Late Devonian (Duperow Formation)									
57	98-28	[3]	48.947288	103.494599	2569	87	nd	nd	Na-Ca-Cl
58	98-40	[3]	48.918441	103.711766	2616	91	5.66	1.2071	Na-Cl
59	98-41	[3]	48.788032	103.566845	2800	88	5.59	1.1976	Na-Cl
60	98-123	[1]	49.558506	103.476746	1989	76	nd	nd	Na-Ca-Cl
61	99-26	[3]	47.176037	103.690634	3373	110	5.72	1.2200	Na-Ca-Cl
62	99-40	[3]	47.309707	103.098512	3489	117	5.65	1.2360	Na-Ca-Cl
63	99-42	[3]	47.105558	103.325994	3446	134	6.27	1.1949	Na-Ca-Cl
64	99-46	[3]	48.619942	103.111918	3087	113	5.79	1.2015	Na-Ca-Cl
65	99-47	[3]	48.580825	103.009742	3091	112	6.13	1.12-1.19	Na-Ca-Cl
66	99-49	[3]	48.479379	102.920699	3090	117	5.28	1.2403	Ca-Na-Cl
67	99-52	[3]	48.472109	102.909722	3093	120	5.25	1.2461	Ca-Na-Cl
68	99-53	[3]	47.914577	103.740754	3484	117	5.19	1.2429	Ca-Na-Cl
69	99-95	[3]	47.222034	103.396170	3459	127	nd	nd	Na-Ca-Cl
70	99-96	[3]	47.388812	103.484373	3410	126	nd	nd	Na-Ca-Cl
71	00-17	[1]	49.124603	104.815804	2386	79	nd	nd	Na-Cl
72	00-44	[1]	49.124603	104.815804	2386	79	nd	nd	Na-Cl
73	00-61	[1]	49.349606	104.791672	2191	70	nd	nd	Na-Cl
74	01-136		48.507830	104.423910	2861	105	6.37	1.2055	Na-Ca-Cl
75	01-141		48.340792	103.768498	3298	110	5.17	1.18-1.250	Ca-Na-Cl
76	01-203	[1]	49.524559	103.403198	1888	76	5.92	1.1918	Na-Cl
Middle Devonian (Dawson Bay Formation)									
77	99-56	[3]	47.905720	104.700100	3218	109	5.99	1.1936	Na-Cl
78	99-57	[3]	47.876400	104.710300	3290	110	5.97	1.1949	Na-Cl
79	00-201	[3]	47.447390	104.962320	3130	109	nd	nd	Na-Ca-Cl
80	01-131		47.661740	105.071660	3013		5.85	1.192	Na-Ca-Cl
Middle Devonian (Prairie Formation)									
81	02-345	[4]	52.095800	106.866700	1025		nd	nd	Ca-Cl
Middle Devonian (Winnipegosis Formation)									
82	98-45	[3]	48.740362	102.942186	3275	104	5.78	1.1656	Na-Ca-Cl
83	98-46	[3]	48.729327	103.352543	3193	104	6.05	nd	Na-Ca-Cl
84	98-58	[3]	49.684620	103.324142	2085	75	6.08	1.1901	Na-Cl
85	99-75	[3]	49.560486	103.474976	2252	81	6.69	1.1990	Na-Cl
86	01-147		48.717810	102.931829	3253	103	7.41	1.01-1.12	Na-Ca-Cl
87	01-151		48.505970	102.969320	3436	102	5.85	1.180-1.250	Na-Ca-Cl
88	01-407	[1]	49.208008	104.805138	2566	74	6.65	1.1645	Na-Cl
89	01-408	[1]	49.189781	104.743988	2603	74	6.36	1.168	Na-Cl
90	01-411	[1]	49.182419	104.731789	2610	74	6.4	nd	Na-Cl
91	02-215		49.427120	102.608704	2192	80	5.82	1.206	Na-Cl
92	02-216		49.422802	102.609100	2197	79	nd	nd	Na-Cl

Table C.1 Continued

No.	Sample ID	Author	BH Latitude	BH Longitude	Depth (m)	Temp (°C)	Ph	density	Water Type
Early to Middle Silurian (Interlake Formation)									
93	98-44	[3]	48.664943	102.856115	3669	122	nd	nd	
94	98-121	[1]	49.523670	103.401176	2358	83	nd	nd	Na-Cl
95	99-34	[3]	46.758284	102.865124	3337	113	5.79	1.1992	Na-Ca-Cl
96	99-35	[3]	46.815203	102.806281	3383	113	6.01	1.12-1.19	Na-Ca-Cl
97	99-36	[3]	47.028696	102.742774	3494	113	6.36	1.12-1.90	Na-Cl
98	99-55	[3]	48.664943	102.856115	3669	122	nd	nd	Na-Ca-Cl
99	99-61	[3]	47.802210	104.318040	3539	112	5.85	1.2102	Na-Cl
100	03-010		49.510906	103.392258	2347	86	nd	nd	
Late Ordovician (Yeoman Formation)									
101	97-15	[3]	49.510906	103.392258	2583	92	6.08	1.175	Na-Cl
102	97-19	[3]	49.527412	103.413475	2575	92	6.19	1.184	Na-Cl
103	99-28	[3]	47.140136	103.613007	3856	113	5.80	1.2226	Na-Ca-Cl
104	99-39	[3]	47.298931	103.793683	3861	110	5.46	1.12-1.19	Na-Ca-Cl
105	99-60	[3]	47.808580	104.308610	3828	102	5.88	1.2073	Na-Cl
106	99-65	[3]	48.958042	103.927671	3216	88	5.86	1.2161	Na-Ca-Cl
107	99-128		49.495594	103.399178	2584	92	nd	nd	Na-Cl
108	00-187		49.328510	104.815643	2729	81	nd	nd	Na-Cl
109	00-192	[3]	49.470104	103.421410	2600	92	6.12	1.1978	Na-Cl
110	01-109		47.861029	103.349897	4103	140	6.25	1.0905	Ca-Na-Cl
111	01-110		47.716207	103.457003	4213	142	5.58	1.2335	Ca-Na-Cl
112	01-111		47.679565	103.317501	4307	137	6.51	1.23	Ca-Na-Cl
113	01-112		47.677990	104.047470	3892	126	6.04	1.1972	Na-Ca-Cl
114	01-135		48.691700	104.080440	3421		5.7	1.2415	Na-Ca-Cl
115	01-140		48.579720	104.140790	3486	91	5.39	1.18-1.25	Na-Ca-Cl
116	01-409	[1]	49.324455	104.816475	2737	82	nd	nd	Na-Cl
117	01-410	[1]	49.331688	104.816475	2730	81	6.79	1.1239	Na-Cl
Middle Ordovician (Winnipeg Formation)									
118	98-10	[3]	49.510300	103.392326	2695	95	nd	nd	Na-Cl
119	98-24	[3]	49.490200	103.442955	2701	95	nd	nd	Na-Cl
120	00-08		49.470688	103.423599	2726	95	nd	nd	Na-Cl
121	00-09		49.489481	103.442902	2700	95	nd	nd	Na-Cl
122	00-11	[1]	49.328510	104.815643	2846	88	nd	nd	Na-Cl
123	00-19	[1]	49.349953	104.821915	2892	88	nd	nd	Na-Cl
124	00-60	[1]	49.349606	104.791672	2850	80	nd	nd	Na-Cl
Cambrian (Deadwood Formation)									
125	01-201	[1]	48.955806	101.970487	2918	93	nd	nd	Na-Ca-Cl
126	01-202	[1]	48.976666	101.939347	2794	80	nd	nd	Na-Ca-Cl

Table C.1 Continued

No.	Sample ID	TDS mg/L	Ca mg/L	K mg/L	Mg mg/L	Na mg/L	Li mg/L	Sr mg/L
Early Cretaceous (Mannville Group)								
1	99-116	11245	<50	<100	<10	3524	0.28	1.63
2	00-101	7845	<20	<40	<5	3581	0.37	0.76
3	01-205	15012	43	17	32.4	5940	0.71	6.03
4	02-128	7420	24	20	4.8	3310	0.366	1.3
Mississippian (Poplar Member)								
5	01-033	12397	640	84	154	3670	2.32	11.8
Mississippian (Ratcliffe Member)								
6	05-106	302245	nd	nd	nd	104100	58	nd
7	05-109	309662	11100	4880	1100	111000	59.6	841
8	05-111	303940	15600	5260	1800	104200	60.6	1050
Mississippian (Midale Member)								
9	99-117	194903	7260	1650	1640	62565	31.2	247
10	00-180	207888	5250	1520	1200	70596	29.1	177
11	00-190	139230	4560	150	967	35898	6.01	127
12	01-128	326852	12300	5370	1490	107153	69.6	839
13	01-129	327667	11900	5500	1430	107736	72.5	809
14	05-103	265092	14200	4680	1600	89370	49.9	1040
15	05-104	266402	11200	4790	1200	92770	45.2	824
16	05-110	274285	16800	5000	1500	90940	57	1420
17	05-115	246964	24300	4830	1700	77460	60.7	940
18	05-117	282599	13800	4460	1400	100000	49	1000
Mississippian (Frobisher Member)								
19	00-116	161392	2230	1270	589	56891	24.7	68.5
20	00-117	147183	2290	1300	586	50503	24.9	67.2
21	02-019							
22	05-112	272789	16800	5180	1600	92550	54,4	1380
23	05-119	250898	10600	4380	1200	87380	52.1	741
Mississippian (Lodgepole Formation)								
24	00-04	29651	979	6810	186	4710	1.68	19.2
Late Devonian (Bakken Formation)								
25	97-23	349056	2510	2130	484	92047	20.4	82.8
26	98-20	254052	2270	1910	396	95790	18.1	68.1
27	98-21	328840	2190	1960	478	89376	20.3	80.8
28	98-43	308167	19800	6370	1530	88814	47.3	1390
29	98-56	254534	2400	1920	409	97300	17.9	67.8
30	99-48	289586	15700	6110	1710	87878	43.3	1070
31	99-69	282825	12100	5160	1420	91053	47.1	727
32	01-108	309209	17600	5310	1450	94091	60.5	1160
33	01-115	313754	18200	5500	1530	96472	66.2	1210
34	01-116	338868	24400	7150	1770	98647	90.1	1820
35	01-117	309081	20800	6220	1780	90597	81.5	1560
36	01-118	318885	11300	5370	1380	106600	60	752
37	01-119	207686	11600	4460	994	64068	49.1	773
38	01-122		9120	5300	1220	116000	57.7	600
39	01-125	248346	4860	4180	623	90270	28.4	265
40	01-126	128124	7200	2540	611	39920	29.3	476
41	01-150	246292	8110	4020	1180	80790	63.6	484
42	01-171	125383	1780	1350	392	46362	16.5	58.7
43	01-404	235557	3430	2580	586	86444	35.6	151
44	02-016							
45	02-205	224505	2150	2040	380	84280	16.1	67

Table C.1 Continued

No.	Sample ID	TDS	Ca	K	Mg	Na	Li	Sr
Late Devonian (Birdbear Formation)								
46	97-14	389722	10300	3220	1330	95480	32.5	481
47	97-32	300898	10600	3280	1350	99739	32.9	501
48	98-18	378087	12600	3750	1590	98012	32.1	668
49	98-125	309775	13900	4020	1740	102867	37.4	682
50	99-25	288570	17300	5750	1740	88627	49.9	645
51	01-105	309074	22100	7110	2020	89728	70.7	900
52	01-106	320098	24400	7240	2330	89886	72.6	1060
53	01-107	300665	21900	6990	2030	86653	69.2	866
54	01-402	248998	6270	3040	899	86591	47.5	285
55	01-403	253006	6450	3310	931	87244	52.8	309
56	01-405	21093	580	200	207	6830	12.3	17.1
Late Devonian (Duperow Formation)								
57	98-28	309162	25400	6790	2850	87915	49.4	1260
58	98-40	320249	5880	9450	805	111609	134	371
59	98-41	308263	18700	4570	2160	94429	165	791
60	98-123	420970	28200	5540	3570	84690	55.1	860
61	99-26	307478	36700	7290	2870	71441	113	1650
62	99-40	334882	47300	9240	3480	66766	121	1850
63	99-42	273348	30400	6800	1990	66437	102	1240
64	99-46	281471	43000	8370	3040	50227	209	1600
65	99-47	226454	35700	8470	2750	42281	133	1370
66	99-49	348089	54800	9810	4810	60935	113	2200
67	99-52	346573	58700	10900	4750	58532	159	2330
68	99-53	346015	56000	10300	3710	58830	198	2520
69	99-95	288748	23200	7210	1500	79262	82.1	990
70	99-96	354058	54600	10300	3650	66576	172	2050
71	00-17	85825	686	360	182	31700	6.99	27.7
72	00-44	96082	1860	758	466	33620	12.9	57.3
73	00-61	29609	1430	336	262	8870	4.74	28.6
74	01-136	311305	33100	7150	3450	74416	242	1770
75	01-141	363496	57000	11000	5050	62581	184	2370
76	01-203	300817	5700	3160	774	109403	56.8	295
Middle Devonian (Dawson Bay Formation)								
77	99-56	289321	19100	8350	1750	83009	80.4	705
78	99-57	284359	18800	7780	1710	82651	77.8	674
79	00-201	176551	12600	3660	1310	46561	39.2	443
80	01-131	286818	33900	10400	3120	62960	119	1110
Middle Devonian (Prairie Formation)								
81	02-345	518581	136000	19900	22300	6392	13.9	4220
Middle Devonian (Winnipegosis Formation)								
82	98-45	257620	28800	6410	1910	62187	41.3	791
83	98-46	244751	18900	4570	1620	69070	28.3	876
84	98-58	304836	6440	5700	4480	103000	51.6	362
85	99-75	407819	7330	5340	2120	104768	46.3	315
86	01-147	53440	4950	1140	567	13880	9.53	148
87	01-151	288932	33100	6490	2550	66536	38.3	1160
88	01-407	252275	2360	3820	403	93389	11.6	94
89	01-408	268821	2260	3820	406	99328	11.3	90.8
90	01-411	309923	3370	3780	506	113787	10.7	117
91	02-215	319951	18300	6720	2890	96127	36.2	773
92	02-216	332044	22500	7520	3200	96349	37.5	921

Table C.1 Continued

No.	Sample ID	TDS	Ca	K	Mg	Na	Li	Sr
Early to Middle Silurian (Interlake Formation)								
93	98-44							
94	98-121	252007	3170	3380	58	56478	13.2	91.2
95	99-34	295552	27600	5630	1960	78299	55.1	941
96	99-35	281975	20400	6010	1510	83182	50.9	736
97	99-36	275629	18700	6050	1440	81477	38.6	662
98	99-55	291680	28400	3710	2050	79747	67.6	1030
99	99-61	310680	19600	6520	1640	92628	48.3	684
100	03-010							
Late Ordovician (Yeoman Formation)								
101	97-15	388866	15400	2940	1760	90706	38.3	575
102	97-19	404607	15300	3200	1860	95081	41.3	597
103	99-28	317683	44100	3910	3130	70345	50.3	1590
104	99-39	313206	33300	7270	2930	76363	97.5	1250
105	99-60	304134	19600	6660	1620	92472	47.4	673
106	99-65	302027	34200	4210	3510	74738	41	1090
107	99-128	288283	16900	3160	1870	89160	40.5	623
108	00-187	270461	3300	4890	496	97361	18.5	149
109	00-192	291958	16100	3140	1850	89397	38.8	647
110	01-109	133332	24200	1840	1520	19870	53.7	866
111	01-110	351930	64700	8350	4250	55178	95.5	1960
112	01-111	177725	36100	3980	2200	23600	58.6	1050
113	01-112	304590	34800	4050	2870	73828	78.7	1350
114	01-135	335774	48000	6230	4870	67302	72.8	1570
115	01-140	336169	43900	5580	4340	73341	69.3	1510
116	01-409	278270	3750	5660	589	97783	26	175
117	01-410	282355	3100	5720	504	100835	24.2	143
Middle Ordovician (Winnipeg Formation)								
118	98-10	305376	8450	2780	908	102000	30.4	372
119	98-24	406588	10900	2890	1030	102970	30	436
120	00-08	414005	7920	2800	879	104295	33.2	351
121	00-09	311369	8580	2710	923	105978	33.2	377
122	00-11	236922	2850	3420	449	86774	13.5	119
123	00-19	208471	2780	5500	414	72570	12.7	122
124	00-60	240631	2920	2590	441	85751	12.9	102
Cambrian (Deadwood Formation)								
125	01-201	325398	33700	3230	1960	85054	23.9	874
126	01-202	320179	27400	3170	1990	90667	27.4	772

Table C.1 Continued

No.	Sample ID	Cl	Br	I	SO_4	HCO_3	Charge Balance
		mg/L	mg/L	mg/L	mg/L	mg/L	
Early Cretaceous (Mannville Group)							
1	99-116	4370	5	1.9	<6	nd	13
2	00-101	4173	6.7	2.5	<2	nd	14.8
3	01-205	7960	5.1	1.6	995	876	0.9
4	02-128	3927	5.2	1.4	<3	1880	0.7
Mississippian (Poplar Member)							
5	01-033	3520	3.8	below detection	4285	218	4.2
Mississippian (Ratcliffe Member)							
6	05-106	197500	569	75.9	nd	nd	
7	05-109	198100	499	63.0	<100	106	
8	05-111	199100	564	75.6	<100	96	
Mississippian (Midale Member)							
9	99-117	120156	234	20.2	959	nd	-1.7
10	00-180	127705	262	22.7	995	nd	-1.7
11	00-190	66503	208	10.2	1396	nd	-0.7
12	01-128	198171	597	68.9	306	138	0.2
13	01-129	198755	608	69	297	153	0.1
14	05-103	175000	635	86.8	<100	121	
15	05-104	172900	642	89.6	<100	136	
16	05-110	182600	651	93.8	300	588	
17	05-115	168900	545	59.3	<100	79	
18	05-117	181900	601	97.6	<100	114	
Mississippian (Frobisher Member)							
19	00-116	97429	155	16.9	2580	nd	-2
20	00-117	89634	140	14.7	2481	nd	-3.3
21	02-019						
22	05-112	179500	645	93.9	680	580	
23	05-119	163000	464	54.3	<100	143	
Mississippian (Lodgepole Formation)							
24	00-04	11740	7.0	1.1	5184	2490	-3.8
Late Devonian (Bakken Formation)							
25	97-23	146530	241	19.8	1834	236	0.8
26	98-20	151349	240	12.7	1807	189	0.8
27	98-21	141789	233	26.7	2145	232	0.7
28	98-43	188910	934	81.7	284	<5	-1.2
29	98-56	150000	235	9.1	1825	208	2.1
30	99-48	175407	827	76.1	327	nd	0.1
31	99-69	170988	630	69.6	306	nd	0.4
32	01-108	188252	716	123.6	425	<5	-0.1
33	01-115	189895	753	128	330	<5	0.9
34	01-116	203814	770	122	260	<5	1.7
35	01-117	187225	706	111	277	<5	1
36	01-118	192736	590	97.8	321	<5	0.8
37	01-119	124875	456	57	292	55	1.3
38	01-122				324	121	
39	01-125	147861	161	3.7	728	94	2.2
40	01-126	76682	292	35.1	224	108	1.8
41	01-150	150353	425	47.7	336	135	-0.7
42	01-171	72147	74	3.95	2790	341	2.1
43	01-404	140797	239	17.6	953	179	1.1
44	02-016						
45	02-205	132918	199	14.2	2124	314	0.9

Table C.1 Continued

No.	Sample ID	Cl	Br	I	SO_4	HCO_3	Charge Balance
Late Devonian (Birdbear Formation)							
46	97-14	171870	496	29	415	67	0.4
47	97-32	184132	480	29.9	425	69	-1
48	98-18	162587	173	3.3	517	150	5.8
49	98-125	184932	572	35.4	476	207	2.2
50	99-25	174458	800	67.6	300	nd	1.5
51	01-105	186240	852	52.6	327	73	1.7
52	01-106	194079	984	46.2	333	94	1
53	01-107	181257	848	52.3	295	84	1.7
54	01-402	150295	462	30.9	614	175	0.3
55	01-403	153146	462	31.1	596	186	0
56	01-405	9300	73.6	1.7	3835	522	1.3
Late Devonian (Duperow Formation)							
57	98-28	183954	763	39	1780	64	3.5
58	98-40	191099	622	27.4	506	108	1.8
59	98-41	186462	762	28.3	363	109	2.3
60	98-123	201807	1028	21.8	196	188	-1
61	99-26	186203	1190	20.6	250	nd	2.3
62	99-40	204598	1490	37.0	312	nd	1.4
63	99-42	165398	963	18.1	530	nd	2.1
64	99-46	173049	1196	25.3	290	nd	1.4
65	99-47	140548	849	19.6	845	nd	0.9
66	99-49	213034	1540	39	306	nd	1.3
67	99-52	208622	1630	34.1	318	nd	3.7
68	99-53	212835	1597	25.1	292	nd	1.3
69	99-95	175561	889	53.4	262	nd	0.5
70	99-96	215138	1540	31.5	303	nd	2.5
71	00-17	52100	41.3	1.71	1510	191	
72	00-44	55600	44.5	1.9	3506	112	-0.5
73	00-61	14300	20.2	0.8	4255	75	-0.1
74	01-136	189223	1130	24.7	339	800	2.5
75	01-141	223001	1691	40.1	428	148	1.4
76	01-203	180349	318	19.8	390	220	1.4
Middle Devonian (Dawson Bay Formation)							
77	99-56	175406	908	12.5	251	nd	0.6
78	99-57	171737	916	13.4	235	nd	1.1
79	00-201	111351	577	9.42	399	nd	-4
80	01-131	173831	1310	20.6	296	47	1.8
Middle Devonian (Prairie Formation)							
81	02-345	324018	5490	73.7	<30	60	1.7
Middle Devonian (Winnipegosis Formation)							
82	98-45	156482	461	5.3	246	35	1.1
83	98-46	148849	435	14.3	330	53	0.4
84	98-58	183665	346	5.0	605	39	1.7
85	99-75	181680	421	16.7	488	249	1.4
86	01-147	32065	88	2	351	180	1.3
87	01-151	177867	554	20.1	275	90	-0.4
88	01-407	150318	85.3	1.9	1576	174	0.6
89	01-408	161174	86.5	2.1	1450	149	0
90	01-411	186629	141	2.1	1387	135	-0.3
91	02-215	194293	618	11.8	126	55	0.6
92	02-216	200736	651	14.0	51	63	1.4

Table C.1 Continued

No.	Sample ID	Cl	Br	I	SO_4	HCO_3	Charge Balance
Early to Middle Silurian (Interlake Formation)							
93	98-44						
94	98-121	95293	74.4	2.33	1861	73	-0.2
95	99-34	180128	925	13.8	216	nd	0.7
96	99-35	169286	784	16.3	261	nd	2.0
97	99-36	166206	691	11.9	180	nd	1.1
98	99-55	175460	747	11.7	259	nd	2.7
99	99-61	188781	769	9.8	231	nd	0.4
100	03-010						
Late Ordovician (Yeoman Formation)							
101	97-15	176816	448	5.2	321	53	-0.2
102	97-19	182655	446	6.0	348	65	0.2
103	99-28	193295	1250	13	199	nd	2.1
104	99-39	190800	1153	42	261	nd	1.3
105	99-60	182267	785	10	232	nd	2.1
106	99-65	183422	809	7	283	nd	2.2
107	99-128	175610	448	4.9	324	nd	0.5
108	00-187	163038	208	4.1	959	nd	-0.4
109	00-192	179840	458	6.1	375	nd	-1.1
110	01-109	80950	503	4.2	234	211	-0.8
111	01-110	215062	1490	10.2	428	393	1.9
112	01-111				274	451	1.2
113	01-112	186519	1002	13	247	79	1.1
114	01-135	206612	1110	7	390	<5	1.3
115	01-140	206370	1000	7	339	52	1.3
116	01-409	168915	220	4.2	902	195	-1.3
117	01-410	170430	201	4.3	1076	268	-0.8
Middle Ordovician (Winnipeg Formation)							
118	98-10	190000	278	5.3	455	<5	-3.1
119	98-24	182430	348	6	292	<5	0.6
120	00-08	184954	299	5.3	416	<5	-1.1
121	00-09	191946	317	5.2	410	<5	-1.9
122	00-11	141543	119	2.4	1501	91	0.4
123	00-19	125658	110	3.0	1142	89	-1.2
124	00-60	146634	102	2.6	1930	92	-2.3
Cambrian (Deadwood Formation)							
125	01-201	199931	617	7.5	357	<5	0.2
126	01-202	195554	594	4.6	351	<5	0.7

Table C.2 The isotopic ($\delta^{37}Cl$ and $\delta^{81}Br$) ranges for the Williston Basin formation waters from the different stratigraphic units.

Stratigraphic Unit	Range of $\delta^{37}Cl$ values	Average $\delta^{37}Cl$ (±Stdv)	Range of $\delta^{81}Br$ values	Average $\delta^{81}Br$ (±Stdv)
Early Cretaceous (Mannville Group)	-1.01 ‰ to +0.16 ‰	-0.62 ‰ (±0.53)		
Mississippian (Madison Group)	-0.06 ‰ to -0.05 ‰	-0.06 ‰ (±0.01)	+0.13 ‰ to +0.26 ‰	+0.19 ‰ (±0.10)
Mississippian (Poplar Member)	-0.10 ‰	-0.10 ‰		
Mississippian (Ratcliffe Member)	-0.25 ‰ to -0.11 ‰	-0.18 ‰ (±0.07)	-0.39 ‰ to +0.04 ‰	-0.18 ‰ (±0.22)
Mississippian (Midale Member)	-0.27 ‰ to +0.97 ‰	+0.02 ‰ (±0.41)	+0.30 ‰ to +0.71 ‰	+0.54 ‰ (±0.16)
Mississippian (Frobisher Member)	-0.09 ‰ to +0.01 ‰	-0.03 ‰ (±0.04)	+0.36 ‰ to +0.70 ‰	+0.59 ‰ (±0.16)
Mississippian (Lodgepole Formation)	-0.31 ‰	-0.31 ‰		
Late Devonian (Bakken Formation)	-0.15 ‰ to +0.82 ‰	+0.25 ‰ (±0.29)	+0.20 ‰ to +2.77 ‰	+1.48 ‰ (±0.78)

Table C.2 Continued

Stratigraphic Unit	Variations in $\delta^{37}Cl$ values	Average $\delta^{37}Cl$ (±Stdv)	Variations in $\delta^{81}Br$ values	Average $\delta^{81}Br$ (±Stdv)
Late Devonian (Birdbear Formation)	-0.18 ‰ to +0.38 ‰	+0.08 ‰ (±0.22)	+0.75 ‰ to +1.01 ‰	+0.88 ‰ (±0.11)
Middle Devonian (Dawson Bay Formation)	-0.16 ‰ to +0.06 ‰	-0.07 ‰ (±0.10)	-0.27 ‰ to +0.18 ‰	+0.01 ‰ (±0.20)
Middle Devonian (Winnipegosis Formation)	-0.46 ‰ to +0.09 ‰	-0.23 ‰ (±0.21)	-0.42 ‰ to +0.53 ‰	+0.19 ‰ (±0.30)
Early to Middle Silurian (Interlake Formation)	-0.25 ‰ to +0.36 ‰	-0.04 ‰ (±0.21)	-.35 ‰ to +0.39 ‰	+0.21 ‰ (±0.31)
Late Ordovician (Yeoman Formation)	-0.73 ‰ to +0.07 ‰	-0.36 ‰ (±0.19)	-1.50 ‰ to +0.45 ‰	-0.58 ‰ (±0.74)
Middle Ordovician (Winnipeg Formation)	-0.09 ‰ to +0.15 ‰	+0.03 ‰ (±0.08)	0.00 ‰ to +0.15 ‰	+0.07 ‰ (±0.07)
Cambrian (Deadwood Formation)	-0.05 ‰ and -0.04 ‰	-0.05 ‰ (±0.01)	-1.41 ‰ and 0.09 ‰	-0.66 ‰ (±1.06)

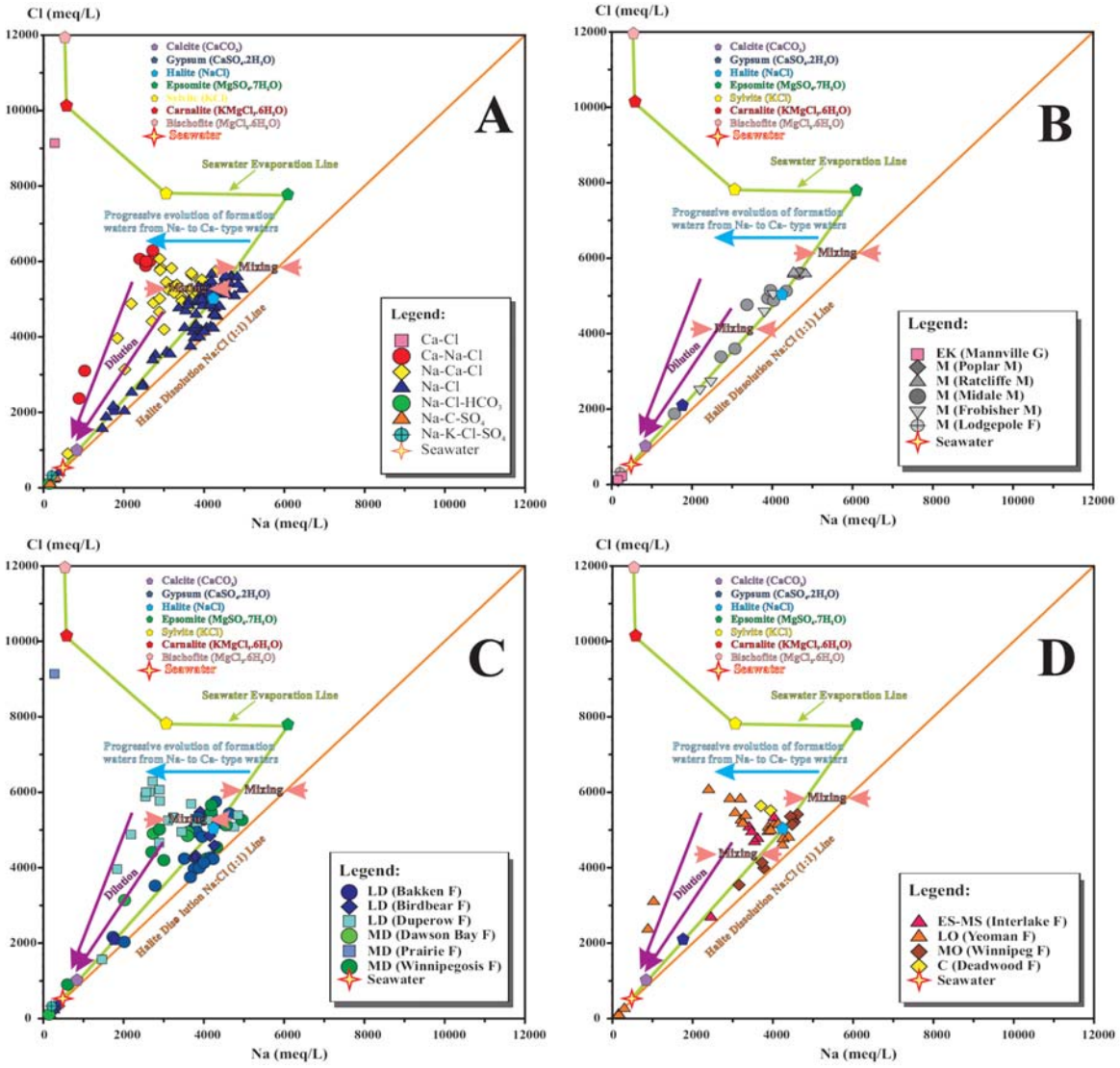

Figure C.1 Cl (meq/L) versus Na (meq/L) of the different water types of the Williston Basin formation waters. A) All data; B) Early Cretaceous and Mississippian stratigraphic units; C) Different Devonian stratigraphic units; D) Silurian, Ordovician and Cambrian stratigraphic units. The plot also illustrates the seawater evaporation trend and the Na:Cl 1:1 halite dissolution line. Some of the possible evolutionary processes and mixing scenarios between end members are also demonstrated.

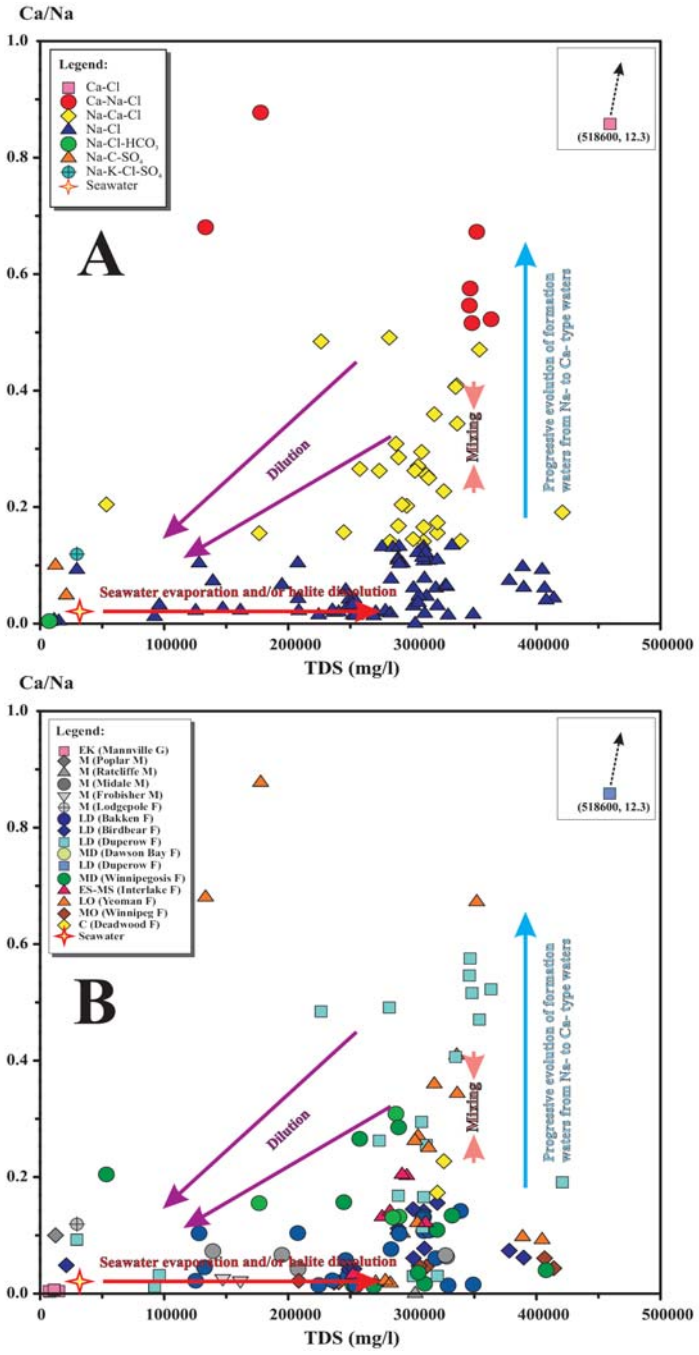

Figure C.2 Ca/Na (mmol) ratios versus TDS (mg/L) of the Williston Basin formation waters (A) based on formation water types and (B) based on the stratigraphic units. The plot shows some possible evolutionary processes and mixing scenarios between different end members.

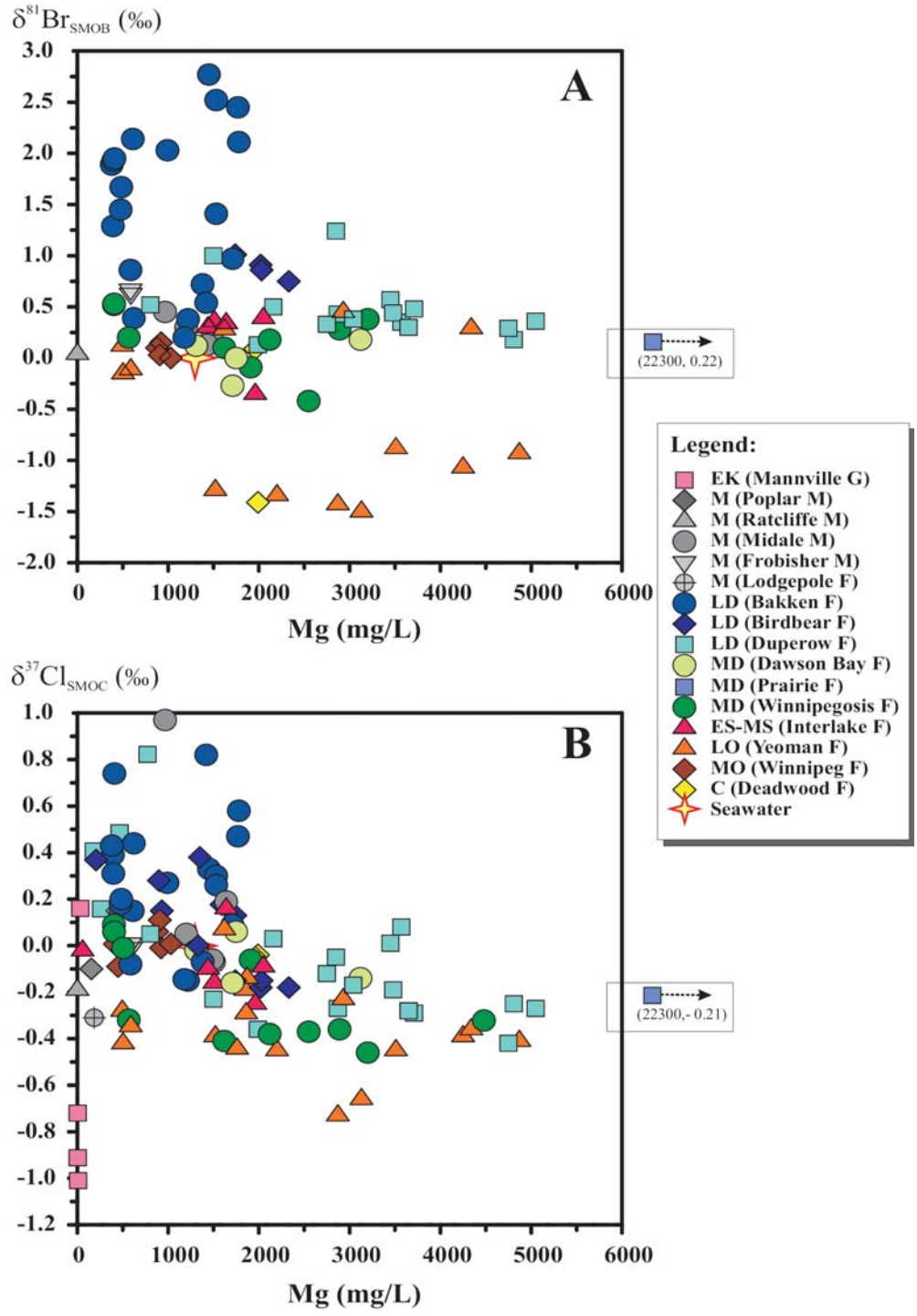

Figure C.3 A) $\delta^{81}Br_{SMOB}$ (‰) versus Mg (mg/L) and B) $\delta^{37}Cl_{SMOC}$ (‰) versus Mg (mg/L) of the Williston Basin formation waters grouped based on the stratigraphic units they were sampled from.

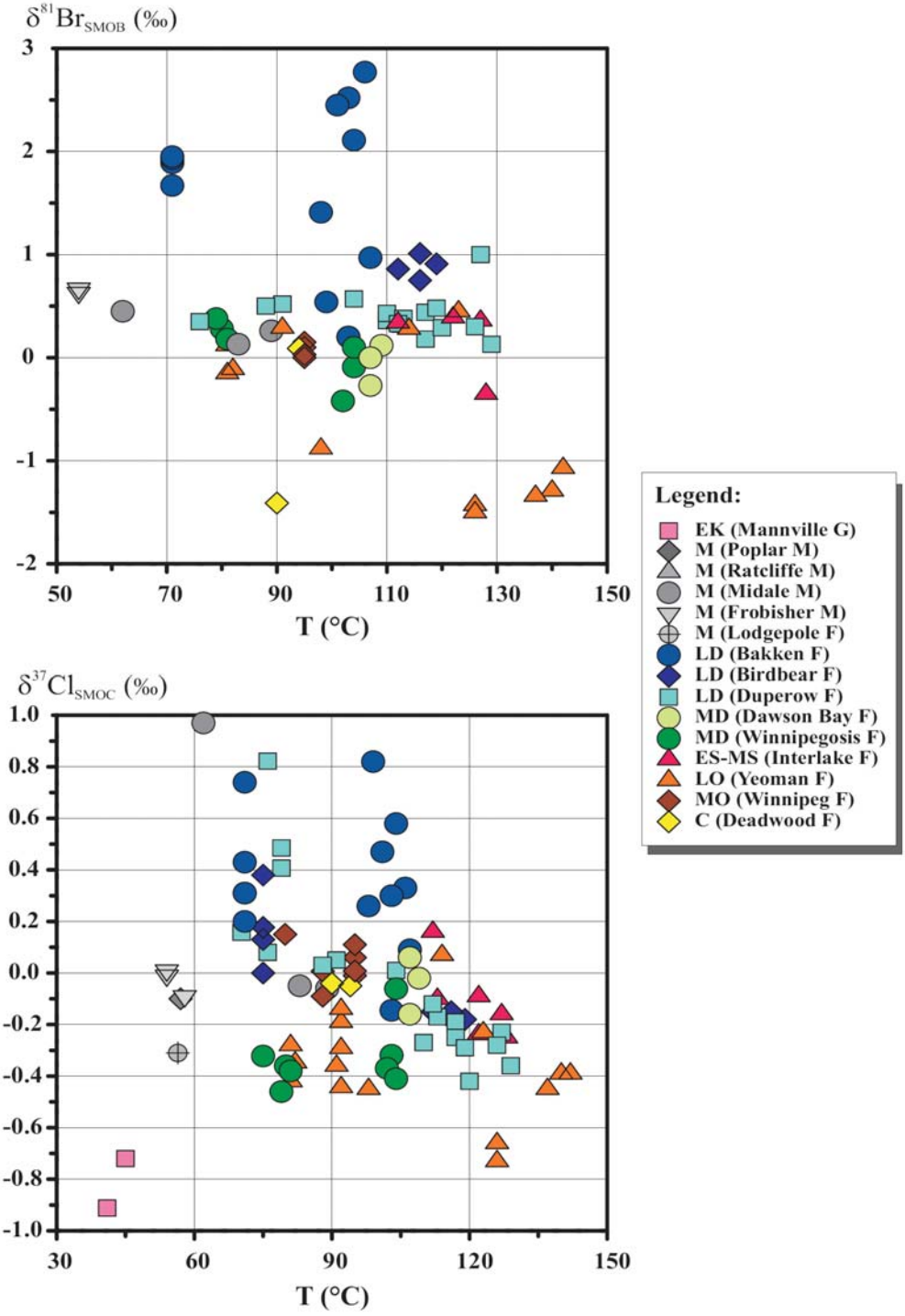

Figure C.4 A) $\delta^{81}Br_{SMOB}$ (‰) versus T (°C) and B) $\delta^{37}Cl_{SMOC}$ (‰) versus T (°C) of the Williston Basin formation waters grouped based on the stratigraphic units they were sampled from.

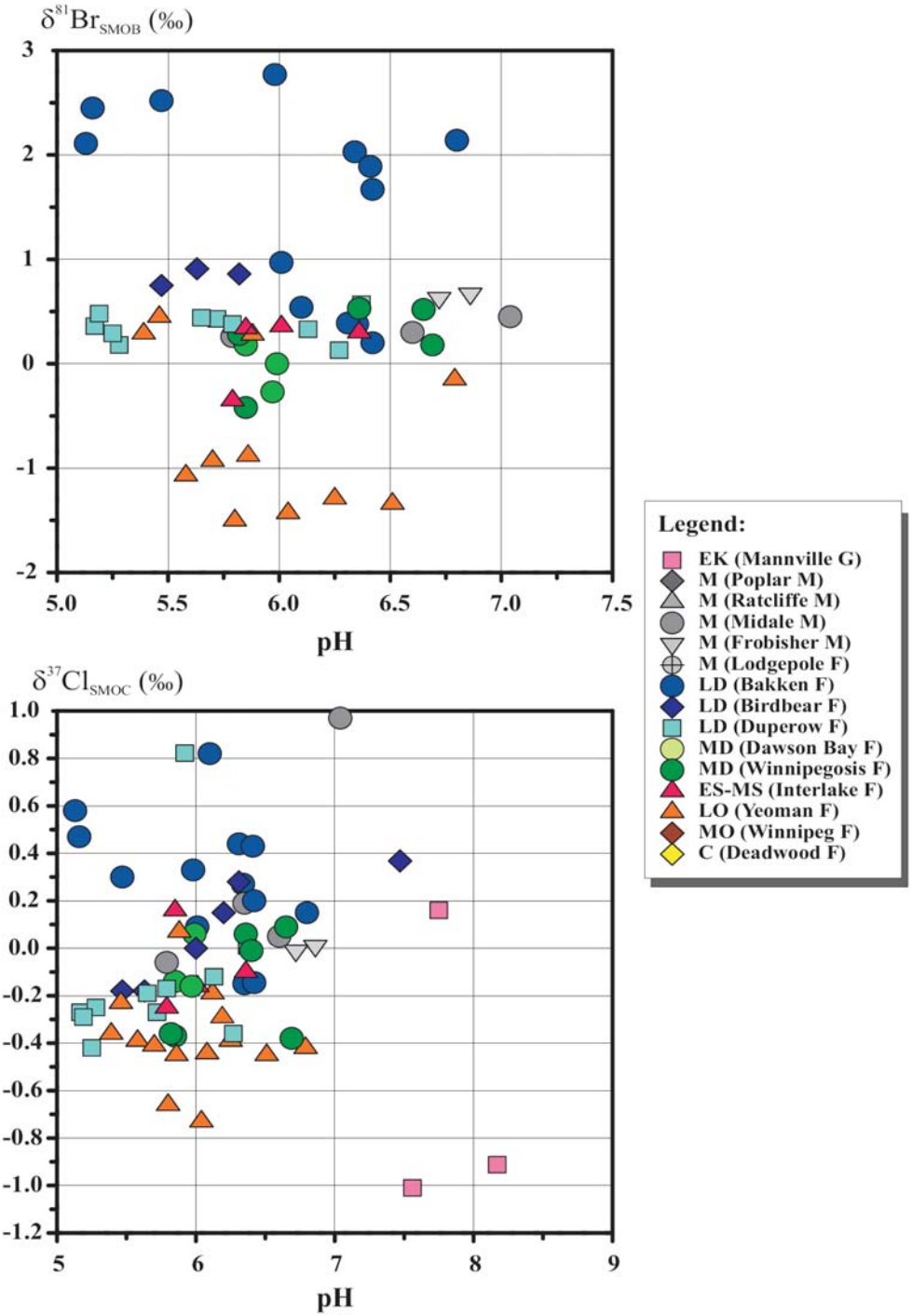

Figure C.5 A) $\delta^{81}Br_{SMOB}$ (‰) versus pH and B) $\delta^{37}Cl_{SMOC}$ (‰) versus pH of the Williston Basin formation waters grouped based on the stratigraphic units they were sampled from.